



2015

# Structure and Molecular Mechanism of a PLP/ GABA Dependent Transcription Regulator GabR

Rui Wu

Loyola University Chicago

## Recommended Citation

Wu, Rui, "Structure and Molecular Mechanism of a PLP/GABA Dependent Transcription Regulator GabR" (2015). *Dissertations*. Paper 1659.  
[http://ecommons.luc.edu/luc\\_diss/1659](http://ecommons.luc.edu/luc_diss/1659)

This Dissertation is brought to you for free and open access by the Theses and Dissertations at Loyola eCommons. It has been accepted for inclusion in Dissertations by an authorized administrator of Loyola eCommons. For more information, please contact [ecommons@luc.edu](mailto:ecommons@luc.edu).



This work is licensed under a [Creative Commons Attribution-Noncommercial-No Derivative Works 3.0 License](https://creativecommons.org/licenses/by-nc-nd/3.0/).  
Copyright © 2015 Rui Wu

LOYOLA UNIVERSITY CHICAGO

STRUCTURE AND MOLECULAR MECHANISM  
OF A PLP/GABA-DEPENDENT  
TRANSCRIPTION REGULATOR GABR

A DISSERTATION SUBMITTED TO  
THE FACULTY OF THE GRADUATE SCHOOL  
IN CANDIDACY FOR THE DEGREE OF  
DOCTOR OF PHILOSOPHY

PROGRAM IN CHEMISTRY

BY

RUI WU

CHICAGO, IL

MAY 2015

Copyright by Rui Wu, 2015  
All rights reserved.

## ACKNOWLEDGMENTS

I would like to begin by expressing my sincerest gratitude to my supervisor Dr. Dali Liu, for introducing me and giving me the opportunity to work in the exciting field of X-ray Crystallography. Dr. Lu was a great and patient mentor who provided immense support throughout my Ph.D. studies by introducing me to tons of great collaborators from who I absorbed tons of knowledge, and for everything that he taught me in these years, both in academia and in general.

I am also forever grateful to Dr. Dr. Ruslan Sanishvili at the Argonne National Laboratory and Dr. Miguel A. Ballicora.

Dr. Ruslan Sanishvili provided great support on six or more projects I've been working on throughout these years and his insightful advice made me a better person. His sharp expertise in X-ray crystallography not only has greatly enriched this dissertation, but also taught me how to approach scientific hypothesis with careful and logical steps. On a personal note, I am forever grateful to him for being a listener when I had doubts of myself, and for giving me a confidence boost when I seemed to lose it.

I would also like to thank Dr. Miguel A. Ballicora for his insightful knowledge on enzyme kinetic and showing me how to produce scientific writing in depth. Chapters 5 and 6 could not be accomplished without the great support and tremendous effects from Dr. Ballicora. More importantly, I have benefited a lot from his artistic approach of encouraging and supporting me at critical moments during this long journey.

I would also like to thank Dr. Till Boecking and his graduate student Walid Al-Zyoud at the University of New South Wales in Australia for a lot of help in determining the Small Angle X-ray Scattering Structures of GabR and GabR and DNA complexes. Those structures have shed light on interpreting the data from the X-ray structures and the DNA binding results. It also paves the way for the future functional study on the GabR, DNA complexes with RNA polymerase, sigma factor, etc.

I would also like to thank Dr. Boris R. Belitsky from Tufts Medical School for hosting me at his lab for almost one month and for his great support on the *in vivo* and *in vitro* aspects of the project. I also benefited a lot from his insightful criticisms on my manuscripts.

I would also like to thank Dr. Quyen Quang from Indiana Medical School for hosting my co-workers and me multiple times at his research lab and assisting with the design of multiple experiments and result interpretations. I am also very grateful for many useful life tips and taking me to the conferences with his research team.

I would also like to thank Dr. Richard Holz, Dr. Richard B. Silverman and Dr. Walter Fast for the opportunities to work on their interesting projects, and their constant guidance and suggestions during the process. I also appreciate the helpful advice from Dr. Jacob Ciszek during the job searching process and Dr. Catherine Putonti for serving on my research committee.

I'm forever grateful to Dr. Carlos M. Figueroa and Dr. Salette Martinez Martinez for teaching me valuable skills at the beginning of graduate school, which have tremendously helped me throughout my research. The postdocs: Hoang V. Lee and Jianbin Zheng and graduate students: Yuguang Wang, Zheng Zhang, Ben Hill, Hyun Lee

and Ken Cleavage, thanks for being such good lab mates and collaborators. I'm also grateful to all the undergraduate students who helped me with my experiments: Hansol lee, Michael Farley, Emily Cybulla, and summer intern Saba Sanishvili, and Nushrat Hoque.

I also want to thank the Chemistry and Biochemistry Department main office staff, Carol Grimm, Stacey Lind, and Denise Hall for their help with paperwork matters; and Matthew Sara from the Stockroom for his help with laboratory / chemicals matters.

I would like to acknowledge my family members - my mum and dad, and my friends: Daniel Kechker, Ronan Garcia, Ambrozewski M. Rachel and Zulfiya Gaziev, for years of lessons and amazing support and encouragement, which have enabled me to complete this dissertation and degree.

## TABLE OF CONTENTS

ACKNOWLEDGMENTS	iii
LIST OF TABLES	viii
LIST OF FIGURES	ix
LIST OF SCHEMES	xii
LIST OF ABBREVIATIONS	xiii
ABSTRACT	xviii
CHAPTER ONE: INTRODUCTION	1
Research Aims: Potential Anti-Virulence Target for Secondary Infections of Cystic Fibrosis (CF)	1
Transcription and the Transcription Factor	3
GntR Family and the Subfamily Classification	4
MocR/GabR	12
CHAPTER TWO: CRYSTAL STRUCTURE OF BACILLUS SUBTILIS GABR, AN AUTOREPRESSOR AND TRANSCRIPTIONAL ACTIVATOR OF GABT	15
Research Significance	15
Introduction	16
GabR is a Head-to-Tail Domain-Swap Homodimer	19
GabR is a Dimer in Solution	23
Conserved Putative DNA-Binding Residues in the N-terminal Winged Helix Domain	25
GabR Binds DNA With High Affinity	32
PLP is Bound in the C-terminal AT-Fold Domain	34
Is GabR an Enzyme?	35
Model for GabR-Mediated Transcriptional Regulation at the gabR and gabT Promoters	41
Biological Implications	44
Materials and Methods	44
CHAPTER THREE: PLP AND GABA TRIGGER GABR-MEDIATED TRANSCRIPTION REGULATION IN BACILLUS SUBTILIS VIA EXTERNAL ALDIMINE FORMATION	54

Research Significance	54
Introduction	55
Crystallography of GabR Eb/O Domain and Asp-AT Completed With Ligands	56
Details of the Effector Binding Site in the GabR Eb/O Domain and Schiff Base Formation Between PLP and GABA	59
External Aldimine as the Final Adduct of GabR-Mediated Reaction	63
Functional Significance of External Aldimine Formation	68
Conclusions	69
Materials and Methods	70
 CHAPTER FOUR: CONCLUSIONS AND FUTURE INVISTIGATIONS	 75
Full Length GabR and Its Overall Structure	75
Effector Binding Domain and Related Biological Function	78
GabR and DNA complex	78
 CHAPTER FIVE: THE CRYSTAL STRUCTURE OF NITROSOMONAS EUROPAEA SUCROSE SYNTHASE REVEALS CRITICAL CONFORMATIONAL CHANGES AND INSIGHTS INTO THE SUCROSE METABOLISM IN PROKARYOTES	   81
Research Significance	81
Introduction	82
Sequence Analysis	84
Protein Expression and Characterization	117
Substrate Specificity of <i>NeuS</i> ase	118
X-ray Diffraction, Data Processing, Model Building, and Refinement	119
Structural Analysis of <i>NeuS</i> ase	120
Site Directed Mutagenesis of Critical Residues	134
Materials and Methods	138
 CHAPTER SIX: CONCLUSIONS	 145
 REFERENCE LIST	 147
 VITA	 158



## LIST OF TABLES

Table 1. Data collection and refinement statistics for full length GabR	50
Table 2. Data collection and refinement statistics for GabR Eb/O domain	58
Table 3. Sucrose synthase genes used for phylogenetic analysis	86
Table 4. Kinetic parameters for substrates of <i>NeuSocSase</i> in the direction of sucrose synthesis	119
Table 5. Data collection and refinement statistics for <i>NeuSocSase</i>	137
Table 6. Activity of wild type and mutants of <i>NeuSocSase</i>	138

## LIST OF FIGURES

Figure 1. Unrooted tree of the proteins of GntR family regulators of <i>M. smegmatis</i> including representatives of all subfamily regulator from different Bacterial Genomes with 1000 bootstrap replicates	7
Figure 2. Quaternary structure of FadR and its corresponding DNA	8
Figure 3. Quaternary structure of PhnF	9
Figure 4. Quaternary structure of CFL2947 from <i>Corynebacterium Glutamicum</i>	9
Figure 5. Quaternary structure of DNA binding domain from AraR and its corresponding DNA fragment	11
Figure 6. Schematic of GabR binding sites at the <i>gabR</i> and <i>gabTD</i> promoters.	12
Figure 7. The GabT-catalyzed aminotransferase reaction	14
Figure 8. Quaternary structure of GabR	19
Figure 9. Quaternary structure of GabR	20
Figure 10. Imidazole is bound in the PLP-binding pocket of apo-GabR	22
Figure 11. Sedimentation velocity analysis of GabR	24
Figure 12. The gel-filtration profile of GabR	25
Figure 13. The GabR N-terminal winged-helix domain	26
Figure 14. The most basic surface on the GabR winged-helix domain	27
Figure 15. GabR electrostatic surface potential	28
Figure 16. Conserved putative DNA-binding residues in GabR	30
Figure 17. Sequence alignment of the winged-helix domain sequences of <i>B. subtilis</i> GabR and <i>E.coli</i> FadR	30

Figure 18. Two DNA-binding domains of GabR can interact on DNA through the “ $\alpha 3$ – $\alpha 3$ dimer interface”	31
Figure 19. Fluorescence polarization assays to measure DNA binding by GabR	33
Figure 20. The PLP-binding pocket of <i>B. subtilis</i> GabR	35
Figure 21. PLP binding in aminotransferases and the arginine switch	36
Figure 22. PLP is bound in the AT-fold domain of GabR	38
Figure 23. BLAST protein sequence alignment	40
Figure 24. A model for transcription regulation at the <i>gabR</i> and <i>gabT</i> promoters	43
Figure 25. Head-to-tail-dimers of the full-length GabR (PDB code: 4NOB), Eb/O domain of GabR and Asp-AT	57
Figure 26. PLP and GABA bound to the truncated Eb/O domain	59
Figure 27. GABA moiety displays a gauche conformation	61
Figure 28. Comparison of the external aldimine vs. internal aldimine in GabR	63
Figure 29. Fluorine NMR spectra	65
Figure 30. Biological effects of GABA and AFPA	69
Figure 31. Small angle X-ray scattering (SAXS) bead model of full length GabR	77
Figure 32. Small angle X-ray scattering (SAXS) bead model of full length GabR superimpose with X-ray crystal structure of full length GabR	77
Figure 33. Small angle X-ray scattering (SAXS) bead model of full length GabR and DNA complex	79
Figure 34. The fitting model of Small Angle X-ray Scattering (SAXS) bead structure of full length GabR and DNA complex and X-ray crystal structure of GabR	80
Figure 35. Phylogenetic tree of SucSases	85
Figure 36. Alignment of sucrose synthases from Table 3	106

Figure 37. The crystal structure of <i>NeuS</i> ucSase	120
Figure 38. The <i>NeuS</i> ucSase monomer structure is shown in backbone trace.	121
Figure 39. The “hinge”	122
Figure 40. Comparison of the open and closed monomeric forms	124
Figure 41. Difference distance matrix map of the GT-B(A) domain	125
Figure 42. Overlap comparison of the fructose binding sites of the open ( <i>NeuS</i> ucSase) and closed ( <i>AthS</i> ucSase, PDB ID 3S29) structures	126
Figure 43. Overlap comparison of the nucleotide binding sites of the open ( <i>NeuS</i> ucSase) and closed ( <i>AthS</i> ucSase, PDB ID 3S29) structures	128
Figure 44. Hinge Analysis of <i>NeuS</i> ucSase	130
Figure 45. Hinge analysis by comparison of the open v. closed conformations	131
Figure 46. Secondary structure rearrangement during conformational changes between open and closed structures of bacterial SucSases	132
Figure 47. The open “latch”	132
Figure 48. Hydrophobic residues contribute to the latch action	133
Figure 49. Conserved hydrophobic residues are involved in substrate binding in both open conformation of <i>NeuS</i> ucSase (A and B), and closed conformation of <i>AthS</i> ucSase (PDB ID: 3S29) (C and D)	135
Figure 50. Three highly conserved catalytic residues in different members of the retaining GT-B glycosyltransferase family	136

## LIST OF SCHEMES

Scheme 1. The Mechanism of First Half of the GABA-AT Reaction	60
Scheme 2. Proposed Reaction Mechanism of AFPA	64

## LIST OF ABBREVIATIONS

GABA	$\gamma$ -amino butyric acid
wHTH	winged Helix-Turn-Helix
PLP	Pyridoxal 5'-Phosphate
AFPA	(S)-4-Amino-5-Fluoropentanoic Acid
CF	Cystic Fibrosis
<i>Bcc</i>	<i>Burkholderia cepacia</i> Complex
<i>B. subtilis</i>	<i>Bacillus Subtilis</i>
<i>B. cenocepacia</i>	<i>Burkholderia Cenocepacia</i>
<i>B. multivorans.</i>	<i>Burkholderia Multivorans</i>
TFs	Transcription Factors
DNA	Deoxyribonucleic Acid
RNA	Ribonucleic Acid
PWM	Parallelism Weight Matrix
GntR	Repressor of the Gluconate Operon
HTH	Helix-Turn-Helix
Pfam	Protein families database
<i>E.coli</i>	<i>Escherichia coli</i>
DBD	DNA Binding Domain
EB/o	Effector Binding and / or oligomerization domain

PDB	Protein Data Bank
CoA	Coenzyme A
RMSD	Root Mean Square Deviation
ABC	ATP-Binding Cassette
GabT	GABA Aminotransferase
SSDH	Succinic Semialdehyde Dehydrogenase
GabD	Succinic Semialdehyde Dehydrogenase
PMP	Pyridoxamine 5'-Phosphate
NAD	Nicotinamide Adenine Dinucleotide
SS	Succinic Semialdehyde
DNase	Deoxyribonuclease
AT	Aminotransferase
Asp-AT	Aspartate Aminotransferase
bp	Base Pair
NMR	Nuclear Magnetic Resonance
BLAST	Basic Local Alignment Search Tool
FP	Fluorescence Polarization
TAMRA	Tetramethylrhodamine
FP <sub>FTD</sub>	Fluorescence Polarization Signal of Free Labeled DNA
FP <sub>GTD</sub>	Fluorescence Polarization Signal of GabR–DNA Complex
K <sub>D</sub>	Dissociation Constant
DEG	Diethylene Glycol
UV	UltraViolet

PRT	PhosphoRibosyl Transferase
LB	Lysogeny Broth
IPTG	Isopropyl- $\beta$ -D-Thiogalactopyranoside
Ni	Nickel
NADP	Nicotinamide Adenine Dinucleotide
NADPH	Nicotinamide Adenine Dinucleotide Dehydrogenase
SAXS	Small Angle X-ray Scattering
GT-B	Retaining Glycosyltransferase Family B
Suc	Sucrose
UDP	Uridine Diphosphpate
UDP-Glc	Uridine Diphosphpate Glucose
Fru-6P	Fructose-6-phophate
ADP	Adenosine Diphosphate
ADP-Glc	Adenosine Diphosphate Glucose
NDP	Nucleoside Diphosphate
NDP-Glc	Nucleoside Diphosphate Glucose
<i>N. europaea</i>	<i>Nitrosomonas europaea</i>
<i>Neu</i> SucSase	<i>Nitrosomonas europaea</i> SucSase
<i>Ath</i> SucSase	<i>Arabidopsis thaliana</i> SucSase
CRC	Comprehensive Cancer Center
BSA	Bovine Serum Albumin
NCBI	National Center for Biotechnology Information database
PEG	Polyethylene Glycol



SSN-1	Sucrose Synthase N-terminal-1
SSN-2	Sucrose Synthase N-terminal-2
<i>T. elongatus</i>	<i>Thermosynechococcus elongatus</i>
Alanine	Ala/A
Arginine	Arg/R
Asparagine	Asn/N
Aspartic Acid	Asp/D
Cysteine	Cys/C
Glutamic Acid	Glu/E
Glutamine	Gln/Q
Glycine	Gly/G
Histidine	His/H
Isoleucine	Ile/I
Leucine	Leu/L
Lysine	Lys/K
Methionine	Met/M
Phenylalanine	Phe/
Proline	Pro/P
Serine	Ser/S
Threonine	Thr/T
Tryptophan	Trp/W
Tyrosine	Tyr/Y
Valine	Val/V

Adenine	A
Cytosine	C
Guanine	G
Thymine	T

## ABSTRACT

GabR is a member of the MocR/GabR subfamily of the GntR family of bacterial transcription regulators. It regulates the metabolism of  $\gamma$ -aminobutyric acid (GABA), an important nitrogen and carbon source for many bacteria. The crystal structures reported here confirmed that this protein has evolved from the fusion of a type I aminotransferase and a winged helix-turn-helix (wHTH) DNA binding protein to form a chimeric protein that adopts a dimeric head-to-tail configuration. The pyridoxal 5'-phosphate (PLP)-binding regulatory domain of GabR is therefore an example of a coenzyme playing a role in transcription regulation rather than in enzymatic catalysis. Our structural and biochemical studies have laid solid the mechanistic foundation for understanding the regulatory functions and mechanism of the MocR/GabR subfamily of transcription regulators.

GabR is also an intriguing case of molecular evolution, displaying the evolutionary lineage between aminotransferase and a resulted regulation domain of a transcription regulator. PLP's native function is not a catalytic co-enzyme but an effector of transcription regulation. The stable chemical species of GabR-PLP-GABA responsible for GabR-mediated transcription activation, has been revealed mechanistic crystallography, NMR spectroscopy and biological assays using both GABA and a

GABA analog (S)-4-Amino-5-Fluoropentanoic Acid (AFPA) as a molecular probe. Our studies provide critical structural and chemical insights for a currently understudied subfamily of bacterial transcription regulators, MocR/GabR-type regulators in the GntR family.

In parallel, I also worked on several other projects. Herein, I dedicated 2 full chapters to demonstrate the progress on the Sucrose Synthase project. We obtained biochemical and structural evidence of sucrose metabolism in non-photosynthetic bacteria. Until now, only sucrose synthases from photosynthetic organisms have been characterized. Here, we provide the crystal structure of the sucrose synthase from the chemolithoautotroph *Nitrosomonas europaea*. This supported that the enzyme functions with an open/close induced fit mechanism. It prefers as substrate adenine-based nucleotides rather than uridine-based like the eukaryotic counterparts, implying there is a strong connection between sucrose and glycogen metabolism in these bacteria. Mutagenesis data showed that the catalytic mechanism must be conserved not only in sucrose synthases, but also in all other retaining GT-B glycosyltransferases.

## CHAPTER ONE

### INTRODUCTION

#### **Research Aims: Potential Anti-Virulence Target for Secondary Infections of Cystic Fibrosis (CF)**

Cystic Fibrosis is a life-threatening genetic disorder that causes thick, sticky mucus to build up in the lungs, digestive tract, and other areas of the body. It is one of the most common chronic lung diseases among children and young adults. In Caucasian populations, the carrier frequency for Cystic Fibrosis is approximately one in twenty-five, with a prevalence of about 1 in 2000 <sup>1</sup>. Nearly 1,000 CF diagnoses are reported annually, and the disease caused 3,708 deaths in the United States from 1999-2006. As of 2007, the medial survival age was 37.4 years, compared to a U.S. life expectancy of 70.7 years in the same year.

The local environment of the cystic fibrosis lung is unique and results in characteristic disease patterns and specific spectrum of cystic fibrosis associated lung pathogens <sup>1</sup>. Susceptibility to *Staphylococcus aureus*, *Pseudomonas aeruginosa* and other bacterial infections is significantly higher in patients with CF, as the lungs become largely ineffective at ridding the body of microbes when mucus build-up begins. Thus, a large number of deaths from CF are attributed to bacterial secondary infections that lead to lung disease in patients. With CF affecting 70,000 people across the world, and the bacteria's high resistance of a wide range of antibacterial agents, the novel antibiotic

development becomes urgent for the treatment of bacterial infections and for an improved life quality of CF patients.

The *Burkholderia cepacia* Complex (*Bcc*) is a subset of at least nine opportunistic pathogens that belong to the gram-negative *Burkholderia* genus associated with infections in CF patients. In efforts to develop more effective CF treatments, this complex is of particular interest in antibiotic development because of the well-documented multi-drug resistance of bacterial strains and the capability of patient-to-patient spread. *Burkholderia cenocepacia* and *Burkholderia multivorans* are two members of the *Bcc* responsible for a majority of the infections seen in CF patients, and they have been reported in both clinical and environmental settings (soil and water) as sources of infection.

These two strains are related to *Bacillus subtilis* by their metabolism of  $\gamma$ -amino butyric acid (GABA) to produce glutamate, which is an important metabolite in bacterial nitrogen metabolism. Similarity existing between *B. subtilis* and *Bcc* strains in their glutamate production mechanisms makes *B. subtilis* an ideal, non-pathogenic model organism for our study on the inhibition/modulation of GABA/glutamate metabolism in *B. cenocepacia* and *B. multivorans* for therapeutically purposes. It also has been recently discovered that GABA is an essential cell-to-cell signal in eukaryotes. It acts as a single signal between eukaryotes and pathogenic bacterial. GABA production has been revealed to be crucial to bacterial stress response, especially acid resistance. All of which make the metabolism of GABA in bacteria a potential target for the development of a strategy to control the virulence of bacterial pathogenesises. GabR is the transcription regulator in *B.*

*subtilis* that represses the transcription of the *gabR* gene while also initiating the transcription of the *gabT* and *gabD* genes, which are key enzymes in glutamate biosynthesis utilizing GABA while responding to the increase of GABA's concentration *in vivo*.

### **The Transcription and the Transcription Factor**

As the first step of gene expression, transcription is a fundamental process that is often highly conserved and tightly regulated process in bacteria. Bacteria cells rely on very sophisticated responses to adapt to micro environmental changes, due to the frequently changing habitats conditions. Though transcription regulation, these responses most frequently lead to the activation and/or repression of a specific sets of genes to control metabolic pathway and adapt to the different environmental condition <sup>2</sup>.

Transcription is the process of synthesis of mRNA by using a single strand of DNA as a template; the process is performed by structurally conserved DNA-dependent RNA polymerase (RNAPs) <sup>3</sup>. Transcription is tightly controlled by the transcription factors (TFs), which are the proteins that bind to specific sequence on the DNA near their target genes, thereby modulating the transcription initiation. TFs perform this function alone or with other proteins in a complex (homoprotein), by promoting (as an activator), or blocking (as a repressor) the recruitment of RNA polymerase to the promoter regions of specific genes.

Based on contemporary X-ray crystallography and advanced computational simulation, TFs mostly revealed as the dimerization motif, both heterodimer and homodimer are common. In general, the dimerization of a protein generally results in the

formation of an enlarged interaction surface, compared to the monomer. The enlarged surface area of the dimer provides increased potential for various protein-protein or protein-DNA interactions essential to transcription. Comparing to a monomer, TFs that dimerize can achieve a higher DNA binding affinity and specificity and twice as many base pairs can be recognized providing distinct DNA-binding specificities <sup>4</sup>.

Taking advantage of the intense and ongoing computationally studies, molecular and biophysical studies over the past decade, scientists have generated an unprecedented amount of information describing the location of the binding site/s, described in Parallelism Weight Matrix (PWM) and further deduced from aligning a set of DNA sequence that are experimentally known, for the transcription regulators <sup>5</sup>. However the understanding of the binding mechanism is still very preliminary. The major challenge for our work is to be able to bridge this gap between the molecular description and the genome-scale overview.

### **GntR family and the subfamily classification**

In 1990, Haydon and Guest first identified and described GntR family of bacterial transcription regulators, named after the first member identified, the *B. subtilis* transcription regulator - GntR - repressor of the gluconate operon <sup>6</sup>. Among all the bacterial transcription regulators, GntR is known as one of the most abundant and widely distributed groups of Helix-Turn-Helix (HTH) transcription factors. To date, the metabolite-response GntR family has approximately 8,561 regulatory proteins in Pfam database (Pfam family GntR: PF00392)<sup>7</sup>, which spread out among 764 bacteria taxa. GntR transcription regulators are often located at the chromosome adjacent to the genes



that they control, which in many cases allows insight into the metabolites that they bind to as effectors. There are also many cases where GntR-like regulators are not located close to the gene it regulates but elsewhere. One of the well-studied examples in this transcription regulator family is orphan regulator FadR/GntR, the fatty acid metabolism regulator in *Escherichia coli*. These studies have intensively focused on both the structural and functional aspects, serving as a critical reference case for our research.

A striking characteristic feature of the GntR family is that the members possess a highly conserved N-terminal DNA-binding domain (DBD), which evolved in DNA binding, and an extensive diverse and heterogeneity C-terminal effector binding and / or oligomerization domain (Eb/O). It was hypothesized that binding of the effector molecules could trigger the conformational changes in the protein, which modulates the DNA-binding properties of the regulator resulting in either activation or repression of transcription. It is not surprising, though, that there are a large number of effector molecules that have not been identified, given the diversity of molecule that they bind and relative large number of the GunR-family members itself.

The HTH DNA binding motif in this GntR family is the traditional tri-helical domain, whose original case demonstrated the critical role in DNA binding within the bacteriophage *Lambda* protein, *cI* and *cro* and the *lac* operon repressor, *LacI* and the generation of cell-type specific gene expression <sup>8</sup>. The there-helical HTH domain is known as the winged-helix-turn-helix domain. In addition to the core three-helix bundle, it also contains a wing form by C-terminal beta-hairpin. In some versions of this domain, the loop between strand elements interacts with the two strands of the wing <sup>9</sup>. The “wing”

feature provides great interactions with the DNA due to the third alpha helix, which can fit well within the major groove of the DNA. This was suggested by the extensive sequence analysis and secondary structural analysis throughout 1980s and 1990s <sup>7</sup>. It is being proposed that these domains descend from a common ancestor.

Since the physiological role of these regulators critically depend upon the effector binding to the operon site of the DNA, therefore analysis based on the alignment of the C terminus and secondary structural predications were used to classify the members of the GntR family. The distinct structural topologies reveal seven major subfamilies: FadR, HutC, MocR, YtrA, and three minor subfamily AraR, DevA, and PlmA (Figure1) <sup>10</sup>.

The most abundant GntR sub-family, FadR subfamily, named after the fatty acid biosynthesis and degradation regulator, functions as a switch that coordinately regulates the machinery required for fatty acid beta-oxidation and the expression of a key enzyme in fatty acid biosynthesis. It contains the majority of the GntR-like regulators, approximately 40 %. The protein in this subfamily contains six or seven-helical C-terminal domain, with the average length of 150-170 amino acid. The crystal structure is available for FadR of *Escherichia coli* (Figure2; PDB ID: 1EX1)<sup>11</sup>.

The HTH domain is fused to a seven alpha helical bundle, which contains a large internal cavity required for binding its regulator molecule. The RMSD on the alpha carbons is 0.717 Å between the bound and unbound of the acyl CoA indicated the protein backbone undergoes conformational shift upon binding to the acyl CoA-its own regulator, further resulting in 7.2 Å movement of the DNA recognition helix preventing DNA binding and subsequently repressing the transcription.

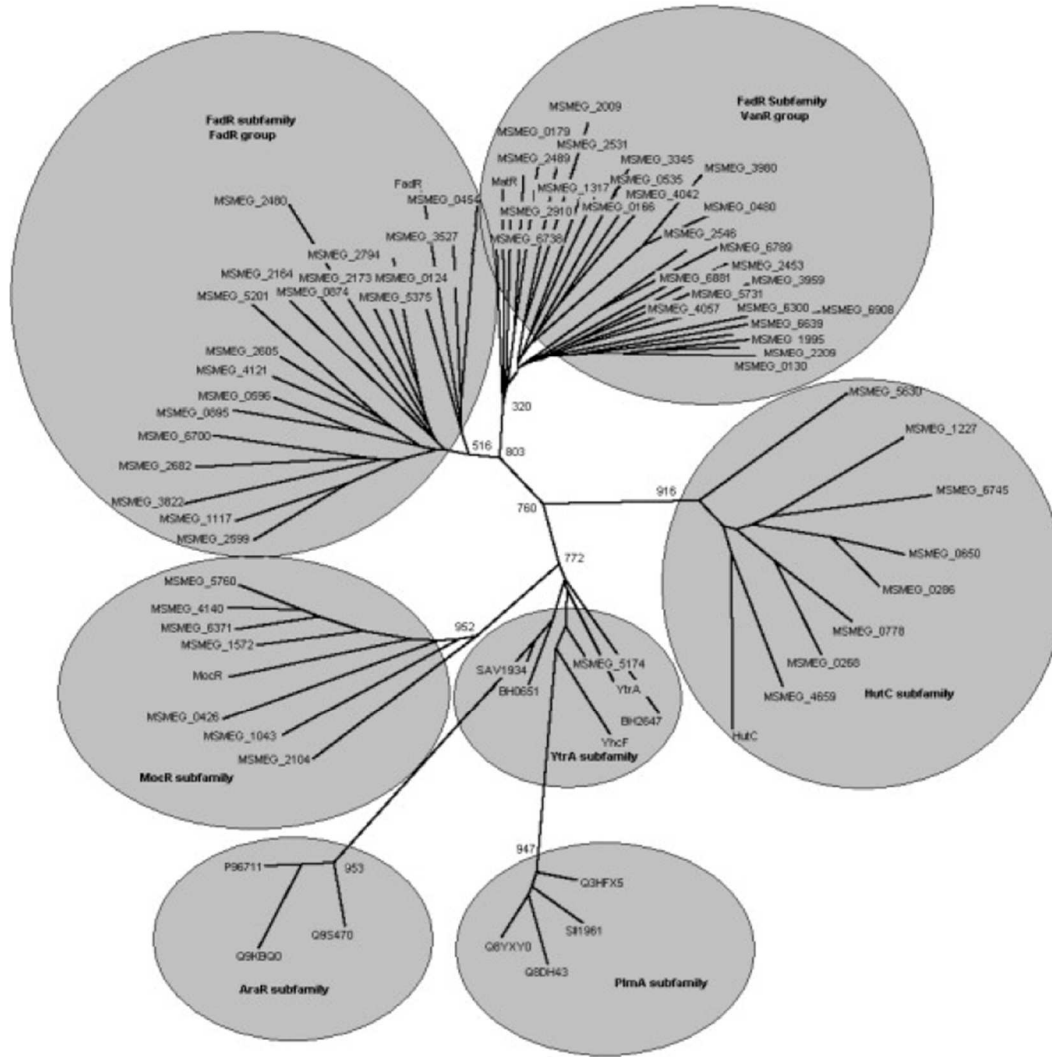


Figure 1. Unrooted tree of the proteins of GntR family regulators of *M. smegmatis* including representatives of all subfamily regulator from different Bacterial Genomes with 1000 bootstrap replicates. All the GntR regulators are clustered into six subfamilies. FadR subfamily is branched again into two groups (FadR and VanR) <sup>10</sup>.

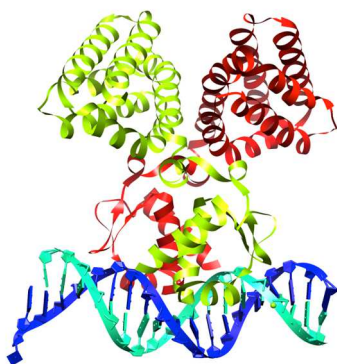


Figure 2. Quaternary structure of FadR and its corresponding DNA.

The second proposed subfamily is the HutC subfamily, named after the histidine utilization operon regulator, comprising about 31 % of the GntR regulators. The C-terminal regulatory domain of HutC response to various of the ligands, such as: histidine<sup>12</sup>; long chain fatty acids<sup>13</sup>; trehalose 6-phosphate or alkylphosphonate<sup>14</sup>, which makes it not so surprising to find out that this subfamily regulate processes as diverse as amino acid uptake and plasmid transfer. The structure of HutC subfamily contains both alpha-helical and beta-sheet on C-terminal domain and averages 170 amino acids in length; Three dimensional crystal structural and analysis of the HutC family member, PhnF from *E. coli* shows that the C-terminal domain had a chorismate lyase-like fold, comprising a six-stranded antiparallel beta-sheets, a two-stranded parallel beta-sheets and four short alpha-helices (Figure3; PDB ID: 2WV0). A large cavity on the surface of the PhnF C terminus indicates the putative effector molecule-binding pocket, which suggested to be conserved in with the other members in the HutC subfamily<sup>15</sup>.

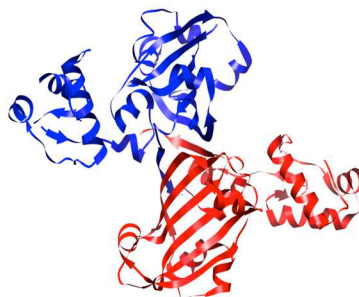
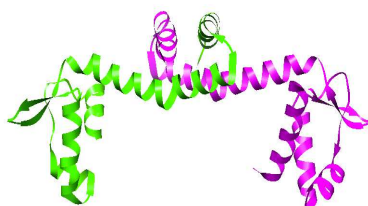


Figure 3. Quaternary structure of PhnF.

The YtrA sub-family represents only 6 % GntR-like regulators to date, among which forms part of operons involved in ATP-binding cassette (ABC) transport system. This sub-family contains the shortest C-terminal domain with about 50 amino acids on average (Figure 4), increasing certain extents of doubts regarding the efficiency for binding of the effector molecule(/s). People hypothesizes that the binding of the small molecules may impair the dimerization of this particular family of the transcription regulators, which could cause the loss of DNA binding, thus further repress the transcription. Combining with the sequence comparison and the secondary structural predication, it was suggested that dimerization is quite necessary for this subfamily and



could be formed by positively

Figure 4. Quaternary structure of CFL2947 from *Corynebacterium glutamicum*.

or negatively charged as well as hydrophobic and aromatic residues<sup>16</sup>. This hypothesis soon proved by the X-ray structure of CFL2947 from *Corynebacterium glutamicum* (Figure 4; PDB ID: 2EK5)<sup>17</sup>.

The DevA sub family of GntR transcription regulators has only be found in bacterium *Streptomyces*<sup>18</sup>. It showed that DevA is required for proper developments in *S. coelicolor*, although the exact roles of these proteins have not been highly elucidated. The C-terminal domain topology is clearly novel comparing to the others subfamilies. The N-terminal domain shares the most similarity with the HutC sub family<sup>18</sup>. Since there are no crystal structures available in this subfamily, the structure-function relationship remains unclear.

AraR is another minor subfamily, which required for the extracellular degradation of arabinose-containing polysaccharides, transport of arabinose, arabinose oligomers, xylose, and galactose, intracellular degradation of arabinose oligomers, and further catabolism of this sugar in *B. subtilis*<sup>19</sup>. The C-terminal domain shows extensive homology to the LacI/ GalR regulator family. The crystal structure of the AraR (Figure 5; PDB ID: 4EGY) demonstrated a high-level repression by co-ordinarily binding two-in-phase<sup>20</sup>, which might correlate with different physiological requirements. The high level of repression is achieved by DNA bending requiring two in-pharse, whereas binding to a single operator, which autoregulates AraR expression, is 10-fold less effective<sup>21</sup>.



Figure 5. Quaternary structure of DNA binding domain from AraR and its corresponding DNA fragment.

PlmA subfamily, the most newly discovered minor subfamily in 2003 that found in cyanobacterial *Anabaena sp.* Strain PCC7120. It has been demonstrated that plmA can affect on a cell's ability to maintain its relative plasmid content. However, regulation mechanism of PlmA remains unclear<sup>22</sup>. Structurally wise, PlmA also has a novel topology on the C-terminal domain, and appears to confine to the Cyanobacteria. The N-terminal DNA binding domain appear to be closely similar to the MocR and YtrA subfamilies suggesting that the E-b/O domain of PlmA may have been divergently replaced during the evolution, despite their similarity in the DNA binding domain.

The MocR subfamily's C-terminal domain is readily distinguishable from others because of its exceptional average length of about 350 amino acids. It is also capable of binding to a vitamin B6 derivative-PLP. The PLP-binding putative aminotransferase domains are closely related by amino acid sequence to the homodimeric type-I aminotransferases. Aminotransferases are of the central importance in amino acid metabolism and in links to carbohydrate and fat metabolism. Type-I aminotransferases almost exclusively exist as dimers in a head-to-tail fashion, and each subunit binds to one molecule of PLP through an internal aldimine linkage with the amino group of the

conserved lysine residue in the PLP binding site. This characteristic feature suggests that the recruitment of such a domain in transcription regulation is likely to facilitate protein-protein interaction/oligomerization.

### MocR/GabR

The representative member of the MocR/GabR subfamily, GabR, is essential for transcriptional activation of the pathway that controls the GABA degradation<sup>23</sup>. GABA is an important nitrogen and carbon source in many bacteria. The GABA-inducible *gabTD* pathway in *B. subtilis* allows utilization of extracellular GABA as the sole nitrogen source to generate glutamate and succinate. The *gabR* gene in *B. subtilis* is located upstream of the *gabTD* operon and is transcribed divergently. GabR functions as the PLP- and GABA-dependent transcriptional activator of the *gabTD* operon and as a negative autoregulator<sup>3</sup>(Figure 6). Mutations in the conserved residues

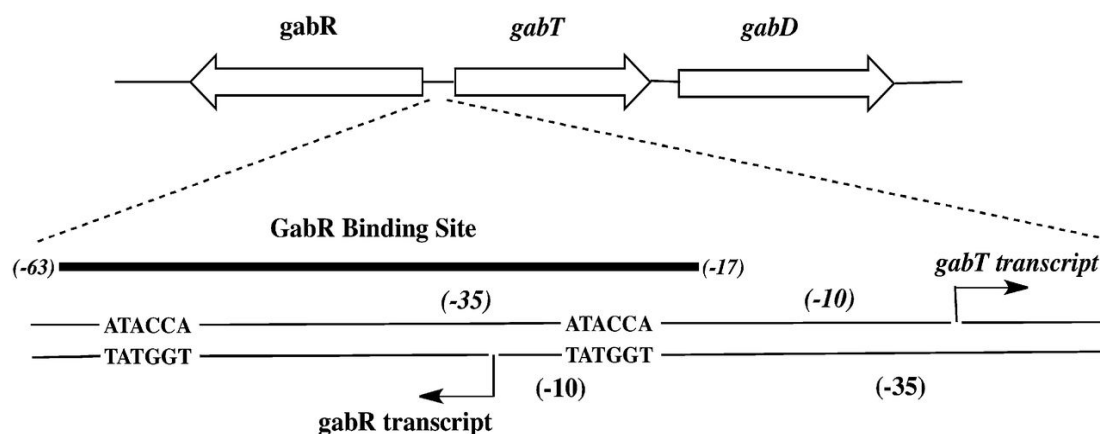


Figure 6. Schematic of GabR binding sites at the *gabR* and *gabTD* promoters. A schematic of the *gabR* and *gabTD* gene loci, as previously elucidated (2), is shown here. The 47-bp GabR binding site (–63 to –17) within the *gabR*–*gabT* regulatory region is shown in detail, and the two direct repeats (ATACCA) are indicated. The arrows indicate the transcription start sites and directions for the *gabR* and *gabT* genes



of the putative aminotransferase domain presumed to be crucial for the folding of the domain and PLP-binding abolished the ability of GabR to activate the *gabT* promoter in vivo but did not affect its activity as an autorepressor <sup>23</sup>. Therefore, while the ability to bind DNA may be sufficient for its autorepressor function, GabR is competent to activate transcription from the *gabT* promoter only in the presence of PLP and GABA.

The *gabT* and *gabD* genes encode the two key enzymes for glutamate biosynthesis: GABA aminotransferase (GabT) and succinic semialdehyde dehydrogenase (SSDH or GabD), respectively. GabT is a type-I aminotransferase that catalyzes the Ping-Pong transamination reaction using GABA as amino group donor,  $\alpha$ -ketoglutarate as amino group acceptor and PLP as co-enzyme to form the products, succinic semialdehyde and glutamate <sup>24</sup>. During the first half-reaction, GABA donates its amino group to PLP, thereby releasing succinic semialdehyde and converting PLP to its pyridoxamine 5'-phosphate (PMP) form (Figure 7). In the second half-reaction,  $\alpha$ -ketoglutarate accepts the amino group to become glutamate and regenerate the PLP form of the enzyme (Figure 7). In the downstream reaction, the NAD-dependent dehydrogenase, GabD converts succinic semialdehyde (SS) to succinate. Null mutants of *gabR*, *gabT* and *gabD* in *B. subtilis* were reported to be incapable of using GABA as the sole nitrogen source <sup>25</sup>, further demonstrating that the functions of GabR, GabT and GabD are all essential for GABA utilization.

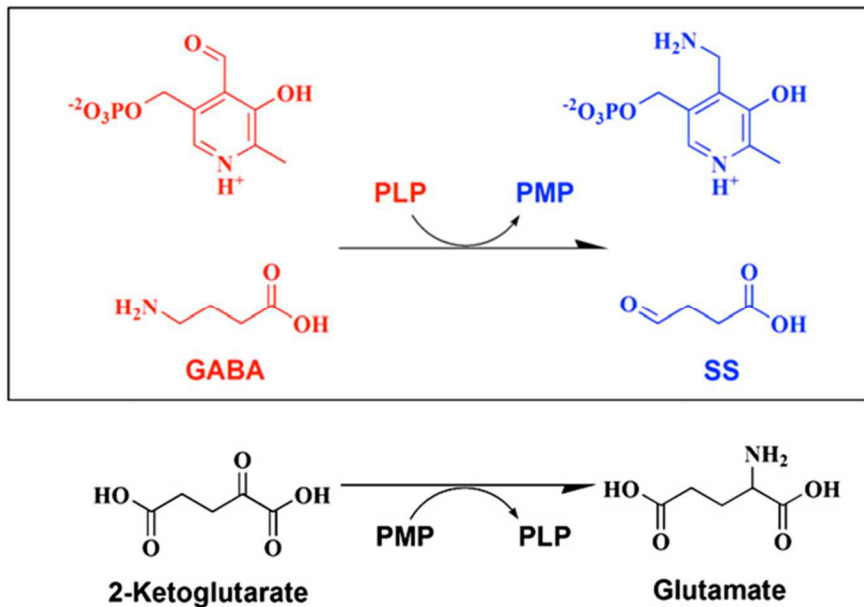


Figure 7. The GabT-catalyzed aminotransferase reaction. The first half reaction (GABA to succinic semialdehyde) of the GabT-catalyzed Ping-Pong transamination is shown in the boxed area. The second half-reaction is shown outside the boxed area.

## CHAPTER TWO

### CRYSTAL STRUCTURE OF BACILLUS SUBTILIS GABR, AN AUTOREPRESSOR AND TRANSCRIPTIONAL ACTIVATOR OF GABT

#### **Research Significance**

*B. subtilis* GabR is a transcription factor that regulates gamma-aminobutyric acid (GABA) metabolism. GabR is a member of the understudied MocR/GabR subfamily of the GntR family of transcription regulators. A typical MocR/GabR-type regulator is a chimeric protein containing a short N-terminal winged-helix-turn-helix DNA-binding domain and a long C-terminal pyridoxal 5'-phosphate (PLP)-binding putative aminotransferase domain. In the presence of PLP and GABA, GabR activates the *gabTD* operon, which allows the bacterium to use GABA as nitrogen and carbon sources. GabR binds to its own promoter and represses *gabR* transcription in the absence of GABA. Here, we report two crystal structures of full length GabR from *B. subtilis*: a 2.7-Å structure of GabR with PLP bound and the 2.55-Å apo structure of GabR without PLP. The quaternary structure of GabR is a head-to-tail domain-swap homodimer. As predicted base on sequence similarity, each monomer comprises two domains: an N-terminal winged-helix DNA-binding domain and a C-terminal PLP-binding type I aminotransferase-like domain. The winged-helix domain contains putative DNA-binding residues conserved in other GntR-type regulators. Together with sedimentation velocity and fluorescence polarization assays, the crystal structure of GabR provides insights into

DNA binding by GabR at the *gabR* and *gabT* promoters. The absence of GabR-mediated aminotransferase activity in the presence of GABA and PLP, and the presence of an active site configuration that is incompatible with stabilization of the GABA external aldimine suggest that a GabR aminotransferase-like activity involving GABA and PLP is not essential to its primary function as a transcription regulator.

## **Introduction**

The MocR/GabR subfamily of chimeric proteins is widespread in bacteria and regulates a variety of biological processes. All members of this subfamily are typically composed of a 60- to 120-residue N-terminal winged-helix DNA-binding domain resembling other bacterial transcriptional regulators from the GntR family, and a large C-terminal putative aminotransferase domain, averaging ~300 aa in size and capable of binding to the vitamin B6 coenzyme, pyridoxal 5'-phosphate (PLP) <sup>25</sup>. The PLP-binding putative aminotransferase domains are closely related by amino acid sequence to homodimeric type I aminotransferases <sup>26,27</sup>. GABA is an important nitrogen and carbon source in many bacteria. The GABA-inducible *gabTD* pathway in *Bacillus subtilis* allows utilization of extracellular GABA as nitrogen and carbon sources. The *gabR* gene is located upstream of the *gabTD* operon and is transcribed divergently. GabR functions as the PLP- and GABA-dependent transcriptional activator of the *gabTD* operon and as a GABA-independent negative autoregulator (figure 6). <sup>24, 25</sup>. Mutations in the conserved residues of the putative aminotransferase domain presumed to be crucial for the folding of the domain and PLP-binding abolished the ability of GabR to activate the *gabT*

promoter in vivo but did not affect its activity as an autorepressor <sup>25</sup>.

The *gabT* and *gabD* genes encode two enzymes for an alternative route of glutamate biosynthesis using GABA: GABA aminotransferase (GabT) and succinic semialdehyde dehydrogenase (GabD), respectively <sup>25</sup>. GabT is a type I aminotransferase <sup>28, 29</sup> that catalyzes the Ping-Pong transamination reaction using GABA as an amino group donor,  $\alpha$ -ketoglutarate as an amino group acceptor and PLP as coenzyme to form the products, succinic semialdehyde (SS) and glutamate. During the first half-reaction,

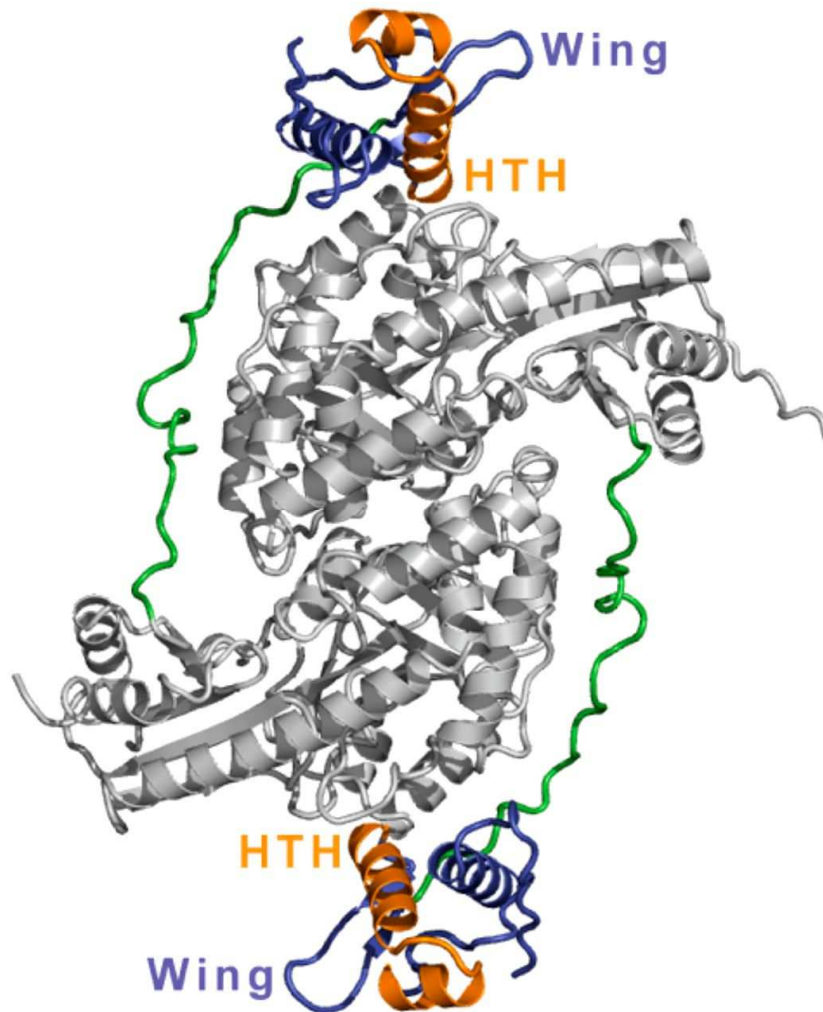
GABA donates its amino group to PLP, thereby releasing SS and converting PLP to pyridoxamine 5'-phosphate (PMP) (Figure 7). In the second half-reaction,  $\alpha$ -ketoglutarate accepts the amino group became glutamate and regenerates the PLP form of the enzyme (Figure 7). In the downstream reaction, the NAD-dependent dehydrogenase, GabD converts SS to succinate. Null mutants of *gabR*, *gabT*, and *gabD* in *B. subtilis* were reported to be incapable of using GABA as the sole nitrogen source <sup>25</sup>.

GabR binds specifically to an extended region of DNA that overlaps the -35 and -10 elements of the *gabT* and *gabR* promoters, respectively <sup>24</sup>(Figure 7). Using DNase I foot printing experiments and native gel-shift experiments with purified GabR, a 47-bp region of DNA (-63 to -17 relative to the *gabT* transcription start site) was identified as the GabR binding site. The 47-bp minimal fragment contains two copies of the direct repeat, ATACCA, which may be essential for GabR binding. Addition of PLP and GABA did not noticeably alter the DNase I footprints, indicating that GabR is capable of binding DNA in the absence of these molecules. Based on the extended 47-bp footprint, it

was proposed that GabR binds to DNA either as a dimer or tetramer<sup>24</sup>. It has been reported that a GabR-catalyzed “partial” aminotransferase- like reaction involving GABA and PLP may be essential for its transcriptional activator function<sup>24</sup>. Interestingly, no “full” two-step Ping-Pong–type GABA aminotransferase activity for GabR could be detected in vivo, and overexpression of GabR was unable to restore GABA aminotransferase activity in strains lacking *gabT*<sup>24</sup>. Here, we report two crystal structures of the PLP-bound and PLP-free forms of full-length *B. subtilis* GabR determined to be 2.7 and 2.55 Å, respectively. The crystal structure of GabR reveals a two-domain protein organized as a distinct head-to-tail domain-swap homodimer. A long linker of 29 aa separates the N-terminal winged-helix domain from the C-terminal domain, which has the same overall fold as type I aminotransferases and is hereby called AT-fold domain. Together with sedimentation velocity and fluorescence polarization data, the GabR structure provides a model for DNA binding at the *gabR-gabT* locus by one or more GabR homodimers. Key amino acid sequence changes in the putative substrate-binding pocket of GabR relative to those of well-characterized type I aminotransferases suggest that a GabR catalytic activity involving GABA and PLP is either absent or very poor under physiological conditions. Our results strongly suggest that the AT-fold domain in *B. subtilis* GabR, in a unique combination with the winged-helix domain, is primarily relegated to a regulatory function at the *gabR* and *gabT* promoters.

### GabR is a Head-to-Tail Domain-Swap Homodimer

Sequence alignments of members of the MocR/GabR subfamily show that these proteins comprise a small N-terminal winged-helix domain and a large C-terminal putative type I aminotransferase domain <sup>16, 25</sup>. The crystal structure of GabR described



here is

Figure 8. Quaternary structure of GabR. GabR is a head-to-tail domain-swap homodimer. The AT-fold domains are shown in light gray. The long linkers connecting the N-terminal winged-helix domains to the C-terminal AT-fold domains are shown in green. The

winged-helix domains are shown in blue-violet. The HTH motifs (orange) and the wing motifs are labeled. An orthogonal view of the structure is shown in Figure 10.

the winged-helix subtype <sup>30</sup> and a C-terminal AT-fold domain (residues 110–470) characteristic of the type I aminotransferase family <sup>31, 32</sup> and containing the signature long bent  $\alpha$ -helix (residues 345–386) connecting two subdomains. A long 29-residue linker (residues 81–109) connects the winged-helix domain to the AT-fold domain (Figure 8 and Figure 9).



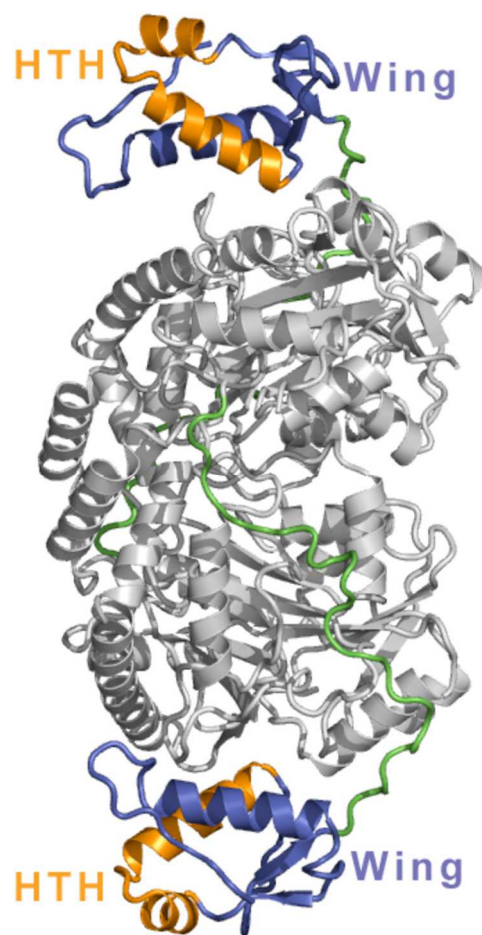


Figure 9. Quaternary structure of GabR. The structure is rotated 90° counterclockwise along the y axis relative to Figure 8.

GabR crystallizes as a homodimer with the two monomers organized in the head-to-tail domain-swapped interfaces. The larger interface is composed of two AT-fold domains, which are also arranged in a head-to-tail manner to form the characteristic homodimeric type I aminotransferase fold. The interface contains a buried area of 1,695 Å<sup>2</sup> with a binding energy of −11.4 kcal/mol, suggesting that this interface stabilizes the

GabR homodimer and is physiological. This interface of GabR, as seen in all type I aminotransferases <sup>31</sup>, contains two PLP-binding pockets bound by one molecule of PLP in each pocket.

The second interface is formed between the winged-helix domain of one monomer and the AT-fold domain of the other monomer. This interface has a buried area of 422 Å<sup>2</sup> with a relatively low free energy of −3.8 kcal/mol, suggesting that the overall quaternary structure of GabR may be dynamic in solution and that the winged-helix domain may undergo large-scale domain movements, especially when bound by DNA. The large dimer interface between the two AT-domains further suggests that any such domain movements by the winged-helix domain do not require restructuring of the AT–AT interface. Interestingly, we note that the extended N-terminal arms of the two monomers of aspartate aminotransferase (Asp-AT) also reach over and interact with the other subunit in that homodimer <sup>32</sup>. Because Asp-AT does not have an N-terminal winged-helix domain, the significance of this “crossing over” of the N-terminal arm to the other subunit in Asp-AT is not clear. Although there is reasonable electron density for the long extended linker that connects the winged-helix domain to the AT-fold domain, the linker does not form any significant contacts with the rest of the protein, suggesting that it may be flexible in solution and may thereby facilitate the proposed winged-helixed domain movements upon DNA binding.

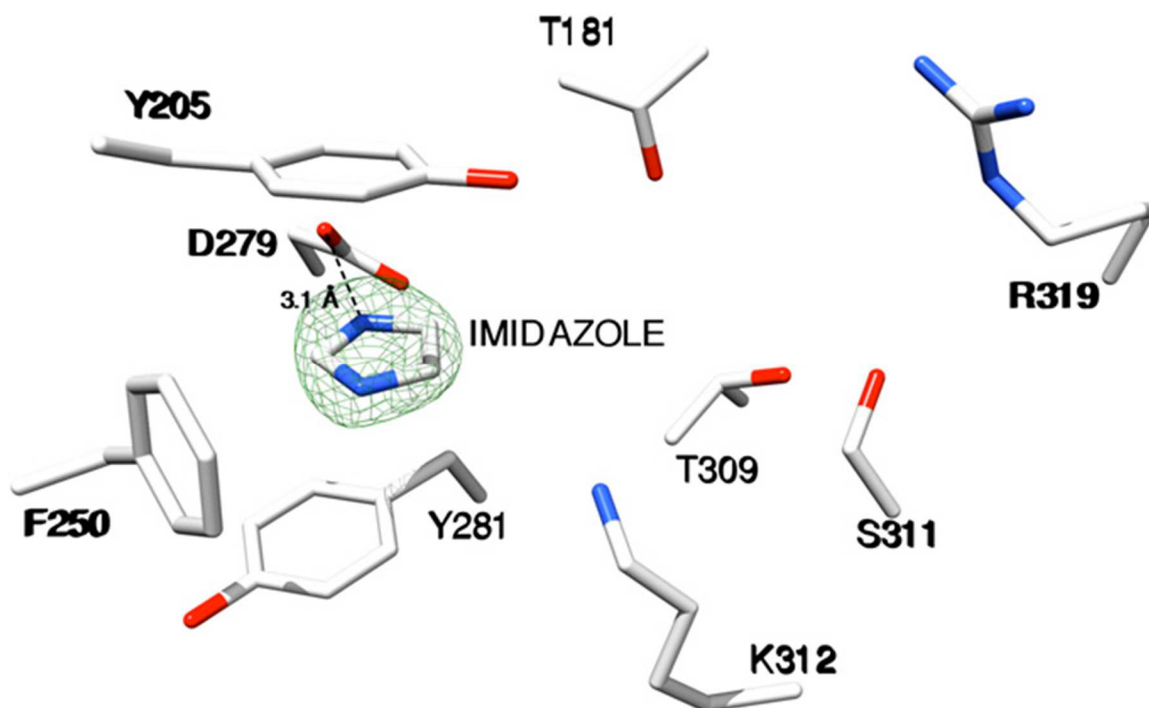


Figure 10. Imidazole is bound in the PLP-binding pocket of apo-GabR. The PLP-binding site of the crystal structure of apo-GabR is shown. The  $2F_o - F_c$  map (green mesh) around the imidazole molecule is shown at  $1\sigma$  level. The imidazole moiety and surrounding side chains are shown as sticks. Carbon atoms are shown in white, oxygen atoms in red, and nitrogen atoms in blue.

We also crystallized GabR without exogenous PLP. In the resulting apo-GabR structure, PLP is no longer bound in the PLP-binding pocket, and instead, a molecule of imidazole is bound in the same pocket (Figure 10). The purified protein is pale yellow in color, suggesting that endogenous PLP from *Escherichia coli* is still bound to GabR immediately after purification. Because imidazole is present in high concentrations in the purification and crystallization buffers, the replacement of PLP by imidazole is most likely a crystallization artifact. The overall similarity between the GabR–imidazole and

GabR–PLP structures suggests that the AT-fold domain maintains its overall structural integrity even when PLP is no longer bound.

### **GabR is a Dimer in Solution**

We performed sedimentation velocity analysis to investigate the oligomeric state of GabR–PLP in solution. In the absence of GABA, the sedimentation velocity plot shows a predominant peak at  $\approx 100$  kDa, suggesting a dimer of GabR in solution even at very low protein concentration (Figure 11; GabR molecular weight, 56 kDa). The plot also shows two minor peaks at about 50 and 10 kDa, which may represent a small proportion of monomer and degradation products, respectively. The sedimentation velocity plot of GabR–PLP in the presence of GABA similarly shows a predominant peak at  $\approx 100$  kDa and two low-molecular-weight peaks (Figure 11), again indicating a dimer of GabR in solution. Also, during protein purification, GabR elutes as one major peak on a Superdex 200 gel-filtration column with an apparent molecular weight of a dimer (Figure 12). Based on the crystal structure, our expectation is that the AT–AT dimer interface in the solution state of GabR may be similar to that found in the crystal structure. Our sedimentation velocity data do not reveal tetramers and higher oligomers in solution; however, further oligomerization of GabR may still occur when GabR binds to DNA.

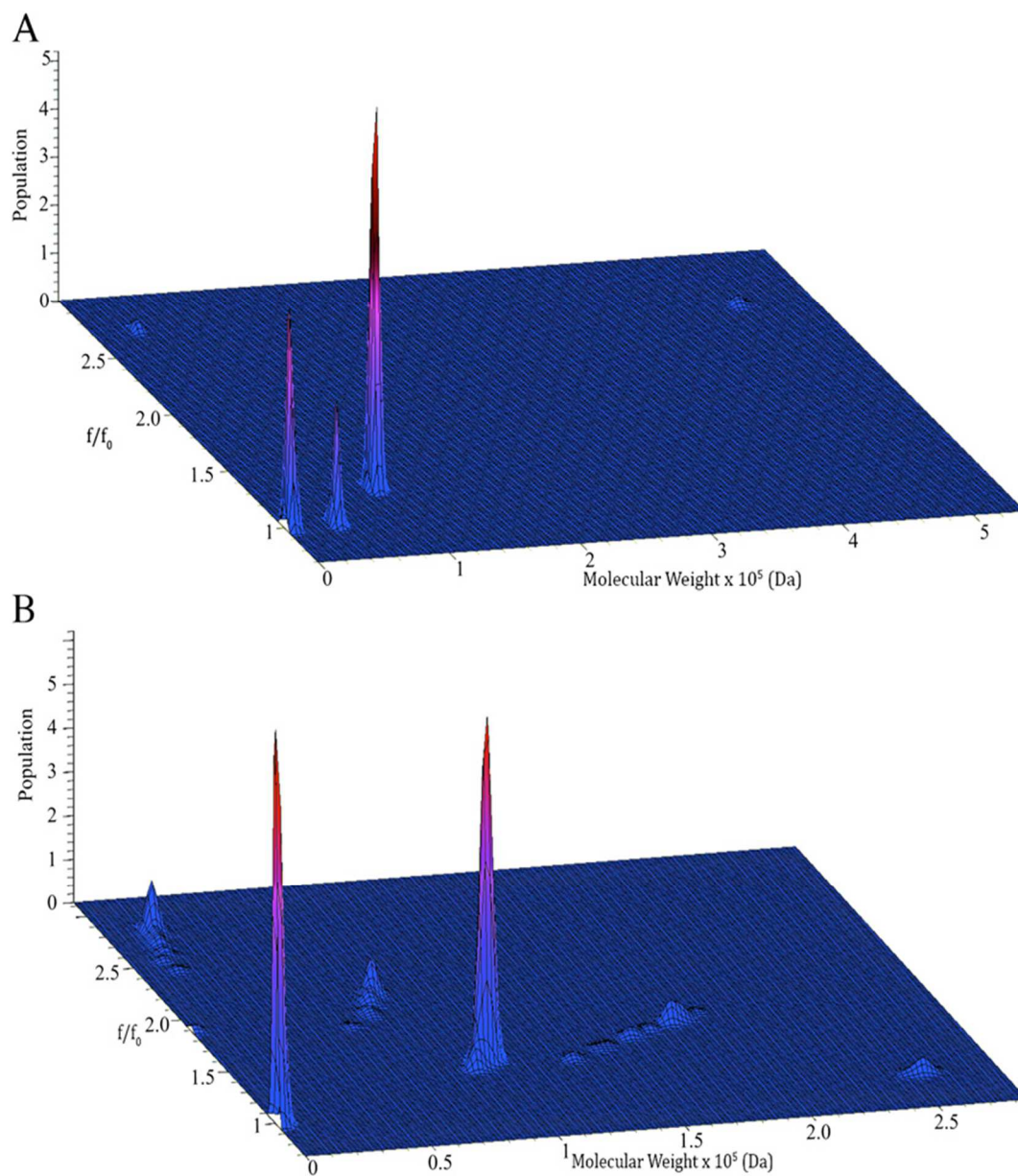


Figure 11. Sedimentation velocity analysis of GabR. (A) Molecular weight of the GabR–PLP sample determined from the global fitting of sedimentation velocity data. (B) Molecular weight of the GabR–PLP sample in the presence of 20 mM GABA

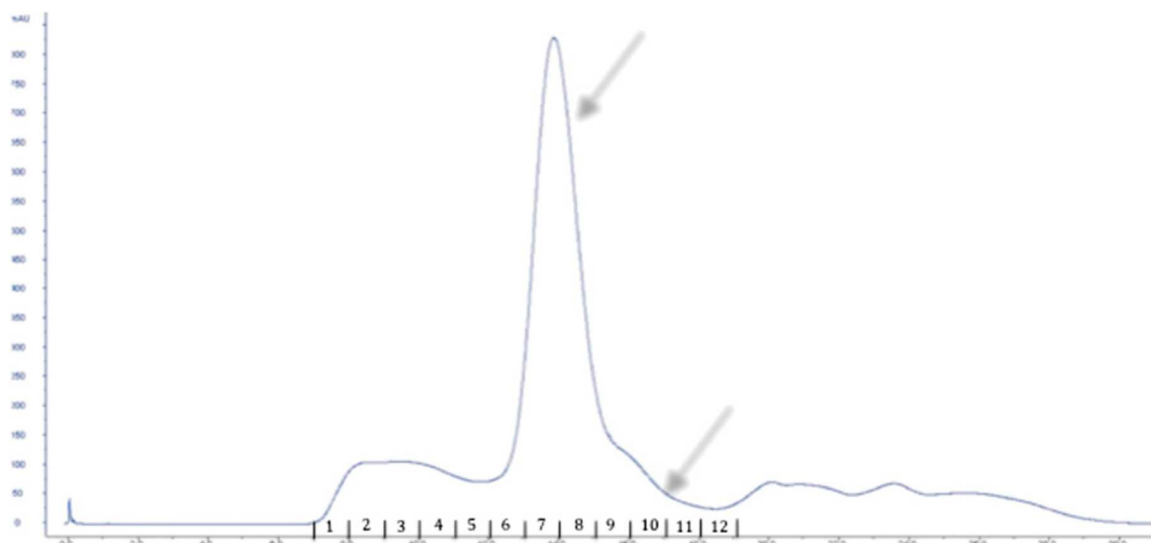


Figure 12. The gel-filtration profile of GabR. The major peak for GabR (fractions 7-9) on Superdex 200 16/60 corresponds to an apparent molecular weight of a dimer. The minor peak (fractions 9-10) corresponds to that for a monomer.

### Conserved Putative DNA-Binding Residues in the N-Terminal Winged Helix

#### Domain

The GabR N-terminal domain (residues 3–80) contains a canonical winged-helix domain ( $\alpha 1$ - $\beta 1$ - $\alpha 2$ -T- $\alpha 3$ - $\beta 2$ -W- $\beta 3$ ), where  $\alpha 2$ -T- $\alpha 3$  (residues 42–66) form the HTH motif and W (residues 71–76) is the wing (Figure 13). In the case of GabR, a second wing is absent. Although many winged-helix proteins contain a second wing, there are several examples of winged-helix proteins that bind DNA and in which the second wing is absent<sup>33</sup>. X-ray and NMR structures of winged-helix proteins in complex with DNA show that the winged-helix domain uses diverse modes of DNA binding, with examples of this domain binding DNA as a monomer, homodimer, or heterodimer<sup>33</sup>.

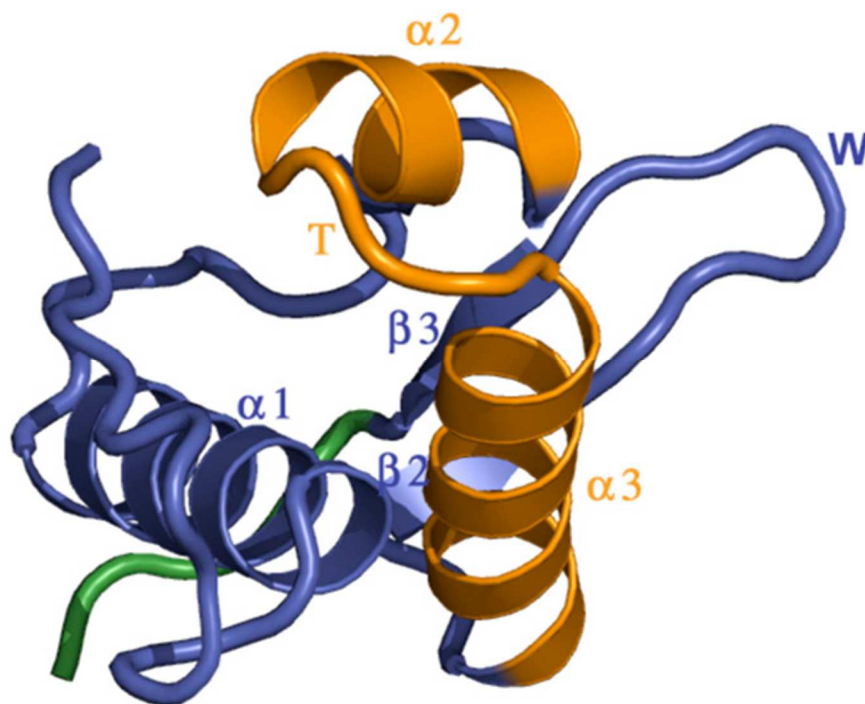


Figure 13. The GabR N-terminal winged-helix domain. The GabR N-terminal winged-helix domain (residues 3–80) is shown in detail. The various secondary structural elements ( $\alpha 1$ - $\beta 1$ - $\alpha 2$ -T- $\alpha 3$ - $\beta 2$ -W- $\beta 3$ ) are labeled. The helix-turn-helix (HTH) motif ( $\alpha 2$ -T- $\alpha 3$ ) is shown in orange. W is the wing ( $\beta 2$ -W- $\beta 3$ ).

In general, the most basic or positively charged surface of the winged-helix domain binds to the negatively charged phosphate backbone or nucleotide side-chain groups<sup>33</sup>. Because the putative DNA-binding domain is conserved among GntR-type transcriptional regulators, we searched the Conserved Domain Database<sup>34</sup> using the GabR winged-helix domain sequence as a query. We found several hits, including *E. coli* acyl-CoA-responsive transcription factor, FadR, and identified three putative DNA-binding residues in GabR (R43, S52, and K75) based on sequence conservation in FadR and other GntR family members. Because these three residues (R43 and S52 in the HTH;

K75 in the wing) also map to the most basic surface on the GabR winged-helix domain (Figure 14) and are fully exposed in the GabR homodimer (Figure 15), we predict that they may constitute a major DNA-binding surface.

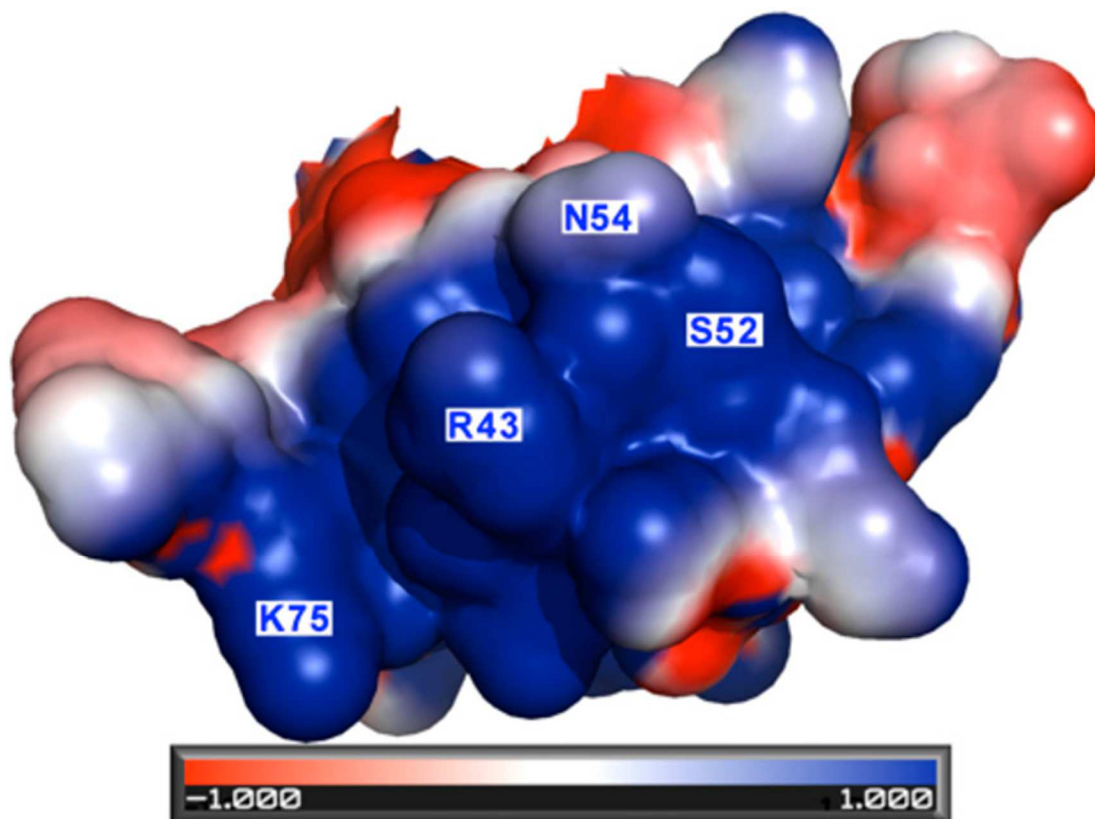


Figure 14. The most basic surface on the GabR winged-helix domain. The electrostatic potential surface of the GabR winged-helix domain is shown. The values  $-1.000$  and  $1.000$  on the scale bar represent acidic and basic electrostatic potential surface charges, respectively. The orientation corresponds to the wingedhelix domain shown on the bottom in Figure 8. The labeled residues denote amino acids that are conserved between GabR and FadR.



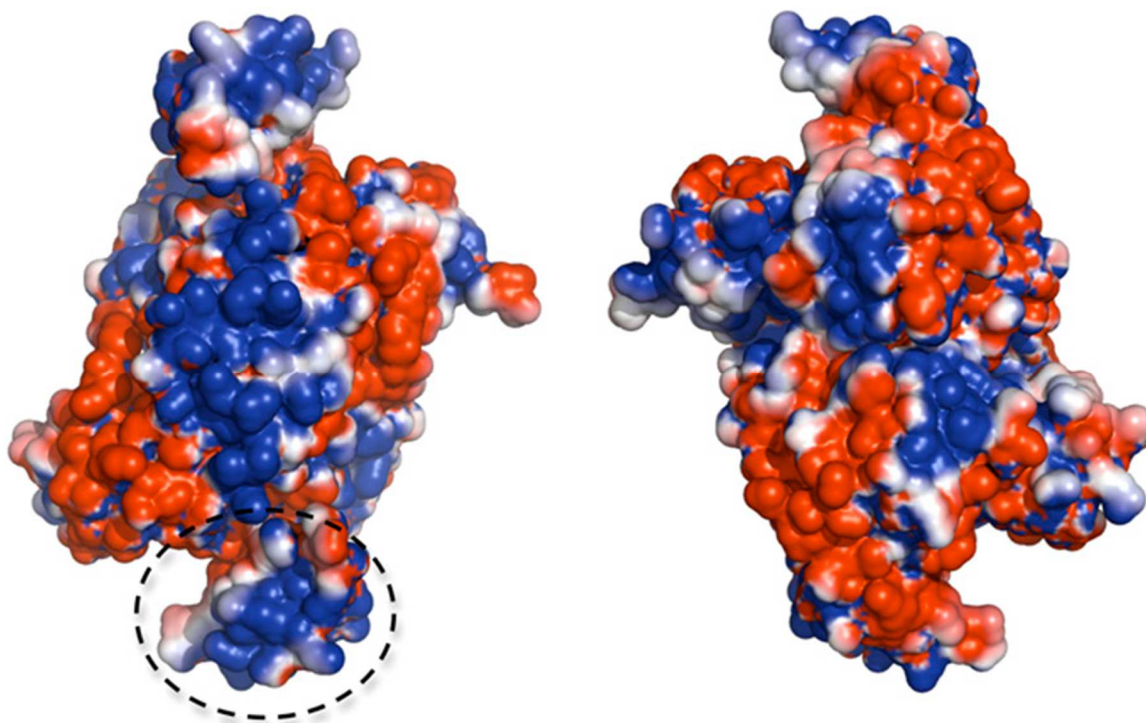
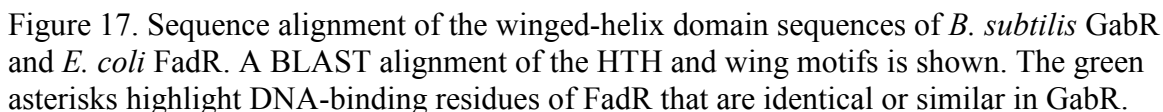
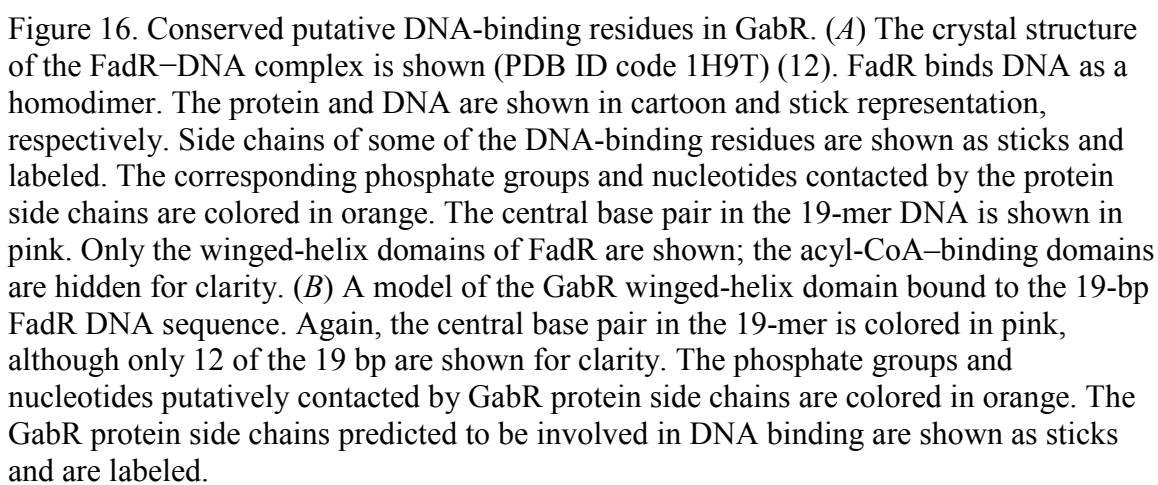


Figure 15. GabR electrostatic surface potential. The electrostatic surface potential representation for the GabR homodimer in two different views. The figure on the Left is in the same orientation as Figure 9. The dotted circle highlights the most basic surface on the winged-helix domain. The figure on the Right is rotated 90° counterclockwise relative to the figure on the Left.

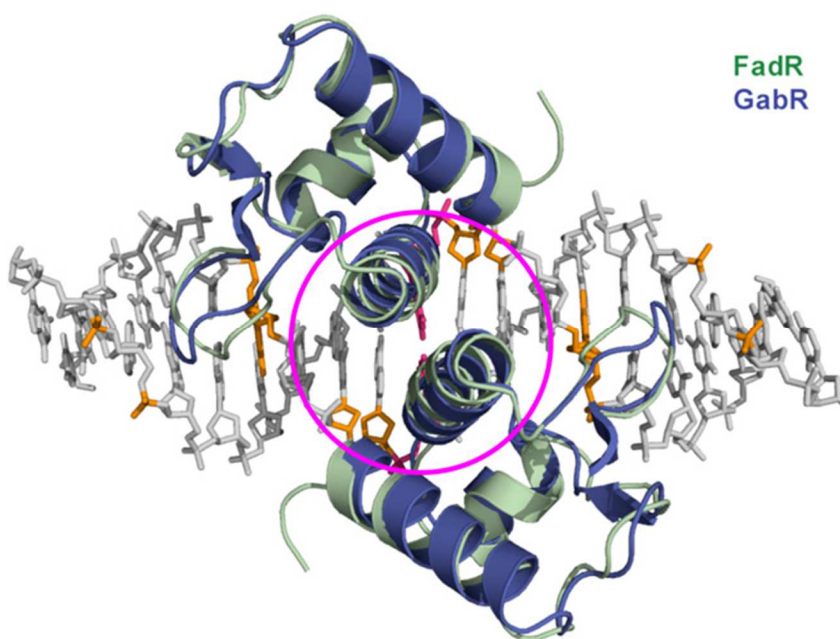
To examine the DNA-binding roles of these conserved residues, we generated a GabR–DNA model by superimposing the structural coordinates of the GabR winged-helix domain onto those of the FadR–DNA complex [Protein Data Bank (PDB) ID code 1H9T<sup>35</sup>]. In the FadR–DNA complex (Figure 16A), two winged-helix domains of a FadR homodimer bind to a 19-bp operator sequence containing two copies of an inverted repeat, TCTGGT, separated only by 3 bp<sup>35</sup>. In contrast, the 47-bp GabR binding site contains two copies of the direct repeat ATACCA separated by 34 bp of DNA. Because we do not know exactly how GabR binds DNA, we only used one copy of the GabR

winged-helix domain for the structural superposition (Figure 16B). The resulting GabR–DNA model (Figure 16B) is identical no matter which FadR monomer we use for the superposition and has several salient features. First, the HTH motif in FadR binds in the major groove of DNA, whereas the wing invades the minor groove (Figure 16A). Residue R35 in helix  $\alpha 2$  of the FadR HTH motif makes two H-bonds with the first guanine in the TCTGGT repeat (Figure 16A).

The conserved arginine residue R43 in GabR (Figure 16B) may form similar sequence-specific contacts with one of the guanines in its direct repeat (double-stranded sequence, ATACCA•TATGGT). In the turn of the HTH motif, FadR residue T44 (S52 in GabR) makes H bonds with the phosphate backbone and provides a hydrophobic contact to the central C–G base pair in the 19-mer, whereas residues in the  $\alpha 3$  recognition helix, which are typically known to bind the major groove of DNA <sup>30</sup>, either contact the central C–G base pair in the 19-mer (T46 in FadR; N54 in GabR) or a phosphate group (T47 in FadR; S55 in GabR) in the major groove. In the FadR wing, residue K67 points between two phosphate groups (Figure 16A). The GabR residue K75 (Figure 16B) could similarly point between two phosphate groups. Because many residues are conserved between FadR and GabR (Figure 17) and because the FadR and GabR DNA repeats have similar sequences, we predict that some of the protein–DNA interactions will be similar between the FadR–DNA and GabR–DNA complexes. However, because the GabR and FadR repeat sequences are dissimilar in type, direction, and spacing, a crystal structure of the GabR–DNA complex is required to elucidate all of the individual pairwise protein–DNA



Second, because the two winged-helix domains of FadR interact with each other on DNA (Figure 16A) <sup>35</sup>, we examined whether such an interface is possible in GabR. The GabR  $\alpha 3$  helix is surface exposed (Figure 8) and has a sequence that is capable of forming an  $\alpha 3$ – $\alpha 3$  interface similar to that of FadR (Figure 17 and Figure 18). Thus, two copies of the GabR winged-helix domain may be able to interact with each other on DNA under specific circumstances, for instance, when the direct repeats that are 34 bp apart are



brought into close proximity.

Figure 18. Two DNA-binding domains of GabR can interact on DNA through the “ $\alpha 3$ – $\alpha 3$  dimer interface.” A superposition of two molecules of GabR onto the FadR–DNA complex is shown. The  $\alpha 3$ – $\alpha 3$  interface is indicated by the magenta circle. The acyl-CoA-binding domains of FadR and putative aminotransferase domains of GabR are not shown for clarity. The protein and DNA are shown in cartoon and stick representation, respectively. Side chains of some of the DNA-binding residues are shown as sticks and labeled. The corresponding phosphate groups and nucleotides contacted by the protein side chains are colored in orange. The central DNA base pair is shown in pink. Only the

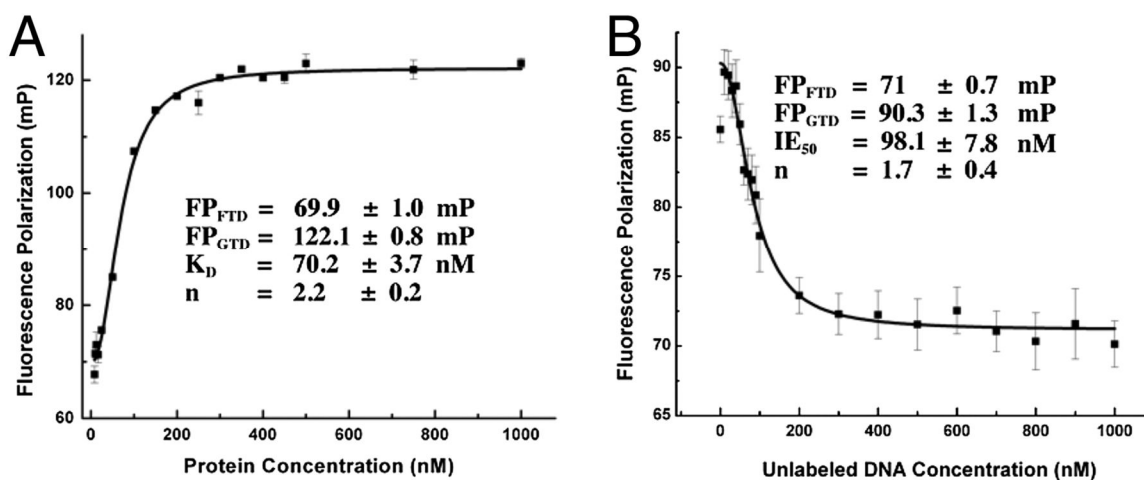
winged-helix domains of FadR are shown. The acyl-CoA-binding domains of FadR are hidden for clarity.

Third, mutating the CC doublets in either of the two GabR direct repeats to GG led to a 10-fold decrease in DNA-binding affinity. Furthermore, mutating both CC doublets to GG completely abolished GabR binding<sup>24</sup>. These observations are consistent with our GabR–DNA model, which suggests that residue R43 of GabR may form sequence-specific contacts with one of the guanines in its direct repeat. As is true for FadR (13)<sup>36</sup>, our GabR–DNA model predicts that mutating conserved residues like R43 and K75 may abrogate or interfere with GabR–DNA interactions

### **GabR Binds DNA with High Affinity**

The binding affinity of GabR for a 49-bp DNA containing the 47-bp GabR binding site was determined by fluorescence polarization and competitive binding assays. Previous studies estimated the apparent dissociationExperimental Procedures gabT fragment to be around 1 nM<sup>24</sup>. When a range of GabR protein concentrations were titrated against the 47-bp carboxytetramethylrhodamine (TAMRA)-labeled DNA, we observed a dose-dependent increase in polarization (Figure 19A), indicative of the binding of GabR protein to DNA. The curve was fitted to the modified Hill equation (in Experiments Procedures) and the dissociation constant of the GabR–DNA complex was determined to be  $70.2 \pm 3.7$  nM. A Hill coefficient of  $2.2 \pm 0.2$  was obtained, indicating positive cooperativity in the binding process. To establish specificity of binding and rule out nonspecific effects from the TAMRA label, a competitive binding assay was performed with unlabeled oligonucleotides containing the same sequence as the

TAMRA-labeled DNA (Figure 19B). A preformed mixture of equimolar concentrations of TAMRA-labeled DNA and GabR was titrated with increasing concentrations of unlabeled DNA. The fluorescence polarization decreased with increasing amounts of unlabeled DNA (Figure 19B). The curve was fitted to the Hill equation (Eq. 2 in Experiments Procedures) and the IE50 of unlabeled DNA for GabR was calculated to be  $98.1 \text{ nM} \pm 7.8 \text{ nM}$ , which is similar to the dissociation constant of the TAMRA-labeled



DNA–GabR complex (Figure 19B). A Hill coefficient of  $1.7 \pm 0.4$  was obtained,

Figure 19. Fluorescence polarization assays to measure DNA binding by GabR. Each data point was measured in triplicate. The average values and errors were plotted and fitted to the Hill equation. The abbreviations used in the figure are as follows:  $FP_{FTD}$ , fluorescence polarization signal of free labeled DNA;  $FP_{GTD}$ , fluorescence polarization signal of the GabR–DNA complex;  $K_D$ , the dissociation constant;  $n$ , the Hill coefficient; and  $IE_{50}$ , the concentration of unlabeled DNA required to bind 50% of protein. (A) Titration of GabR against 50 nM TAMRA-DNA. The GabR concentrations were varied from 0 to 1,000 nM. Error bars are too small to be displayed if the errors are less than 1/1,000th of the measured value. (B) Competitive binding assay. Titration of unlabeled DNA (0–1,000 nM) against a fixed concentration of preformed GabR-labeled DNA complex (100 nM each of GabR and TAMRA-DNA).

supporting the same type of positive cooperativity as shown in (Figure 19A). Although the precise binding stoichiometry of GabR for DNA is still unknown, the dissociation constants that we determined suggest a high-affinity GabR–DNA complex. The Hill coefficients in both titrations indicate positive cooperativity in the binding of GabR dimers to DNA.

### **PLP is bound in the C-terminal AT-Fold Domain**

Like in other type I aminotransferases <sup>31, 32</sup>, the AT-fold domain of GabR has two subdomains, the large subdomain containing the invariant lysine (K312) that forms the Schiff base with PLP and the small subdomain that typically interacts with the  $\alpha$ -carboxylate group of the substrate. One molecule of PLP is bound per GabR monomer as an internal aldimine at K312. We next compared the PLP-binding pocket of *B. subtilis* GabR (Figure 20) with those of *E. coli* Asp-AT (PDB ID: 2AAT), the best-characterized member of the type I aminotransferase family; and pig liver GABA-AT bound to the substrate analog,  $\gamma$ -ethynyl GABA (GEG) (PDB ID: 1OHY) <sup>32, 37</sup>. The active site residues that facilitate PLP binding are conserved in all three cases. For example, the phosphate group of PLP is situated very close to the N terminus of a nearby helix in all cases and is stabilized by hydrogen bonds from polar residues (T181, T309, and S311 in the case of GabR) to the phosphate oxygens. The salt bridge between an arginine residue (residue R319) and the phosphate group is also conserved in GabR, although the phosphate group has a different orientation compared with those in Asp-AT and GABA-AT. The primary function of PLP is to stabilize the negative charge generated at the C $\alpha$  atom of the

transition state or external aldimine (Schiff base between an amino acid substrate and PLP) by delocalizing the negative charge through the  $\pi$ -electron system of the cofactor. A conserved aspartate residue [D279 in GabR, D222 in *E. coli* Asp-AT, D223 in chicken mitochondrial Asp-AT<sup>27</sup>, and D298 in GABA-AT; Figs. 5A and 6A] promotes this electron sink nature of PLP by maintaining PLP in the protonated state through interaction with the pyridinium nitrogen.

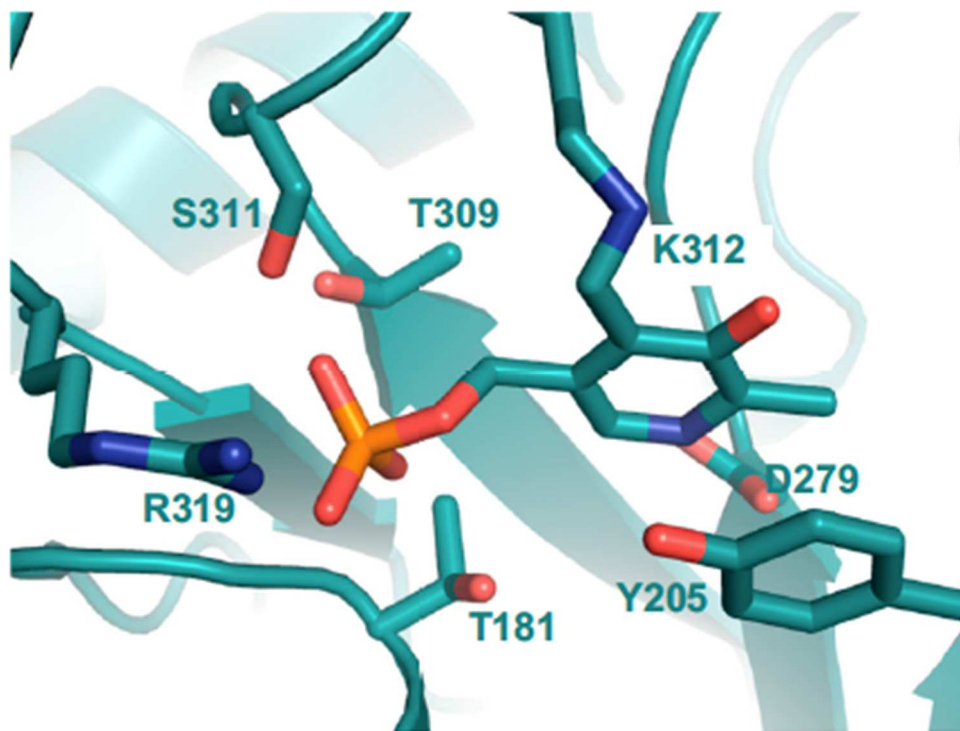
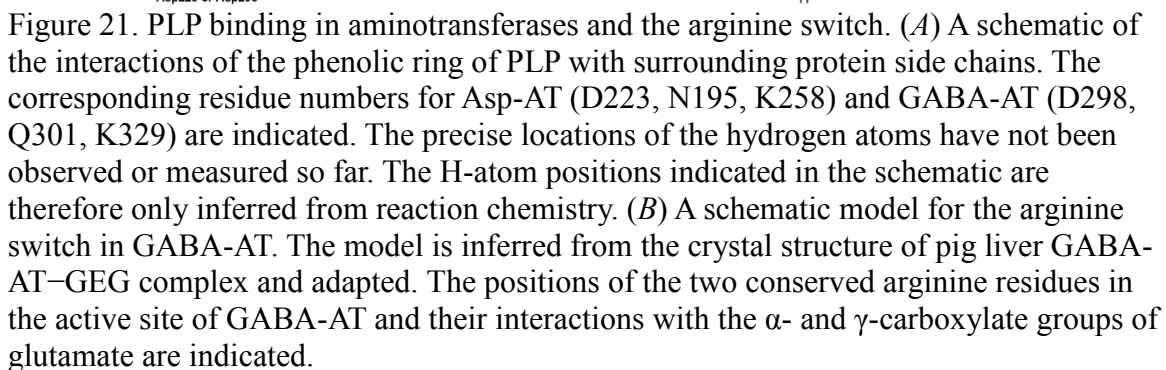


Figure 20. The PLP-binding pocket of *B. subtilis* GabR. The GabR residues that interact with PLP are labeled.

### Is GabR an enzyme?

We were currently unable to obtain crystals of a GabR–PLP–GABA complex, and therefore, we examined the putative GABA-binding site in GabR–PLP to understand whether GabR might catalyze an aminotransferase reaction involving GABA.





elements vary significantly and contain insertions of  $\alpha$ -helices and  $\beta$ -strands in different

parts of the structures, making it difficult to obtain secondary structure-based superposition. Therefore, we manually superimposed the pyridine ring of PLP to compare the putative substrate-binding pockets in all cases.

If GabR were a bona fide aminotransferase, then the active site must be able to interact with a keto acid such as  $\alpha$ -ketoglutarate. In the active sites of Asp-AT and GABA-AT, two conserved arginines stabilize such a keto acid to subsequently form the related amino acid (Figure 21A)<sup>31</sup>. However, we found two key differences in the “active site” of GabR, compared with these aminotransferases, which may compromise its ability to transaminate GABA. First, the GabR active site may contain only one structurally conserved arginine (R207) that is, however, not conserved by sequence. In Asp-AT and GABA-AT, the equivalent arginine residue (R292\* in the other subunit of the dimer in Asp-AT and R192 in GABAAT (Figure 21B), is known to form a bidentate hydrogen bond/ion pair with the  $\gamma$ -carboxylate of a dicarboxylate substrate such as glutamate, whereas the second arginine (R386 in Asp-AT and R445 in GABA-AT; Figure 21B) makes a similar direct contact with the  $\alpha$ -carboxylate of the glutamate. Furthermore, GABA-AT employs an arginine switch to distinguish between GABA and glutamate<sup>31, 37</sup>. When GABA binds, R192 stays in place to contact the carboxylate of GABA (Figure 22), which is located in the same position as the  $\gamma$ -carboxylate of glutamate, while R445 moves away to accommodate GABA and engages instead in a salt bridge with a nearby glutamate residue (E270; Figure 22A). Because only the first arginine residue in GabR may be structurally conserved (R207; Figure 22B) while the second arginine is not, this

suggests that GabR may bind GABA but not glutamate or other dicarboxylate substrates. In the absence of conserved arginines, aromatic amino acid aminotransferases and branched-chain aminotransferases use large-scale rearrangements of the active site hydrogen-bond network or hydrophobic cavities lined with polar residues to accommodate two different amino acids in the same site (refs. 9 and 15, and references therein). However, because these features are not preserved in GabR, these alternative substrate-binding mechanisms are unlikely for GabR. The second key difference in the active site of GabR is related to its ability to stabilize the GABA external aldimine. When the amino acid substrate forms an external aldimine, the imine N atom of the amino acid and phenolic O atom of PLP could share an H-atom. Therefore, the phenolic O must be optimally oriented to accept the hydrogen from the imine N during reprotonation and hydrolysis to form PMP and release the deaminated substrate (Figure 21A). In Asp-AT,

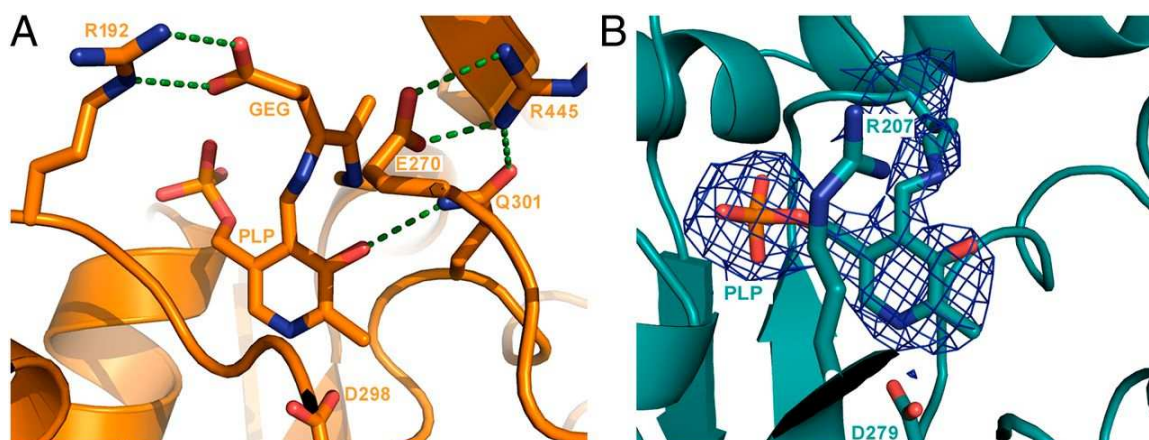


Figure 22. PLP is bound in the AT-fold domain of GabR. (A) The substrate-binding pocket in the GABA-AT-GEG structure. The secondary structure elements are shown in cartoon form. Side chains of the key residues that interact with PLP and substrate analog, GEG, are shown in stick representation and labeled. Hydrogen bonds are shown as dotted green lines. (B) The putative substrate-binding pocket in the crystal structure of GabR. The figure is drawn as described in A. The  $2F_o - F_c$  map (blue mesh) around PLP is

shown at 1.2 $\sigma$  level.

an asparagine (N195; Figure 21A) interacts with the phenolic O to hold it in place, and in GABA-AT, a glutamine residue (Q301; Figure 21A) and a water molecule perform the same function. In GabR, there is no such interaction with the phenolic O, implying that the GABA external aldimine might not be optimally oriented for catalysis.

A sequence alignment of 10 MocR/GabR protein sequences from different strains of *B. subtilis*, *E. coli*, *Pseudomonas aeruginosa*, *Salmonella enterica*, and *Streptococcus pneumoniae* revealed an overall lack of evolutionary conservation for the arginine switch. Although the residues involved in PLP-binding (equivalent of *B. subtilis* GabR residues, D279, R319, and K312) are conserved in the examined homologs, we found the residue corresponding to *B. subtilis* GabR (R207) to be highly variable. In contrast to GabR, all of the PLP-interacting residues and the two substrate-interacting arginines are identical between *B. subtilis* GabT, a known GABA aminotransferase, and pig liver GABA-AT (Figure 23). Such a contrast indicates the functional divergence of GabR from its evolutionary relatives. Together, these critical differences in the active site architecture of GabR strongly suggest that GabR may bind GABA in a different manner than a true transaminase and may only catalyze the “full” transamination reaction with poor efficiency, if at all. Without the ability to accommodate glutamate effectively, GabR may not be able to complete the second half-reaction and enzymatically regenerate the PLP form of GabR. Consistent with our crystal structure and with previous reports

that GabR does not rescue GabT activity<sup>24</sup>, we were unable to measure a GABA-AT activity for GabR in coupled steady-state enzyme assays (described in Experiments Procedures). Also, UV-visible scanning spectrophotometry experiments of GabR in the presence of PLP and GABA did not reveal any of the spectral shifts typically produced by

```

35  KGEAELYDLDGRRFIDFAGAIGTLNVGHSHPKVVEAVKRQ---AEELIHPGFNVMMYPT  91
    +  G  L  D+DG R +D      I ++ +G+SHP +V+ V++      +  +  P  ++
51  ESRGNYLVDVDGNRMLDLYSQISSIPIGYSHPALVKLVQQPQNVSTFINRPALGILPPEN  110

92  YIE-LAEKLCGIAPGSHEKKAIFLNSGAEAVENAVKIARKY--TKRQG-----  136
    ++E L E L  +AP      +  I +  G+ + ENA K      +  +K +G
111 FVEKLRESLLSVAPKGMSQ-LITMACGSCSNENAFKTIFMWYRSKERGQSAFSKEELET  169

137 -----VVSFTRGFHGRITNMTSMSTSKVKPYKFGFGPFAPEVYQAPFPY--YYQ  182
    ++SF      FHGRIT  ++ T      +K      F  +  APFP  Y
170 MINQAPGCPDYSILSFMGAFHGRITMGCLATTHSKAIHKIDIPSFDWPI--APFRLKYPL  227

183 KPAGMSDESYDDMVIQAFNDDFFIA-SVAPETVACVVMPEVQEGGFIIPSKRFVQHVASF  241
    +      ++  +  ++  D  +      +TVA +++EP+Q EGG      S  F  +  +
228 EEFVKENQQEEARCLEEVEDLIVKYRKKKKTVAGIIVEPIQSEGDNHASDDFFRKL RDI  287

242 CKEHGIVFVADEIQTFGARTGTYFAIEHF--DVVPDLITVSKSLAAGLPLSGVIGRAEML  299
    ++HG  F+  DE+QTG      TG ++A EH+  D      D++T SK  +      ++G      E
288 SRKHGCAFLVDEVQTGGGSTGKFWAHEHWGLDDPADVMTFSKKM-----MTGGFFHKEEF  342

300 DAAAPGELGGTYAGSPLGCAALAVLDIIEEGLNERSEEIGKIIEDKAYEWKQEF-FI  358
    AP  +  T+  G  P      V++II+  E  L  +  GK++      +  +  +P  FI
343 RPNAPYRIFNTWLGDPSKNLLLAEVINI I KREDLLSNAAHAGKVLLTGLLDLQARYPQFI  402

359 GDIRRLGAMAAIEIVKDPDTREPDKTKAAAI AAYANQNGLLLLTAGINGNIIRFLTPLVI  418
    +R  G  +  +      PD++      +  +  A  G++L  G      IRF  LV
403 SRVRGRGTFCSFDT-----PDESIRNKLISIARNKGVML--GGCGDKSIRFRPTLVF  452

419 SDSLLNEGLSIL  430
    D  +  L+I
453 RDHHAHLFLNIF  464

```

Figure 23. BLAST protein sequence alignment. Sequence alignment between *B. subtilis* GabT GABA aminotransferase (upper sequence; 1–436) and pig liver GABA-AT (lower sequence; 1–472) are shown. The two proteins share 25% sequence identity and 43% similarity between their AT domains. The conserved residues interacting with the substrate carboxylate groups (R192 and R445), the pyridinium N and phenolic O of PLP

(D298 and Q301, respectively), and the invariant Schiff base lysine (K329) are highlighted. The residue numbers in parentheses denote residues from pig liver GABA-AT.

the PLP or PMP intermediates in a PLP-dependent transamination reaction. Together, these experiments suggest that GabR may have very poor or no GABA aminotransferase activity under physiological conditions. Although the trifunctional NAD-dependent *S. enterica* repressor, NadR is an example of a cofactor-dependent protein containing an N-terminal DNA-binding domain and two catalytically active domains [a middle adenylyltransferase domain and a C-terminal nicotinamide ribose kinase <sup>4</sup>], there is also precedence for adaptation of enzymes to regulatory roles in other proteins. For instance, PyrR, a UMP-dependent transcription attenuator for pyrimidine biosynthesis in *B. subtilis* contains a type I phosphoribosyltransferase (PRT) domain without measurable catalytic activity <sup>38</sup>. The *B. subtilis* purine repressor PurR has a two-domain architecture like GabR: an N-terminal wingedhelix domain and a C-terminal PRT domain devoid of catalytic activity <sup>39</sup>. It is of course possible that GabR recognizes other substrates or possesses a different PLP-dependent enzymatic activity that may or may not be related to its function as a PLP and GABA-dependent transcriptional activator of *gabT*. However, so far, no other enzymatic activity for GabR has been reported.

### **Model for GabR-Mediated Transcriptional Regulation at the *gabR* and *gabT***

#### **Promoters**

Based on the crystal structure of GabR, the sedimentation velocity data and the model for the GabR–DNA complex, we propose three possible modes for GabR binding

and regulation at the *gabR* and *gabT* promoters (Figure 24). Because we do not know the precise GabR:DNA binding ratio, we consider different models with one or more GabR dimers bound to DNA. In model 1, two copies of GabR dimers bind to the 47-bp DNA with only one winged-helix domain from each dimer binding to each direct repeat. That the Hill coefficient for the GabR–DNA complex is close to 2 (Figure 19) further suggests that GabR may cooperatively bind DNA as a dimer of dimers in the same way that a dimer of  $\lambda$ cII dimers binds its DNA operator <sup>40</sup>. In the  $\lambda$ cII–DNA crystal structure, as in model 1, only one monomer from each  $\lambda$ cII dimer binds its DNA sequence comprising two direct repeats. Even though the spacings between the direct repeats in the binding sites of  $\lambda$ cII and GabR are different (6 and 34 bp, respectively), the cooperative binding of GabR to DNA as a dimer of dimers is still possible. In model 2, only one copy of the GabR dimer binds to the 47-bp DNA and both winged-helix domains of the dimer are involved in DNA binding. In this model, the two winged-helix domains of one GabR dimer may be rearranged and some bending of DNA may occur. The small buried surface area (422 Å<sup>2</sup>) between the winged-helix domain and AT-fold domains suggests that the position of the wingedhelix domain may be dynamic in

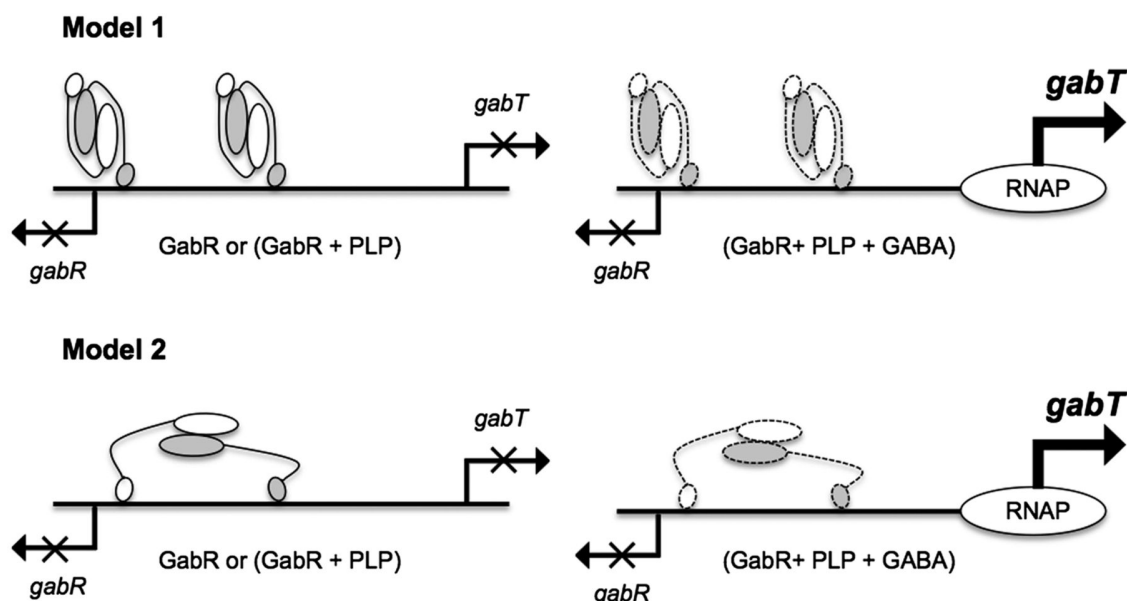


Figure 24. A model for transcriptional regulation at the *gabR* and *gabT* promoters. Different models for GabR binding in the *gabR*–*gabT* regulatory region are depicted. The GabR homodimer is represented as a cartoon with one monomer shown in white and the other colored gray. The larger oval represents the AT-fold domain and the smaller oval represents the winged-helix domain. Putative conformational changes in the presence of GABA are indicated by symbols with dashed lines.

solution and that the proposed domain movements are possible using large-scale movements facilitated by the long linker. We recognize that other viable models still exist. For example, the second winged-helix domain of a GabR dimer may bind to unidentified *cis* binding sites located at larger distances from the *gabR*–*gabT* locus to form large DNA loops. Intriguingly, a large basic surface at the AT–AT interface begs the question whether this surface is somehow also involved in DNA binding (Fig. S8). These models suggest that GABA may bring about conformational changes in GabR or the GabR–DNA complex, and that these changes may be necessary to activate *gabT* transcription, for instance, by recruiting RNA polymerase to the *gabT* promoter (Figure



24). Crystal structures of GabR–DNA complexes with and without GABA may help unravel some of these unknowns.

### **Biological Implications**

Our studies suggest that GabR may not possess “full” GABA aminotransferase activity, although it requires PLP and GABA to activate transcription at the *gabT* promoter. It is likely that the primary function of GabR in *B. subtilis* is to regulate transcription at the *gabR* and *gabT* promoters and that the AT-fold domain of GabR has adapted to primarily serve as an effector binding domain. How the AT-fold domain of GabR assists the wingedhelix domain in transcriptional regulation and how GABA mechanistically affects *gabT* activation by GabR still remain to be determined.

In summary, these studies were published in the in the Proceedings of the National Academy of Sciences of the United States of America (PNAS): Raji Edayathumangalam, Rui Wu, Yuguang Wang, Roman Garcia, Wei Wang, Cheryl Kreinbring, Jingling Liao, Todd Stone, Quyen Q. Hoang, Boris Belitsky, Gregory A. Petsko, Dagmar Ringe, and Dali Liu. (2013) 110 (44), 17820-17825.(Equal contribution first author)

### **Materials and Methods**

*Protein Expression and Purification.* The full-length coding region of the *Bacillus subtilis* *gabR* gene (residues 1–479) was subcloned from a pBAD construct into pETite C-His vector (Lucigen), which encodes an inducible T7 expression system. The C-terminally His6-tagged protein was expressed in *Escherichia coli* strain BL21 (DE3).

Transformed cells were grown in LB media containing kanamycin at 37 °C to OD600 of  $\approx 0.6$  and induced with 0.5 mM isopropyl- $\beta$ -D-thiogalactopyranoside (IPTG) at 37 °C for 4 h. Cells were harvested, resuspended in buffer containing twofold PBS buffer and 10 mM imidazole (pH 7.5), and sonicated. Insoluble material was removed by centrifugation. The GabR-His6 protein (molecular weight, 56 kDa) was purified to homogeneity by affinity chromatography Ni-NTA (GE Healthcare) and gel filtration (HiLoad 16/60 Superdex 200 pg; GE Healthcare) in buffer containing twofold PBS (274 mM NaCl, 5.4 mM KCl, 16 mM Na<sub>2</sub>HPO<sub>4</sub>, 2.92 mM KH<sub>2</sub>PO<sub>4</sub>, pH 7.4), 475 mM imidazole (pH 7.5), 1 mM pyridoxal 5'-phosphate (PLP), and 5% (vol/vol) glycerol. The protein requires high salt and imidazole concentrations to stay soluble without precipitation. Alternatively, the presence of 5% (vol/vol) glycerol and 0.5% Nonidet P-40 in the buffer helps to keep GabR soluble without the need for NaCl and imidazole. Purified GabR-His6 protein was concentrated (Centricon Plus centrifugal filter units; Millipore) and stored at 4 °C for short term ( $\approx 4$  wk) or flash frozen in  $\approx 50$ - $\mu$ L aliquots in liquid nitrogen after the addition of 15% (vol/vol) glycerol and stored at  $-80$  °C for long-term use. The concentrated sample of purified GabR was pale yellow in color, indicating that PLP was bound to the protein.

*Analytical Ultracentrifugation Analysis.* The oligomeric state of GabR–PLP in solution was analyzed by sedimentation velocity using a Beckman-Coulter Optima XL-I ultracentrifuge. The experiments were conducted at low protein concentrations (30, 50, and 80  $\mu$ g/mL) in the presence of 0.5 mM PLP and in the presence and absence of 20 mM

GABA. In each experiment, 450  $\mu$ L of the protein solution was loaded into a sector-shaped centrifugation cell at concentrations corresponding to OD230 values of 0.3, 0.5, and 0.8. The samples were spun at 48,000 rpm (Beckman AN60Ti Rotor) for 5 h with radial scans capturing the boundary distribution every 2 min until the sample had almost completely pelleted. Boundary profiles from sedimentation velocity scans were collected and analyzed using the UltraScan II software suite. Initial model-independent van Holde–Weischet analysis of the data clearly showed no evidence of mass action over the concentration range investigated, thereby confirming an absence of dynamic equilibrium between species. Therefore, all data were fit to a 50-iteration global genetic algorithm–Monte Carlo (GA-MC50) model, which showed a narrow and randomly distributed residual, indicative of good data quality and model fitting.

*Fluorescence Polarization DNA-Binding Assay.* Fluorescence polarization data for the GabR–DNA complex were obtained using an EnVision 2102 Multilabel Plate Reader (Perkin-Elmer). Two 49-bp complementary single-stranded DNA oligonucleotides containing the 47-bp GabR binding region (5' TCTGATACCATCAAAAAGTTATAATTGGTACTTTTCATCATACCAAAGA-3') were purchased from Integrated DNA Technologies. The oligonucleotides were either unlabeled or labeled at the 3' end with the fluorophore, TAMRA. The double-stranded oligonucleotides were prepared by annealing a mixture containing equimolar concentrations of the two single-stranded oligonucleotides. For the fluorescence polarization assay, varying concentrations of the GabR protein was titrated against a

fixed concentration of TAMRA-labeled DNA (50 nM). GabR protein was serially diluted in the DNA binding buffer [20 mM Tris·HCl, pH 8.0, 50 mM KCl, 2 mM MgCl<sub>2</sub>, 5% (vol/vol) glycerol, 1 mM EDTA, 1 mM DTT, and 0.05% Nonidet P-40]. The TAMRA-DNA (50 nM) was mixed with the serially diluted GabR protein (final concentration, 0–1,000 nM) and 100 µL of each sample mixture was loaded into the individual wells of a 384-well microplate. In the competitive binding assay, varying concentrations of unlabeled DNA were titrated against a fixed concentration of preformed GabR-labeled DNA complex (100 nM GabR and 100 nM TAMRA-DNA). The fluorescence polarization (FP) signals of the GabR–DNA mixtures were measured with fixed excitation (531 nm) and emission (595 nm) wavelength filters at room temperature. Fluorescence intensity remained constant throughout the polarization measurements. The fluorescence polarization signal for each sample was calculated and plotted against the GabR protein concentrations in the fluorescence polarization assay and against the concentrations of unlabeled DNA in the competitive binding assay. Each data point is the average of three independent measurements. The titration plot for GabR versus TAMRA-DNA was fitted to a modified Hill equation (Eq. S1) in ORIGIN software to calculate the dissociation constants and Hill coefficient. For the competitive binding assay, the IE50 value and Hill coefficient were obtained by fitting the data points to the Hill equation. (Eq. S2).

$$(\text{FPGTD} - \text{FPFTD}) = [\text{TAMRA-DNA}]^n / K_D^n + [\text{TAMRA-DNA}]^n; \quad [1]$$

where FPGTD represents FP signal when TAMRA-DNA is saturated with GabR; FPFTD

represents FP when all TAMRADNA is free in solution without any GabR bound; KD is the dissociation constant for the GabR–TAMRA-DNA complex; and n is the Hill coefficient.

$$(FPGTD - FPFTD) = [\text{Unlabeled DNA}]^n / (IE_{50}^n + [\text{Unlabeled DNA}]^n), \quad [2]$$

where FPGTD, FPFTD, and n are the same as in Eq. S1; IE50 represents the concentration of unlabeled DNA needed to bind 50% of protein.

*Crystallization.* Crystals of GabR were obtained by the hangingdrop method using protein at 5 or 10 mg/mL. The initial sparse matrix screen was set up with the Gryphon crystallization robot (Art Robbins Instruments) to obtain initial crystallization hits, which were further optimized manually to obtain crystals with the best size and morphology. The optimized crystallization solution contained 33% (vol/vol) PEG400, 200 mM calcium acetate, and 200 mM imidazole, pH 7.5. The hanging drops were incubated at 20 °C or room temperature. Crystals appeared in 5 d and grew to maximum size in 1–2 wk. Crystals with good morphology and size were picked directly from the hanging drops and flash-cooled in liquid nitrogen. The heavy metal derivatives were prepared by soaking crystals in 10 mM ethylmercury phosphate for 1 h before flash-cooling in liquid nitrogen. The heavy metal soaking condition also included 1 mM PLP.

*Data Collection and Processing.* Single-wavelength anomalous dispersion (SAD) data were collected at beamlines 19-ID and 19-BM at Advanced Photon Source, Argonne National Laboratory. X-ray diffraction data for the mercury derivative of holo-GabR (Table 1, Dataset 1) and for holo- and apo-GabR native crystals (Table 1, Datasets

2 and 3) were collected at the wavelengths of 1.0039 and 0.9792 Å, respectively. The datasets were indexed, integrated, and scaled with either the HKL package <sup>41</sup> or iMosflm and Scala programs in the CCP4 program suite <sup>42</sup>. The datasets were all scaled in the space group P212121 to resolutions of 3.1, 2.7, and 2.55 Å, respectively. The data statistics are reported in Table 1.

Table 1. Data collection and refinement statistics for full length GabR

Datasets	(1) GabR-PLP, mercury derivative	(2) GabR-PLP, native	(3) apo-GabR, native
Wavelength (Å)	1.0039	0.9792	0.9792
Space Group	P2 <sub>1</sub> 2 <sub>1</sub> 2 <sub>1</sub>	P2 <sub>1</sub> 2 <sub>1</sub> 2 <sub>1</sub>	P2 <sub>1</sub> 2 <sub>1</sub> 2 <sub>1</sub>
Resolution range (Å)	30-3.1 (3.15-3.1)	50-2.71 (2.76-2.71)	49.3-2.55
Unit cell (a b c) (Å)	98.1 101.1 211.2	97.2 101.3 211.2	99.9 101.4 213.2
Total unique reflections	39106	57413	68270
Multiplicity	6.7 (6.8)	4.8 (3.8)	5.8 (5.6)
Completeness (%)	100 (100)	99 (97.9)	95.8 (90.7)
Linear R <sub>merge</sub> <sup>a</sup> (%)	10.7 (71.6)	0.102 (ND)	11.7 (68.7)
I/σ	21.9 (2.9)	18.7 (1.0)	9.4 (2.2)
Average Wilson B- factor	67.7	59.9	38.7
R <sub>cryst</sub> <sup>b</sup>	0.2124		0.1947
R <sub>free</sub> <sup>c</sup>	0.2556		0.2461
Number of atoms	15247		15514
<i>Macromolecules</i>	15108		15139
<i>Ligands</i>	99		73
<i>Water</i>	40		300
RMSD <sup>d</sup> bonds (Å)	0.005		0.010
RMSD <sup>d</sup> angles (°)	1.02		1.405
Ramachandran favored (%)	94.0		89.8
Ramachandran outliers (%)	1.5		3.5
Average B-factor (Å <sup>2</sup> )	82.7		47.4
<i>Macromolecules</i>	82.6		63.0
<i>Solvent</i>	55.2		50.5

The values for the highest resolution bin are in parentheses.

$$^a\text{Linear } R_{\text{merge}} = \Sigma |I_{\text{obs}} - I_{\text{avg}}| / \Sigma I_{\text{av}}$$

$$^bR_{\text{cryst}} = \Sigma |F_{\text{obs}} - F_{\text{calc}}| / \Sigma F_{\text{obs}}$$

<sup>c</sup>Five percent of the reflection data were selected at random as a test set and only these data were used to calculate  $R_{\text{free}}$ .

<sup>d</sup>RMSD, root mean square deviation.

ND, Not Determined/Calculated by the program

*Sequence and Structure Analyses.* GabR homologs were identified in the sequence database using BLAST ; multiple sequence alignment using BLAST; conserved domain searches using CDD (4) <sup>34</sup>; buried surface area from PDBePISA server ([http://www.ebi.ac.uk/msd-srv/prot\\_int/cgi-bin/piserver](http://www.ebi.ac.uk/msd-srv/prot_int/cgi-bin/piserver)); and structural similarity using DALI <sup>43</sup>. Secondary structure superimpositions were done in Coot. Electrostatic surface potentials were calculated with PyMOL (The PyMOL Molecular Graphics System, version 1.5.0.4; Schrödinger). Figs. 3, 4, 6, and 9, and Figs. S2, S4, S5, S7, and S8 were drawn with PyMOL.

*Structure Solution, Model Building, and Refinement.* Automated substructure solution by AutoSol in PHENIX <sup>44</sup> found 15 heavy atom peaks in the mercury dataset (Table 1, Dataset 1) and identified fourfold noncrystallographic symmetry (NCS) using superposition of the mercury sites. AutoBuild in PHENIX automatically built ~80% of the residues. The initial phases were extended and refined to 2.7 Å using the native holo-GabR dataset (Table 1, Dataset 2) to yield improved maps and further improved by



fourfold NCS averaging and density modification. The remainder of the model was built manually in Coot <sup>45</sup> guided by the structure of *Thermococcus profundus* multiple substrate aminotransferase [Protein Data Bank (PDB) ID code 1WST], a homolog obtained from the FFAS03 server (<http://ffas.burnham.org/ffas-cgi/cgi/ffas.pl>). Several loops accounting for gaps in the model were placed and refined by a combination of manual building and the fit\_loops routine in PHENIX. Next, MR-SAD using the model and the mercury dataset identified five more mercury sites and led to even better maps. Several iterative rounds of manual model building and refinement using the maximum-likelihood amplitude targets in PHENIX and Rosetta using simulated annealing (in the initial stages) and automatic NCS restraints were required to obtain the final model. The initial model (□80% complete) had Rcryst and Rfree values of 0.393 and 0.484, respectively, for all data between 45.0 and 2.7 Å. The Rcryst and Rfree values of the final model (98% complete) are 0.229 and 0.265, respectively. The final model of the GabR–PLP complex consists of two homodimers of GabR in the asymmetric unit with □470 residues out of 479 accounted for in each monomer. The final model also contains 1 molecule of PLP per monomer, 16 molecules of ethylmercury, and 52 water molecules. The quality of the final model is summarized in Table S1. This model has been deposited in the PDB and is available with ID code 4N0B. The native dataset of apo-GabR (Table 1, Dataset 3), which was processed to a resolution of 2.55 Å, was phased by molecular replacement using the final model of GabR as the input model.

The Rfactor and Rfree values of the final model from the native dataset are 0.195

and 0.246, respectively. Other model statistics are summarized in Table S1. This model has been deposited in the PDB with ID code 4MGR. The density for PLP is lacking in this structure, as expected. We interpreted a difference density peak in the PLP-binding pocket as imidazole (Figure 10) because imidazole is a major component in the protein purification and crystallization buffer.

*GabR Enzyme Assay.* Activity was measured using varying concentrations of GabR protein in an assay buffer containing 100mM Tris·HCl, 5 mM DTT, 100 mM KCl, 100  $\mu$ M PLP, 20 mM GABA, 20 mM  $\alpha$ -ketoglutarate, 500  $\mu$ M NADP<sup>+</sup>, and 3 units of aldehyde dehydrogenase (ADH). In the coupled assay, ADH consumes the product of the first half-reaction (succinic semialdehyde) to produce succinate. The coupled reaction is measured spectrophotometrically (absorbance change at 340 nm) from the concomitant reduction of the cofactor, NADP<sup>+</sup> to NADPH.

## CHAPTER THREE

### PLP AND GABA TRIGGER GABR-MEDIATED TRANSCRIPTION REGULATION IN BACILLUS SUBSILIS VIA EXTERNAL ALDIMINE FORMATION

#### **Research Significance**

The *Bacillus subtilis* protein GabR activates the biosynthesis of glutamate from  $\gamma$ -aminobutyric acid (GABA) at the transcription level upon binding to pyridoxal-5'-phosphate (PLP) and GABA. We herein report that the external aldimine formed between PLP and GABA is apparently responsible for triggering the GabR-mediated transcription activation. A crystal structure of the GabR effector-binding/oligomerization (Eb/O) domain (residues 88-479) in complex with both PLP and GABA revealed the formation of a PLP-GABA Schiff base. Details of the GABA binding site in the Eb/O domain structure suggest that binding monocarboxylic  $\gamma$ -amino acid such as GABA should be preferred over dicarboxylic acid ligands. A reactive GABA analog, (*S*)-4-amino-5-fluoropentanoic acid (AFPA), was used as a molecular probe to examine the reactivity of PLP in both GabR and a homologous aspartate aminotransferase (Asp-AT) from *E. coli* as control. The comparison between the complex structures of Eb/O-PLP-AFPA and Asp-AT-PLP-AFPA revealed that GabR is incapable of facilitating further steps of the transamination reaction after the formation of the external aldimine. Results of *in vitro* and *in vivo* assays using full-length GabR support the conclusion that AFPA is a

agonistic ligand capable of triggering GabR-mediated transcription activation via formation of an external aldimine with PLP

## Introduction

Bacterial transcription regulators are often directly responsive to the changes in metabolite concentration <sup>15, 16</sup>. GabR responds to the increase of GABA concentration in bacterial cells <sup>25</sup> and upregulates glutamate regeneration from GABA. Belonging to the MocR/GabR subfamily in the GntR family of bacterial transcription regulators <sup>16, 25</sup>. GabR-type regulators characteristically have a large C-terminal Eb/O domain, which is homologous to the type I aminotransferases <sup>31</sup>, and a small N-terminal “winged-helix-turn-helix” (wHTH) DNA-binding domain <sup>26</sup>. In *B. subtilis*, GabR represses its own transcription <sup>24, 25</sup>. With both PLP and GABA bound, GabR activates the transcription of two genes, *gabT* and *gabD*, which encode the enzymes GABA aminotransferase (GABA-AT) and succinic semialdehyde dehydrogenase (SSA-DH) respectively, forming a pathway for glutamate regeneration from GABA <sup>24, 25</sup>.

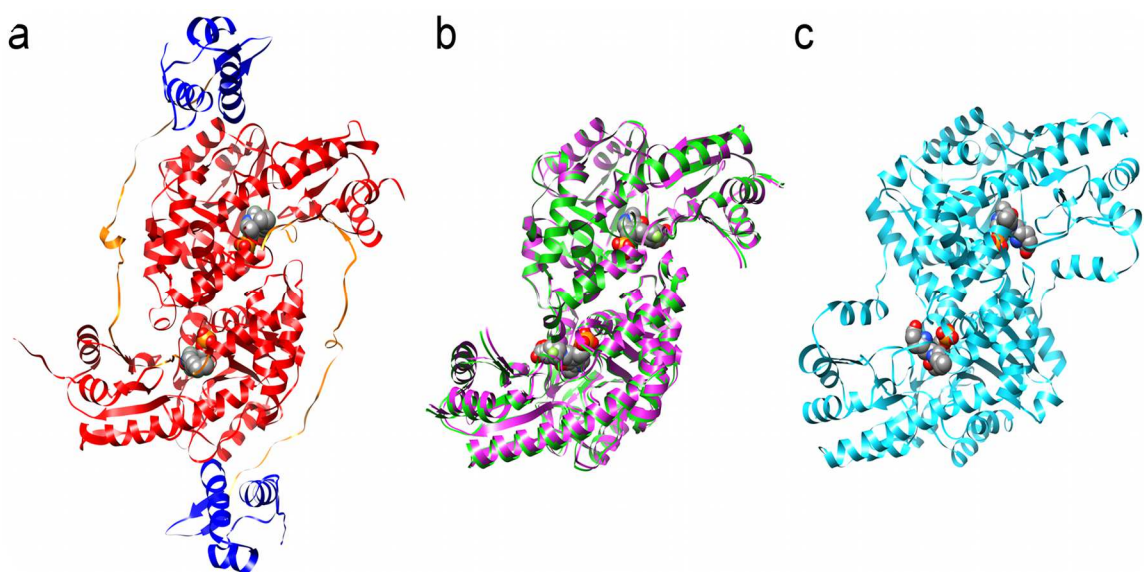
Previously, we have reported the crystal structures of full-length GabR as a “head-to-tail” dimer <sup>46</sup>, in which electron density supported the existence of PLP bound to K312 of the Eb/O domain in the form of an internal aldimine. Although the PLP-binding site of GabR is largely conserved compared to that of type I aminotransferases, no aminotransferase activity has been detected for GabR <sup>46</sup>. To our knowledge, the existence of PLP in MocR/GabR-type transcription regulators is the only case known in nature where PLP functions as an effector in transcription regulation, including the other reported case of a MocR regulator PdxR that controls the biosynthesis of PLP in bacteria

<sup>47-49</sup>. A previous report on GabR has shown that a “second metabolite pair” of pyridoxamine-5'-phosphate (PMP) and succinic semialdehyde (SSA) could also cause transcription activation upon binding to GabR <sup>24</sup>. The first half of the “Ping-Pong” transamination catalyzed by GABA-AT (Schemes 1 and 2) in fact converts PLP and GABA to PMP and SSA, reversibly <sup>50</sup>. It was hypothesized that certain step(s) of the aminotransferase reaction might be required to trigger GabR-mediated transcription activation <sup>24</sup>. Such hypothesis has not been proven, and the chemical identity of the GabR-PLP-GABA complex that results in transcription activation remained unknown. Using X-ray crystallography, NMR spectroscopy and biological assays, an external aldimine species formed between PLP and GABA when both bound to the effector binding site of GabR has been identified and is apparently responsible for triggering GabR-mediated transcription activation.

### **Crystallography of GabR Eb/O Domain and Asp-AT Complexed with Ligands**

Three complex structures with PLP-ligand adducts bound were obtained through co-crystallization. X-ray crystal structures were determined and refinement of all three complex structures converged with good statistics (Table 2). The Schiff base adducts were built into the electron density maps (*fo*-*fc*) in the final rounds of refinement. The formed adduct was confirmed by the simulated annealing omit difference maps (*fo*-*fc*) generated in Phenix <sup>51</sup>. The final models for EB/O-PLP-GABA, EB/O-PLP-AFPA and Asp-AT-PLP-AFPA have been deposited in the Protein Data Bank (PDB) with accession codes XXXX, YYYY and ZZZZ, respectively. The full length GabR was truncated to its

Eb/O domain (residues 88-479), expressed, purified and co-crystallized with PLP and GABA. The complex structures Eb/O-PLP-GABA and Eb/O-PLP-AFPA were solved with molecular replacement and refined at 2.23 Å resolution and 2.25 Å resolution, respectively. The complex structure of Asp-AT-PLP-AFPA was solved and refined at 1.53 Å resolution. The overall structure of the Eb/O domain retains the same “head-to-



tail” homodimer architecture as those in the full-length GabR and type I aminotransferases (Figure 25).

Figure 25. Head-to-tail-dimers of the full-length GabR (PDB code: 4N0B), Eb/O domain of GabR and Asp-AT. Bound PLP's are shown in spheres. a) In the full length GabR, the Eb/O domains are in red, the flexible linker regions are in orange, and the DNA-binding domains are in blue. b) An overlay of two dimeric structures of the GabR Eb/O domain in complexes with GABA (magenta) and AFPA (green). c) The dimeric structure of *E. coli* Asp-AT (PDB code 1SFF, cyan).

Table 2. Data collection and refinement statistics for GabR Eb/O domain

Protein	GabR-EBO/GABA	GabR-EBO/AFPA	Asp-AT/AFPA
Data processing			
Space group	C222 <sub>1</sub>	C222 <sub>1</sub>	C222 <sub>1</sub>
Cell dimension			
α, β, γ (°)	90.0; 90.0; 90.0	90.0; 90.0; 90.0	90.0; 90.0; 90.0
a, b, c (Å)	92.4; 128.9; 65.1	96.6; 127.5; 67.6	84.9; 154.9; 79.3
Resolution (Å)	49.2 - 2.23	50.8 - 2.25	29.0-1.53
<sup>a</sup> R <sub>merge</sub> (%)	7.5 (46.4) <sup>b</sup>	8.3 (64.4) <sup>b</sup>	6.8 (68.7) <sup>b</sup>
I/σ (I)	29.3(4.7) <sup>b</sup>	12.6(1.2) <sup>b</sup>	34.0(1.7) <sup>b</sup>
Completeness (%)	99.8(97.9) <sup>b</sup>	96.2(78.4) <sup>b</sup>	98.2(83.4) <sup>b</sup>
Multiplicity	5.5 (4.9) <sup>b</sup>	3.1 (2.5) <sup>b</sup>	12.2 (5.6) <sup>b</sup>
No. Reflections	248492	132836	1914313
No. Unique Reflections	19166	19311	147549
Refinement			
<sup>c</sup> R <sub>work</sub> / <sup>d</sup> R <sub>free</sub> (%)	17.44/21.07	18.82/23.70	14.88/16.55
No. of Atoms			
Protein	2921	2292	3465
Ligand	22	24	32
Water	136	182	510
B-factors(Å <sup>2</sup> )			
Protein	40.41	42.24	23.72
Ligand (Lowest/Highest)	28.60/41.18	24.80/43.97	13.05/27.80
<sup>e</sup> RMSD (from ideal values)			
Bond length (Å)	0.005	0.003	0.007
Bond angle (°)	0.862	0.604	1.128
Ramachandran plot			
Most Favored (%)	96.69	96.40	97.17
Allowed (%)	3.04	3.32	2.61
Outliers (%)	0.28	0.28	0.22

<sup>a</sup>  $R_{\text{merge}} = \sum |I_{\text{obs}} - I_{\text{avg}}| / \sum I_{\text{avg}}$

<sup>b</sup> The values for the highest resolution bins are in parentheses.

<sup>c</sup>  $R_{\text{work}} = \sum |F_{\text{obs}} - F_{\text{calc}}| / \sum F_{\text{obs}}$

<sup>d</sup> Five percent of the reflection data was selected at random as a test set, and only these data were used to calculate  $R_{\text{free}}$ .

<sup>e</sup> RMSD, root mean square deviation

### Details of the Effector Binding Site in the GabR Eb/O Domain and Schiff Base

## Formation between PLP and GABA

In the effector-binding pocket of the Eb/O domain, the omit map difference electron density (*fo*-*fc*) revealed the existence of a Schiff base formed between PLP and GABA (Figure 26a). Three basic residues, R207, R430 and H114, from the same subunit interact with the carboxylate of the GABA moiety. In a complex structure of GABA-AT-PLP-aminooxyacetate (AOA) (Figure 26a), the PLP-AOA adduct mimicks the PLP-GABA external aldimine, whose carboxylate interacts with one of the conserved arginine

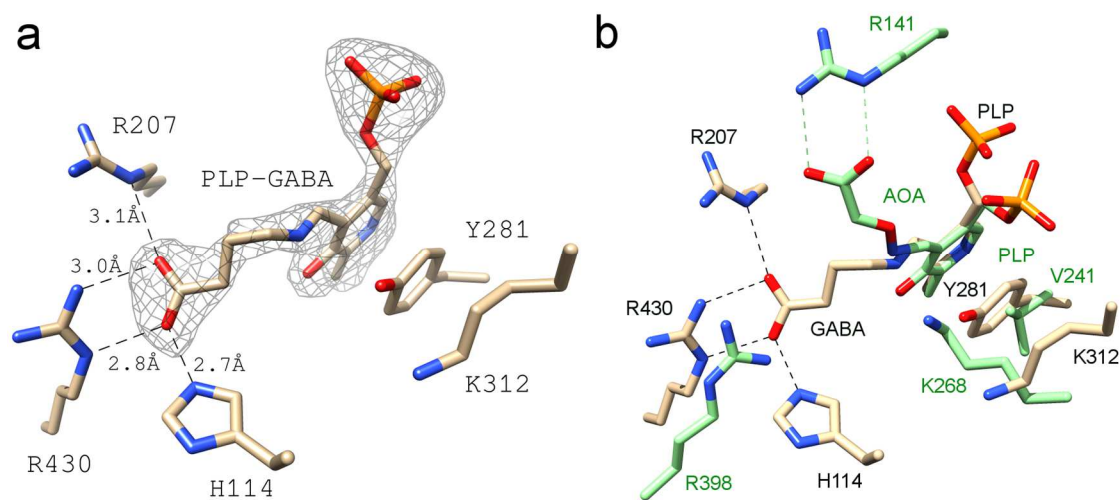
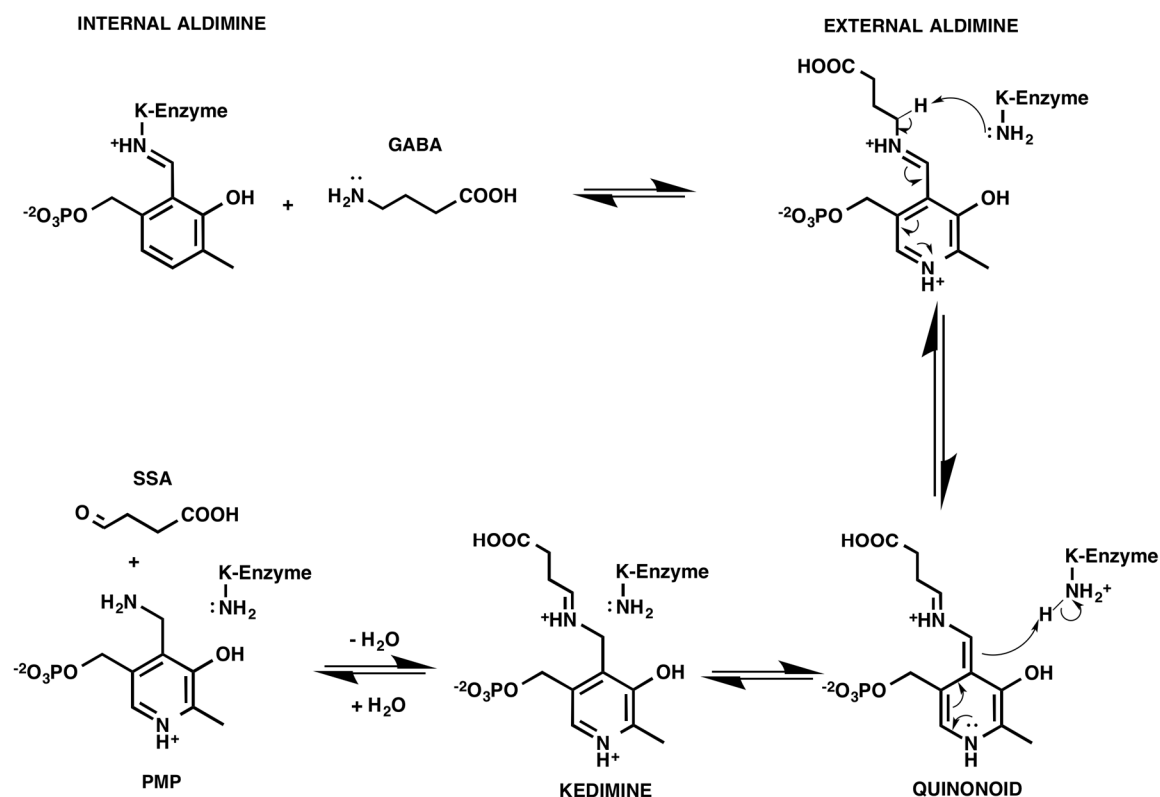


Figure 26. PLP and GABA bound to the truncated Eb/O domain. a) The simulated annealing omit map (fo-fc) is shown around the PLP-GABA Schiff base at  $3\sigma$ . b) Eb/O-PLP-GABA in comparison to GABA-AT with aminooxyacetate (AOA) bound to PLP mimicking the PLP-GABA external aldimine (green, PDB code: 1SFF). transamination reaction (Scheme 1).



residues (R141)<sup>52</sup>. Compared with the homologous type I aminotransferases such as GABA-AT (Figure 26B), GabR is missing one (R141 in GABA-AT) of the two conserved arginines, which are involved in binding to dicarboxylic acid substrates<sup>37, 52</sup>, such as *L*-glutamate or 2-ketoglutarate, in the second-half of a typical

This observed structural difference suggests that GabR has evolved to preferentially recognize monocarboxylic acids, such as GABA, and orient the ligand in favor of forming a Schiff base with PLP.



Scheme 1. The Mechanism of First Half of the GABA-AT Reaction.

Interestingly, the preserved basic residues in GabR are not aligned with GABA-AT residue R141, which is proposed to interact with the GABA carboxylate<sup>33, 52</sup>. While

the aminooxyacetate (AOA)-PLP adduct, which mimics the GABA-PLP in the *E. coli* GABA-AT structure, binds to the active site in an anti conformation, the PLP-GABA Schiff base in GabR is in a gauche conformation (Figure 3b). The dihedral torsional angle of C2-C1-O-N in the PLP-AOA “structural mimic” is measured to be  $156.7^\circ$  ( $13.3^\circ$  off from an ideal anti-conformation) in UCSF Chimera. In the complex structure of Eb/O-PLP-GABA, the GABA moiety displays a gauche conformation (Figure 27).

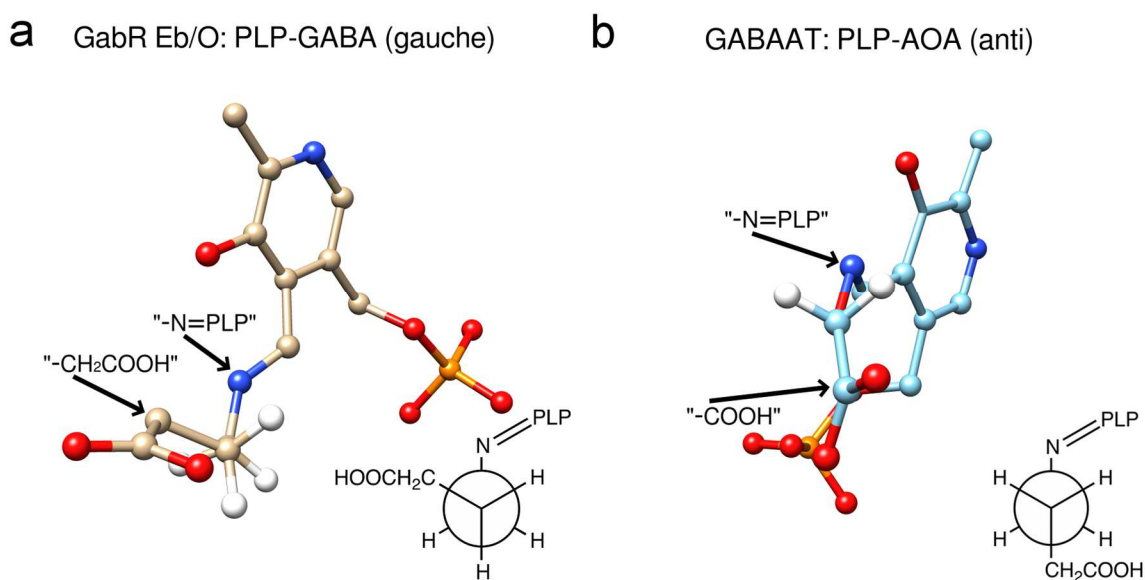


Figure 27. GABA Moiety Displays a Gauche Conformation. (a) The GABA bound in the Eb/O domain is in a gauche conformation. The PLP-GABA external aldimine is shown in stick and ball form. The C $\gamma$  atom is placed (hidden) behind the C $\beta$  atom, in the same orientation as the Newman projection for the dihedral torsional angle C $\alpha$ -C $\beta$ -C $\gamma$ -N in the PLP-GABA. A Newman projection of a PLP-GABA Schiff base is shown in a gauche conformation. (b) The aminooxyacetate (AOA)-PLP imine bound in *E. coli* GABA-AT (PDB code: 1SFF) mimicking the PLP-GABA Schiff base was shown in ball and stick form. The O atom is placed (hidden) behind the C1 atom in the same orientation as the Newman projection for the dihedral torsional angle C2-C1-O-N in the PLP-AOA. A Newman projection of a PLP-GABA Schiff base is shown in an anti-conformation.

The dihedral torsional angle of C $\alpha$ -C $\beta$ -C $\gamma$ -N in PLP-GABA Schiff base was measured to be 77.3° (17.3° off from an ideal gauche conformation) in UCSF Chimera. Compared to the anti conformation, the gauche conformation is of higher energy and a relatively minor conformation for GABA molecule dissolved in an aqueous environment in the cell. Herein, we speculate that GabR's preference for a gauche conformation could be an evolutionary outcome to sense the GABA's concentration buildup instead of detecting the basal GABA level inside the cell. Alternatively, we speculate that the chemical strain could be released and provide extra energy for GabR's action after or during transcription activation.

In all PLP-dependent enzymes, a conserved lysine forms an internal aldimine with PLP in a resting form and acts as a key catalytic residue during catalytic reactions, such as in the first half of the "Ping-Pong" transamination<sup>31</sup> (Scheme 1). The conserved K312<sup>46</sup>(Figure 28) was previously proven to be essential for GabR's function, although the catalytic capacity to facilitate transamination was never detected for GabR<sup>24</sup>. In the Eb/O-PLP-GABA complex structure (Figure 2a), Y281 is observed to block K312 from accessing the PLP-GABA Schiff base, preventing the reformation of the internal aldimine as well as further transamination-like catalysis, in which the freed catalytic lysine would deprotonate the carbon adjacent to the nitrogen atom of GABA (Scheme 1)<sup>33, 37</sup>. As a result, GabR is unlikely to catalyze the first half of the transamination reaction shown in Scheme 1. As we previously reported<sup>46</sup>, in the absence of GABA, Y281 is found in a different orientation, allowing internal aldimine formation (Figure 28). The observed

obstruction by Y281 supersedes the previous speculation that GabR's inability to stabilize the external aldimine might be the reason for no observed transaminase activity<sup>46</sup>.

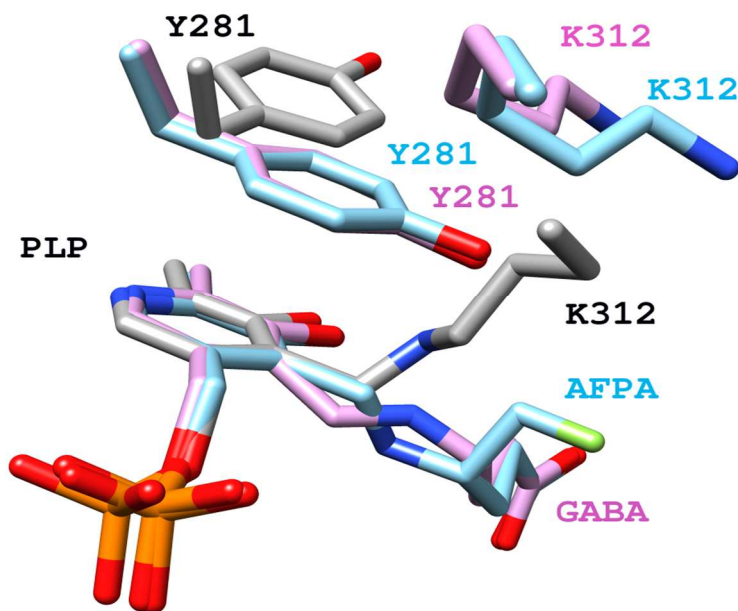
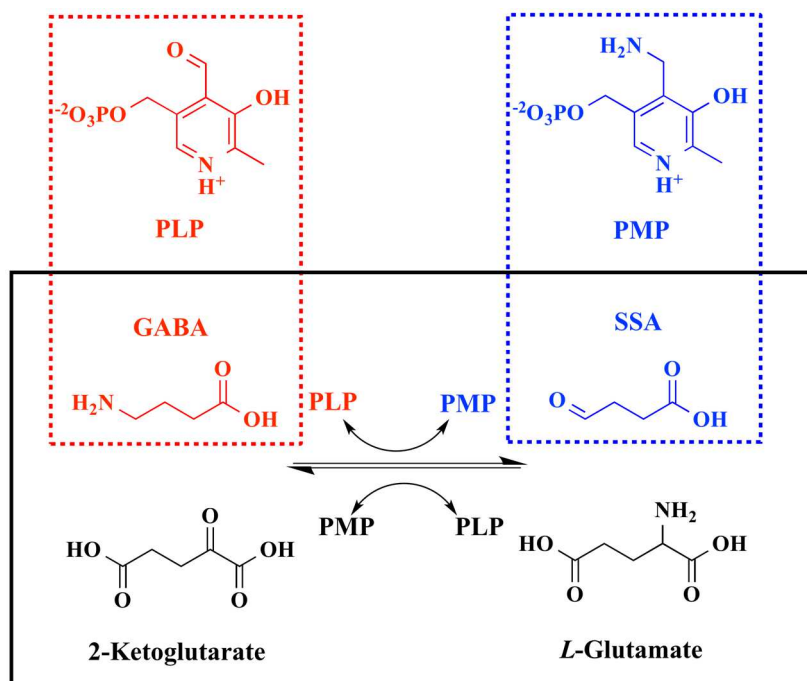


Figure 28. Comparison of the external aldimine vs. internal aldimine in GabR. Schiff bases, K312, and Y281 are shown in stick form. Labels and carbon atoms for internal aldimine (PDB code: 4N0B) are in black and grey, respectively. Labels and carbon atoms for Eb/O-PLP-GABA are in magenta. Labels and carbon atoms for Eb/O-PLP-AFPA are in cyan.

### External Aldimine as the Final Adduct of GabR-Mediated Reaction

The Eb/O-PLP-GABA complex structure at 2.23 Å resolution could not allow us to distinguish between external aldimine and ketimine (Scheme 1) for the chemical identity of the PLP-GABA Schiff base observed. Therefore, we used a mechanism-based inactivator, (*S*)-4-amino-5-fluoropentanoic acid (AFPA), which was designed to

irreversibly inactivate PLP-dependent aminotransferases<sup>53</sup>, as a molecular probe. A previously proposed inactivation mechanism of an aminotransferase, mammalian GABA-AT, by AFPA is shown in Scheme 2. Once a typical aminotransferase reaction progresses beyond the external aldimine 1 stage, the AFPA moiety loses the fluorine group, resulting in a reactive intermediate. Eventually, AFPA inactivates the PLP-dependent aminotransferase via a ternary adduct, in which the AFPA moiety is covalently linked to both PLP and the catalytic lysine, or alternatively forms external aldimine 3. The catalytic lysine freed after the formation of the external aldimine 1 plays a critical role in assisting the irreversible inactivation of the PLP enzyme. The formation of the proposed ternary adduct should provide evidence that the reaction between AFPA and PLP can progress beyond the external aldimine 1, reaching quinonoid or ketimine intermediates (Schemes 2 and Figure 29 )



Scheme 2. Proposed Reaction Mechanism of AFPA. The green dashed box (1) shows the final adduct in the GabR Eb/O domain; the red dashed box (2) shows the expected adduct for Asp-AT; the blue dashed box (3) indicates an alternative external aldimine species

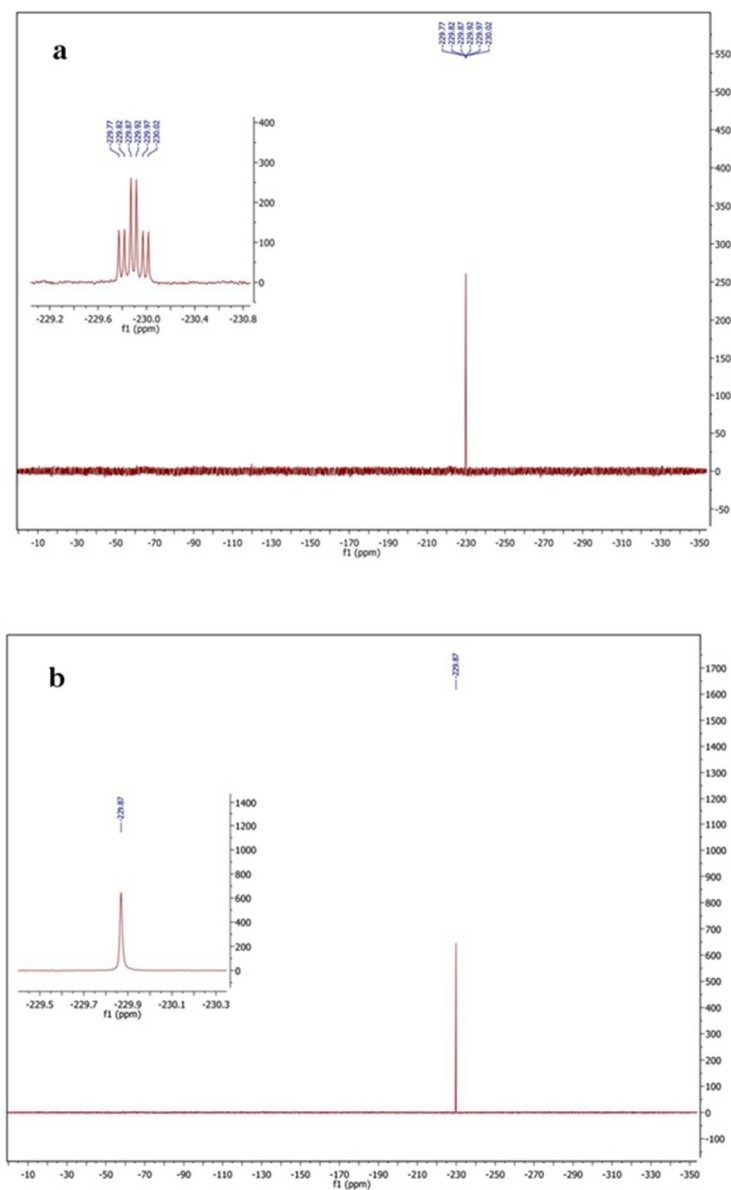


Figure 29. Fluorine NMR Spectra. a) Fluorine NMR showing a triplet of doublets ( $J_1 = 25.3$  Hz,  $J_2 = 21.4$  Hz). b) Proton-decoupled fluorine NMR spectrometry that shows a singlet.

In contrast, the intact fluorine group of AFPA should indicate that the reaction cannot proceed beyond the formation of the external aldimine 1. *E. coli* Asp-AT, a

homolog of the GabR Eb/O domain, has been used successfully as a model enzyme to study mechanism-based inactivators of PLP-dependent enzymes<sup>54-56</sup>. Due to the desirable crystallographic behavior of Asp-AT in various co-crystallization conditions, we chose it as a control for the co-crystallization experiment with AFPA.

Both the GabR Eb/O domain and Asp-AT were co-crystallized with PLP and AFPA. The structure of the Eb/O-PLP-AFPA complex (refined at 2.25 Å resolution) confirms the formation of external aldimine with the fluorine atom intact in the final adduct (Figure 30). To validate the existence of the fluorine atom, extra rounds of refinement were done after deletion of the fluorine atom; the omit map difference density (*fo-fc*) strongly supports the presence of the fluorine atom in the complex. Residue Y281 is observed to be in the same position as that in Eb/O-PLP-GABA complex structure (Figure 27), preventing the access of K312 to the PLP-AFPA Schiff base, which otherwise could potentially push the reaction further along the proposed inactivation pathway (Scheme 2).

Furthermore, the AFPA-treated protein sample was subjected to NMR studies to eliminate the possibility of an alternative adduct (adduct 3 in Scheme 2, via pathway b in Scheme 2). Pathway b and adduct 3 were never previously proven in the studies of the AFPA inactivation. However, it is chemically plausible that a hydroxyl or water could react with the reactive intermediate and replace the eliminated fluorine group; the resulting adduct 3 would be structurally similar to the external aldimine proposed here (adduct 1 in Scheme 2). At 2.25 Å resolution obtained for the complex structure Eb/O-



PLP-AFPA, it is impossible to distinguish adduct 3 from adduct 1 even with the omit map difference density ( $fo-fc$ ) validation shown (as green mesh) in Figure 30a. Fluorine NMR spectrometry was hence employed to eliminate this hypothetical possibility. The results are shown in Figure 29. Figure S29a is the fluorine NMR spectrum that shows a triplet of doublets ( $J_1 = 25.3$  Hz,  $J_2 = 21.4$  Hz), since the fluorine atom is split by its two neighboring hydrogen atoms, then split again by another hydrogen atom on the adjacent carbon in the external aldimine form. Figure S1b represents the proton-decoupled fluorine NMR spectrum that shows a singlet, because the fluorine atom and the protons are decoupled. As concluded, the fluorine atom remains intact in the same environment as intact AFPA, even after treatment with a saturated amount of GabR protein.

As a positive control, the structure of the Asp-AT-PLP-AFPA complex (refined at 1.53 Å resolution) showed that the proposed ternary adduct 3 (has formed via pathway a in Scheme 2 (Figure 30b), indicating that the catalytic actions of the conserved lysine have occurred in Asp-AT but not in the GabR Eb/O domain. On the basis of structural information and NMR results, it was concluded that the external aldimine 1 is the final chemical species when both PLP and AFPA are bound to the GabR Eb/O domain. This suggests that the observed Schiff base in the Eb/O-PLP-GABA complex structure is also an external aldimine.

For aminotransferases in general, the external aldimine intermediate can be transiently observed spectroscopically<sup>57</sup>. However, mutation of a catalytic residue<sup>58</sup> or chemical modification of the ligands such as the amino acid<sup>52</sup> or PLP<sup>59</sup> was required to

trap a stable external aldimine in an aminotransferase. GabR is, to our knowledge, the first reported protein capable of forming a stable external aldimine between PLP and GABA for its function in transcription regulation. Only mild global conformational changes are introduced in the PLP-bound Eb/O domain upon binding to GABA and formation of the external aldimine. A least squares structural comparison revealed that the Eb/O domains of the GabR-PLP dimer (PDB: 4N0B) aligned well with those of the Eb/O-PLP-GABA complex or the Eb/O-PLP-AFPA complex, with RMSD values for C $\alpha$  atoms around 1.12 Å and 1.13 Å, respectively. Conformational changes could be more pronounced in the linker region between Eb/O and wHTH domains, and within the wHTH domains in the full-length dimeric GabR; these conformational changes likely contribute to the triggering of transcription activation.

### **Functional Significance of External Aldimine Formation**

To extrapolate the functional interpretation from the GabR Eb/O domain to the full length GabR, both *in vivo* and *in vitro* assays were conducted to compare the biological effects of GABA and AFPA. When examining GabR-mediated activation *in vivo* using a *gabT-lacZ* fusion<sup>25</sup> (Figure 31a), both GABA and AFPA triggered GabR-mediated transcription activation in *B. subtilis* cells. *In vitro*, GabR, PLP, RNA polymerase, and the *gabT* promoter-containing DNA fragments were mixed with radioactively labeled nucleotides as described previously<sup>24</sup>. The *gabT* transcript was formed upon addition of either GABA or AFPA (Figure 31b). In contrast to *in vivo* results, AFPA triggered the GabR-mediated transcription activation *in vitro* with a higher

potency than did GABA. The GabR-PLP-AFPA complex may be a better transcriptional activator than the GabR-PLP-GABA complex. However, the bacterial cellular uptake of GABA may be more efficient than that of AFPA, resulting in a more pronounced biological effect *in vivo* upon the addition of GABA.

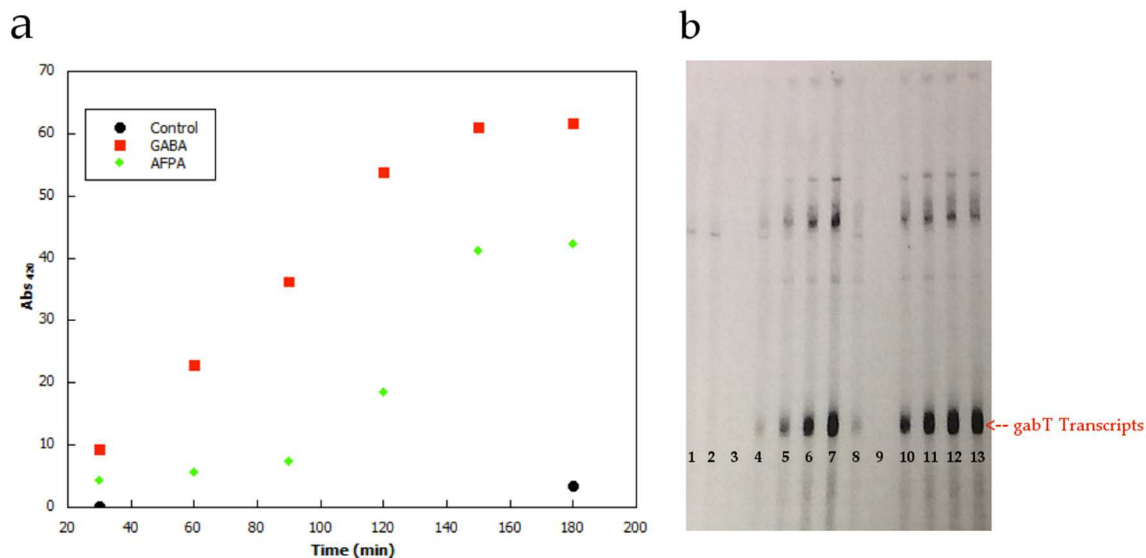


Figure 30. Biological effects of GABA and AFPA. a) The *gabT-lacZ* expression is monitored by absorbance at 420nm produced by the *lacZ* reaction using ONPG over time. b) Self-developed film indicating the newly synthesized *gabT* mRNA. Lane 1: Control without GABA or AFPA. Lanes 2-7: GABA added at concentration of 0.625, 1.25, 2.5, 5, 10 & 20 mM, respectively. Lanes 8-13: AFPA added with concentration of 0.625, 1.25, 2.5, 5, 10 & 20 mM, respectively.

## Conclusions

We have shown that PLP bound to the GabR Eb/O domain reacts with the effector GABA to form a stable external aldimine, which apparently triggers the transcription from the *gabT* promoter in *B. subtilis*. This conclusion offers an explanation for the previous results that the effector pair of PMP and SSA can also trigger GabR-mediated transcription activation *in vitro*<sup>24</sup>. Through a reverse transamination-like reaction

(Scheme 1), SSA and PMP can potentially form a Schiff base, presenting a structure similar to the PLP-GABA external aldimine<sup>24</sup>. However, SSA and PMP may not work as an actual effector pair *in vivo*. With an evolutionarily modified PLP/GABA binding site, the GabR Eb/O domain is capable of preferentially binding to GABA and forming an external aldimine. To perform the role of a transcription regulator, GabR employs Y281 to subdue the Eb/O domain's catalytic potential by stabilizing the external aldimine formed and preventing its further modification.

In summary, these studies were submitted to the Proceedings of the National Academy of Sciences of the United States of America (PNAS) for publication: Rui Wu, Ruslan Sanishvili, Boris R. Belitsky, Jose I. Juncosa, Hoang V. Le, Helaina J.S. Lehrer, Michael Farley, Richard B. Silverman, Gregory A. Petsko, Dagmar Ringe, and Dali Liu. (2015)

## **Materials and Methods**

*Materials.* Chemicals for the assays were purchased from Fisher Scientific (Pittsburgh, PA) and Sigma-Aldrich (St. Louis, MO); Cloning vectors were obtained from Integrated DNA Technologies (Coralville, IA). *Escherichia coli* BL21 (DE3) cells was purchased from New England BioLabs (Ipswich, MA). Bacterial growth media and antibiotics were obtained from Fisher Scientific and Sigma-Aldrich. Crystallization screen solutions and other crystallization supplies were purchased from Hampton Research (Aliso Viejo, CA) and Emerald Bio (Bedford, MA). All chemicals were of the highest quality available.

*Protein Expression and Purification.* Full-length GabR protein and *L*-aspartate aminotransferase from *E. coli* were expressed and purified as described <sup>24</sup>. The GabR Eb/O domain was overexpressed in *E. coli* and purified using a similar method. Transformed *E. coli* BL21 (DE3) cells were grown in 1L of LB supplemented with 50 µg/ml kanamycin at 37 °C and 250 rpm until OD<sub>600</sub> nm reached ~ 0.6. Protein expression was induced by the addition of 0.5 mM isopropyl-beta-D-1-thiogalactopyranoside (IPTG). Cells were incubated at 25 °C and harvested after 16 h by centrifuging at 4800 rpm and 4 °C for 10 min. The cell paste was resuspended in the lysis buffer containing 1 x PBS and 10 mM imidazole, pH 8.0 followed by sonication. The resulting suspension was centrifuged twice at 16,500 rpm and 4 °C for 20 min, and the soluble fraction was

loaded onto a 10 ml His-Trap column (GE Life Sciences, Piscataway, NJ) containing  $\text{Ni}^{2+}$  and previously equilibrated with lysis buffer. Elution of the retained proteins was achieved with a linear imidazole gradient (25 column volume, 10 mM-485 mM). Fractions containing truncated EB/O domain were pooled, concentrated to 2 mL, and loaded onto a 16/60 Superdex 200 size exclusion column (GE Life Sciences) that was previously equilibrated with 84% elution buffer. Fractions containing enzyme were pooled, concentrated, and used freshly after exchanging into suitable buffers for the crystallization and biological assays. The wild type Asp-AT was overexpressed and purified with the protocol used by Onuffer and Kirsch <sup>60</sup>.

*Crystallization of the GabR-Eb/O and X-ray Diffraction Data Collection.* After the initial crystallization screen and optimization, the GabR-Eb/O domain was crystallized via hanging drop methods at 25 °C. The hanging drops were prepared with 1  $\mu\text{L}$  of 12 mg/mL pre-incubated protein with inhibitor solution and 1  $\mu\text{L}$  of the reservoir solution that contained 0.1 M Tris (pH 8.5) buffer and 20 % ethanol. Crystals were harvested in about 10 days. For cryo-cooling, crystals were transferred to the reservoir solution with 20 % glycerol as cryo protectant, and were flash-cooled by plunging in liquid nitrogen. The cocrystallization of Asp-AT and AFPA were conducted according to previous studies <sup>54, 55</sup> The diffraction data were collected at GM/CA@APS beamlines 23ID-B and 23ID-D at Advance Photon Source (Argonne National Laboratory, Argonne, IL). The wavelength used for data collection was 1.0332 Å, and diffraction images were

recorded on 4x4 tiled CCD detectors (Rayonix, Evanston, IL) with 300×300 mm<sup>2</sup> sensitive are. All data were indexed, integrated, scaled and merged using HKL2000 <sup>41</sup>.

*Phasing, Model Building, and Refinement.* Diffraction data were phased with molecular replacement using the program Phaser <sup>61</sup> in the CCP4 software suite <sup>42</sup>. Previously solved full-length GabR structure <sup>46</sup>, truncated to contain residues 107-479, was used as the search model. Rigid body refinement followed by restrained refinement was carried out in Refmac5. Model building was conducted using the program COOT <sup>45</sup>. Iterative rounds of model building and refinement generated the final coordinates.

*In Vivo and in Vitro Assays for GabR-Dependent Transcription Activation.* The *in vivo* assay was conducted as previously described <sup>24</sup>, using GABA or AFPA as effectors (0.625 – 20 mM). *In vitro* GabR-dependent RNA polymerase reactions were performed as previously described <sup>24</sup>. The PCR-fragment (50nM) contained the gabR-gabT regulatory region. The total reaction was carried in transcription buffer containing: 40 mM Tris-HCl, 100 mM KCl, 10 mM MgCl<sub>2</sub>, 5% glycerol, 0.1 mM EDTA, 1 mM DTT, 0,1 mg/mL of BSA with four units of RNasin, 150 μM ATP, CTP, and GTP, 20 μM UTP, 0.5 to 1 μl Ci of <sup>32</sup>P-labeled UTP, and 0.02-0.04 unit of *E. coli* RNA polymerase. The reaction was incubated at 37 °C for 15 min and terminated by additional of 4 μL of the 20 mM EDTA, 95% formamide dye solution. The samples were subsequently heated at 80 °C for 5 min. The samples were then analyzed without further purification using 7 M urea / 5-6% polyacrylamide DNA sequencing gels. GABA was purchased from Sigma. AFPA was synthesized according to previous publication <sup>53</sup>.

*Nuclear Magnetic Resonance (NMR) Spectroscopy.* The protein (100 mg) was treated with AFPA. The molar ratio of the protein and AFPA was 2:1 to minimize free AFPA in the solution. The sample was concentrated to a volume of 0.4 mL by centrifugation. Deuterium oxide (0.15 mL) was added, and the solution was transferred to a 5 mm standard NMR tube. Fluorine NMR and proton-decoupled fluorine NMR spectra were taken at the Northwestern IMSERC facility on an Agilent DD2 500 MHz spectrometer with an Agilent 5 mm HFX probe at 26 °C.  $^{19}\text{F}$  NMR  $\delta$  229.87 (td,  $J_1=25.3$  Hz,  $J_2=21.4$  Hz); proton-decoupled  $^{19}\text{F}$  NMR  $\delta$  229.87 (s).

*Structural Analysis and Figure Making.* All structural analyses were conducted in COOT <sup>45</sup> and UCSF Chimera <sup>53</sup>. Structure comparison of the PLP/amino acid binding site was conducted in two steps (Figure 2b & Figure 6): First, the overall structural comparison/overlap was conducted in UCSF Chimera using the Needleman-Wunsch algorithm. Second, manual adjustments were done by overlapping the pyridine ring of the PLP to achieve better pattern matching for the conserved key residues in the PLP/amino acid binding site for comparison. All structural figures were made in UCSF Chimera.



## CHAPTER FOUR

### CONCLUSIONS AND FUTURE INVESTIGATIONS

#### **Full length GabR and Its Overall Structure**

In conclusion, the studies presented herein have as provided useful information to elucidate the transcription regulatory mechanism of GabR, gain insight into the functionality of a unique MocR subfamily member, gain insight into the regulation pathway of the GABA shunt pathway, and provided some detailed molecular and chemical information for future anti-virulence drug discovery.

The obtained X-ray crystal structures of full length GabR provided information on the domain arrangements of MocR subfamily's transcription. To our best knowledge, these structures are the first X-ray crystal structures revealed in the GntR/MocR family. In addition, we also build model obtained from the small angle X-ray scattering (SAXS) from protein solution sample (Figure 31), and structure impose indicated a high agreement between the bead model and the X-ray crystal structure (Figure 32). These suggested that the head-to-tail homodimer is probably physiologically and in the functional geometry before transcription initiation. More detailed structure analysis provides offer more information:

(1) To allow us to propose a model for the DNA and protein complex, further to speculated how the interaction between DNA and GabR could position the regulatory domain in the proper position and set the “perfect” geometry to initiate the transcription.

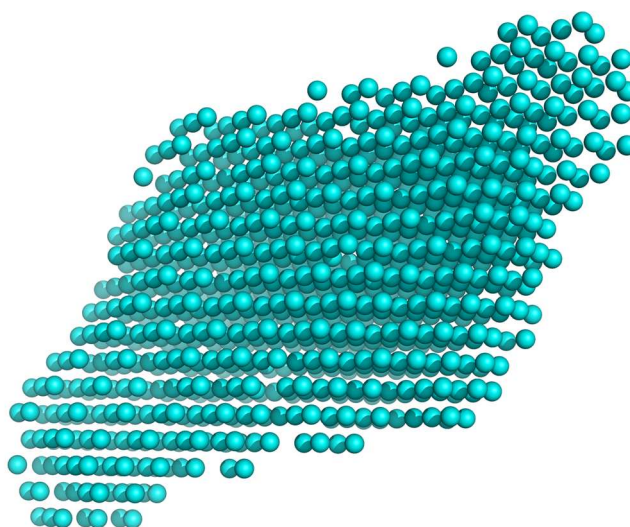


Figure 31. Small Angle X-ray Scattering (SAXS) bead model of full length GabR.

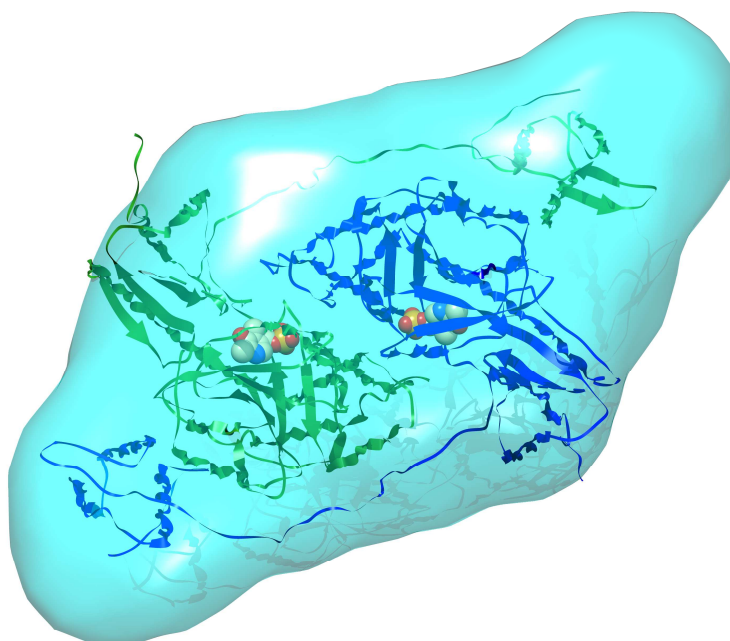


Figure 32. Small Angle X-ray Scattering (SAXS) bead model of full length GabR superimpose with X-ray crystal structure of full length GabR.

(2) The reveal of the effector/s (GABA and PLP) binding pocket in effector binding and/or regulatory domain offer us a bold hypothesis that nature may recycled the vitamin B6 and “borrow” a partial reaction from aminotransferase to regulate the

\

transcription initiation.

(3) The linker region between the DNA binding domain and the effectors binding and /or regulatory domain shown to be the first case in GntR transcription regulator super family. The long linker suggests a rather dramatic conformational changes could happen upon binding to the effectors during the initiation of the transcription.

### **Effector Binding Domain and Related Biological Function**

Although these structures have provided much needed answers in terms of static image before GabR associate with the effector GABA. There are still more details that need to be addressed to elucidate how effector triggers the transcription initiation.

Further studies revealed several Eb/O domain structures in complex with GABA, and molecular probe molecule AFPA. These two structures paved the way toward understanding how GabR functions. Our results suggest that upon binding to effector (GABA) or effectors analog (APFA), the internal aldimine would undergo a reaction with coming effector to form external aldimine. Using multiple approaches, such as: NMR, *in vivo* transcription assay, *in vitro* transcription assay, we were able to determine that the external aldimine is a critical chemical species that triggers the transcription initiation.

### **GabR and DNA Complex**

One of the disadvantage of having only the Eb/O domain is no structural information could support during the initiation of the transcription if there is a conformational changes on the geometry between Eb/O and DNA binding domain, or if

the DNA binding domain have re-located upon binding to effectors. This will hopefully be addressed in the near future. Meanwhile a SAXS bead model of the GabR/DNA complex (Figure 33 and Figure 34) shed some light on how the DNA and GabR would interact. Notably, the DNA fragment is at the bented confirmation from the interpretation from the SAXS bead model. Looks apparent to us this bented geometry somehow facilitate the transcription initiation, more specifically maybe facilitating RNA polymerase, sigma factor and other important component to bind to initiate the transcription.



Figure 33. Small Angle X-ray Scattering (SAXS) bead model of full length GabR and DNA complex.

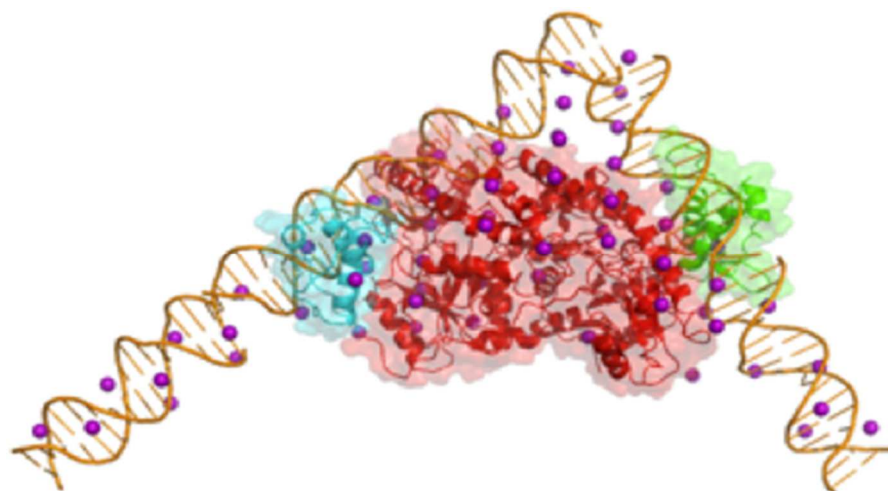


Figure 34. The fitting model of Small Angle X-ray Scattering (SAXS) bead structure of full length GabR and DNA complex and X-ray crystal structure of GabR.

## CHAPTER FIVE

### THE CRYSTAL STRUCTURE OF NITROSOMONAS EUROPAEA SUCROSE SYNTHASE REVEALS CRITICAL CONFORMATIONAL CHANGES AND INSIGHTS INTO THE SUCROSE METABOLISM IN PROKARYOTES

#### **Research Significance**

In this chapter we report the first crystal structure of a prokaryotic sucrose synthase from the non-photosynthetic bacterium *Nitrosomonas europaea*. The obtained structure was in an open form, whereas the only other available structure from the plant *Arabidopsis thaliana* was in a closed conformation. Comparative structural analysis revealed a “hinge-latch” combination, which is critical to transition between the open and closed forms of the enzyme. The *N. europaea* sucrose synthase shares the same fold as the GT-B family of the retaining glycosyltransferases. In addition, a triad of conserved homologous catalytic residues in the family showed to be functionally critical in the *N. europaea* sucrose synthase (Arg567, Lys572, Glu663). This implies that sucrose synthase shares not only a common origin with the GT-B family, but also a similar catalytic mechanism. The enzyme was proven to prefer transferring glucose from ADP-glucose rather than UDP-glucose like the eukaryotic counterparts. This predicts that these prokaryotic organisms have a different sucrose metabolic scenario from plants. Nucleotide preference determines where the glucose moiety is targeted after sucrose is degraded.

## Introduction

In plants, sucrose (Suc) is a major photosynthetic product and plays a key role not only for carbon partition but also in sugar sensing, development, and regulation of gene expression<sup>62-64</sup>. It was first thought that Suc metabolism was a characteristic of plants but it was later found in other oxygenic photosynthetic organisms<sup>65, 66</sup>. In the last decade, Salerno and coworkers demonstrated the importance of Suc for carbon and nitrogen fixation in filamentous cyanobacteria<sup>67, 68</sup>. More recently, genomic and phylogenetic analyses revealed the existence of Suc-related genes in non-photosynthetic prokaryotes such as proteobacteria, firmicutes, and planctomycetes<sup>65, 66, 69</sup>. It has been suggested that these organisms acquired the genes of Suc metabolism by horizontal gene transfer<sup>65, 66, 69</sup>. However, analysis of the enzymes encoded by such genes is currently lacking.

*Nitrosomonas europaea* is a chemo-litho-autotrophic bacterium that obtains energy by oxidizing ammonia to hydroxylamine and nitrite in presence of oxygen<sup>70</sup>. It is a member of the  $\beta$ -proteobacteria group with a putative photosynthetic ancestor<sup>71</sup>. *N. europaea* has potential for many biotechnological applications, including bioremediation of water contaminated with chlorinated aliphatic hydrocarbons<sup>72</sup> or ammonia, in combination with *Paracoccus denitrifi*<sup>70</sup>. *N. europaea* displays some metabolic resemblance to photosynthetic organisms, but with marked differences. For instance, it possesses all the coding genes for enzymes of the Calvin-Benson cycle, but with two exceptions that could be replaced by other glycolytic enzymes<sup>73</sup>. All the genes coding for enzymes from the tricarboxylic acid cycle were found in *N. europaea*<sup>73</sup>; however, activity of  $\alpha$ -ketoglutarate dehydrogenase is non-detectable<sup>74</sup>.

The evidence from genomic studies suggests that *N. europaea* can synthesize Suc<sup>73</sup>; however, the biochemical properties of enzymes from Suc metabolism have not been characterized. Generally, in plants, Suc is synthesized from UDP-glucose (UDP-Glc) and fructose-6-phosphate (Fru-6P) in a reaction catalyzed by Suc-6-phosphate synthase (EC 2.4.1.14), followed by removal of the phosphate group by Suc-6-phosphatase (EC 3.1.3.24). The disaccharide can be degraded to Glc and Fru by invertases (EC 3.2.1.26) or cleaved by UDP to form UDP-Glc and Fru by Suc synthase (SucSase, EC 2.4.1.13)<sup>63, 64</sup>. However, some plant SucSases have a certain degree of substrate promiscuity<sup>75-82</sup>, and *Thermosynechococcus elongatus* prefers ADP<sup>77</sup>. For that reason, a general reversible reaction could be written as:



Besides its physiological role, SucSase catalyzes a reversible reaction and its activity can be measured in both directions *in vitro*. In filamentous cyanobacteria, the products derived from Suc cleavage contribute to other biological processes, such as polysaccharides synthesis<sup>83</sup>. Therefore, understanding the catalysis and the regulation of SucSase is of great significance. Recently, Zheng et al.<sup>84</sup> reported the crystal structure of the *Arabidopsis thaliana* SucSase (*Ath*SucSase) in complex with UDP and fructose in a closed conformation. This enzyme is a homotetramer composed of four identical subunits of ~90 kDa and belongs to group 4 of the GT-B retaining glycosyltransferase family (<http://www.cazy.org/GlycosylTransferases.html>)<sup>85</sup>. The reaction mechanism for this enzyme family has not been elucidated. But, it has been suggested that it favors the S<sub>N</sub>i-like reaction mechanism proposed by Lairson et al.<sup>84-86</sup>.



Although several cyanobacterial <sup>69, 77, 80</sup> and plant <sup>75, 78, 87-90</sup> SucSases have been characterized, the enzyme from non-photosynthetic bacteria has never been studied and no structural information of any SucSase from bacterial sources is available. In this work we report the recombinant expression and biochemical characterization of *N. europaea* SucSase (*NeuSucSase*) and its crystal structure. We also determined the catalytic implications of highly conserved residues and the specificity for nucleotide substrates.

### Sequence Analysis

To know how *NeuSucSase* relates to other SucSases from divergent organisms we constructed a phylogenetic tree using 117 amino acid sequences retrieved from the NCBI database (Figure 35, Table 3, and Figure 37). The tree comprised seven major branches, containing the sequences from cyanobacteria (group I; 21 sequences), proteobacteria (groups II and III; 17 sequences), the moss *Physcomitrella patens* subsp. *patens* (group IV; 4 sequences), and vascular plants (groups V, VI, and VII; 75 sequences) (Figure 35). The shape of the tree shown in Figure 35 is similar to the one published by Kolman et al. <sup>69</sup>. Group I is subdivided in two branches, containing the sequences encoded by the *susA* (cyan) and *susB* (orange) genes (Figure 35) <sup>69</sup>. Most sequences from proteobacteria are included in group III (including  $\beta$ -,  $\gamma$ - and  $\delta$ -)

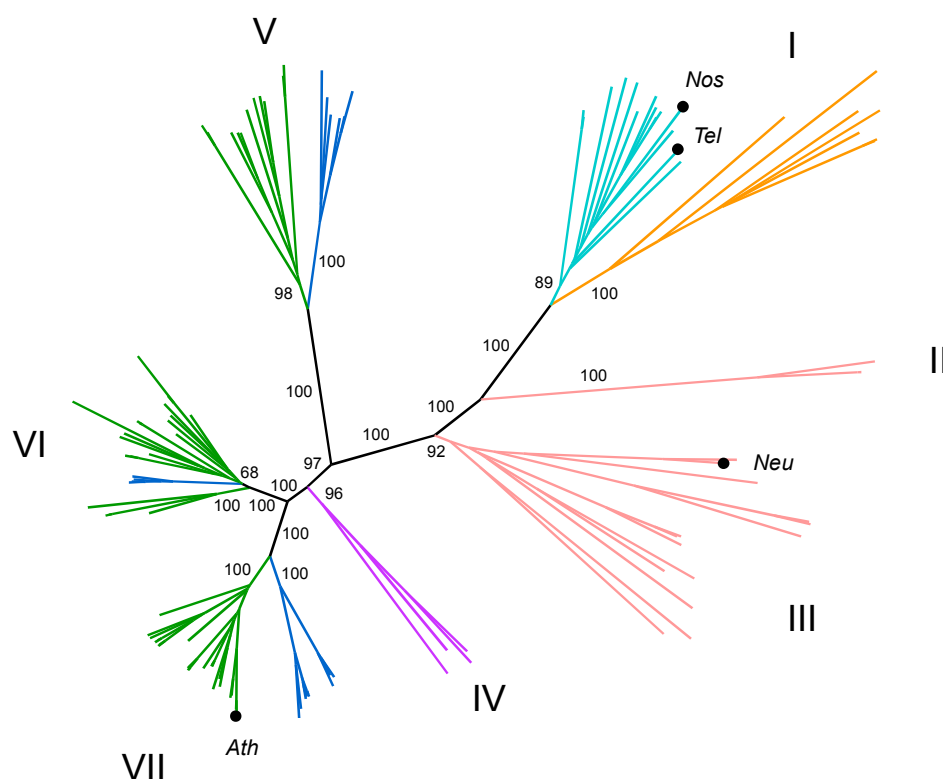


Figure 35. Phylogenetic tree of SucSases. Group I contains sequences from cyanobacteria and is divided in two major branches, *susA* (cyan) and *susB* (orange) proteins; groups II and III (pink) contain sequences from proteobacteria; group IV contains the sequences from the moss *P. patens* (violet); and groups V, VI, and VII, which contain the sequences from vascular plants are further divided in two branches, dicots (green) and monocots (blue). Numbers for major branches are the bootstrap values obtained during tree reconstruction, as described in the “Materials and Methods” section. *Neu*, *N. europaea*; *Ath*, *A. thaliana* SucSase 1; *Nos*, *Nostoc* sp. PCC 7120 *susA*; *Tel*, *T. elongatus*. proteobacteria); though, the sequences from  $\delta$ -proteobacterium MLMS-1 and *Desulfurivibrio alkaliphilus* AHT2 are in a diverging branch (group II)

Table 3. Sucrose synthase genes used for phylogenetic analysis. Different colors belong to different branches in Fig. 35.

Accession (GI)	Organism	Phylum	Type	Annotation
158339122	<i>Acaryochloris marina</i> MBIC11017	cyanobacteria		sucrose synthase
75908500	<i>Anabaena variabilis</i> ATCC 29413	cyanobacteria		sucrose synthase
209523126	<i>Arthrospira maxima</i> CS-328	cyanobacteria		sucrose synthase
284053161	<i>Arthrospira platensis</i> str. Paraca	cyanobacteria		sucrose synthase
218440696	<i>Cyanothece</i> sp. PCC 7424	cyanobacteria		sucrose synthase
220907171	<i>Cyanothece</i> sp. PCC 7425	cyanobacteria		sucrose synthase
332712456	<i>Lyngbya majuscula</i> 3L	cyanobacteria		sucrose synthase
254416162	<i>Microcoleus chthonoplastes</i> PCC 7420	cyanobacteria		sucrose synthase
334117431	<i>Microcoleus vaginatus</i> FGP-2	cyanobacteria		sucrose synthase
159031025	<i>Microcystis aeruginosa</i> PCC 7806	cyanobacteria		unnamed protein product
119512682	<i>Nodularia spumigena</i> CCY9414	cyanobacteria		sucrose synthase
186682280	<i>Nostoc punctiforme</i> PCC 73102	cyanobacteria		sucrose synthase
17232477	<i>Nostoc</i> sp. PCC 7120	cyanobacteria		sucrose synthase
22298591	<i>Thermosynechococcus elongatus</i> BP-1	cyanobacteria		sucrose synthase
75909957	<i>Anabaena variabilis</i> ATCC 29413	cyanobacteria		sucrose synthase
220909283	<i>Cyanothece</i> sp. PCC 7425	cyanobacteria		sucrose synthase
332708740	<i>Lyngbya majuscula</i> 3L	cyanobacteria		sucrose synthase
119510624	<i>Nodularia spumigena</i> CCY9414	cyanobacteria		sucrose synthase
298489784	<i>Nostoc azollae</i> 0708	cyanobacteria		sucrose synthase
186685043	<i>Nostoc punctiforme</i> PCC 73102	cyanobacteria		sucrose synthase

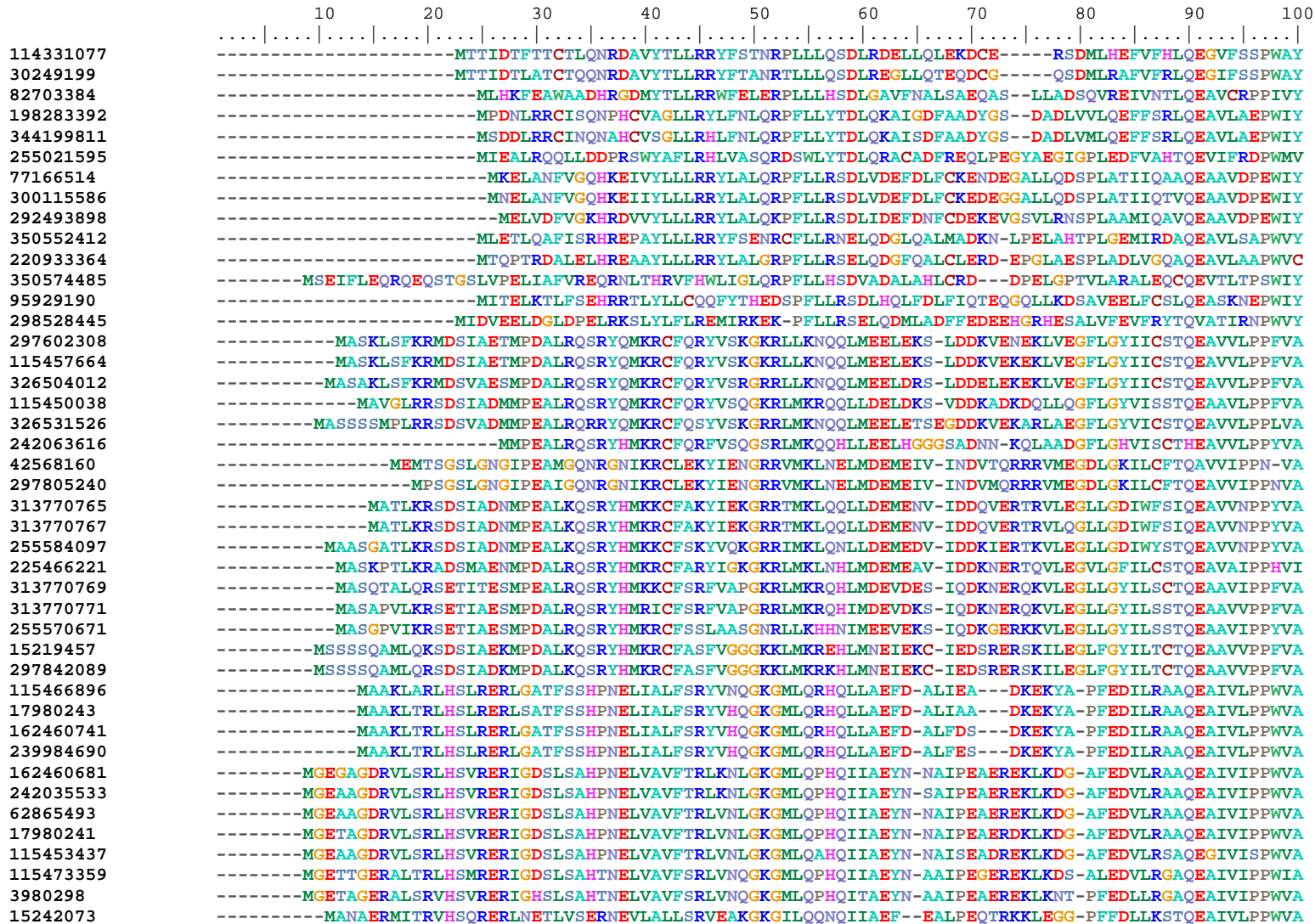
17228554	<i>Nostoc</i> sp. PCC 7120	cyanobacteria		sucrose synthase
<hr/>				
168009716	<i>Physcomitrella patens</i> subsp. patens	streptophyta	moss	predicted protein
168029793	<i>Physcomitrella patens</i> subsp. patens	streptophyta	moss	predicted protein
168035060	<i>Physcomitrella patens</i> subsp. patens	streptophyta	moss	predicted protein
168058907	<i>Physcomitrella patens</i> subsp. patens	streptophyta	moss	predicted protein
297795665	<i>Arabidopsis lyrata</i> subsp. lyrata	streptophyta	eudicot	hypothetical protein
297805240	<i>Arabidopsis lyrata</i> subsp. lyrata	streptophyta	eudicot	hypothetical protein
297812265	<i>Arabidopsis lyrata</i> subsp. lyrata	streptophyta	eudicot	hypothetical protein
297814081	<i>Arabidopsis lyrata</i> subsp. lyrata	streptophyta	eudicot	hypothetical protein
297818772	<i>Arabidopsis lyrata</i> subsp. lyrata	streptophyta	eudicot	hypothetical protein
297842089	<i>Arabidopsis lyrata</i> subsp. lyrata	streptophyta	eudicot	hypothetical protein
15219457	<i>Arabidopsis thaliana</i>	streptophyta	eudicot	sucrose synthase 6
42568160	<i>Arabidopsis thaliana</i>	streptophyta	eudicot	sucrose synthase 5
22331535	<i>Arabidopsis thaliana</i>	streptophyta	eudicot	sucrose synthase 4
15235300	<i>Arabidopsis thaliana</i>	streptophyta	eudicot	sucrose synthase 3
15239816	<i>Arabidopsis thaliana</i>	streptophyta	eudicot	sucrose synthase 2
15242073	<i>Arabidopsis thaliana</i>	streptophyta	eudicot	sucrose synthase 1
151176306	<i>Beta vulgaris</i>	streptophyta	eudicot	sucrose synthase 1
14530225	<i>Beta vulgaris</i>	streptophyta	eudicot	sucrose synthase
38425095	<i>Beta vulgaris</i>	streptophyta	eudicot	sucrose synthase
6682841	<i>Citrus unshiu</i>	streptophyta	eudicot	sucrose synthase
6683114	<i>Citrus unshiu</i>	streptophyta	eudicot	sucrose synthase
115310620	<i>Coffea arabica</i>	streptophyta	eudicot	sucrose synthase
115310618	<i>Coffea arabica</i>	streptophyta	eudicot	sucrose synthase

4468153	<i>Craterostigma plantagineum</i>	streptophyta	eudicot	sucrose synthase
4468151	<i>Craterostigma plantagineum</i>	streptophyta	eudicot	sucrose synthase
324984223	<i>Gossypium barbadense</i>	streptophyta	eudicot	sucrose synthase
324984221	<i>Gossypium barbadense</i>	streptophyta	eudicot	sucrose synthase
324984229	<i>Gossypium hirsutum</i>	streptophyta	eudicot	sucrose synthase
258489633	<i>Gossypium hirsutum</i>	streptophyta	eudicot	sucrose synthase 1
3915046	<i>Medicago sativa</i>	streptophyta	eudicot	sucrose synthase
4584690	<i>Medicago truncatula</i>	streptophyta	eudicot	sucrose synthase
345286419	<i>Orobancha ramosa</i>	streptophyta	eudicot	sucrose synthase 2
345286417	<i>Orobancha ramosa</i>	streptophyta	eudicot	sucrose synthase 1
3915037	<i>Pisum sativum</i>	streptophyta	eudicot	sucrose synthase 2
3766299	<i>Pisum sativum</i>	streptophyta	eudicot	sucrose synthase
3377764	<i>Pisum sativum</i>	streptophyta	eudicot	nodule-enhanced susy
313770771	<i>Populus trichocarpa</i>	streptophyta	eudicot	sucrose synthase 7
313770769	<i>Populus trichocarpa</i>	streptophyta	eudicot	sucrose synthase 6
313770767	<i>Populus trichocarpa</i>	streptophyta	eudicot	sucrose synthase 5
313770765	<i>Populus trichocarpa</i>	streptophyta	eudicot	sucrose synthase 4
313770763	<i>Populus trichocarpa</i>	streptophyta	eudicot	sucrose synthase 3
313770761	<i>Populus trichocarpa</i>	streptophyta	eudicot	sucrose synthase 2
313770759	<i>Populus trichocarpa</i>	streptophyta	eudicot	sucrose synthase 1
255550319	<i>Ricinus communis</i>	streptophyta	eudicot	sucrose synthase
255551835	<i>Ricinus communis</i>	streptophyta	eudicot	sucrose synthase
255564236	<i>Ricinus communis</i>	streptophyta	eudicot	sucrose synthase
255570671	<i>Ricinus communis</i>	streptophyta	eudicot	sucrose synthase
255584097	<i>Ricinus communis</i>	streptophyta	eudicot	sucrose synthase

304651490	<i>Solanum lycopersicum</i>	streptophyta	eudicot	sucrose synthase isoform 4
304651488	<i>Solanum lycopersicum</i>	streptophyta	eudicot	sucrose synthase isoform 3
3660531	<i>Solanum lycopersicum</i>	streptophyta	eudicot	sucrose synthase
31455440	<i>Solanum tuberosum</i>	streptophyta	eudicot	sucrose synthase 4
28629438	<i>Solanum tuberosum</i>	streptophyta	eudicot	sucrose synthase 2
29289943	<i>Solanum tuberosum</i>	streptophyta	eudicot	sucrose synthase
225431790	<i>Vitis vinifera</i>	streptophyta	eudicot	hypothetical protein
225437428	<i>Vitis vinifera</i>	streptophyta	eudicot	hypothetical protein
225444613	<i>Vitis vinifera</i>	streptophyta	eudicot	hypothetical protein
225466221	<i>Vitis vinifera</i>	streptophyta	eudicot	hypothetical protein
62865493	<i>Bambusa oldhamii</i>	streptophyta	monocot	sucrose synthase
17980241	<i>Bambusa oldhamii</i>	streptophyta	monocot	sucrose synthase
17980243	<i>Bambusa oldhamii</i>	streptophyta	monocot	sucrose synthase
326531526	<i>Hordeum vulgare</i> subsp. vulgare	streptophyta	monocot	predicted protein
326504012	<i>Hordeum vulgare</i> subsp. vulgare	streptophyta	monocot	predicted protein
241896730	<i>Hordeum vulgare</i> subsp. vulgare	streptophyta	monocot	sucrose synthase
3980298	<i>Hordeum vulgare</i> subsp. vulgare	streptophyta	monocot	sucrose synthase 2
239984690	<i>Hordeum vulgare</i> subsp. vulgare	streptophyta	monocot	sucrose synthase
115450038	<i>Oryza sativa</i> Japonica Group	streptophyta	monocot	Os02g0831500
115452927	<i>Oryza sativa</i> Japonica Group	streptophyta	monocot	Os03g0340500
115453437	<i>Oryza sativa</i> Japonica Group	streptophyta	monocot	Os03g0401300
115457664	<i>Oryza sativa</i> Japonica Group	streptophyta	monocot	Os04g0309600
115466896	<i>Oryza sativa</i> Japonica Group	streptophyta	monocot	Os06g0194900
115473359	<i>Oryza sativa</i> Japonica Group	streptophyta	monocot	Os07g0616800
297602308	<i>Oryza sativa</i> Japonica Group	streptophyta	monocot	Os04g0249500

242063616	<i>Sorghum bicolor</i>	streptophyta	monocot	hypothetical protein
242035533	<i>Sorghum bicolor</i>	streptophyta	monocot	hypothetical protein
242035817	<i>Sorghum bicolor</i>	streptophyta	monocot	hypothetical protein
162458268	<i>Zea mays</i>	streptophyta	monocot	sucrose synthase 2
162460681	<i>Zea mays</i>	streptophyta	monocot	sucrose synthase 2
162460741	<i>Zea mays</i>	streptophyta	monocot	sucrose synthase 1
<hr/>				
114331077	<i>Nitrosomonas eutropha</i> C91	$\beta$ -proteobacteria		sucrose synthase
82703384	<i>Nitrospira multiformis</i> ATCC 25196	$\beta$ -proteobacteria		sucrose synthase
30249199	<i>Nitrosomonas europaea</i> ATCC 19718	$\beta$ -proteobacteria		sucrose synthase
94264333	delta proteobacterium MLMS-1	$\delta$ -proteobacteria		sucrose synthase
94266940	delta proteobacterium MLMS-1	$\delta$ -proteobacteria		sucrose synthase
95929190	<i>Desulfuromonas acetoxidans</i> DSM 684	$\delta$ -proteobacteria		sucrose synthase
297569306	<i>Desulfurivibrio alkaliphilus</i> AHT2	$\delta$ -proteobacteria		sucrose synthase
298528445	<i>Desulfonatronospira thiodismutans</i> ASO3-1	$\delta$ -proteobacteria		sucrose synthase
77166514	<i>Nitrosococcus oceani</i> ATCC 19707	$\gamma$ -proteobacteria		sucrose synthase
292493898	<i>Nitrosococcus halophilus</i> Nc4	$\gamma$ -proteobacteria		sucrose synthase
300115586	<i>Nitrosococcus watsonii</i> C-113	$\gamma$ -proteobacteria		sucrose synthase
350552412	<i>Thiorhodospira sibirica</i> ATCC 700588	$\gamma$ -proteobacteria		sucrose synthase
350574485	<i>Thiorhodovibrio</i> sp. 970	$\gamma$ -proteobacteria		sucrose synthase
220933364	<i>Thioalkalivibrio sulfidophilus</i> HL-EbGr7	$\gamma$ -proteobacteria		sucrose synthase
255021595	<i>Acidithiobacillus caldus</i> ATCC 51756	$\gamma$ -proteobacteria		sucrose synthase
198283392	<i>Acidithiobacillus ferrooxidans</i> ATCC 53993	$\gamma$ -proteobacteria		sucrose synthase
<hr/>				

Figure 36. Alignment of sucrose synthases from Table 3.





297812265 -----MANAERMITRVHSQERERLNETLVSENEVLALLSRVEAKGKGILQQNQIIAEF--EALPEETQKKLEGG-PFFDLLKSTQEAIVLPPWVA  
22331535 -----MANAERVITRVHSQERERLDATLVAQKNEVFALLSRVEAKGKGILQHHQIIAEF--EAMPLETQKKLQGG-AFFEFLRSAQEAIVLPPFVA  
297818772 -----MANAERVITRVHSQERERLDATLIAQKNEVLALLSRVEAKGKGILQHHQIIAEF--EAMPLETQKKLQGG-AFFEILRSAQEAIVLPPFVA  
313770759 -----MAERALT RVHSIRERVDETLKAHRNEIVALLTRIEGKKGILQHHQIVAEF--EAIPEDTRKTLAGG-AFAEVLIRSTQEAIIVPPWIA  
313770761 -----MSVLTRVQSIRERLDETLKTHRNEIVALLTRIEGKKGILQHHQIIAEF--EAIPPEIRKILAGG-AFSEVLIRSTQEAIVLPPWVA  
255550319 -----MAERVITRVHSIRERLDETLAANRNEIVALLTRIEGKKGILQHHQIIAEF--EAIPEDIRKNLLDS-VFGEVLIRSTQEAIVLPPWVA  
324984223 -----MANPVITRVHSLRERLDETLAHRNEILALLSRIEGKKGILQHHQIIIEF--EAIPENRKKLADG-AFFEVLKASQEAIVLPPWVA  
258489633 -----MANPVITRVHSLRERLDETLAHRNEILALLSRIEGKKGILQHHQIIIEF--EAIPENRKKLADG-AFFEVLKASQEAIVLPPWVA  
324984221 -----MADRVTITRVHSLRERLDETLAHRNEILALLSRIEGKKGILQHHQIIIEF--EAIPENRKKLANG-AFFEVLKASQEAIVLPPWVA  
324984229 -----MADRVTITRVHSLRERLDETLAHRNEILALLSRIEGKKGILQHHQIIIEF--EAIPENRKKLANG-AFFEVLKASQEAIVLPPWVA  
6683114 -----MAERALT RVHSLRERLDETLAHRNEILALLSRIEGKKGILQHHQIIIEF--ESISEENRKHLEEG-AFGEVLRATQEAIVLPPWVA  
4584690 -----MATERLITRVHSLRERLDETLTANRNEILALLSRLEAKGKGILQHHQIVAEF--EEIPEESRQKLTG-AFGEVLIRSTQEAIVLPPWVA  
3915046 -----MATERLITRVHSLRERLDETLTANRNEILALLSRLEAKGKGILQHHQIVAEF--EEIPEESRQKLTG-AFGEVLIRSTQEAIVLPPWVA  
3766299 -----MATDRLITRVHSLRERLDETLTANRNEILALLSRLEAKGKGILQHHQIVAEF--EEIPEENRQKLTG-AFGEVLIRSTQEAIVLPPWVA  
3777764 -----MATDRLITRVHSLRERLDETLTANRNEILALLSRLEAKGKGILQHHQIVAEF--EEIPEENRQKLTG-AFGEVLIRSTQEAIVLPPWVA  
225444613 -----MADGVLITGVHSLRERLDETLAHRNEILALLSRIEGKKGILQHHQIIIEF--EALPEVNRRKLSG-PFGDILKSIQEAIIVPPWIA  
3660531 -----MAERVLTITRVHSLRERLDETLAHRNEILALLSRIEGKKGILQHHQIIIEF--DAIRQDDKDLNEH-AFEEILLKSTQEAIVLPPWVA  
31455440 -----MAERVLTITRVHSLRERLDETLAHRNEILALLSRIEGKKGILQHHQIIIEF--DAIRQDDKDLNEH-AFEEILLKSTQEAIVLPPWVA  
304651488 -----MAQVLTITRVHSLRERLDETLAHRNEILALLSRIEGKKGILQHHQIIIEF--ESIHKEDKDLNDH-AFEEVLKSTQEAIVLPPWVA  
28629438 -----MAERVLTITRVHSLRERLDETLAHRNEILALLSRIEGKKGILQHHQIIIEF--ESIHKEDKDLNDH-AFEEVLKSTQEAIVLPPWVA  
115310618 -----MAERVLTITRVHSLRERLDETLAHRNEILALLSRLETHGKGILQHHQIIIEF--EEINKDGKQIHDH-AFEEVLKSTQEAIVLPPWVA  
345286417 -----MAERVLTITRVHSLRERLDETLAHRNEILALLSRVEAHGKGILQHHQIIIEF--EAIQADKAKLQDH-AFQEVLRSTQEAIVLPPWVA  
38425095 -----MASRLITRVPSLKERLDETLTAQRNEIISFLSKIASHGKGILQHHQIIIEF--EAVAD--KHKLADG-PFGEVLRHTQETIVLPWTIT  
15235300 -----MANPKLITRVPSLKERLDETLTAQRNEIISFLSKIASHGKGILQHHQIIIEF--EAVAD--KHKLADG-PFGEVLRHTQETIVLPWTIT  
297814081 -----MANPKLITRIISTDRVDQTLAHRNELVALLSRYVDQGGKILQPHNLIDELESVIGDDATKQSLSDG-PFGEILKSAMEAIIVPPFVA  
6682841 -----MAAPKLSRIPSIIRERVDQTLAHRNELVALLSRYVDQGGKILQPHNLIDELESVIGDDATKQSLSDG-PFGEILKSAMEAIIVPPFVA  
255564236 -----MAAPKLSRIPSIIRERVDQTLAHRNELVALLSRYVDQGGKILQPHNLIDELESVIGDDATKQSLSDG-PFGEILKSAMEAIIVPPFVA  
313770763 -----MANPKLITRIPSMRERVDQTLAHRNELVALLSRYVDQGGKILQPHNLIDELESVIGDDATKQSLSDG-PFGEILKSAMEAIIVPPFVA  
3915037 -----MSTHPKLTITRVPSIRDRVDQTLAHRNELVALLSRYVDQGGKILQPHNLIDELESVIGDDATKQSLSDG-PFGEILKSAMEAIIVPPFVA  
225437428 -----MSTHPKLTITRVPSIRDRVDQTLAHRNELVALLSRYVDQGGKILQPHNLIDELESVIGDDATKQSLSDG-PFGEILKSAMEAIIVPPFVA  
162458268 -----MSAPKLDNRNPSIRDRVDQTLAHRNELVALLSRYVDQGGKILQPHNLIDELESVIGDDATKQSLSDG-PFGEILKSAMEAIIVPPFVA  
242035817 -----MSAPKLDNRNPSIRDRVDQTLAHRNELVALLSRYVDQGGKILQPHNLIDELESVIGDDATKQSLSDG-PFGEILKSAMEAIIVPPFVA  
115452927 -----MSGPKLDRTPSIRDRVDQTLAHRNELVALLSRYVDQGGKILQPHNLIDELESVIGDDATKQSLSDG-PFGEILKSAMEAIIVPPFVA  
241896730 -----MAAPKLDNRNPSIRDRVDQTLAHRNELVALLSRYVDQGGKILQPHNLIDELESVIGDDATKQSLSDG-PFGEILKSAMEAIIVPPFVA  
304651490 -----MSNPKLSRIPSMRERVDQTLAHRNELVALLSRYVDQGGKILQPHNLIDELESVIGDDATKQSLSDG-PFGEILKSAMEAIIVPPFVA  
29289943 -----MSNPKLSRIPSMRERVDQTLAHRNELVALLSRYVDQGGKILQPHNLIDELESVIGDDATKQSLSDG-PFGEILKSAMEAIIVPPFVA  
115310620 -----MATIKLQKLPSIRERVDQTLAHRNELVALLSRYVDQGGKILQPHNLIDELESVIGDDATKQSLSDG-PFGEILKSAMEAIIVPPFVA  
4468153 -----MATPKLTIPSMRERVDQTLAHRNELVALLSRYVDQGGKILQPHNLIDELESVIGDDATKQSLSDG-PFGEILKSAMEAIIVPPFVA  
345286419 -----MSNPKLTIPSMRERVDQTLAHRNELVALLSRYVDQGGKILQPHNLIDELESVIGDDATKQSLSDG-PFGEILKSAMEAIIVPPFVA  
4468151 -----MTHEKAPASPCMRERVDQTLAHRNELVALLSRYVDQGGKILQPHNLIDELESVIGDDATKQSLSDG-PFGEILKSAMEAIIVPPFVA  
151176306 -----MAPKLTIPSMRERVDQTLAHRNELVALLSRYVDQGGKILQPHNLIDELESVIGDDATKQSLSDG-PFGEILKSAMEAIIVPPFVA  
14530225 -----MAPKLTIPSMRERVDQTLAHRNELVALLSRYVDQGGKILQPHNLIDELESVIGDDATKQSLSDG-PFGEILKSAMEAIIVPPFVA  
15239816 -----MPTGRFETMREWVDAISAQRNELLSLFSRYVDQGGKILQSHQLIDEFLKTVKVDGTTLEDLNSK-PFMKVLQSAEEAIIVPPFVA  
297795665 -----MPTGRFETMREWVDAISAQRNELLSLFSRYVDQGGKILQSHQLIDEFLKTVKVDGTTLEDLNSK-PFMKVLQSAEEAIIVPPFVA  
225431790 -----MPHRYDGQSMRERVDQTLAHRNELVALLSRYVDQGGKILQSHQLIDEFLKTVKVDGTTLEDLNSK-PFMKVLQSAEEAIIVPPFVA  
255551835 -----MPLSSFRDRVDILSVYRVELVSLTTHVABGKGILQTHDLLCELDNVVVDDEAMEKLRRS-PFVEVLQSTQEAIIVPPFVA  
168009716 -----MATQPALRRLNSIQERVDQKVVQSNRNLILDLLSRYVDQGGKILQSHQLIDEFLKTVKVDGTTLEDLNSK-PFMKVLQSAEEAIIVPPFVA

168035060 -----MAANGVAPKKPVLQRLNSIQERVQSAVQEHRNVIIIDLLSRVYKQGRTHLQPHHIVDELN-SLTEADRVTEIKDS-AFGLLLLNCQEAIVLPFWLG  
168058907 -----MSQPRPTLRLRLTSLKERVSSLSQEHRNELLLHLQGVVAAQGRSILQPHHLQDQLA-AVHDA---AHIQDT-AIGKILLQNCQEAIVSPFWVG  
168029793 -----MDGIATQAGALPRMTSMNKIQGSLDHRNENLRILSKLATAKRALMQPHEVIDLN-KAAEESGSLKIMDG-PLARVFSLCQEAIVLAPWVG  
94266940 -----MYDDLGSFIDEAEIPLLRREFLLSLPPSEPPPLLRNDVLAQFQQCEAHSEVDEPLG-----CWRFLRKVQEIQLQADDLLV  
94264333 -----MYDDLGSFIDEAEIPLLRREFLLSLPPSEPPPLLRNDVLAQFQQCESHPEVDDPLG-----CWRFLRKVQEIQLQADDLLV  
297569306 -----MENDLGCFFVDEQDVAPLREFFLLSLQRPPEPPLLRNDILAFQGFQAGQFPAAEGLAG-----AWRFLRKVQEVLLADDLLI  
254416162 -----MLNLIQNVLDCEERNDLRQFASQLKQSGPRYLLRNDILSDFSKYCAQCEKPDYFYHSSNLGKLIYYTQEIILQESLY  
332712456 -----MLNLIQDVLSEDEKSDLRHFTSOLKTAEPYRYLLRNEILAAFNEYCTKHKKSEYFYHSSHLGKLIYYTQEIILQESLY  
17232477 -----MSELMQAILDSEEHDLRGFISELRQQDKNYLLRNDILNVYAEYCSKQCKPETSQYKFSNLSKLIYYTQEIILQESLY  
75908500 -----MSELMQAILDSEEHDLRAFISELRQQDKNYLLRNDILNVYSEYCSKQCKSETSYKFSNLSKLIYYTQEIILQESLY  
186682280 -----MSELQAVIDSEERSDLRSFSELRQQEKYLLRNDILNVYSEYCSKQCKSEYKFTSSLGKLIYYTQEIILQESLY  
119512682 MCGGGVSFVLPVKNNANLMLGVPMSIELQAVIDSEEEKSDLRSFASQLRQEEKNYLLRNDILNVFIDYCSKSEKSETSAASSRLGKLIYYTQEIILQESLY  
334117431 -----MSELQAVIASDEKTELRFVSDLRALGNKYLLRNDIVNAFAAYCTKYEKPEQFHQSSLLSKLIYYVQEIILQESLY  
218440696 -----MSGLIETVLNSEEKIVLWQFIGELRTSDKRYLLRNDIVCAFEDFCRKNQNSQ-KIDSSPLGQMIHYTQEIILQESLY  
159031025 -----MAELIEAIANSNEKKDLQQFLHLQRLQLEKPYLLRNDLLTAFADYCRQDKPASFRQLLSLAKLIYYTQEIILQESLY  
220907171 -----MSELITAVLASSEERRELKEFLQLQQRQDNRYLLRNEILAAFSSQYGEAEAGKPEKFFHSSQLGKLINFYQEIILQESLY  
22298591 -----MTCVLLKAVVESDERADLRQFSRILQLGEKRYLLRNDILDADAFADYCRDQERPVPVPPSESRLSKLIVFYTQEIIVDNESLY  
158339122 -----MSQLIQAVLNSDEKTDLRQFASVHNQPERYRYLLRNDILSFADYDFCEKYKTPAFQLSSRLQKLIYYTQEIILQESLY  
284053161 -----MSELIQNVLESDEKQDLRQFSELRISEKRYLLRNDILQAFADYCLKFKQAAHFVDSHSLGKLIYYTQEIILQESLY  
209523126 -----MSELIQNVIDSDEKQDLRQFASLELRISEKRYLLRNDILQAFADYCLKFKQSDHFVHSSNLGKLIYYTQEIILQESLY  
17228554 -----MHSELFHPIFANGEEKAAALQQLIIALDASGKRYFLRNEILHTFSQYCCQAQKPTFYFYSSSSVGLKIYQTHEIVLAEDGTW  
75909957 -----MHSELFHPIFANGEEKAAALQQLIIALDSSGKRYFLRNEILHTFSQYCCQAQKPTFYFYSSSSVGLKIYQTHEIVLAEDGTW  
186685043 -----MYELVQAVNFGDEKTAHLQIYTLSSASGKRYLLRNEILQAFADYCHESQKPAYFYHSSSLGKLIYYTHEIIIEESTW  
119510624 -----MHSELFETVLNKDEKITLRQFISELSDTKRYFLRNEILHNFAEFCHQYQKPTFYFYSSSSIGRLIHNTHEMILDEQGTW  
298489784 -----MYELQAVLTSDEKITALRQFLILLHDFDKCYFLRNEILQAFNTYCHQSEKPTFYFYHSSSLGTLHYTHEIIIEESTW  
220909283 -----MRDLVESVLTDEKIDLARFLDRLIQQKQYFLRNEILQHFSSYCHREAEKAAHFYFASYLGLKLIYYTHEILQEGAVW  
332708740 -----MSSLLRAVLQSEKADLRQFISQLRSEQERYFLRNQILQAFDNYCTTHDKPAYFKRTSSIAELLNLYTHEIILEKNLW

## Clustal Consensus

```

110      120      130      140      150      160      170      180      190      200
114331077      FVLRLPGIAELEFEVRMHQEHLMPEKITITINEFLGFKKE--TVTKG-EA--IESILEVDFGPFNRAFPKLRESRSIGQGVIFLNRQLSSEMFT-RIE--AGSTRLL
30249199      LALRPEIAKAWFEMRIHQEHLIPEKLTITSEFLKFKKE--TVVKG-EA--TESVLEVDGPFNRFGRPLKESRSIGQGVIFLNRKLSSEMFS-RIE--AGHTSL
82703384      MAAREEAAGCWYARLHLDRLIPEAVITVSEYLAFKKE--LLVNPEGA--NEPVLIEDFAPFNKGSPKLKEIRSIGQGVIFLNRQLAGGLLFG--QLG--LGSDKL
198283392      LAWPRSPGRWITYLRMHWEQLHLETLAPSDYLAFKKE--RQVLPAND--QEPILTVDFEDFRAAPYHLQDEDTIGQGLIYMNRRLAGRLFG-NIK--TGRQSI
344199811      LAWSPSPGRWTYLRLEHRLKLEHLLLETLTAGDYLAFKKE--RQVLPAND--QEPVLTVDFEDFLAVSYRLHDEATIGQGLMYNRRLAGQLFG-DIK--AGRSI
255021595      FAWRPRPGRWIIYVRIHREQLALEELSTDAYLQAKE--GIVGLGAE--GEAVLTVDFRDFRPVSRRLRDESTIGDGLTHLNRRLAGRIFS-DLA--AGRSQI
77166514      LSVRPRIANWEYYRIHTEVMHIEITVVSQFLEFKERLVLGPTQP--QSWPLKIDMGPFNREFPRLRETRSIGRGMDFLNRHLSNQLFN-ELE--TGGQYL
300115586      LSVRPRIANWEYYRIHTEVMHIEITVVSQFLEFKERLVLGTSQP--QSWPLKIDMGPFNREFPRLKETRSIGRGMDFLNRHLSNQLFN-ELE--TGGQYL
292493898      LSIIRPGIASWEYYRIHAEVIGITETVITISQFLEFKARVLVGQQD--EPWPLKVDMGPFNREFPRLRESETRSIGRGMDFLNRHLSQLFK--ELE--TGGQCL
350552412      FAVRPRVGRWYLRHLHVDLDYPDSVEASEFLGFKERLISAQAG---TERPLEFDIEPFDRGFPKLRESRSIGRGMEFLNRKLSSQLFD--GGD--QGLEKL
220933364      LALRPRIGRWQFLRIHADDLSVEDLGVSEFLAIKERLVCAPR---HGRPLEFDIEPFNREFPRLRETRSIGRGVEFLNRKLSSQLFD--RAN--GGDLKL
350574485      LALRRRVARWQFVRLHETMDAPQSVSAEYLAFKERTATCGPE--DPGWLEIDMSPFYRDQFLKEEGSIRGGVEFLNRKLSSRLFE-ELG--KGLDRRL
95929190      LAARSTIGHWNYRLHSEETIEIDEIDVSEYLEFKERLVGYEAPS--DEYILLELDMTPFNREFPKLQEARSIGRGVEFLNRHLSSKLFV--EKR--EGSRKI
298528445      LAVRPEIAKAWQYFRFHVEDVLFEDEIGASDYLKFDEMQVNSTQV--DEFLLEIDIEPFNREFPRLKNEYTYIGKGVDFLNRHLSQGFFQ--DKK--RGHEKL
297602308      FAVRMNPGIWEYVVKHSDDLSVEGITPSEYLKFKETLYDEKWAKDDNS--LEVDFGALDLSTPHLTPSSIGNGLQVFSKFMSSKLG--GKP--ESMKPL
115457664      FAVRMNPGIWEYVVKHSDDLSVEGITPSEYLKFKETLYDEKWAKDDNS--LEVDFGALDLSTPHLTPSSIGNGLQVFSKFMSSKLG--GKP--ESMKPL

```

326504012 FAVRMNPGIWEYVKVHADDLSVEGITPSEYLFKFDLTLYDEKWAKDDNS--LEVDFGALDLSTPRLTLPSSIGNGMQFVSKFMSSKLN--GKP--ESMKPL  
115450038 FAVRMNPGIWEYVKVHSANLSVEQMTPSDYLKNKEALVDDKWAGYDDSSQLEVDGALDLSTPHLTLPSSIGKGAHLVSRFMSSKLT--DNK----KPL  
326531526 FAVRTNPGVWEFIRVHSGDLSVEQITPADYLKCKETLYDEKWARDNNS--LEVDGALDLSTPHLALPSSIGNGMQFISRFMSSKLS--GKP--ESMKPL  
242063616 LAVRRNPGVWEYITVHSGDLTVQQTTPSDYLKRRK-----EILFLYDNSSQLEVLNGLALDLSTPRLTLPSSIGNGMHLVSRFLSSRLGGGGGR--TKNKAL  
42568160 FAVRGTPGNWQYVKVNSSNLSVEALSSTQYLKLEFLFDENWANDENA--LEVDGALDFTLPWLSLSSSIGNGLSFVSSKLGGRLN-----DNPQSL  
297805240 FAVRGNPGIWQYTKVNSSNLSVEALSSTQYFKLKELLFDENWANDENA--LEVDGALDFTLPWLSLSSSIGNGVSVFSSKLGSRN-----DNPQSL  
313770765 FSIRPSPGFWEYVKVNSANLSVEGITVTDYLFKFKEMIYDENWAKDANA--LEVDGAFDFSVPHLTLSSSSIGNGLGFVSKFVTSKLSG--RL--ENAPPL  
313770767 LSIRPSPGFWEFVKVNSADLSVEGITATDYLKFKEMIYDENWAKDANA--LEVDGAFDFSVPHLTLSSSSIGNGLGFVSKFATSLSG--RL--ESAPPL  
255584097 FAIRPSPGFWEFVRVNSADLAVDGINVSEYLFKFKEMIFESWAKDVNT--LEVDGAFDFSMPLTLSSSIGNGHNFVSKFITSKLNG--RP--ENAPPL  
225466221 FSIRSNPGFWEYVKVSSDDLSEAITAADYLFKFKEMVFDENWAKDDNA--LELNFSAFDFPMPLTLSSSIGNGVSLVSKFMTSKLNG--NS--QSAQPL  
313770769 FAVRPNPGFWEYVKVNAEDLSVDEGISVSEYLLQKEMVFEKWNANENA--LELDFGAMDFSTPRLTLSSSIGNGVNYMSKFMSSKLSG--SS--EAAKPL  
313770771 FAVRPNPGFWEYVKVNAEDLSVDGISVSEYLLQKEMVFEKWNANENA--LELDFGAMDFSTPRLTLSSSIGNGLNYMSKFMSSKLRG--NS--DAAKPL  
255570671 FAVRPNPGFWEYVKVNAEDLNVGDISPSEYLLQKEMVFEKWNANENA--LEIDFGAIDFSIPRLNLSSSSIGNGMSFISKFMSSNLCG--SY--SSAKPL  
15219457 LAARPNGFWEYVKVNSGDLTVDEITATDYLKLEKESVFEKWNANENA--LEIDFGAIDFTSPRLSLSSSIGNGADYISKFISSKLG--KS--DKLEPL  
297842089 LAARPNGFWEYVKVNSGDLTVDEITANDYLLKLEKESVFEKWNANENA--LEIDFGAIDFTSPRLSLSSSIGNGADYISKFISSKLG--KS--GRLEPL  
115466896 LAIRPRPGVWDYIRVNVSELAVELSVSEYLLQKEMVFEKWNANENA--SNFVLELDFEPFNASFPSPMSKISIGNGVQFLNRHLSSKLFQ--DK--ESLYPL  
17980243 LAIRPRPGVWDYIRVNVSELAVELSVSEYLLQKEMVFEKWNANENA--SNFVLELDFEPFNASFPSPMSKISIGNGVQFLNRHLSSKLFQ--DK--ESLYPL  
162460741 LAIRPRPGVWDYIRVNVSELAVELSVSEYLLQKEMVFEKWNANENA--SNFVLELDFEPFNASFPSPMSKISIGNGVQFLNRHLSSKLFQ--DK--ESLYPL  
239984690 LAIRPRPGVWDYIRVNVSELAVELTVSEYLLQKEMVFEKWNANENA--SKFVLELDFEPFNASFPSPMSKISIGNGVQFLNRHLSSKLFQ--DK--ESLYPL  
162460681 LAIRPRPGVWEYVRNVSELAVELRVPEYLLQKEMVFEKWNANENA--NNFVLELDFEPFNASFPSPMSKISIGNGVQFLNRHLSSKLFH--DK--ESMYPL  
242035533 LAIRPRPGVWEYVRNVSELAVELRVPEYLLQKEMVFEKWNANENA--NNFVLELDFEPFNASFPSPMSKISIGNGVQFLNRHLSSKLFH--DK--ESMYPL  
62865493 LAIRPRPGVWEYVRNVSELAVELRVPEYLLQKEMVFEKWNANENA--NNFVLELDFEPFNASFPSPMSKISIGNGVQFLNRHLSSKLFH--DK--ESMYPL  
17980241 LAIRPRPGVWEYVRNVSELAVELRVPEYLLQKEMVFEKWNANENA--NNFVLELDFEPFNASFPSPMSKISIGNGVQFLNRHLSSKLFH--DK--ESMYPL  
115453437 LAIRPRPGVWEYVRNVSELAVELTVSEYLLQKEMVFEKWNANENA--NNFVLELDFEPFNASFPSPMSKISIGNGVQFLNRHLSSKLFH--DK--ESMYPL  
115473359 LAIRPRPGVWEYLRINVSQLGVEELSVPEYLLQKEMVFEKWNANENA--NNFVLELDFEPFNASFPSPMSKISIGNGVQFLNRHLSSKLFH--DK--ESMYPL  
3980298 LAIRPRPGVWEYVRNVSELGVEELSVLRYLQKEMVFEKWNANENA--NNFVLELDFEPFNASFPSPMSKISIGNGVQFLNRHLSSKLFH--DK--ESMYPL  
15242073 LAVRPRPGVWEYLRVNLHALVVEELQPAEFLHFKEELVDGKVN--GNFTLELDFEPFNASFPSPMSKISIGNGVQFLNRHLSSKLFH--DK--ESLPL  
297812265 LAVRPRPGVWEYIRVNLHALVVEELQPAEFLHFKEELVDGKVN--GNFTLELDFEPFNASFPSPMSKISIGNGVQFLNRHLSSKLFH--DK--ESLPL  
22331535 LAVRPRPGVWEYVRVNLHDLVVEELQASEYLLQKEMVFEKWNANENA--GNFTLELDFEPFNAAFPPRPTLNKYIGNGVQFLNRHLSSKLFH--DK--ESLHPL  
297818772 LAVRPRPGVWEYVRVNLHDLVVEELQASEYLLQKEMVFEKWNANENA--GNFTLELDFEPFNAAFPPRPTLNKYIGNGVQFLNRHLSSKLFH--DK--ESLHPL  
313770759 LALRPRPGVWEYIRLNVQALVVEELRVAEYLLHFKEELVDGGSN--GNFVLELDFEPFNASFPSPMSKISIGNGVQFLNRHLSSKLFH--DK--ESLHPL  
313770761 LAVRPRPGVWEYVRNVQALVVEELRVAEYLLHFKEELVDGGSN--GNFVLELDFEPFNASFPSPMSKISIGNGVQFLNRHLSSKLFH--DK--ESLHPL  
255550319 LAVRPRPGVWEYIRVNVHALVVEELRVAEYLLHFKEELVDGGSN--GNFVLELDFEPFNASFPSPMSKISIGNGVQFLNRHLSSKLFH--DK--ESLHPL  
324984223 LAVRPRPGVWEYIRVNVHALVVEELTVAEYLLHFKEELVDGGSN--GNFVLELDFEPFNSSFPSPMSKISIGNGVQFLNRHLSSKLFH--DK--ESMHPL  
258489633 LAVRPRPGVWEYIRVNVHALVVEELTVAEYLLHFKEELVDGGSN--GNFVLELDFEPFNSSFPSPMSKISIGNGVQFLNRHLSSKLFH--DK--ESMHPL  
324984221 LAVRPRPGVWEYIRVNVHALVVEELTVAEYLLHFKEELVDGGSN--GNFVLELDFEPFNSSFPSPMSKISIGNGVQFLNRHLSSKLFH--DK--ESMHPL  
324984229 LAVRPRPGVWEYIRVNVHALVVEELTVAEYLLHFKEELVDGGSN--GNFVLELDFEPFNSSFPSPMSKISIGNGVQFLNRHLSSKLFH--DK--ESMHPL  
6683114 LAVRPRPGVWEYIRVNVHALVVEELTVAEYLLHFKEELVDGGSN--GNFVLELDFEPFNSSFPSPMSKISIGNGVQFLNRHLSSKLFH--DK--ESMHPL  
4584690 LAVRPRPGIWEYLRVNVHALVVENLQPAEFLKFKEELVDGSAN--GNFVLELDFEPFTASFPSPMSKISIGNGVQFLNRHLSSKLFH--DK--ESLHPL  
3915046 LAVRPRPGIWEYLRVNVHALVVENLQPAEFLKFKEELVDGSAN--GNFVLELDFEPFTASFPSPMSKISIGNGVQFLNRHLSSKLFH--DK--ESLHPL  
3766299 LAVRPRPGVWEYLRVNVHALVVENLQPAEFLKFKEELVDGSAN--GNFVLELDFEPFTASFPSPMSKISIGNGVQFLNRHLSSKLFH--DK--ESLHPL  
3377764 LAVRPRPGVWEYLRVNVHALVVENLQPAEFLKFKEELVDGSAN--GNFVLELDFEPFTASFPSPMSKISIGNGVQFLNRHLSSKLFH--DK--ESLHPL  
225444613 FAVRPRPGVWEYIRVNVSAVVVEELLVPEYLLHFKEELVDGGSN--GNFVLELDFEPFTASVPRPTLSKISIGNGVQFLNRHLSSKLFH--DK--DSMQPL  
3660531 LAIRLRPGVWEYVRNVNALSVEELTVPEFLQKEMVFEKWNANENA--GNFVLELDFEPFTASFPKPTLTLSKISIGNGVQFLNRHLSSKLFH--DK--ESMTPL  
31455440 LAIRLRPGVWEYIRVNVNALSVEELTVPEFLQKEMVFEKWNANENA--GNFVLELDFEPFTASFPKPTLTLSKISIGNGVQFLNRHLSSKLFH--DK--ESMTPL  
304651488 LAIRLRPGVWEYVRNVNALSVEELTVPEFLQKEMVFEKWNANENA--GNFVLELDFEPFTASFPKPTLTLSKISIGNGVQFLNRHLSSKLFH--DK--ESMTPL  
28629438 LAIRLRPGVWEYVRNVNALSVEELTVPEFLQKEMVFEKWNANENA--GNFVLELDFEPFTASFPKPTLTLSKISIGNGVQFLNRHLSSKLFH--DK--ESMTPL

115310618 LAIRLRPGVWEYVRNVHALVVEELTVPEYLHFKEELVDGSKN---GNFVLELDFEPFTASFPKPTLTKYIGDGVFEFLNRHLSAKMFH--DK--ESMAPL  
345286417 LAIRLRPGVWEYVRNVNALVVEELTVPQYLHFKEELVNGAAN---GNFVLELDFEPFTASFPKPTLTLSIGNGVFEFLNRHLSAKMFH--DR--ESMTPL  
38425095 LAVRPRPGIWEYIRVNDALAVEELTPSQFLHVKEELVDGSTN---GNFVLELDFEPFTASFPKPTLTLSIGNGVFEFLNRHLSAKMFH--DK--ESMRPL  
15235300 LAVRPRPGVWEYVRNVFELSVEQLTVSEYLRKFKEELVDGPNS---DPFVLELDFEPFNANVPRPSRSSSIGNGVQFLNRHLSVSMFR--NK--DCLEPL  
297814081 LAVRPRPGVWEYVRNVFELSVEQLTVSEYLRKFKEELVDGPNS---DPFVLELDFEPFNANVPRPSRSSSIGNGVQFLNRHLSVSMFR--NK--DCLEPL  
6682841 IAVRPRPGVWEYVRNVYELSVESYELHFKEELVDAAFN---ERFVLELDFEPFNATFPRPNRSSSIGNGVQFLNRHLSVSMFR--NK--DCLEPL  
255564236 IAIRPRPGIWEYVRNVHDLVSEQLDVSQYLRKFKEELVDGSSN---DPVLELDFEPFNADVPKPHRSSSIGNGVQFLNRHLSVSMFR--NK--DCLEPL  
313770763 VSIIRPRPGVWEYVRVDVSQLNVEELTVSQYLRKFKEELVDGPN---DPVLELDFEPFNAAFPRPTRSSSIGNGVQYLRHLSVSMFR--NK--DTLEPL  
3915037 IAVRPRPGVWEYVRNVFELSVEQLTVSEYLSKFKEELVDGKSN---DNILELDFEPFNASFPKPTRSSSIGNGVQFLNRHLSVSMFR--NK--DCLEPL  
225437428 IAVRPRPGVWEYVRNVHLSVDQLSVSEYLRKFKEELVDGMFN---DYYVLELDFEPFNASFPKPTRSSSIGNGVQFLNRHLSVSMFR--NK--ESLEPL  
162458268 IAVRPRPGVWEYVRNVHLSVEQLTVSEYLRKFKEELVDGQHN---DPVLELDFEPFNVSVPKPNRSSSIGNGVQFLNRHLSVSMFR--NR--DCLEPL  
242035817 IAVRPRPGVWEYVRNVHLSVEQLTVSEYLRKFKEELVDGQHN---DPVLELDFEPFNASVPKPNRSSSIGNGVQFLNRHLSVSMFR--NR--DCLEPL  
115452927 IAVRPRPGVWEYVRNVHLSVEQLTVSEYLRKFKEELVDGQYN---DPVLELDFEPFNASVPKPNRSSSIGNGVQFLNRHLSVSMFR--NK--DCLEPL  
241896730 IAVRPRPGVWEYVRNVHLSVEQLTVSEYLRKFKEELVDGQHN---NPVLELDFEPFNATLIPRPSRSSSIGNGVQFLNRHLSVSMFR--NR--DCLEPL  
304651490 IAVRPRPGVWEYVRNVYDLVSEQLTVPEYLRKFKEELVDGEDH---HLFVLELDFEPFNASVPKPNRSSSIGNGVQFLNRHLSVSMFR--SN--ESLDEL  
29289943 IAVRPRPGVWEYVRNVYDLVSEQLTVPEYLRKFKEELVDGEDN---DLFVLELDFEPFNASVPKPNRSSSIGNGVQFLNRHLSVSMFR--SK--ESLDEL  
115310620 IAVRPRPGVWEYVRNVYELSDQLSISEYLRKFKEELVDGRSE---DHLVLELDFEPFNATFPRPTRSSSIGNGVQFLNRHLSVSMFR--NK--DSLEPL  
4468153 LAVRPRPGVWEYVRNVYQLSVDELTVSEYLRKFKEELVDGGID---DNFVLELDFEPFNASFPKPTRSSSIGNGVQFLNRHLSVSMFR--NK--DCLEPL  
345286419 IAIRPRPGVWEYVRNVYELSDDELTVSEYLRKFKEELVDGQHD---DHYVLELDFEPFNATFPRPTRSSSIGNGVQFLNRHLSVSMFR--NK--ESLDEL  
4468151 LAVRPRPGVWEYVRNVYELSDDELTVSEYLRKFKEELVDGQHD---DHYVLELDFEPFNATFPRPTRSSSIGNGVQFLNRHLSVSMFR--NK--DSLEPL  
151176306 IAVRPRPGVWEYVRNVSELNVEQLTVSEYLRKFKEELVDGKAD---DHYVLELDFEPFNESVPKPNRSSSIGNGVQFLNRHLSVSMFR--NK--DCLEPL  
14530225 IAVRPRPGVWEYVRNVSELNVEQLTVSEYLRKFKEELVDGKAD---DHYVLELDFEPFNESVPKPNRSSSIGNGVQFLNRHLSVSMFR--NK--DCLEPL  
15239816 LAIRPRPGVREYVRNVYELSDHLLTVSEYLRKFKEELVNGHAN---GDYVLELDFEPFNATLPRPTRSSSIGNGVQFLNRHLSVSMFR--NK--ESMEPL  
297795665 IAVRPRPGVWEYVRNVYELSDHLLTVSEYLRKFKEELVNGHAN---GDYVLELDFEPFNATLPRPTRSSSIGNGVQFLNRHLSVSMFR--NK--ESMEPL  
225431790 IAIRPRPGVWEYVRNVYELNVDQLSVSEYLRKFKEELVDGQIK---GNVLELDFEPFNATFPRPTRSSSIGNGVQFLNRHLSVSMFR--NK--ESLEPL  
255551835 MAIRPRPGVWEYVRNVYELSDHLLTVSEYLRKFKEELVDGECN---ESYVLELDFEPFNATFPRPTRSSSIGNGVQFLNRHLSVSMFR--QK--ESLEPL  
168009716 FAVRPRPGIWEYVRINVVEELTLEELSVSEYLSFKEQLAN-GTEY---DPFVLELDFAPFNANFPMTRPSSIGHGVQFLNRHLSKLFH--TP--DSMEPL  
168035060 LAVRPRPGIWEYLRINVVEELTLEELSVSEYLSFKEQLANSTDVP---DGFLELDFEPFNANFPMTRPSSIGHGVQFLNRHLSKLFH--TA--DGIEPL  
168058907 FAVRPRPGIWEYVRINVVEELTLEELSVSEYLSFKEQLANSTDVP---DGFLELDFEPFNANFPMTRPSSIGHGVQFLNRHLSKLFH--NP--ESMEPL  
168029793 LAIRPRPGIWEYVRINVVEELTLEELSVSEYLSFKEQLANSTDVP---DGFLELDFEPFNANFPMTRPSSIGHGVQFLNRHLSKLFH--NP--ESMEPL  
94266940 IVYRHRANCLIFAINQSDKLLKLSVGDFLAIKERLLRPELPP---QORTLNINLAPFYDYGPTLKDPNTIGQGIKFLNRHMSGRLANHPEK---WNRFL  
94264333 IVYRHRANCLIFAINQSDKLLKLSVGDFLAIKERLLRPELPP---QORTLNINLAPFYDYGPTLKDPNTIGQGIKFLNRHMSGRLANHPEK---WNRFL  
297569306 ILVYRHRANCLIFAINQSDKLLKLSVGDFLAIKERLLRPELPP---QORTLNINLAPFYDYGPTLKDPNTIGQGIKFLNRHMSGRLANHPEK---WNRFL  
254416162 LIIRPKIAEQEAF-QVLELTVETIITQTLTLDVDRFVNHYPN---EGDVLLELDFEPFNATFPRPTRSSSIGNGVQFLNRHLSKLFQDPRQ---WQESL  
332712456 LIIRPKIAEQEAF-QVLELTVETIITQTLTLDVDRFVNHYPN---EGDVLLELDFEPFNATFPRPTRSSSIGNGVQFLNRHLSKLFQDPRQ---WQESL  
17232477 FIIRPKIAEQEVY-RLTADLDVEPMTVQELLDLDRDLVNFHYPH---EGDVLLELDFEPFNATFPRPTRSSSIGNGVQFLNRHLSKLFQDPRQ---WQESL  
75908500 FIIRPNIAEQEVY-RLTADLDVEPMTVQELLDLDRDLVNFHYPH---EGDVLLELDFEPFNATFPRPTRSSSIGNGVQFLNRHLSKLFQDPRQ---WQESL  
186682280 FIIRSKIAEQEVY-WLTSDLSEIEMTVQELLDLDRDLVNFHYPH---EGDVLLELDFEPFNATFPRPTRSSSIGNGVQFLNRHLSKLFQDPRQ---WQESL  
119512682 FIIRPKIAEQEVY-RLTEDLVNEMSVQELLDLDRDLVNFHYPH---EGDVLLELDFEPFNATFPRPTRSSSIGNGVQFLNRHLSKLFQDPRQ---WQESL  
334117431 VIVRPRPGIWEYVRINVVEELTLEELSVSEYLSFKEQLANSTDVP---DGFLELDFEPFNANFPMTRPSSIGHGVQFLNRHLSKLFH--TP--DSMEPL  
218440696 IVYRPKIARQEVY-RLREDTPIELHVSQQLDVRDHFVNQFHPD---EGDVFEIDFEPFYDYSPTIRDSKNIGKGVQFLNRHLSKLFQDPRQ---WQESL  
159031025 LVVRPQIALSQAF-RLTDDLTCEPISVQELLDLDRDLVNFHYPH---EGDVLLELDFEPFNATFPRPTRSSSIGNGVQFLNRHLSKLFQDPRQ---WQESL  
220907171 LVLRPNIASQSVF-RITSDLAEEEMRVKELLTVRDLVQRHHPH---EGELLELDFEPFYDYSPTIRDAKNIGKGMQLLTRYLSSKLFQDPRQ---WQESL  
22298591 WIVRPRPGIWEYVRINVVEELTLEELSVSEYLSFKEQLANSTDVP---DGFLELDFEPFNANFPMTRPSSIGHGVQFLNRHLSKLFH--TP--DSMEPL  
158339122 LIIRPKIAEQEAF-QVLELTVETIITQTLTLDVDRFVNHYPN---EGDVLLELDFEPFNATFPRPTRSSSIGNGVQFLNRHLSKLFQDPRQ---WQESL  
284053161 LIVRPRPGIWEYVRINVVEELTLEELSVSEYLSFKEQLANSTDVP---DGFLELDFEPFNANFPMTRPSSIGHGVQFLNRHLSKLFH--TP--DSMEPL  
209523126 LIVRPRPGIWEYVRINVVEELTLEELSVSEYLSFKEQLANSTDVP---DGFLELDFEPFNANFPMTRPSSIGHGVQFLNRHLSKLFH--TP--DSMEPL

```

17228554 FVVRPRIASQEVWRLTSDIAKFDSMSIDAFLDVSDRLVNAYEP-----NILEIDLNSFYEASPSISDPRNIGQGLAFLNRYLCSQIATDPQY---WVELV
75909957 FVVRPRIANQEVWRLTSDIAKFDSMPIDAFLDVSDRLVNAYEP-----NILEIDLSSFYEASPSISDPRNIGQGLAFLNRYLCSQIATDPQY---WVELV
186685043 FVIRPKIANQEVWRLTANLDSFEQMTQQALLDVRDLVNRYQP-----GILEIDLHPFYEDSPRIDDPNIGQGLAYLNRYLCNQLLTDPQY---WVELV
119510624 FVVRPRIGSQQMWRLQADFSGFEPMPQAWLDVSDRLVNRYQP-----HILEIDFQPPFAESTRITDPRNIGQGLAFLNRYLCDQLSNDTHY---WLEVI
298489784 FVVRPRIASQEVWRLTADFTHFDLMTTPKAFLDVSDRLVNRYQP-----HILEIDLHPFYQTSPRISDPRIGQGLTFLNHYLCNQFVSDPQY---WLETF
220909283 LLVRSTINDQQIWQISTDLNRYGRMSPHDLLEVRDRLVNRSQS-----SILEINVPFFYNMAYAVEDPRNIGQGLAFLNHYLCNQVVSIDRTR---WLDVL
332708740 LLLRTRVASQEIYRLAADLTSFEPMPVEELLSLRDRWVKRYFPE--KGGLEIDVGPFYKNTPTIRDPKIGNGLEFLNRYLSSQLFADSEQ---WLEEL
Clustal Consensus      *          :          :          : . . . :          : * *          : .

```

210 220 230 240 250 260 270 280 290 300

```

114331077 LHLFLGVHTID-----GQQLMFTSNSHNINMVRSQLRQALEMLEAVDGTTPWAEELSSDMSKIGFAPGWGHNAARVAETMNMMLDILEAPSPSALEA
30249199 LHLFLGVHAIE-----GQQLMFSNNSHDIHAVRNQLRQALEMLETLDGTTPIWIELAPKMNQLGFAPGWGHANRVAETMNMMLDILEAPSPSALEE
82703384 LHLFLTVHSMD-----GKQLMLGGNFADVPAALRSGLRRALSMLKYPDDTEWKDVAEPLGGIGFAPGWGNCVGRVSETMSILLVDILEAPSPQILES
198283392 LDFLAVHKLN-----GQSLMVHDQPPDFEALR---QTVQYLATLPKTKPWTEFAAEMTYRGFAPGWGDTAGRVRETMRLLMDLLDAPSAEGLQA
344199811 LDFLAVHKLN-----GQSLMVHDQPPDFEALR---RTVQYLATLPKTKQAWTEIAAEMTHRGFAPGWGDTVGRVRETMRLLMDLLDAPSAEGLQA
255021595 LEFLSLHRLD-----GQNLMLSGNNTDFDSLRL---QTVQYLGTLPRETPWAEIREDMRRRGFAPGWGNTAGRVRETMRLLMDLLDSPSPALES
77166514 LSFLSVHHCN-----GQPLMLNDRIQDVQGLRCAALRLAMDFLGGFQEAEEWDVAVGHKLQELGFERGWGRTAARIQDSFSILLMDILEAPEPGNLEH
300115586 LSFLSVHHCN-----GQPLMLNDRIQDVQGLRRAALRLAMDFLGGFQEAEEWDVAVGHKLQELGFERGWGRTAARMQDSFSILLMDILEAPEPGNLEH
292493898 LNFLRMHSHR-----GQPLMLNDRIQDLRGLRRALRLAMDFLGGFQEAEEWDVAVGHKLQELGFERGWGRTAARMQDSFSILLMDILEAPEPGNLEH
350552412 FHLFLHEHCCE-----GQILMINERVNRVNEELRGVIRRCCKLLNGYARHTPWAEEVAPLLRDVGLPEGWGSDVGRILETLRLSLLDLEAPSPETLER
220933364 FRFLREHRCN-----GRLLMINDRIRDVDAIRVAIRDAEQRLARLKRDPWADFAPLQDLGFEPGWGRTAGRVQETRLRLSELLEAPSPESLER
350574485 LNFLRMHSHR-----GQVLMNDTITDVAGLRNALRQALLPLRRRAASTPYEELAPDLRLGFEPGWGCDAAARVNTMGLLLDILEAPSPQITIEE
95929190 LDFLRVHQHR-----STQMLMNGMIEDVPGLOALARKGVKFLKNCEDETCWDDPTMMSYGFQPGWGRTELEDILEMFHMLMDILEAPDPQNLK
298528445 FEFLRLHQIE-----GKQLMLNGHIEVSGLSALRKALTFLLKKQDPSQKWSGISRHMQLGFPGWGKDVERVRENLELLREILEAPTNPILAS
297602308 LDYLLTLNRY-----GEKLMINDTIDTVSKLQATALLLAEVFFVSGLPKYTPYLKFEQRFQEWGLEKGGWDTAERCKETLNCLSEVLQAPDPINMEK
115457664 LDYLLTLNRY-----GEKLMINDTIDTVSKLQATALLLAEVFFVSGLPKYTPYLKFEQRFQEWGLEKGGWDTAERCKETLNCLSEVLQAPDPINMEK
326504012 LDYLLALNRY-----GEKLMVNDTIDTVNKLQATALLLAEVFFVSGLPKFTPYLKFQRFQEWGLEKGGWGENAERCKETLNFLSEVLQAPDPINMEK
115450038 LDYLLALSHR-----GDKLMINDILDVTKLQATALLLAEVYVAGLHPDNYSEFEQKFQEWGLEKGGWDTAETCKETLSSSLSEVLQAPDPINMEK
326531526 LDYLLALNRY-----GEKLMISDSLDTADKLQATALLLAEVFFVASLEKSTPYQQFEQKFQEWGLEKGGWDTAETCRETNLFSEVLQAPDPINMEK
242063616 LDYLLALRYRRRPGDQQQINNKLISDITLDTVGKLQALLLAQAFVSEQHPDTPYQQMAHRFQEWGLEKGGWDTAEACGHTLACLAELVQAPDPASIEHR
42568160 VDYLLSLEHQ-----GEKLMMNETLNTARKLEMSLILADVFLSELPKDTPFQAFELRFKECGFEKGGWESAGRVKETMRILSEILQAPDPQNIDR
297805240 VDYLLSLEHQ-----GEKLMMNETLNTARKLEMSLILADVFLSELPKDTPFQAFELRFKECGFEKGGWESAGRVKETMRILSEILQAPDPHNIDR
313770765 VDYLLSLNRQ-----GEKLMINETLGTGKLQMALIVAEEVYLSGLAKDTPYQNFETISFKEWGFEKGGWDTAERVKETMRCLSEVLQAPDPINMEK
313770767 VDYLLSLNHE-----GEKLMINETLSSVRKLRLMALIVAEEYLSGLPKDTPYQNFETISFKAWGFEKGGWNTAERVKETMRCLSEVLQAPDPINMEK
255584097 VDYLLSLTHH-----GEKLMINETLSTVAKLQMALIVAEEVYLSGLAGDTPYQNFETISFKEWGFEKGGWDTAERAKETMRSLSEVLQAPDPINMEK
225466221 VDYLLSLNHQ-----GEKLMITNTLNTPTKLQMALIVAEEVFFVSALPKDTPYPSFELRFKEWGFEGKGGWNTAERVKETMRSLSEALEAPDPINMEK
313770769 LDYLLALNHQ-----GENLMINQTLDTVAKLQALIVAEEVVSAFPKDTPYQDFQQRRLRELGFETGWGDTAERVKETMRLLSESLQAPYPMKLQL
313770771 LDYLLALDHQ-----GENLMINQALDSVSKLQALIVAEEVVSAFPKDAPYQDFQQSLKRLGFEGKGGWDTAERVKETMRMLSESLQAPEPVKLEL
255570671 LDYLLALNRY-----GENLMINEKLDTVAKLQKALVSVFSSKEAAYKNVQDQSLKEMGFEGKGGWNTAERVKETMRLLSESLQAPDPINMEK
15219457 LNYLLRLNHH-----GENLMINDDLNTVAKLQKSLMLAVIVVSTYSKHTPYETFAQRLKEMGFEGKGGWDTAERVKETMIILSEVLEAPDNGKLDL
297842089 LNYLLRLNHH-----GENLMINDDLNTVAKLQKSLMLAVIVVSTYPKHTPYETFAIRLKEMGFEKGGWDTAERVKETMVMLSEVLEAPDNVKLDL
115466896 LNFLKAHNHK-----GTTMMLNDRIQSLRGLQSSLRKAEYLYMGIPQDTPYSEFNHRFQELGLEKGGWDCAKRVLDTIHLLLDLLEAPDPANLEK
17980243 LNFLKAHNHK-----GTTMMLNDRIQSLRGLQSSLRKAEYLYMSFPQDTPYSEFNHRFQELGLEKGGWDTAKRVLDTIHLLLDLLEAPDPANLEK
162460741 LNFLKAHNYK-----GTTMMLNDRIQSLRGLQSSLRKAEYLYSVQDTPYSEFNHRFQELGLEKGGWDTAKRVLDTIHLLLDLLEAPDPANLEK
239984690 LNFLKAHNYK-----GTTMMLNDRIQSLRGLQSSLRKAEYLYSIPEDTPSPSEFNHRFQELGLEKGGWDTAKRVLDTIHLLLDLLEAPDPASLEK
162460681 LNFLRAHNYK-----GMTMMLNDRIRSLSALQGLARKAEHLLSTLQADTPYSEFHHRFQELGLEKGGWDCAKRAQETIHLLLDLLEAPDPSTLEK

```



242035533 LNFLRAHNYK-----GMTMMLNDRIRSLQALRKAEEHLSTLQADTPYSEFHHRFQELGLEKGGWGDCAKRAQETIHLLLDLLEAPDPSTLEK  
62865493 LNFLRAHNYK-----GMTMMLNDRIRSLQALRKAEEHLSGLSADTPSYSDFHHRFQELGLEKGGWGDCAKRAQETIHLLLDLLEAPDPSTLEK  
17980241 LNFLRAHNYK-----GMTMMLNDRIRSLQALRKAEEHLSGLSADTPSYSDFHHRFQELGLEKGGWGDCAKRAQETIHLLLDLLEAPDPSTLEK  
115453437 LNFLRAHNYK-----GMTMMLNDRIRSLQALRKAEEHLSGLSADTPYSEFHHRFQELGLEKGGWGDCAKRSQETIHLLLDLLEAPDPSTLEK  
115473359 LNFLRAHNYK-----GMTMMLNDRIRSLDALQALRKAEEHLAGITADTPYSEFHHRFQELGLEKGGWGDCAQVRVRETIHLLLDLLEAPEPSALEK  
3980298 LNFLRAHNYK-----GMAMMLNDRIRSLGTLQALRKAETHLSGLPADTPYSEFHHRFQELGLEKGGWGDCAQRASSETIHLLLDLLEAPDPSSLEK  
15242073 LKFLRLHSHQ-----GKNLMLS EKIQLNLTQHILRKAEEYLAELKSETLYEEFEAKFEEIGLERGGWGDNAERVLDIMIRLLLDLLEAPDPCTLET  
297812265 LKFLRRHSHQ-----GKNLMLS EKIQLNLTQHILRKAEEYLAELKPEPTYEEFEAKFEEIGLERGGWGDNAERVLDIMIRLLLDLLEAPDPCTLET  
22331535 LKFLRLHSHQ-----GKTLMLNDRIRSLQALRKAEEYLMELKPEPTYEEFEAKFEEIGLERGGWGDNAERVLDIMIRLLLDLLEAPDPCTLET  
297818772 LKFLRLHSHQ-----GKTLMLNDRIRSLQALRKAEEYLMELKPEPTYEEFEAKFEEIGLERGGWGDNAERVLDIMIRLLLDLLEAPDPCTLET  
313770759 LKFLRVHSHQ-----GKTLMLNDRIRSLQALRKAEEYLMELKPEPTYEEFEAKFEEIGLERGGWGDNAERVLDIMIRLLLDLLEAPDPCTLET  
313770761 LKFLRVHSHQ-----GKTLMLNDRIRSLQALRKAEEYLMELKPEPTYEEFEAKFEEIGLERGGWGDNAERVLDIMIRLLLDLLEAPDPCTLET  
255550319 LEFLRVHSHQ-----GKTLMLNDRIRSLQALRKAEEYLMELKPEPTYEEFEAKFEEIGLERGGWGDNAERVLDIMIRLLLDLLEAPDPCTLET  
324984223 LEFLRVHSHQ-----GKTLMLNDRIRSLQALRKAEEYLMELKPEPTYEEFEAKFEEIGLERGGWGDNAERVLDIMIRLLLDLLEAPDPCTLET  
258489633 LEFLRVHSHQ-----GKTLMLNDRIRSLQALRKAEEYLMELKPEPTYEEFEAKFEEIGLERGGWGDNAERVLDIMIRLLLDLLEAPDPCTLET  
324984221 LEFLRVHSHQ-----GKTLMLNDRIRSLQALRKAEEYLMELKPEPTYEEFEAKFEEIGLERGGWGDNAERVLDIMIRLLLDLLEAPDPCTLET  
324984229 LEFLRVHSHQ-----GKTLMLNDRIRSLQALRKAEEYLMELKPEPTYEEFEAKFEEIGLERGGWGDNAERVLDIMIRLLLDLLEAPDPCTLET  
6683114 LEFLRVHSHQ-----GKTLMLNDRIRSLQALRKAEEYLMELKPEPTYEEFEAKFEEIGLERGGWGDNAERVLDIMIRLLLDLLEAPDPCTLET  
4584690 LEFLRVHSHQ-----GKTLMLNDRIRSLQALRKAEEYLMELKPEPTYEEFEAKFEEIGLERGGWGDNAERVLDIMIRLLLDLLEAPDPCTLET  
3915046 LEFLRVHSHQ-----GKTLMLNDRIRSLQALRKAEEYLMELKPEPTYEEFEAKFEEIGLERGGWGDNAERVLDIMIRLLLDLLEAPDPCTLET  
3766299 LEFLRVHSHQ-----GKTLMLNDRIRSLQALRKAEEYLMELKPEPTYEEFEAKFEEIGLERGGWGDNAERVLDIMIRLLLDLLEAPDPCTLET  
3377764 LEFLRVHSHQ-----GKTLMLNDRIRSLQALRKAEEYLMELKPEPTYEEFEAKFEEIGLERGGWGDNAERVLDIMIRLLLDLLEAPDPCTLET  
225444613 LEFLRVHSHQ-----GKTLMLNDRIRSLQALRKAEEYLMELKPEPTYEEFEAKFEEIGLERGGWGDNAERVLDIMIRLLLDLLEAPDPCTLET  
3660531 LEFLRVHSHQ-----GKTLMLNDRIRSLQALRKAEEYLMELKPEPTYEEFEAKFEEIGLERGGWGDNAERVLDIMIRLLLDLLEAPDPCTLET  
31455440 LEFLRVHSHQ-----GKTLMLNDRIRSLQALRKAEEYLMELKPEPTYEEFEAKFEEIGLERGGWGDNAERVLDIMIRLLLDLLEAPDPCTLET  
304651488 LEFLRVHSHQ-----GKTLMLNDRIRSLQALRKAEEYLMELKPEPTYEEFEAKFEEIGLERGGWGDNAERVLDIMIRLLLDLLEAPDPCTLET  
28629438 LEFLRVHSHQ-----GKTLMLNDRIRSLQALRKAEEYLMELKPEPTYEEFEAKFEEIGLERGGWGDNAERVLDIMIRLLLDLLEAPDPCTLET  
115310618 LEFLRVHSHQ-----GKTLMLNDRIRSLQALRKAEEYLMELKPEPTYEEFEAKFEEIGLERGGWGDNAERVLDIMIRLLLDLLEAPDPCTLET  
345286417 LEFLRVHSHQ-----GKTLMLNDRIRSLQALRKAEEYLMELKPEPTYEEFEAKFEEIGLERGGWGDNAERVLDIMIRLLLDLLEAPDPCTLET  
38425095 LEFLRVHSHQ-----GKTLMLNDRIRSLQALRKAEEYLMELKPEPTYEEFEAKFEEIGLERGGWGDNAERVLDIMIRLLLDLLEAPDPCTLET  
15235300 LEFLRVHSHQ-----GKTLMLNDRIRSLQALRKAEEYLMELKPEPTYEEFEAKFEEIGLERGGWGDNAERVLDIMIRLLLDLLEAPDPCTLET  
297814081 LEFLRVHSHQ-----GKTLMLNDRIRSLQALRKAEEYLMELKPEPTYEEFEAKFEEIGLERGGWGDNAERVLDIMIRLLLDLLEAPDPCTLET  
6682841 LEFLRVHSHQ-----GKTLMLNDRIRSLQALRKAEEYLMELKPEPTYEEFEAKFEEIGLERGGWGDNAERVLDIMIRLLLDLLEAPDPCTLET  
255564236 LEFLRVHSHQ-----GKTLMLNDRIRSLQALRKAEEYLMELKPEPTYEEFEAKFEEIGLERGGWGDNAERVLDIMIRLLLDLLEAPDPCTLET  
313770763 LEFLRVHSHQ-----GKTLMLNDRIRSLQALRKAEEYLMELKPEPTYEEFEAKFEEIGLERGGWGDNAERVLDIMIRLLLDLLEAPDPCTLET  
3915037 LEFLRVHSHQ-----GKTLMLNDRIRSLQALRKAEEYLMELKPEPTYEEFEAKFEEIGLERGGWGDNAERVLDIMIRLLLDLLEAPDPCTLET  
225437428 LEFLRVHSHQ-----GKTLMLNDRIRSLQALRKAEEYLMELKPEPTYEEFEAKFEEIGLERGGWGDNAERVLDIMIRLLLDLLEAPDPCTLET  
162458268 LEFLRVHSHQ-----GKTLMLNDRIRSLQALRKAEEYLMELKPEPTYEEFEAKFEEIGLERGGWGDNAERVLDIMIRLLLDLLEAPDPCTLET  
242035817 LEFLRVHSHQ-----GKTLMLNDRIRSLQALRKAEEYLMELKPEPTYEEFEAKFEEIGLERGGWGDNAERVLDIMIRLLLDLLEAPDPCTLET  
115452927 LEFLRVHSHQ-----GKTLMLNDRIRSLQALRKAEEYLMELKPEPTYEEFEAKFEEIGLERGGWGDNAERVLDIMIRLLLDLLEAPDPCTLET  
241896730 LEFLRVHSHQ-----GKTLMLNDRIRSLQALRKAEEYLMELKPEPTYEEFEAKFEEIGLERGGWGDNAERVLDIMIRLLLDLLEAPDPCTLET  
304651490 LEFLRVHSHQ-----GKTLMLNDRIRSLQALRKAEEYLMELKPEPTYEEFEAKFEEIGLERGGWGDNAERVLDIMIRLLLDLLEAPDPCTLET  
29289943 LEFLRVHSHQ-----GKTLMLNDRIRSLQALRKAEEYLMELKPEPTYEEFEAKFEEIGLERGGWGDNAERVLDIMIRLLLDLLEAPDPCTLET  
115310620 LEFLRVHSHQ-----GKTLMLNDRIRSLQALRKAEEYLMELKPEPTYEEFEAKFEEIGLERGGWGDNAERVLDIMIRLLLDLLEAPDPCTLET  
4468153 LEFLRVHSHQ-----GKTLMLNDRIRSLQALRKAEEYLMELKPEPTYEEFEAKFEEIGLERGGWGDNAERVLDIMIRLLLDLLEAPDPCTLET  
345286419 LEFLRVHSHQ-----GKTLMLNDRIRSLQALRKAEEYLMELKPEPTYEEFEAKFEEIGLERGGWGDNAERVLDIMIRLLLDLLEAPDPCTLET  
4468151 LEFLRVHSHQ-----GKTLMLNDRIRSLQALRKAEEYLMELKPEPTYEEFEAKFEEIGLERGGWGDNAERVLDIMIRLLLDLLEAPDPCTLET

151176306 LDFLRVKHKH-----GVVVMLNDRIQTIQRQLQSALSKAEDYLIKLPADTPYSEFEFVIQGMGFERGWGDTAERVLEMMHLLLDILQAPDPSTLET  
14530225 LDFLRVKHKH-----GVVVMLNDRIQTIQRQLQSALSKAEDYLIKLPADTPYSEFEFVIQGMGFERGWGDTAERVLEMMHLLLDILQAPDPSTLET  
15239816 LEFLRTHKHD-----GRPMMLNDRIQNIPILQGALARAEELFSKLPLATPYSEFEFELQMGFERGWGDTAQKVSEMVHLLLDILQAPDPSVLET  
297795665 LEFLRTHKHD-----GRSMMLNDRIQNIPILQGALARAEELFSKLPLATPYSEFEFELQMGFERGWGDTAQKVSEMVHLLLDILQAPDPSVLET  
225431790 LDFLRAHKHD-----GHVVMLNDRIQNISRQLSALARAEEYLSKLPPLTPTYSEFEFELQMGFEKGWGDTAQVRSEMVHLLLEILQAPDPSTLET  
255551835 LEFLRTHKHD-----GHALMLNDRIQNLSLHYALARAAEHLSKFPNPTPFSEFEFDLQSMGFERGWGDRAERSEMVHLLMDILQAPDPASLES  
168009716 YEFRLMHTYR-----GQTLMMLNDRIASLVRLRPQLVKAEALEFLERCKHPDDLEFAHQQLGLGLEKGWGNAGRAETIKMLQDLLQAPDPDTLEK  
168035060 FQFLRMHTYR-----GQTLMMLNDRIISLRRLRPQLVKADDILSKLPEDTPTFDAHKLQGLGLEKGWNTAGRVEITIKLEDLLQAPDPDTLEK  
168058907 FQFLRLHTYR-----GETLMMLNERIATFSRFRPQLVRAEEALSCLPEDTPTSSFAHRQLQGLGLEKGWNTAGRVLQTLKLLDLQAPDPDTLEK  
168029793 VEFMRVHKYK-----DQTTLLNESITNVVRLRALIKAEEYLICKLPNDQPKDFYSKLGLEGLERGWDTAGRVELMHLLLDILQAPDPDILEK  
94266940 YEFKLKHQLH-----GIQLLLDGERVRNPVQLEDALAAALDFLERCHWPDDLERLRQLRRRLGFLDGWDSLPRILETMHMLQDILEQPDEANLEE  
94264333 YEFKLKHQLH-----GTQLLLDGERVRNPVQLEDALAAALDFLERCHWPDDLERLRQLRRRLGFLDGWDSLPRILETMHMLQDILEQPDEANLEE  
297569306 YEFKLKHQLH-----GTQLLLDGSLVRSPHEELBEALSAMDPLERCYPDDLARISQRLGRGLGFLAGWGNLSLPRMLETMHMLQDILEQPDEANLEE  
254416162 FNFLSLHEVQ-----GTQLLIN-GRKSQQQLSDQVKLAGFVSVDRAEDEPYESFRFKLQDMGFEGAGWNTASRVRETLELIDDELIDSPDHQVLEA  
332712456 YGFLKVRHFH-----GNQLLIN-ERIHNHQLSEQVKLALEFVSDRDPDEYDKFRFKLQEMGFEPGWGNTASRVRETLAMDELIDDELIDSPDHQVLEA  
17232477 FNFLRLHNYN-----GIQLLIN-HQIQSQQLSQQVKNALNFVSDRPNDEPYEQFRLQLQTMGFEPGWGNTASRVRTLNLIDELIDSPDPQTLEA  
75908500 FNFLRLHNYN-----GIQLLIN-YQIQSQQLSQQVKKALNFVSDRPHDEPYEQFRLQLQAMGFEPGWGNTASRVRTLNLIDELIDSPDPQTLEA  
186682280 LNFLRLHHYN-----GVQLLVN-DRIQSQQLSEQVKKAIGFVNNRPDDEPYEQFRFQLQMGFEPGWGNTAARVRETLNLIDELIDSPDPQTLEA  
119512682 LNFLRLHNYN-----GVQLLIN-DRITTQQQLSTQIKAITFVSDRPHDEPYEQFRFELQMTGFEPGWGNTAKRGVDTLIDELIDSPDPQTIEA  
334117431 FNFLRLHRYN-----GVQLLIN-DRIKSQEQLSEQVKKALTFFVSDLSEEEGYERFRLVLQMGGFEGAGWNTAARVHETLGLIDELIDSPDPQTLEA  
218440696 FNFLSLHCYN-----GITLLIN-GRKNQHQLSEQVKDAIFFLNQFSDIPEEDFRYEFGSMGFEPGWGNTAGRVEKTSILDELIDSPDQVLEA  
159031025 FQFLRMHNYN-----GITLLIN-DRIGNQRQLSQQVKALDFLESYSEEPYSNLRFELQSLGFEPGWGNTASRMRESLELIDLGLIDAPDHQVLEA  
220907171 FQFLSLHRYD-----GNQLLIS-ERIKNHQLSMQVKQALHLVNSQPPQALFSDDFRELQNGFEPGWGNTAARVRETLLELIDSPDHQVLEA  
22298591 FNFLRIHRYN-----GYQLLIN-ERIRSPQHLSQVKQALVVLSDRPPTAYSEFRFELQNLGFEPGWGNTAVRVDTLEILDQLDSDPDHGVLEA  
158339122 FSFLKLHSYN-----GTQLLIN-QRIQSPHLSSECVKQAISLVGGLPPEQYPDEFERNFQELGFEPGWGNTAARVLETEMLDELIDSPDQVLEA  
284053161 YQFLSLHSYN-----GLQLLIN-DRITNQNLQSYAIKKAISLLNKRSKPKEYEKFRFELQETIGFEPGWGNTARRALETELIDDELIDSPDHQVLEA  
209523126 YQFLSLHSYN-----GLQLMIN-DRITNQNLQSHAIKKAISLLNKRSKPKEYENFRFELQETIGFEPGWGNTARRALETELIDDELIDSPDHQVLEA  
17228554 YLALRGLQYD-----GINLMIG-DAIPSGIHAKQIHAAIKFLSALPPEEPYEFKYIELQKLGFEPGWGNTAQRILETITILLDKLIDSPQPAVLEA  
75909957 YLALRGLQYD-----GINLMIG-DAIPSGIHAKQIHAAIKFLSALPPEEPYEFKYIELQALGFEPGWGNTAERILETITILLDRILDSPQPAVLEA  
186685043 FQALQGLQYD-----GIRLLLS-DRIPSGIHAKQIKALKLVNERSPHPEYEFKFSIDLQELGFEPGWGNTAARVSETLELIDRLIYSEPGEILEA  
119510624 FQALYQLTYD-----QKPLLIS-DRIPSGIHLVKQIKALKFLNQPPPPEEPYANFRPHLQELGFEPGWGNTSGRISETLELLEQLIDNPQPAILEA  
298489784 FQALQGIQFN-----GMKVLIS-DRISHGIQFAKLIKPAITLLSELPPDEPYAQFRSHLQELGLEAGWGNNAGRVRTLELLEQLRIDTPQTYILEA  
220909283 FRVLCGHEYD-----GLSLLIN-BQIGSGEDLYKQVQALWFIRQRPGEDEWEQLHYYLEKLGFAGWGNDRASRVETLELLEQLYIMDSPAPPILEA  
232708740 LKLNQAHHYD-----HTPLLLN-NRIDSTTQLFEKLKEALTIVGELPAHTPYEKFRFELQVLGFEGAGWNTAGRVRTLELLELRLMDAPDAHVLEA

Clustal Consensus :: : \* : \*

350552412 FLARIPMIFSLILSPHGGFQANVLGRPDGTGGQVYIILDQVRALEREMRSLQAQGLH---IEPRILVVTTRLIPEAQGTS CDQPFVERINGTRNAQILRV  
220933364 FLARIPMIFSLILSPHGGFQAGVLGLPDTGGQVYIILDQVRALEREMRDLAEQGLD---IEPRIRVVTTRLIPEARGTS CDQPEEAVSGTENARILRV  
350574485 FLGRIPMIFSIAILSPHGWFGQSNVLGRPDGTGGQVYIILDQVRALEREMRLAEQGD---IDPEVIVITRLIPESEGTSDQRIEPIAGTQNARILRV  
95929190 FLGRIPMIFSIIVVSPHGYFGQENVLGLPDTGGQVYIILDQVRALEKEMKEQIYRQGLD---IEPSIVVLTTRLIPHCGDTS CNQPEEQIAGTSNATIVRV  
298528445 FLSRIPMIFKLIVVSPHGYFGQSNVLGRPDGTGGQIVYIILDQVRALEKEMRRQIKEQGLE---IEPEIVVLTTRLIPEAGDTCNQRQEDIVGTSNARILRV  
297602308 FFSRVPSIFNIVIFSIGHGYFGQEKVLGLPDTGGQVYIILDQVRAMEEELLQRIKQQGLH---VTPKILVLTTRLIPDAKGT KCNVELEPVENTKYSHILRV  
115457664 FFSRVPSIFNIVIFSIGHGYFGQEKVLGLPDTGGQVYIILDQVRAMEEELLQRIKQQGLH---VTPKILVLTTRLIPDAKGT KCNVELEPVENTKYSHILRV  
326504012 FFSRVPSIFNIVIFSIGHGYFGQEKVLGLPDTGGQVYIILDQVRAMEEELLQRIKQQGLH---ITPKILVLTTRLIPDSKGT KCNVELEPVENTKYSHILRV  
115450038 FFSRVPSIFNIVIFSIGHGYFGQEKVLGLPDTGGQVYIILDQVRALEDELLQRIKQQGLN---ATPKILVLTTRLIPEAKGT KCNVELEPIENTKHSNILRV  
326531526 FFSRVPSVFNIVIFSIGHGYFGQEKVLGLPDTGGQVYIILDQVRALEEELLQRIKQQGLN---VTPKILVLTTRLIPDAKGT KCNVELEPVENTKHSNILRV  
242063616 FFSRVPSVFDVVIFSVHGYFGQEKVLGLPDTGGQVYIILDQVRALEEELLQRIKQQGLT---FTPNILVLTTRLIPEAKGT KCNVELEPIENTKHSNILRV  
42568160 FFAFVPRIFNVVIFSVHGYFGQDVLGLPDTGGQVYIILDQVRALEEELLQRIKQQGLN---FKPQILVVTTRLIPDAKGT KCNVELEPIFGTKYSNILRI  
297805240 FFAFVPRIFNVVIFSVHGYFGQDVLGLPDTGGQVYIILDQVRALEEELLQRIKQQGLN---FKPQILVVTTRLIPDAKGT KCNVELEPIFGTKYSNILRI  
313770765 FLSRLPTVFNIVIFSIGHGYFGQADVLGLPDTGGQVYIILDQVRALEEELLQRIKQQGLN---VKPQIVVATRLIPDARGTTCNLEFEAIDGTYKSNILRV  
313770765 FLSRLPTVFNIVIFSIGHGYFGQADVLGLPDTGGQVYIILDQVRALEEELLQRIKQQGLN---VKPQIVVATRLIPDARGTTCNLEFEAIDGTYKSNILRV  
255584097 FLSRVPTIFNVVIFSIGHGYFGQANVLGLPDTG-----GQVTRILIPDARGTTCNLEFEAIDGTYKSNILRV  
225466221 FLSRLPTIFNVVIFSIGHGYFGQSDVLGLPDTGGQVYIILDQVRALEEELLQRIKQQGLN---VKPQILVVTTRLIPDARGTTCNLEFEAIDGTYKSNILRV  
313770769 LFSRIPNMFNIVIFSIGHGYFGQSDVLGLPDTGGQVYIILDQVRALEEELLQRIKQQGLN---VKPQILVVTTRLIPDARGTTCNLEFEAIDGTYKSNILRV  
313770769 LFSRIPNMFNIVIFSIGHGYFGQSDVLGLPDTGGQVYIILDQVRALEEELLQRIKQQGLN---VKPQILVVTTRLIPDARGTTCNLEFEAIDGTYKSNILRV  
2555840671 LFSRIPNMFNIVIFSIGHGYFGQSDVLGLPDTGGQVYIILDQVRALEEELLQRIKQQGLN---MKPQILVVTTRLIPDARGTTCNLEFEAIDGTYKSNILRV  
15219457 LFSRLPTVFNIVIFSIGHGYFGQDVLGLPDTGGQVYIILDQVRALEEELLQRIKQQGLN---FKPQILVVTTRLIPEARGT KCNVELEPIFGTKYSNILRV  
297842089 LFSRLPTVFNIVIFSIGHGYFGQDVLGLPDTGGQVYIILDQVRALEEELLQRIKQQGLN---FKPQILVVTTRLIPEARGT KCNVELEPIFGTKYSNILRV  
115466896 FLGTIPMMFNVVILSPHGYFAQSNVLGYPDGTGGQVYIILDQVRALEEELLQRIKQQGLD---ITPKILVTRLLPDAGTTCGQRLKVKVGT EHTDILRV  
17980243 FLGTIPMMFNVVILSPHGYFAQSNVLGYPDGTGGQVYIILDQVRALEEELLQRIKQQGLD---ITPKILVTRLLPDAGTTCGQRLKVKVGT EHTDILRV  
162460741 FLGTIPMMFNVVILSPHGYFAQSNVLGYPDGTGGQVYIILDQVRALEEELLQRIKQQGLD---ITPKILVTRLLPDAGTTCGQRLKVKVGT EHTDILRV  
239984690 FLGTIPMMFNVVILSPHGYFAQSNVLGYPDGTGGQVYIILDQVRALEEELLQRIKQQGLD---ITPKILVTRLLPDAGTTCGQRLKVKVGT EHTDILRV  
162460681 FLGTIPMMFNVVILSPHGYFAQSNVLGYPDGTGGQVYIILDQVRALEEELLQRIKQQGLD---ITPKILVTRLLPDAGTTCGQRLKVKVGT EHTDILRV  
242035533 FLGTIPMMFNVVILSPHGYFAQSNVLGYPDGTGGQVYIILDQVRALEEELLQRIKQQGLD---ITPKILVTRLLPDAGTTCGQRLKVKVGT EHTDILRV  
62865493 FLGTIPMMFNVVILSPHGYFAQSNVLGYPDGTGGQVYIILDQVRALEEELLQRIKQQGLN---ITPRILVTRLLPDAGTTCGQRLKVKVGT EHTDILRV  
17980241 FLGTIPMMFNVVILSPHGYFAQSNVLGYPDGTGGQVYIILDQVRALEEELLQRIKQQGLN---ITPRILVTRLLPDAGTTCGQRLKVKVGT EHTDILRV  
115453437 FLGTIPMMFNVVILSPHGYFAQSNVLGYPDGTGGQVYIILDQVRALEEELLQRIKQQGLN---ITPRILVTRLLPDAGTTCGQRLKVKVGT EHTDILRV  
115473359 FLGTIPMMFNVVILSPHGYFAQSNVLGYPDGTGGQVYIILDQVRALEEELLQRIKQQGLN---ITPRILVTRLLPDAGTTCGQRLKVKVGT EHTDILRV  
3980298 FLGTIPMMFNVVILSPHGYFAQSNVLGYPDGTGGQVYIILDQVRALEEELLQRIKQQGLD---ITPKILVTRMLPDAGTTCGQRLKVKVGT EHTDILRV  
15242073 FLGRVPMFNVVILSPHGYFAQSNVLGYPDGTGGQVYIILDQVRALEEELLQRIKQQGLN---IKPRILVTRLLPDAGTTCGQRLKVKVGT EHTDILRV  
297812265 FLGRVPMFNVVILSPHGYFAQSNVLGYPDGTGGQVYIILDQVRALEEELLQRIKQQGLD---IKPRILVTRLLPDAGTTCGQRLKVKVGT EHTDILRV  
22331535 FLGRIPMVFNVVILSPHGYFAQSNVLGYPDGTGGQVYIILDQVRALEEELLQRIKQQGLD---ITPRILVTRLLPDAGTTCGQRLKVKVGT EHTDILRV  
297818772 FLGRIPMVFNVVILSPHGYFAQSNVLGYPDGTGGQVYIILDQVRALEEELLQRIKQQGLD---ITPRILVTRLLPDAGTTCGQRLKVKVGT EHTDILRV  
313770759 FLGRIPMVFNVVILSPHGYFAQSNVLGYPDGTGGQVYIILDQVRALEEELLQRIKQQGLD---ITPRILVTRLLPDAGTTCGQRLKVKVGT EHTDILRV  
313770761 FLGRIPMVFNVVILSPHGYFAQSNVLGYPDGTGGQVYIILDQVRALEEELLQRIKQQGLD---ITPRILVTRLLPDAGTTCGQRLKVKVGT EHTDILRV  
255550319 FLGRIPMVFNVVILSPHGYFAQSNVLGYPDGTG-----GQITRLLPDAGTTCGQRLKVKVGT EHTDILRV  
324984223 FLGRIPMVFNVVILTPHGYFAQSNVLGYPDGTGGQVYIILDQVRALEEELLQRIKQQGLN---ITPRILVTRLLPDAGTTCGQRLKVKVGT EHTDILRV  
258489633 FLGRIPMVFNVVILTPHGYFAQSNVLGYPDGTGGQVYIILDQVRALEEELLQRIKQQGLN---ITPRILVTRLLPDAGTTCGQRLKVKVGT EHTDILRV  
324984221 FLGRIPMVFNVVILTPHGYFAQSNVLGYPDGTGGQVYIILDQVRALEEELLQRIKQQGLN---ITPRILVTRLLPDAGTTCGQRLKVKVGT EHTDILRV  
324984229 FLGRIPMVFNVVILTPHGYFAQSNVLGYPDGTGGQVYIILDQVRALEEELLQRIKQQGLN---ITPRILVTRLLPDAGTTCGQRLKVKVGT EHTDILRV  
6683114 FLGRIPMVFNVVILTPHGYFAQSNVLGYPDGTGGQVYIILDQVRALEEELLQRIKQQGLD---ITPRILVTRLLPDAGTTCGQRLKVKVGT EHTDILRV  
4584690 FLDRIPMVFNVVILSPHGYFAQSNVLGYPDGTGGQVYIILDQVRALEEELLQRIKQQGLD---ITPRILVTRLLPDAGTTCGQRLKVKVGT EHTDILRV  
3915046 FLDRIPMVFNVVILSPHGYFAQSNVLGYPDGTGGQVYIILDQVRALEEELLQRIKQQGLD---ITPRILVTRLLPDAGTTCGQRLKVKVGT EHTDILRV



3766299 FLDRIPMFNVVILSPHGYFAQDDVLGYPD TGGQVVYILDQVRALESEMLNRIKKQGLD---IVPRILIITRLLPDAVGTT CGQRLEKVGTEHCHILRV  
3377764 FLDRIPMFNVVILSPHGYFAQDDVLGYPD TGGQVVYILDQVRALESEMLNRIKKQGLD---IVPRILIITRLLPDAVGTT CGQRLEKVGTEHCHILRV  
225444613 FLGRIPMFNVVILSPHGYFAQDNVLGYPD TGGQVVYILDQVRAMETEMLLRIKQGLD---ITPKIIIVTRLPPDAVGTT CNQRIEKVYGETHSIILRV  
3660531 FLGRIPMFNVVILSPHGYLAQENVLGYPD TGGQVVYILDQVPALEREMLKRIKEQGLD---IIPRILIVTRLPPDAVGTT CGQRLEKVGTEHSHILRV  
31455440 FLGRIPMFNVVILSPHGYFAQENVLGYPD TGGQVVYILDQVPALEREMLKRIKEQGLD---IIPRILIVTRLPPDAVGTT CGQRLEKVGAEHSHILRV  
304651488 FLSRIPMFNVVILSPHGYFAQENVLGYPD TGGQVVYILDQVPALEREMLKRIKEQGLD---IKPRILIVTRLPPDAVGTT CGQRLEKVFGETHSHILRV  
28629438 FLSRIPMFNVVILSPHGYFAQENVLGYPD TGGQVVYILDQVPALEREMLKRIKEQGLD---IKPRILIVTRLPPDAVGTT CGQRLEKVFGETHSHILRV  
115310618 FLGRIPMFNVVILSPHGYFAQENVLGYPD TGGQVVYILDQVPALEREMLKRIKEQGLD---VKPRILIITRLPPDAGTT CGQRLEKVGSEYSHILRV  
345286417 FLGRIPMFNVVILSPHGYFAQENVLGYPD TGGQVVYILDQVPALEREMLKRIKEQGLD---ITPRILIVTRLPPDAVGTT CGQRLEKVFGETHSHILRV  
38425095 FLGRIPMFNVVILTPHGYFAQANVLGYPD TGGQVVYILDQVRALEHEMLLRIKQGLD---IIPRILIVSRLPPDAVGTT CGQRLEKVFGETHSHILRV  
15235300 FLGMVPMFNVVILSPHGYFGQANVLGLPD TGGQVVYILDQVRALEHEMLLRIKQGLD---ISPSILIVTRLIPDAKGTTCNQRLERVSGETEHTHILRV  
297814081 FLGMVPMFNVVILSPHGYFGQANVLGLPD TGGQVVYILDQVRALEHEMLLRIKQGLD---ITPRILIVTRLIPDAKGTTCNQRLERVSGETEHTHILRV  
6682841 FLGRIPMFNVVILSPHGYFGQANVLGLPD TGGQVVYILDQVRALEHEMLLRIKQGLD---ISPKILIVTRLIPDAKGTTCNQRLERVSGETEHTHILRV  
255564236 FLGRIPMFNVVILSPHGYFGQANVLGLPD TGGQVVYILDQVRALEHEMLLRIKQGLD---GQVTRLIPDAKGTTCNQRLERVSGETEHTHILRV  
313770763 FLGRVPMFNVVILSPHGYFGQANVLGLPD TGGQIVYILDQVRALEHEMLLRIKQGLD---FKPKILIVTRLIPDSKGTSCNQRLERVSGETEHTHILRV  
3915037 FLGRVPMFNVVILSPHGYFGQANVLGLPD TGGQVVYILDQVRALEHEMLVRIKQGLD---FTPRILIVTRLIPDAKGTTCNQRLERVSGETEHTHILRV  
225437428 FLGRIPMFNVVILSPHGYFGQANVLGLPD TGGQVVYILDQVRALEHEMLLRMKQGLD---VTPRILIVTRLIPDAKGTTCNQRLERVSGETEHTHILRV  
162458268 FLGRIPMFNVVIVSPHGYFGQANVLGLPD TGGQIVYILDQVRALEHEMLVRLKQGLD---VSPKILIVTRLIPDAKGTSCNQRLERISGTQHTYILRV  
242035817 FLGRIPMFNVVIVSPHGYFGQANVLGLPD TGGQIVYILDQVRALEHEMLVRLKQGLD---FSPKILIVTRLIPDAKGTSCNQRLERISGTQHTYILRV  
115452927 FLGRIPMFNVVIVSPHGYFGQANVLGLPD TGGQIVYILDQVRALEHEMLVRLKQGLD---FTPKILIVTRLIPDAKGTSCNQRLERISGTQHTYILRV  
241896730 FLGRIPMFNVVIVSPHGYFGQANVLGMPD TGGQIVYILDQVRALEHEMLVRLKQGLD---VTPKILIVTRLIPDSKGTSCNQRLERISGTQHTYILRV  
304651490 FLGRIPMFNVVILSPHGYFGQANVLGLPD TGGQVVYILDQVRALEHEMLLRIKQGLN---FKPRILVTRLIPDAKGTTCNQRLERISGTQHTYILRV  
29289943 FLGRIPMFNVVILSPHGYFGQANVLGLPD TGGQVVYILDQVRALEHEMLLRIKQGLN---FKPKILVTRLIPDAKGTTCNQRLERISGTQHTYILRV  
115310620 FLGRVPMFNVVILSPHGYFGQANVLGLPD TGGQIVYILDQVRALEHEMLLRIKQGLD---VTPRILIVTRLIPDAKGTTCNQRLERVSGETEHTHILRV  
4468153 FLGRIPMFNVVILSIHGYFGQANVLGLPD TGGQIVYILDQVRALEHEMLKRIKQGLS---IIPQILIVTRLIPDAKGTSCNQRLERISGCEHSHILRV  
345286419 FLGRVPMFNVVILSVHGYFGQANVLGLPD TGGQIVYILDQVRALEHEMLLRIKQGLQ---ITPRILVTRLIPDAADTSCNQRLERISGCEHSHILRV  
4468151 FLGQLPMFNVVILSIHGYFAQTDVLGLPD TGGQVVYILDQVRAMENEMIKRIKNHGLN---ITPRILIVTRLIPDAKGTTCNQRLERISGCEHSHILRV  
151176306 FLGRIPMFNVVILSVHGYFGQANVLGLPD TGGQIVYILDQVRSLEHEMLQRIKQGLD---VTPRILIVSRLIPDAKGTTCNQRMKEKVSGETEHASILRV  
14530225 FLGRIPMFNVVILSVHGYFGQANVLGLPD TGGQIVYILDQVRSLEHEMLQRIKQGLD---VTPRILIVSRLIPDAKGTTCNQRMKEKVSGETEHASILRV  
15239816 FLGRIPMFNVVILSPHGYFGQANVLGLPD TGGQVVYILDQVRALEHEMLLRIKQGLQ---VIPKILIVTRLIPDAKGTTCNQRLERVSGETEHAHILRI  
297795665 FLGRIPMFNVVILSPHGYFGQANVLGLPD TGGQVVYILDQVRALEHEMLLRIKQGLQ---VIPKILIVTRLIPDAKGTTCNQRLERVSGETEHAHILRI  
225431790 FLGRIPMFNVVIVSPHGYFGQANVLGLPD TGGQIVYILDQVRALEHEMLLRIKQGLD---VIPKILIVTRLIPDAKGTTCNQRLERISGTQHTHILRV  
255551835 FLGMLPMFNVVIVSPHGYFGQANVLGLPD TGGQVVYILDQVRALEHEMLLRIKQGLD---GQVTRLIPDAKGTTCNQRLERISGTQHTYILRV  
168009716 FLARIPMFNVVIVSPHGYFGQANVLGLPD TGGQVVYILDQVRALEHEMLLRIKQGLD---IIPQIVILTRLIPNAIGTT CNQRIEKVGSRTSHILRI  
168035060 FLARIPMFNVVIVTPHGYFGQANVLGLPD TGGQVVYILDQVRALEHEMLLRIKQGLD---IVPKIVILTRLIPNAIGTT CNQRIEKVGSRTSHILRI  
168058907 FLARIPMFNVVIVTPHGYFGQANVLGLPD TGGQVVYILDQVRALEHEMLLRIKQGLD---FKP---QILTRLIPNANGTTVQRIEKVGSRTSHILRV  
168029793 FLARIPMFNVVIVTPHGYFGQANVLGLPD TGGQVVYILDQVRALEHEMLLRIKQGLD---IEPQIVVTRLIPNANGTT CNQRIEKVGSRTSHILRV  
94266940 FLARIPMFNVVIVTPHGYFGQANVLGLPD TGGQVVYILDQVRALEHEMLLRIKQGLD---LEIEPKILITRLIPENEGTTADQRLERVPVDTANVAILRV  
94264333 FLSRIPMFNVVILSPHGYFGQANVLGLPD TGGQVVYILDQVRALEHEMLLRIKQGLD---LEIEPKILITRLIPENEGTTADQRLERVPVDTANVAILRV  
297569306 FLSRIPMFNVVILSPHGYFGQANVLGLPD TGGQVVYILDQVRALEHEMLLRIKQGLD---LEIAEKILIVSRLIPENEGTSADQRLERVPVDTANVAILRV  
254416162 FLSRIPMFNVVILSPHGYFGQANVLGLPD TGGQVVYILDQVRALEHEMLLRIKQGLD---LEIAEKILIVSRLIPENEGTSADQRLERVPVDTANVAILRV  
332712456 FISIRIPMFNVVILSVHGYFGQANVLGLPD TGGQVVYILDQVRALEHEMLLRIKQGLD---LNIQPKVILTRLIPNNDGTRCNERLEKVGHTENAWILRV  
17232477 FISIRIPMFNVVILSVHGYFGQANVLGLPD TGGQVVYILDQVRALEHEMLLRIKQGLD---LNIQPKVILTRLIPNNDGTRCNERLEKVGHTENAWILRV  
75908500 FISIRIPMFNVVILSVHGYFGQANVLGLPD TGGQVVYILDQVRALEHEMLLRIKQGLD---LNIQPKVILTRLIPNNDGTRCNERLEKVGHTENAWILRV  
186682280 FISIRIPMFNVVILSVHGYFGQANVLGLPD TGGQVVYILDQVRALEHEMLLRIKQGLD---LNIQPKVILTRLIPNNDGTRCNERLEKVGHTENAWILRV  
119512682 FISIRIPMFNVVILSVHGYFGQANVLGLPD TGGQVVYILDQVRALEHEMLLRIKQGLD---LNIQPKVILTRLIPNNDGTRCNERLEKVGHTENAWILRV  
334117431 FISIRIPMFNVVILSVHGYFGQANVLGLPD TGGQVVYILDQVRALEHEMLLRIKQGLD---LNIQPKVILTRLIPNNDGTRCNERLEKVGHTENAWILRV



15219457 PFVITNKG-VLRQVSRFDIYPYLERFTQD--ATSKILQRLDCKPDLIIIGNYTDGNLVASLMATKLGVTQGTIAHALEKTKYEDSDAKWKELDPKYHFSQ  
297842089 PFVITDKG-ILRQVSRFDIYPYLERFTQD--ATSKILQRLDCKPDLIIIGNYTDGNLVASLMATKIGVTQGTIAHALEKTKYEDSDAKWKELDPKYHFSQ  
115466896 PFRSENG-ILRKWISRFDVWPFLTYTTED--VANEIMREMQAKPDLIIIGNYSDGNLVATLLAHKLGVTQCTIAHALEKTKYPNSDIYLDKFDSQYHFSQ  
17980243 PFRTENG-ILRKWISRFDVWPFLTYTTED--VANEIMREMQAKPDLIIIGNYSDGNLVATLLAHKLGVTQCTIAHALEKTKYPNSDIYLDKFDSQYHFSQ  
162460741 PFRNENG-ILRKWISRFDVWPFLTYTTED--VSSEIMKEMQAKPDLIIIGNYSDGNLVATLLAHKLGVTQCTIAHALEKTKYPNSDIYLDKFDSQYHFSQ  
239984690 PFRTENG-IR-KWISRFDVWPFLTYTTEDVNDVANELMREMOTKPDIIIGNYSDGNLVATLLAHKLGVTQCTIAHALEKTKYPNSDIYLDKFDSQYHFSQ  
162460681 PFRTENG-IVRKWISRFEVWPYLETYTDD--VAHEIAGELQANPDLIIIGNYSDGNLVACLLAHKMGVTHCTIAHALEKTKYPNSDIYWKFFEDHYHFSQ  
242035533 PFRTENG-IVRKWISRFEVWPYLETYTDD--VAHEIAGELQANPDLIIIGNYSDGNLVACLLAHKMGVTHCTIAHALEKTKYPNSDIYWKFFEDHYHFSQ  
62865493 PFRTENG-IVRKWISRFEVWPYLETFTDD--VAHEIAGELQANPDLIIIGNYSDGNLVACLLAHKMGVTHCTIAHALEKTKYPNSDIYWKFFEDHYHFSQ  
17980241 PFRTENG-IVRKWISRFEVWPYLETFTDD--VAHEIAGELQANPDLIIIGNYSDGNLVACLLAHKMGVTHCTIAHALEKTKYPNSDIYWKFFEDHYHFSQ  
115453437 PFRTENG-IVRKWISRFEVWPYLETFTDD--VAHEIAGELQANPDLIIIGNYSDGNLVACLLAHKMGVTHCTIAHALEKTKYPNSDIYWKFFEDHYHFSQ  
115473359 PFRTENG-TVRKWISRFEVWPYLETYTDD--VAHEISGELQATPDLIIIGNYSDGNLVACLLAHKLGVTCTIAHALEKTKYPNSDIYWKFFEDHYHFSQ  
3980298 PFKTEDG-IVRKWISRFEVWPYLEAYTDD--VAHEIAGELQANPDLIIIGNYSDGNLVACLLAHKLGVTGTHCTIAHALEKTKYPNSDIYWKFFEDHYHFSQ  
15242073 PFRTEKG-IVRKWISRFEVWPYLETYTTED--AAVELSKELNGKPDIIIGNYSDGNLVASLLAHKLGVTQCTIAHALEKTKYPNSDIYWKLLDDKYHFSQ  
297812265 PFRTEKG-IVRKWISRFEVWPYLETYTTED--AAVELSKELNGKPDIIIGNYSDGNLVASLLAHKLGVTQCTIAHALEKTKYPNSDIYWKLLDDKYHFSQ  
22331535 PFRTEKG-IVRKWISRFEVWPYLETFTED--VAAEISKELQKPDIIIGNYSDGNLVASLLAHKLGVTQCTIAHALEKTKYPNSDIYWKLLDDKYHFSQ  
297818772 PFRTEKG-IVRKWISRFEVWPYLETFTED--VAAEISKELQKPDIIIGNYSDGNLVASLLAHKLGVTQCTIAHALEKTKYPNSDIYWKLLDDKYHFSQ  
313770759 PFRDQKG-MVRKWISRFEVWPYLETFTED--VAAEIAKELQKPDIIIGNYSDGNLVASLLAHKLGVTCTIAHALEKTKYPNSDIYWKFFDEKYHFSQ  
313770761 PFRDEKG-MVRKWISRFEVWPYLETYTDD--VAAEIAKELQKPDIIIGNYSDGNLVASLLAHKLGVTCTIAHALEKTKYPNSDIYWKFFDEKYHFSQ  
255550319 PFRTEKG-IVRKWISRFEVWPYLETYTTED--VATEIGKELQKPDIIIGNYSDGNLVASLLAHKLGVTCTIAHALEKTKYPNSDIYWKLLDDKYHFSQ  
324984223 PFRTEKG-IVRKWISRFEVWPYLETYTTED--VAHEISKELQKPDIIIGNYSDGNLVASLLAHKLGVTQCTIAHALEKTKYPNSDIYWKLLDDKYHFSQ  
258489633 PFRTEKG-IVRKWISRFEVWPYLETYTTED--VAHEISKELQKPDIIIGNYSDGNLVASLLAHKLGVTQCTIAHALEKTKYPNSDIYWKLLDDKYHFSQ  
324984221 PFRTEKG-IVRKWISRFEVWPYLETYTTED--VAHEISKELQKPDIIIGNYSDGNLVASLLAHKLGVTQCTIAHALEKTKYPNSDIYWKLLDDKYHFSQ  
324984229 PFRTEKG-IVRKWISRFEVWPYLETYTTED--VAHEISKELQKPDIIIGNYSDGNLVASLLAHKLGVTQCTIAHALEKTKYPNSDIYWKLLDDKYHFSQ  
6683114 PFRTEKG-VVRKWISRFEVWPYLETYTTED--VAVEIAKELQKPDIIIGNYSDGNLVASLLAHKLGVTQCTIAHALEKTKYPNSDIYWKLLDDKYHFSQ  
4584690 PFRDTKG-IVRKWISRFEVWPYLETYTTED--VAHELAKELQKPDIIIGNYSDGNLVASLLAHKLGVTQCTIAHALEKTKYPNSDIYWKFFEEKYHFSQ  
3915046 PFRDEKG-IVRKWISRFEVWPYLETYTTED--VAHELAKELQKPDIIIGNYSDGNLVASLLAHKLGVTQCTIAHALEKTKYPNSDIYWKFFEEKYHFSQ  
3766299 PFRDQKG-IVRKWISRFEVWPYLETYTTED--VAHELAKELQKPDIIIGNYSDGNLVASLLAHKLGVTQCTIAHALEKTKYPNSDIYWKFFEEKYHFSQ  
3377764 PFRDQKG-IVRKWISRFEVWPYLETYTTED--VAHELAKELQKPDIIIGNYSDGNLVASLLAHKLGVTQCTIAHALEKTKYPNSDIYWKFFEEKYHFSQ  
225444613 PFRTEKG-IVRKWISRFEVWPYLETYTTED--VAKELATELQKPDIIIGNYSDGNLVASLLAHKLGVTQCTIAHALEKTKYPNSDIYWKLLDDKYHFSQ  
3660531 PFRTEKG-IVRKWISRFEVWPYMETTFIED--VAKEISAELOAKPDLIIIGNYSEGNLAASLLAHKLGVTQCTIAHALEKTKYPNSDIYWKFFDEKYHFSQ  
31455440 PFRTEKG-IVRKWISRFEVWPYMETTFIED--VAKEISAELOAKPDLIIIGNYSEGNLAASLLAHKLGVTQCTIAHALEKTKYPNSDIYWKFFDEKYHFSQ  
304651488 PFRTEKG-IVRKWISRFEVWPYMETTFIED--VGKEITAELOAKPDLIIIGNYSEGNLAASLLAHKLGVTQCTIAHALEKTKYPNSDIYLNKFDEKYHFSQ  
28629438 PFRTEKG-IVRKWISRFEVWPYMETTFIED--VGKEITAELOAKPDLIIIGNYSEGNLAASLLAHKLGVTQCTIAHALEKTKYPNSDIYLNKFDEKYHFSQ  
115310618 PFRTEKG-VVRKWISRFEVWPYMETTFIED--VAKEVTAELOAKPDLIIIGNYSEGNLAASLLAHKLGVTQCTIAHALEKTKYPNSDIYLNKFDEKYHFSQ  
345286417 PFRTEKG-ILRKWISRFEVWPYMETTFIED--VAKEITAELOAKPDLIIIGNYSEGNLAASLLAHKLGVTQCTIAHALEKTKYPNSDIYLNKFDEKYHFSQ  
38425095 PFRTEKG-IVRRWISRFEVWPYLETYTTED--VANEIAGELQAKPDLIIIGNYSDGNLVASLLAHKLGVTQCTIAHALEKTKYPNSDIYWKSFEEKYHFSQ  
15235300 PFRSEKG-ILRKWISRFDVWPYLENYAQD--AAEIVGELQGVPDFIIGNYSDGNLVASLLAHKMGVTQCTIAHALEKTKYPNSDIYWKDFDNKYHFSQ  
297814081 PFRSDKG-ILHKWISRFDVWPYLENYAQD--AAEIVGELQGVPDFIIGNYSDGNLVASLLAHKMGVTQCTIAHALEKTKYPNSDIYWKDFDNKYHFSQ  
6682841 PFRSEKG-ILRQWISRFDVWPYLENYAQD--VGEITAELOAKPDLIIIGNYSDGNLVASLLAHKMGVTQCTIAHALEKTKYPNSDIYWKFFDEKYHFSQ  
255564236 PFRSEKG-ILRKWISRFDVWPYLETLLS-----EIVAELOQIPDFIIGNYSDGNLVASLLAHKMGVTQCTIAHALEKTKYPNSDIYWKFFDDKYHFSQ  
313770763 PFRSEHG-ILRKWISRFDVWPYLETFAED--AAEIVAELOQIPDFIIGNYSDGNLVASLLAHKMGVTQCTIAHALEKTKYPNSDIYWKFFDDKYHFSQ  
3915037 PFRSEKG-ILRKWISRFDVWPFLTFAED--VASEIAAELOQCPDFIIGNYSDGNLVASLLAHKMGVTQCTIAHALEKTKYPNSDIYWKFFEDKYHFSQ  
225437428 PFRTDKG-ILRKWISRFDVWPYLETFAED--AAEIAAELOQGVPELIIIGNYSDGNLVASLLAHKLGVTQCTIAHALEKTKYPNSDIYWKFFDDKYHFSQ  
162458268 PFRNENG-ILKKWISRFDVWPYLETFAED--AAGEIAAELOQGTDFIIGNYSDGNLVASLLAHKMGITQCNIAHALEKTKYPNSDIYWKFFDEKYHFSQ  
242035817 PFRNENG-ILKKWISRFDVWPYLETFAED--AAGEIAAELOQGTDFIIGNYSDGNLVASLLAHKMGITQCNIAHALEKTKYPNSDIYWKFFDEKYHFSQ  
115452927 PFRNENG-ILRKWISRFDVWPYLEKFAED--AAGEIAAELOQGTDFIIGNYSDGNLVASLLAHKMGITQCNIAHALEKTKYPNSDIYWKFFDEKYHFSQ





82703384 YTADLIAMNSADFIITSTFQEIAGTEQTVGQYETYQNYTMPGLYRVVNGIDVDFPKFNIVSPGADAEVYFSYLDH-ERRLDALIPDIERLLYGDDPGVPC  
198283392 FTADLIAMNSSDIIVTSTYQEIAGNDREVGGYEGYQNYSLPGLYRVENGIDVDFTKFNIVSPGADAHYFFPYAS-EARLRYLHDDIDALLFGEEPADR  
34419811 FTADLIAMNSADIIVTSTYQEIAGNDHEVGGYEGHQNYSPLGLYRVENGIDVDFTKFNIVSPGADAHYFFPYAS-EERLRYLHDDIDALLFGEEPADR  
255021595 FTADLIAMNAADIIVTSTYQEIAGNDREIGQYEGHQDYTLPLGLYRVENGIDVDFSKFNIVSPGADPRFYFSYART-EERPSFLEPEIESLLFGREPADR  
77166514 FTGDLIAMNSADFIIVTSTYQEIAGNKNSVGQYESYSAYTLPGLYQVIHGIDVDFPKFNIVSPGADGEVYFPYTD-KRRLSGLRQEIIEALIWGDERP-DA  
300115586 FTGDLIAMNSADFIITSTYQEIAGNKNSVGQYESYSAYTLPGLYQVIHGIDVDFPKFNIVSPGADGEVYFPYTD-KRRLSGLRQEIIEALIWGDDRS-DT  
292493898 FTADFIAMNSADFIITSTYQEIAGDRSSVGQYESYGAYILPGLYQVVGIDVDFPKFNIVSPGADAEVYFPYRER-KRRLRGLRREIEELIWGNRP-DA  
350552412 FTADLIAMNAADFIITSTYQEIAGTDHSGVGGYESYSAFSLPGLYRVVKGIDVDFPKFNIVSPGADAEVYFSYKDS-ERRLHGLHDELQTLIFGTPSE-DM  
220933364 FTADLIAMNAADFIITSTYQEIAGTGEDIGQYESYMSFSLPDLYRVVKGIDVDFPKFNIVSPGADDRVYFPYTE-ERRITGLHEEIEALLFGGHRD-DA  
350574485 FTADLIAMNTADFIITSTYQEIAGTDESLGQYESYMNFTMPGLYRVVAGVDVDFPKFNIVSPGADDEIYFPFTE-ERRLAHLHGEIEQLIFGEPVPGQS  
95929190 FTADLVSMNAADFIITSTYQEIAGTEESLGQYESYSFTMPALYRVVINGINIVDFPKFNIVSPGADDRVYFPYDE-ENRLTELHDELHELIYGDHME-GS  
298528445 FTADLIAMNTADFIITSTYQEIAGTEESVGQYETYNFTMPDLYRVVSGIDVDFPKFNIVSPGADENVYFPYDE-DRRLTELHDELSDYIYGPFGD-WA  
297602308 FTADMISMNTSDFIITSTYQEIAGSKEKPGQYEHYAFATMPGLCRYATGINVDFPKFNIAAPGADQSIYFPFTQK-QKRLTDLHPQIDELLYSKDDTDEH  
115457664 FTADMISMNTSDFIITSTYQEIAGSKEKPGQYEHYAFATMPGLCRYATGINVDFPKFNIAAPGADQSIYFPFTQK-QKRLTDLHPQIDELLYSKDDTDEH  
326504012 FTADMFMNTTDFIITSTYQEIAGSKEKPGQYEHYAFATMPGLCRYATGINVDFPKFNIAAPGADQSVYFPFTQK-QKRLTNLHPQIEELLYSKEDTDEH  
115450038 FTADMIAMNTSDFIISTYQEIAGSKEKPGQYESHYAFATMPGLCRYATGINVDFPKFNIAAPGADQSVYFPFTQK-QKRLTDLHPQIEELLYSKEDNNEH  
326531526 FTADMIAMNTSDFIISTYQEIAGSKDKPGQYESHYAFATMPGLCRYATGINVDFPKFNIAAPGADQTVYFPFTQK-QARLTDLHPQIEELLYSKEDNNEH  
242063616 FTADMIAMNTSDFIISTYQEIAGSKDKPGQYESHYAFATMPGLCRYATGINVDFPKFNIAAPGADQSVYFPFTQK-QKRLTDLHPQIEALVYKEENDEH  
42568160 FTADLISMNSADFIISTYQEIAGSKERAGQYESHMSFTVPLGLYRVVSGINVDFPKFNIAAPGADDSIYFPFTAQ-DRRFTKFYTSIDELLYSQSENDEH  
297805240 FTADLISMNSADFIISTYQEIAGSKERAGQYESHMSFTVPLGLYRVVSGINVDFPKFNIAAPGADDSIYFPFTAQ-DRRFTKFYPSIEELLYSQSENDEH  
313770765 FMADIVAMNATDFIISTYQEIAGSKDRTGQYESHAAFTLPGLCRVVSQVNVDFPKFNIAAPGADQSVYFPHTEK-QSRFTQFNPDIIEELLYSKVVNDEH  
313770767 FMADTIAMNATDFIISTYQEIAGSKDRPGQYESHASFTLPGLCRVVSQVNVDFPKFNIAAPGADQSVYFPYTEK-QSRFTKFHPAIEELLYSKVVNDEH  
255584097 FIADTISMNAADFIISTYQEIAGSKERPGQYESHSAFTLPGLCRVVSQVNVDFPKFNIAAPGADQSVYFPNTEK-QKRFSQFHSIEELLYSKVEENDEH  
225466221 FTADTISMNAADFIISTYQEIAGSKDRPGQYESHSAFTLPGLCRVVSQVNVDFPKFNIAAPGADQSVYFPYMER-HKRLTSFQPAIEELLYSKDDNNEH  
313770769 FTADMIAMNSADFIITSTYQEIAGSNVRPGQYESHTAFTMPGLCRVVSQVNVDFPKFNIAAPGADQSVYFPYTEK-QKRLTSFHPAIEELLYSKEDNNEH  
313770771 FTADMIAMNTADFIITSTYQEIAGSKNRPGQYESHVAFTMPGLCRVVSQVNVDFPKFNIAAPGADQTVYFPYTEK-QKRLTSFHPAIEELLYSKEDNNEH  
255570671 FTADMIAMNAADFIITSTYQEIAGSKDRPGQYESHKAFTMPGLCRVVSQVNVDFPKFNIAAPGADQSVYFPYTEK-RRRLTSFHPAIEELLYSKEDNNEH  
15219457 FTADLIAMNVTDFIITSTYQEIAGSKDRPGQYESHTAFTMPGLCRVVSQVNVDFPKFNIAAPGADQSVYFPYTEK-DKRFTKFHPSIQELLYNEKDNEH  
297842089 FTGDLIAMNVTDFIITSTYQEIAGSKDRPGQYESHTAFTMPGLCRVVSQVNVDFPKFNIAAPGADQSVYFPYTEK-EKRFTKFHPSIQELLYNEKDNEH  
115466896 FTADLIAMNHTDFIITSTFQEIAGSKDVTGQYESHIAFTLPGLYRVVHGIDVDFPKFNIVSPGADMSVYFPYTEA-DKRLTAFHPEIEELLYSEVENDEH  
17980243 FTADLIAMNHTDFIITSTFQEIAGSKDVTGQYESHIAFTLPGLYRVVHGIDVDFPKFNIVSPGADMSVYFPYTEA-DKRLTAFHPEIEELLYSDVENSEH  
162460741 FTADLIAMNHTDFIITSTFQEIAGSKDVTGQYESHIAFTLPGLYRVVHGIDVDFPKFNIVSPGADMSVYFPYTEA-DKRLTAFHPEIEELLYSDVENSEH  
239984690 FTADLIAMNHTDFIITSTFQEIAGSKDSVGQYESHIAFTLPDLYRVVHGIDVDFPKFNIVSPGADMTVYFPYTEA-DKRLTAFHSEIEELLYSDVENSEH  
162460681 FTADLIAMNHTDFIITSTFQEIAGNKDVTGQYESHMAFTMPGLYRVVHGIDVDFPKFNIVSPGADLSIYFPYTES-HKRLTSLHPEIEELLYSQTENTEH  
242035533 FTADLIAMNHTDFIITSTFQEIAGNKDVTGQYESHMAFTMPGLYRVVHGIDVDFPKFNIVSPGADLSIYFPYTES-HKRLTSLHPEIEELLYSQTENTEH  
62865493 FTADLIAMNHTDFIITSTFQEIAGNKDVTGQYESHMAFTMPGLYRVVHGIDVDFPKFNIVSPGADLSIYFPYTES-HKRLTSLHPEIEELLYSDVDNNEH  
17980241 FTADLIAMNHTDFIITSTFQEIAGNKDVTGQYESHMAFTMPGLYRVVHGIDVDFPKFNIVSPGADMSIYFPYTES-HKRLTSLHPEIEELLYSDVDNNEH  
115453437 FTADLIAMNHTDFIITSTFQEIAGNKDVTGQYESHMAFTMPGLYRVVHGIDVDFPKFNIVSPGADMSIYFPYTES-HKRLTSLHPEIEELLYSDVDNNEH  
115473359 FTADLIAMNHTDFIITSTFQEIAGNKETVQYESHMAFTMPGLYRVVHGIDVDFPKFNIVSPGADMSIYFPYTES-QKRLTSLHLEIEELLYSDVENTEH  
3980298 FTADLIAMNHTDFIITSTFQEIAGNKDVTGQYESHMAFTMPGLYRVVHGIDVDFPKFNIVSPGADMSIYFPYTES-QKRLTSLHLEIEELLYSDVENTEH  
15242073 FTADIFAMNHTDFIITSTFQEIAGSKETVQYESHTAFTLPGLYRVVHGIDVDFPKFNIVSPGADMSIYFPYTEE-KRRLTKFHSEIEELLYSDVENKEH  
297812265 FTADIFAMNHTDFIITSTFQEIAGSKDVTGQYESHTAFTLPGLYRVVHGIDVDFPKFNIVSPGADMSIYFPYTEE-KRRLTKFHSEIEELLYSDVENKEH  
22331535 FTADLIAMNHTDFIITSTFQEIAGSKDVTGQYESHRSFTLPGLYRVVHGIDVDFPKFNIVSPGADMSIYFAYTEE-KRRLTAFHLEIEELLYSDVENEH  
297818772 FTADLIAMNHTDFIITSTFQEIAGSKDVTGQYESHTAFTLPGLYRVVHGIDVDFPKFNIVSPGADMSIYFAYTEE-KRRLTAFHLEIEELLYSDVENEH  
313770759 FTADLIAMNHTDFIITSTFQEIAGSKDVTGQYESHTAFTLPGLYRVVHGIDVDFPKFNIVSPGADMSIYFPYTEE-KRRLTKFHSEIEELLYSDVENEH  
313770761 FTADLIAMNHTDFIITSTFQEIAGSKDVTGQYESHTAFTLPGLYRVVHGIDVDFPKFNIVSPGADMSIYFPYTEE-KRRLTKFHSEIEELLYSDVENEH  
255550319 FTADLIAMNHTDFIITSTFQEIAGSKDVTGQYESHTAFTLPGLYRVVHGIDVDFPKFNIVSPGADMSIYFPYTEE-KRRLTKFHSEIEELLYSDVENEH

324984223 FTADLFAMNHTDFIITSTFQEIAGSKDVGQYESHTAFTLPGLYRVVHGIDVDFPKFNIVSPGADMEIYFPYTEE-KRRLKHFHTEIEDLLYSKVENEH  
258489633 FTADLFAMNHTDFIITSTFQEIAGSKDVGQYESHTAFTLPGLYRVVHGIDVDFPKFNIVSPGADMEIYFPYTEE-KRRLKHFHTEIEDLLYSKVENEH  
324984221 FTADLFAMNHTDFIITSTFQEIAGSKDVGQYESHTAFTLPGLYRVVHGIDVDFPKFNIVSPGADMEIYFPYTEE-KRRLKHFHTEIEDLLYSKVENEH  
324984229 FTADLFAMNHTDFIITSTFQEIAGSKDVGQYESHTAFTLPGLYRVVHGIDVDFPKFNIVSPGADMEIYFPYTEE-KRRLKHFHTEIEDLLYSKVENEH  
6683114 FTADLIAMNHTDFIITSTFQEIAGSKDVGQYESHTAFTLPGLYRVVHGIDVDFPKFNIVSPGADMSIYFPYTEE-KRRLKSFHPEIEELLYSDVENKEH  
4584690 FTADLFAMNHTDFIITSTFQEIAGSKDVGQYESHTAFTLPGLYRVVHGIDVDFPKFNIVSPGADQTIYFPYTEE-SRRLTSFYPEIEELLYSSVENEH  
3915046 FTADLFAMNHTDFIITSTFQEIAGSKDVGQYESHTAFTLPGLYRVVHGIDVDFPKFNIVSPGADQTIYFPYTEE-SRRLTSFYPEIEELLYSSVENEH  
3766299 FTADLFAMNHTDFIITSTFQEIAGSKDVGQYESHTAFTLPGLYRVVHGIDVDFPKFNIVSPGADQTIYFPYTEE-SRRLTSFYPEIEELLYSTVENEH  
3377764 FTADLFAMNHTDFIITSTFQEIAGSKDVGQYESHTAFTLPGLYRVVHGIDVDFPKFNIVSPGADQTIYFPYTEE-SRRLTSFYPEIEKLLYSTGGNEH  
225444613 FTADLIAMNHTDFIITSTFQEIAGSKDVGQYESHTGFTMPGLYRVVHGIDVDFPKFNIVSPGADMTIYFSYTEE-KMRLKALHPEIEELLYSPVENKEH  
3660531 FTADLIAMNHTDFIITSTFQEIAGSKDVGQYESHMAFTMPGLYRVVHGIDVDFPKFNIVSPGADINLYFPYSES-EKRLTAFHPEIEELLYSDVENDDH  
31455440 FTADLIAMNHTDFIITSTFQEIAGSKDVGQYESHMAFTMPGLYRVVHGIDVDFPKFNIVSPGADINLYFSYSET-EKRLTAFHPEIEELLYSDVENDEH  
304651488 FTADLIAMNHTDFIITSTFQEIAGSKDVGQYESHMAFTMPGLYRVVHGIDVDFPKFNIVSPGADVNLVFPYSEK-EKRLTTFHPEIEDLLFSDEVENEH  
28629438 FTADLIAMNHTDFIITSTFQEIAGSKDVGQYESHMAFTMPGLYRVVHGIDVDFPKFNIVSPGADVNLVFPYSEK-EKRLTTFHPEIEDLLFSDEVENEH  
115310618 FTADLIAMNHTDFIITSTFQEIAGSKDVGQYESHMAFTMPGLYRVVHGIDVDFPKFNIVSPGADTNLYFPYHTEK-EKRLTSFHPEIEELLYSDVENEH  
345286417 FTADLIAMNHTDFIITSTFQEIAGSKDVGQYESHMAFTMPGLYRVVHGIDVDFPKFNIVSPGADMNLYFPYTEK-EKRLTALHPEIEELLYSNVENEH  
38425095 FTADLIAMNHTDFIITSTFQEIAGNKDVGQYESHMAFTLPGLYRVVHGIDVDFPKFNIVSPGADLSIYFNYTEE-KKRLTALHPEIEELLYSETQNEH  
15235300 FTADLIAMNADFIITSTFQEIAGTKNTVGQYESHGAFTLPGLYRVVHGIDVDFPKFNIVSPGADMTIYFPYSEE-TRRLTALHGSIEEMLYSPDQTDEH  
297814081 FTADLIAMNADFIITSTFQEIAGTKNTVGQYESHGAFTLPGLYRVVHGIDVDFPKFNIVSPGADMAIYFPFSEE-TKRLTALHSSIEEMLYSPQOTDEH  
6682841 FTADLIAMNADFIITSTFQEIAGTKNTVGQYESHTAFTLPGLYRVVHGIDVDFPKFNIVSPGADMDIYFPYSEK-QKRLTALHGSIEQLLFDPQNDDEH  
255564236 FTADILAMNADFIITSTFQEIAGSKNTVGQYESHTAFTLPGLYRVVHGIDVDFPKFNIVSPGADMSIYFPYSEK-QKRLTALHGSIEKMLYDPEQTDDEW  
313770763 FTADVLAMNADFIITSTFQEIAGTKNTVGQYESHTAFTLPGLYRVVHGIDVDFPKFNIVSPGADMDIYFPYSDK-QKRLTTLHGSIEKMLYDSEQTTDDW  
3915037 FTADLIAMNADFIITSTFQEIAGTKNTIGQYESHTAFTLPGLYRVVHGIDVDFPKFNIVSPGADMTIYFPYSDK-EKRLTALHSSIEKLLYGTEQTDDEY  
225437428 FTADLIAMNADFIITSTFQEIAGSKNTVGQYESHTAFTLPGLYRVVHGIDVDFPKFNIVSPGADMCYFPYSDV-EKRLTALHGSIEKLLYDPEQNEEH  
162458268 FTADIIAMNADFIITSTFQEIAGSKNTVGQYESHTAFTLPGLYRVVHGIDVDFPKFNIVSPGADMSIYFPYHTEK-AKRLTSLHGSIEENLIYDPEQNDDEH  
242035817 FTADIIAMNADFIITSTFQEIAGSKNTVGQYESHTAFTLPGLYRVVHGIDVDFPKFNIVSPGADMSIYFPYHTEK-AKRLTSLHGSIEENLIYDPEQNDQH  
115452927 FTADIIAMNADFIITSTFQEIAGSKNTVGQYESHTAFTLPGLYRVVHGIDVDFPKFNIVSPGADMSIYFPYTEK-AKRLTSLHGSLENLISDPEQNDDEH  
241896730 FTADIIAMNADFIITSTFQEIAGSKNTVGQYESHTAFTLPGLYRVVHGIDVDFPKFNIVSPGADMSIYFPYTEK-AKRLTALHGSIESLIYDPEQNDDEH  
304651490 FTADLLSMNHSDFIITSTFQEIAGTKNTVGQYESHTAFTLPGLYRVVHGIDVDFPKFNIVSPGADMTIYFPYFDK-EKRLTSLHPSIEKLLFDPEQNEVH  
29289943 FTADLLSMNHSDFIITSTFQEIAGTKNTVGQYESHTAFTLPGLYRVVHGIDVDFPKFNIVSPGADMTIYFPYSDK-EKRLTSLHPSIEKLLFDPEQNEVH  
115310620 FTADLLAMNHSDFIITSTFQEIAGTNNTVGQYESHTAFTLPGLYRVVHGIDVDFPKFNIVSPGADMAIYFPYSDT-EKRLTSFHGSIEENLLFDPEQNDDEH  
4468153 FTADLLAMNNSDFIITSTFQEIAGTKNSVGQYESHGAFTLPGLYRVVHGIDVDFPKFNIVSPGADDDGIYFSYSEK-ERRLTSYHDCLEKLLFDPEQTEEH  
345286419 FTADLLAMNHSDFIITSTFQEIAGTKSTVGQYESHASFTLPGLYRVVHGIDVDFPKFNIVSPGADDECIYFPYSEK-DKRLTALHESLEKLI FDPQQTDEH  
4468151 FTADLLAMQHSDFIITSTFQEIAGTRNVVGQYESHVAFTMPGLYRVVHGIDVDFPKFNIVSPGADSEIYFPYTDK-EKRLTNLQASIEKLLFDPEQNEEH  
151176306 FSADLMAMNHADFIITSTFQEIAGTKNTVGQYESHKAFTFPGLYRVVHGIDVDFPKFNIVSPGADMAIYFPFSEK-EHRLTSLHSFIEQLLFKPEQNEEH  
14530225 FSADLMAMNHADFIITSTFQEIAGTKNTVGQYESHKAFTFPGLYRVVHGIDVDFPKFNIVSPGADMAIYFPFSEKDVCLTSLHRLIEQLLFKPEQNEEH  
15239816 FTADLIAMNADFIITSTFQEIAGSKNNVGQYESHTAFTMPGLYRVVHGIDVDFPKFNIVSPGADMTIYFPYSDK-ERRLTALHESIEELLYSFAEQNDEH  
297795665 FTADLIAMNADFIITSTFQEIAGSKNNVGQYESHTAFTMPGLYRVVHGIDVDFPKFNIVSPGADMTIYFPYSDK-ERRLTALHESIEELLYSFAEQNDEH  
225431790 FTADLIAMNADFIITSTFQEIAGSKNVGQYESHTAFTLPGLYRVVHGIDVDFPKFNIVSPGADMSIYFSYSEK-ERRLTALHDSIESLLYDSEQNDDH  
255551835 FTADIIAMNADFIITSTFQEIAGSKNNVGQYESHTAFTLPGLYRVVHGIDVDFPKFNIVSPGADSCYFPYSDR-ERRLTALHGAIEELLYDPEQNEEH  
168009716 FTADLIAMNHADFIITSTFQEIAGSAKTVGQYESHQAFTMPGLYRVVNGVNVDFPKFNIVSPGADMDVYFPYTDK-ERRLTALHPTIEDLLFGTEQSDDEH  
168035060 FTADLIAMNHADFIITSTFQEIAGSAKTVGQYESHQAFTMPGLYRVVNGIDVDFPKFNIVSPGADMTVYFPYTDK-QHRLTKLHPAIEKLLFSSDQTDEH  
168058907 FTADLIAMNSADFIITSTFQEIAGSADTVGQYESHQAFTMPGLYRVVNGIDVDFPKFNIVSPGADMNIIYFPADK-ERRLTSLQESIEELLYSPEQTDDEH  
168029793 FTADLIAMNQADFIITSTFQEIAGSEDTVGQYESHVAFTLPGLYRVVNGIDVDFPKFNIVSPGADTIYVFSYTEK-DRRLTDLHDKIEKLLYDPEQTAEH  
94266940 FMVDLIAMNQANFIVTSTAQEITGTENSIGQYESYQFFTMPGLLNITSGIDLHPRFNVI PPVGNQEVYFPWNRK-RSRPTKLRRRVSELLFSGEDD-DC  
94264333 FMVDLIAMNQANFIVTSTAQEITGTENSIGQYESYQFFTMPGLLNITSGIDLHPRFNVI PPVGNQEVYFPWNRK-RSRPTKLRRRVSELLFSGEDD-DC  
297569306 FMADLLAMNQANFIITSTAQEITGTENSIGQYESYQFFTMPGLVNVISGINLFHPRFNVI PPVGNQEVYFPYNRK-RGRVKVMRREVTLLFEQEDA-DC

```

254416162 FTADLIAMNAANFIISSTYQEIVGKPDVSGQYESYQNFTMPDLYHVVGNGIELFSKFNVPPGVNEQVYFPYTRS-EDRVPRDCERLEELLFTLDDPSQV
332712456 FTADLIAMNAANFIISSTYQEIVGTADSVGQYESYQNFTMPDLYHVINGIELFSKFNVPPGVNETVFFPYTRT-QGRVASDIKRLEDEFLFTLDDPSQV
17232477 FTADLIAMNAANFVISSTYQEIVGTPDSIGQYESYKCFMPELYHVVGNGIELFSKFNVPPGVNENSYFPYTQT-QNRIESDRDRLEMLFTLEDSSQI
75908500 FTADLIAMNAANFVISSTYQEIVGTSVSGQYESYKCFMPELYHVVGNGIELFSKFNVPPGVNENSYFPYTHT-QDRIESDRDRLEMLFTLEDSSQI
186682280 FTADLIAMNAANFVVSSTYQEIVGTPDSVSGQYESYKCFMPELYHVVGNGIELFSKFNVPPGVNENSYFPYTRT-KDRVESDRQRLAETLFTLEDPTQI
119512682 FTADLIAMNAANFVVSSTYQEIVGTPDSVSGQYESYKCFMPELYHVVGNGIELFSKFNVPPGVNENSYFPYTRK-EDRVEADSDRLADILFTLEDPHQI
334117431 FTADLIAMNAANCIVSSTYQEIVGQPDVSGQYESYHCFMPELYHVVGNGIELFSKFNVPPGVNENSYFPYTRI-EDRVQGDRLNELLFTLEDPEQV
218440696 FTADLIAMNAANCIISSTYQEIVGRTDSVSGQYESYHCFMPELYHVVGNGIELFSKFNVPPGVNENSYFPYTRT-DEVPNKREHLEDLLFTLEDPSQV
159031025 FTADLISMNAANFIISSTYQEIVGTSVSGQYESYKCFMPELYHVVGNGIELFSKFNVPPGVNENSYFPYTNR-EERLLGGERLEELLFTLEAPRRV
220907171 FTADLIVMNAANFIISSTYQEIVGTPDSVSGQYESYHCFMPELYHVVGNGIELFSKFNVPPGVNENSYFPYTKV-EERLVTERRLEELLFTLDDPAQV
22298591 FTADLIAMNAANFIISSTYQEIVGTPDSIGQYESYHCFMPELYHVVGNGIELFSKFNVPPGVNENSYFPYTHY-TERLEGDRQLEELLFTLEDPPQI
158339122 FTADLIAMNAANFIISSTYQEIVGTPDSIGQYESYHCFMPELYHVVGNGIELFSKFNVPPGVNENSYFPYTHY-TERLEGDRQLEELLFTLEDPPQI
284053161 FTADLIAMNAANFIISSTYQEIVGTPDSIGQYESYHCFMPELYHVVGNGIELFSKFNVPPGVNENSYFPYTHY-TERLEGDRQLEELLFTLEDPPQI
209523126 FTADLIAMNAANFIISSTYQEIVGTPDSIGQYESYHCFMPELYHVVGNGIELFSKFNVPPGVNENSYFPYTHY-TERLEGDRQLEELLFTLEDPPQI
17228554 FTADLITMNAADFIITSSYQEIVGTPDSIGQYESYHCFMPELYHVVGNGIELFSKFNVPPGVNENSYFPYTHY-TERLEGDRQLEELLFTLEDPPQI
75909957 FTADLITMNAADFIITSSYQEIVGTPDSIGQYESYHCFMPELYHVVGNGIELFSKFNVPPGVNENSYFPYTHY-TERLEGDRQLEELLFTLEDPPQI
186685043 FTADLISMNAADFIITSSYQEIVGTPDSIGQYESYHCFMPELYHVVGNGIELFSKFNVPPGVNENSYFPYTHY-TERLEGDRQLEELLFTLEDPPQI
119510624 FTADLISMNAADFIITSSYQEIVGTPDSIGQYESYHCFMPELYHVVGNGIELFSKFNVPPGVNENSYFPYTHY-TERLEGDRQLEELLFTLEDPPQI
298489784 FTADLISMNAADFIITSSYQEIVGTPDSIGQYESYHCFMPELYHVVGNGIELFSKFNVPPGVNENSYFPYTHY-TERLEGDRQLEELLFTLEDPPQI
220909283 FTADLITMNAADFIITSSYQEIVGTPDSIGQYESYHCFMPELYHVVGNGIELFSKFNVPPGVNENSYFPYTHY-TERLEGDRQLEELLFTLEDPPQI
332708740 FTADLIAMNSADFIITSSYQEIVGTPDSIGQYESYHCFMPELYHVVGNGIELFSKFNVPPGVNENSYFPYTHY-TERLEGDRQLEELLFTLEDPPQI
Clustal Consensus : * * : . : : : : * : * * : : . * * . * : : . : * * . * : : : :

```

610 620 630 640 650 660 670 680 690 700

```

114331077 RGILQDSKPLIFTMARLDRIKNTGLVSYGASQRLRLANLVIVGGKIDPQHSSDHHEEQEIHQMHLMDEYKLDQVVRWLGMRLDKNLAGELYRYIA
30249199 RGYLQDPDKPLIFTMARLDRIKNTGLVSYGASQRLRLANLVIVGGKIDPQHSSDHHEEQEIHRMHQLMDEHELDQVVRWLGMRLDKNLAGELYRYIA
82703384 RGYFADPAKPLIFTMARLDTVKNLTGLAAWFGQCEALSTAAANLVIVGGHIDPAASCDGEERAIEHMHALMNEYKLEGRMRWLGTRLKKNLAGELYRHA
198283392 RGVLKERDKPIIFSMARMHIKNLSGLAEIFGASERLRKANLVIIIGHVLDLQNSQDEEEGAQIQRMHIMDAHQLDGQMRWIGTLLEKNVAGELYRVIG
344199811 RGVLKDRDKPIIFSMARMHIKNLSGLAALFGASERLRKANLVIIIGHVLDLQNSQDEEEGAQIQRMHIMDAHQLDGQMRWIGTLLEKNVAGELYRVIG
255021595 RGVLEDRQKPLLLSMARMHIKNLSGLAEIYGRSSRLRGLANLVIIIGHVLDVGNSSDAEEREEIRRMHEIMDHYQLDGLRWVQALLDKTVAGELYRVVA
77166514 RGKLQDHTKPLLLFTIARLDRIKNTGLVEWYGRCELRRLKANLVIVVGGYIDKSQSDADSEEQQAQIARMHQLMEEYGLDQVVRWLGVMQLKNLAGELYRFIA
300115586 RGKLQDRSKPLLLFTIARLDRIKNTGLVEWYGRCELRRLKANLVIVVGGYIDKSQSDADSEEQQAQIARMHQLMEEYGLDQVVRWLGVMQLKNLAGELYRFIA
292493898 RGRQLQDKGKPLLLFTMARLDRIKNTGLVEWYGRCELRRLKANLVIVVGGYIDKSQSDADSEEQQAQIARMHQLMEEYGLDQVVRWLGVMQLKNLAGELYRFIA
350552412 RGTLLKHPERPLIFTMARLDRIKNTGLVQWYAENALREANLVIVVAGYTDAGKSADREEQEIHYLHHLFTTHGLDEQVVRWLGVRLLDKVVFAGELYRFIA
220933364 RGVLAAPERPVIFMARLDRIKNTGLVQWYAENALREANLVIVVAGYTDAGKSADREEQEIHYLHHLFTTHGLDEQVVRWLGVRLLDKVVFAGELYRFIA
350574485 RGQLQDRDKPLLLSMARLDRIKNIIGGLVDWYARAPELNRNVNLVVVAGHVVDGNASGDDEEREQIDYIHYLMNTHGLDQVVRWLGVMQLKNLAGELYRFIA
95929190 RGLLDDKDKPLIFTMARLDKVKNTGLVECYAKSERLRKANLVIVVAGYTDAGKSADREEQEIHYLHHLFTTHGLDEQVVRWLGVMQLKNLAGELYRFIA
298528445 KGELQDRTKPIIFSMARLDRIKNTGLVEWYGRCELRRLKANLVIVVAGYTDAGKSADREEQEIHYLHHLFTTHGLDEQVVRWLGVMQLKNLAGELYRFIA
297602308 IGYLADRNPPIIFSMARLDKVKNTGLVEWYGRCELRRLKANLVIVVAGYTDAGKSADREEQEIHYLHHLFTTHGLDEQVVRWLGVMQLKNLAGELYRFIA
115457664 IGYLADRNPPIIFSMARLDKVKNTGLVEWYGRCELRRLKANLVIVVAGYTDAGKSADREEQEIHYLHHLFTTHGLDEQVVRWLGVMQLKNLAGELYRFIA
326504012 IGYLADRNPPIIFSMARLDKVKNTGLVEWYGRCELRRLKANLVIVVAGYTDAGKSADREEQEIHYLHHLFTTHGLDEQVVRWLGVMQLKNLAGELYRFIA
115450038 IGYLADRNPPIIFSMARLDKVKNTGLVEWYGRCELRRLKANLVIVVAGYTDAGKSADREEQEIHYLHHLFTTHGLDEQVVRWLGVMQLKNLAGELYRFIA
326531526 IGYLADRNPPIIFSMARLDKVKNTGLVEWYGRCELRRLKANLVIVVAGYTDAGKSADREEQEIHYLHHLFTTHGLDEQVVRWLGVMQLKNLAGELYRFIA
242063616 IGYLADRNPPIIFSMARLDKVKNTGLVEWYGRCELRRLKANLVIVVAGYTDAGKSADREEQEIHYLHHLFTTHGLDEQVVRWLGVMQLKNLAGELYRFIA
42568160 IGYLADRNPPIIFSMARLDKVKNTGLVEWYGRCELRRLKANLVIVVAGYTDAGKSADREEQEIHYLHHLFTTHGLDEQVVRWLGVMQLKNLAGELYRFIA
297805240 IGYLADRNPPIIFSMARLDKVKNTGLVEWYGRCELRRLKANLVIVVAGYTDAGKSADREEQEIHYLHHLFTTHGLDEQVVRWLGVMQLKNLAGELYRFIA

```

313770765 IGYLEDKKKPIIFSMARLDTVKNLTGLTEWYGKNRRLGLVNLVIVGGFFDPNKSKDREEMAEIKKMHLEIKYQLKGQIRWIAAQTDRKRNGELYRCIA  
313770767 IGYLEDKKKPIIFSMARLDTVKNLTGLTEWYGKNRRLGLVNLVIVGGFFDPNKSKDREEMAEITKMHGLIKKYRLNGQFRWIAAQTDRNRNGELYRCIA  
255584097 IGYLADKKKPIIFSMARFDTVKNLTGLTEWYGKNRRLNLVNLVIVAGFFDPKSKDREEMAEIKKMHALIDKYQLKGQIRWIAAQTDRQRNGELYRCIA  
225466221 IGFLADRRKPIIFSMARLDIVKNITGLTEWFGNNKRLRLVNLVIVAGFFDPKSKDREEMAEIKKMHITLIEKYQLKGQIRWIAAQNDRRRNGELYRCIA  
313770769 IGYLADRRKPIIFSMARLDTVKNITGLTEWFGKNTKLRNLVNLVIVAGFFDPKSKNDREETAEIKKMHALIEKYQLKGQFRWIAAQTDRYRNGELYRCIA  
313770771 IGYLADKKKPIIFSMARLDTVKNITGLTEWYGKNAKLRNLVNLVIVAGFFDPKSKNDREETAEIKKMHSLIEKYQLKGQFRWIAAQSDRYRNGELYRCIA  
255570671 IGYLADRRKPIIFSMARLDTVKNITGLTEWYGKNRRLNLVNLVIVAGFFDPKSKDREETAEINKMHALIEKYQLKGQIRWIAAQTDRYRNGELYRCIA  
15219457 MGYLADREKPIIFSMARLDTVKNITGLTEWYGKDKRLREMANLVVAGFFDMSKSNDRREEKAEIKKMHDLIEKYKLKGKFRWIAAQTDRYRNGELYRCIA  
297842089 MGYLAEREKPIIFSMARLDTVKNITGLTEWYGKDKRLREMANLVVAGFFDMSKSNDRREEKAEIKKMHDLIEKYKLKGKFRWIAAQTDRYRNGELYRCIA  
115466896 KFVLKDKNKPIIFSMARLDVKNMTGLVEMYGKNAHLRDLANLVIVCGDHG-NQSKDREEQAEFKKMYGLIDQYKLKGHIRWISAQMNVRVNGELYRYIC  
17980243 KFVLKDKNKPIIFSMARLDVKNMTGLVEMYGKNAHLRDLANLVIVAGDHG-KESKDREEQAEFKKMYSLIDEYKLKGHIRWISAQMNVRVNGELYRYIC  
162460741 KFVLKDKKKPIIFSMARLDVKNMTGLVEMYGKNARLRELANLVIVAGDHG-KESKDREEQAEFKKMYSLIDEYKLKGHIRWISAQMNVRVNGELYRYIC  
239984690 KFVLKDRNKPIIFSMARLDVKNMTGLVEMYGKNAHLKDLANLVIVAGDHG-KESKDREEQAEFKKMYSLIEEYKLKGHIRWISAQMNVRVNGELYRYIC  
162460681 KFVLNDRNKPIIFSMARLDVKNLTGLVELYGRNRLQELVNLVIVCGDHG-NPSKDKEEQAEFKKMFDLIEQYNLNGHIRWISAQMNVRVNGELYRYIC  
242035533 KFVLNDRNKPIIFSMARLDVKNLTGLVELYGRNRLQELVNLVIVCGDHG-NPSKDKEEQAEFKKMFDLIEQYNLNGHIRWISAQMNVRVNGELYRYIC  
62865493 KFVLKDRNKPIIFSMARLDVKNLTGLVELYGRNRLQELVNLVIVCGDHG-NPSKDKEEQAEFKKMFDLIEQYNLNGHIRWISAQMNVRVNGELYRYIC  
17980241 KFVLKDRNKPIIFSMARLDVKNLTGLVELYGRNRLQELVNLVIVCGDHG-NPSKDKEEQAEFKKMFDLIEQYNLNGHIRWISAQMNVRVNGELYRYIC  
115453437 KFVLKDRNKPIIFSMARLDVKNLTGLVELYGRNRLQELVNLVIVCGDHG-NPSKDKEEQAEFKKMFDLIEQYNLNGHIRWISAQMNVRVNGELYRYIC  
115473359 KFVLKDKKKPIIFSMARLDVKNLTGLVELYGRNRLQELVNLVIVCGDHG-KESKDKEEQAEFKKMFNLIEQYNLNGHIRWISAQMNVRVNGELYRYIC  
3980298 KFVLKDKKKPIIFSMARLDVKNLTGLVELYGRNRLQELVNLVIVCGDHG-KVSKDKEEQAEFKKMFDLIEKYNLNGHIRWISAQMNVRVNGELYRYIC  
15242073 LCVLKDKKKPIILFTMARLDVKNLSSLVEWYGKNTRLRELANLVIVGGDRR-KESKDNEEKAEEMKKMYDLIEEYKLNQGFWRWISSQMDVRVNGELYRYIC  
297812265 LCVLKDKKKPIILFTMARLDVKNLSSLVEWYGKNTRLRELANLVIVGGDRR-KESKDNEEKAEEMKKMYDLIEEYKLNQGFWRWISSQMDVRVNGELYRYIC  
22331535 LCVLKDKKKPIIFTMARLDVKNLSSLVEWYGKNTRLRELANLVIVGGDRR-KESQDNEEKAEEMKKMYELIEEYKLNQGFWRWISSQMDVRVNGELYRYIC  
297818772 LCVLKDKKKPIILFTMARLDVKNLSSLVEWYGKNTRLRELANLVIVGGDRR-KESQDNEEKAEEMKKMYDLIEEYKLNQGFWRWISSQMDVRVNGELYRYIC  
313770759 LCVLKDRNKPIILFTMARLDVKNLSSLVEWYGKNTKLRELANLVIVGGDRR-KESKDLEEQAEMKKMYSHIEKYNLNGQFRWISSQMDVRVNGELYRYIC  
313770761 LCVLKDRNKPIILFTMARLDVKNLTGLVEWYGKNTKLRELANLVIVGGDRR-KESKDLEEQAEMKKMYSHIEKYNLNGQFRWISSQMDVRVNGELYRYIC  
255550319 LCVLKDRSKPIIFTMARLDVKNLTGLVEWYGKNAKLRELANLVIVGGDRR-KESKDLEEQAEMKKMHGLIEKYNLNGQFRWISSQMDVRVNGELYRYIC  
324984223 LCVLNDRNKPIILFTMARLDVKNLTGLVEWYGKNAKLRELANLVIVGGDRR-KESKDLEEQAEMKKMFELIEKYNLNGQFRWISSQMDVRVNGELYRYIC  
258489633 LCVLNDRNKPIILFTMARLDVKNLTGLVEWYGKNAKLRELANLVIVGGDRR-KESKDLEEQAEMKKMFELIEKYNLNGQFRWISSQMDVRVNGELYRYIC  
324984221 LCVLNDRNKPIILFTMARLDVKNLTGLVEWYGKNAKLRELANLVIVGGDRR-KESKDLEEQAEMKKMFELIDKYNLNGQFRWISSQMDVRVNGELYRYIC  
324984229 LCVLNDRNKPIILFTMARLDVKNLTGLVEWYGKNAKLRELANLVIVGGDRR-KESKDLEEQAEMKKMFELIDKYNLNGQFRWISSQMDVRVNGELYRYIC  
6683114 LCVLKDRNKPIILFTMARLDVKNLTGLVEWYGKNAKLRELANLVIVGGDRR-KESKDLEEQAEMKKMYSLIDQYKLNGQFRWISSQMDVRVNGELYRYIC  
4584690 ICVLKDRNKPIIFTMARLDVKNITGLVEWYGKNAKLRELANLVIVGGDRR-KESKDLEEIAEMKKMYGLIETKYKLNGQFRWISSQMDVRVNGELYRYIC  
3915046 ICVLKDRNKPIIFTMARLDVKNITGLVEWYGKNAKLRELANLVIVGGDRR-KESKDLEEIAEMKKMYGLIETKYKLNGQFRWISSQMDVRVNGELYRYIC  
3766299 ICVLKDRSKPIIFTMARLDVKNITGLVEWYGKNAKLRELANLVIVGGDRR-KESKDLEEQAEMKKMYEHIEKYKLNGQFRWISSQMDVRVNGELYRYIC  
3377764 ICVLKDRNKPIIFTMARLDVKNITGLVEWYGKNAKLRELANLVIVGGDRR-KESKDLEEQAEMKKMYEHIEKYKLNGQFRWISSQMDVRVNGELYRYIC  
225444613 LCVLKDRNKPIIFSMARLDVKNLTGLVEWYGKNTRLRELANLVIVGGDRR-KESKDLEEQAEMKKMHGLIEKYKLNGQFRWISSQMDVRVNGELYRYIA  
3660531 LCVLKDRTPILFTMARLDVKNLTGLVEWYAKNPRLRLGLVNLVIVGGDRR-KESKDLEEQAEMKKMYELIETHNLNGQFRWISSQMDVRVNGELYRYIA  
31455440 LCVLKDRTPILFTMARLDVKNLTGLVEWYAKNPRLRLGLVNLVIVGGDRR-KESKDLEEQAEMKKMYELIETHNLNGQFRWISSQMDVRVNGELYRYIA  
304651488 LCVLKDRNKPIIFTMARLDVKNLTGLVEWYAKNPRLRELANLVIVGGDRR-KESKDLEEQAEMKKMYELIKTHNLNGQFRWISSQMDVRVNGELYRYIA  
28629438 LCVLKDRNKPIIFTMARLDVKNLTGLVEWYAKNPRLRELANLVIVGGDRR-KESKDLEEQAEMKKMYELIKTHNLNGQFRWISSQMDVRVNGELYRYIA  
115310618 LCVLKDKKKPIILFTMARLDVKNLTGLVELYAKNPRLRELANLVIVGGDRR-KESKDLEEQAEMKKMYSLIETYNLNGQFRWISSQMDVRVNGELYRYIA  
345286417 LCVLKDKNKPIIFTMARLDVKNPTGLVELYAKSPKLRQLVNLVIVGGDRR-KESKDLEEQAEMKKMYNLIETYNLNGQFRWISSQMDVRVNGELYRYIA  
38425095 ICVLKDRKKPIIFSMARLDVKNMTGLVEWYGKNAKLRELANLVIVGGDRR-KESKDTEEKEMKKMYSLIEEYNLNGQFRWISSQMDVRVNGELYRYIA  
15235300 VGTLSDRSKPIIFSMARLDVKNISGLVEMYSKNTKLRELANLVIVAGNIDVNSKDREEIVEIEKMHNLKMYKLDGQFRWITAQTNRARNGELYRYIA  
297814081 VGTLSDRSKPIIFSMARLDVKNISGLVEMYSKNTKLRELANLVIVAGNIDVNSKDREEIAEIEKMDNLVKS YKLDGQFRWITAQTNRARNGELYRYIA  
6682841 VGTLSDRSKPIVFSMARLDVKNMTGLVECYGKNSRLRELANLVIVAGYIDVNSKDREEIAEIEKMHNLKMYKLDGQFRWIAAQTNRARNGELYRYIA



255564236 IGTLDKSKPLIFSMARLDVKNITGLVEMYGKNAKLRELVLNVLVIVAGYIDVKKSKDREEIAEIEKMHDLMKKYNLEGGFRWITAQTNRARNGELYRYIA  
 313770763 IGTLDKSKPIIFSMARLDVKNISGLVECYGKNARLRELVLNVLVIVAGYIDVKKSDREEIEIEIEKMHDLMKKYKLDGGFRWLTAQTNRARNGELYRYIA  
 3915037 IGSLTDRSKPIIFSMARLDVKNITGLVESYAKNSKLRELVLNVLVIVAGYIDVKKSSDREEIEIEIEKMHDLMKQYNLNGEFRWITAQTNRARNGELYRYIA  
 225437428 IGMNDRSKPIIFSMARLDQVKNTGLVECYAKNAKLREMANLVVIVAGYNDVKKSDREEIIEIEKMHDLMKKEYNLHGQFRWISSQTNRARNGELYRYIA  
 162458268 IGHLDDRSKPIIFSMARLDVKNITGLVEAFKCAKLRELVLNVLVIVAGYNDVKKSKDREEIAEIEKMHDLIKTHNLFQGFWRWISAQTNRARNGELYRYIA  
 242035817 IGHLDDRSKPIIFSMARLDVKNITGLVEAFKCTKLRELVLNVLVIVAGYNDVKKSKDREEIAEIEKMHDLIKTYNLFQGFWRWISAQTNRARNGELYRYIA  
 115452927 IGHLDDRSKPIIFSMARLDVKNITGLVEAYAKNARLRELVLNVLVIVAGYNDVKKSKDREEIAEIEKMHDLIKTYNLFQGFWRWISAQTNRARNGELYRYIA  
 241896730 IGHLDPSKPIIFSMARLDVKNITGLVKAYSKNAKLRLVLNVLVIVAGYNDVKKSKDREEIAEIEKMHDLIKTYNLFQGFWRWISAQTNRARNGELYRYIA  
 304651490 IGSLNDQSKPIIFSMARLDVKNITGLVECYAKNATLRELANLVVIVAGYNDVKKSDREEIAEIEKMHDLIKTYNLFQGFWRWISAQTNRARNGELYRYIA  
 29289943 IGNLNDQSKPIIFSMARLDVKNITGLVECYAKNATLRELANLVVIVAGYNDVKKSDREEIAEIEKMHDLIKTYNLFQGFWRWISAQTNRARNGELYRYIA  
 115310620 IGTLDKASKPIIFSMARLDVKNITGLVECYAKNAELRELANLVVIVAGYNDVKKSDREEIEIEIEKMHDLIKTYNLFQGFWRWISAQTNRARNGELYRYIA  
 4468153 IGVLDQSKPIIFSMARLDVKNITGLVECYAKNAKLRELANLVVIVAGYNDVKKSDREEIAEIEKMHDLIKTYNLFQGFWRWISAQTNRARNGELYRYIA  
 345286419 VGFLDPKPIIFSMARLDVKNISGLVELYAKNARLRELANLVVIVAGYIDVKKSSDREEIEIEIEKMHDLIKTYNLFQGFWRWISAQTNRARNGELYRYIA  
 4468151 IGVLDKSKPIIFSMARLDVKNITGLVECYAKNAKLRELANLVVIVAGYNDVKKSSDREEIEIEIEKMHDLIKTYNLFQGFWRWISAQTNRARNGELYRYIA  
 151176306 IGVLDTSKPIIFSMARLDVKNITGLVECYGKNAKLRELANLVVIVAGYNDVKKSDREEIAEIEKMHDLIKTYNLFQGFWRWISAQTNRARNGELYRYIA  
 14530225 IGVLDTSKPIIFSMARLDVKNITGLVECYGKNAKLRELANLVVIVAGYNDVKKSDREEIEIEIEKMHDLIKTYNLFQGFWRWISAQTNRARNGELYRYIA  
 15239816 VGLSDQSKPIIFSMARLDVKNITGLVECYAKNSKLRELANLVVIVAGYIDVKKSDREEIEIEIEKMHDLIKTYNLFQGFWRWISAQTNRARNGELYRYIA  
 297795665 VGLSDQSKPIIFSMARLDVKNITGLVECYAKNSKLRELANLVVIVAGYIDVKKSDREEIEIEIEKMHDLIKTYNLFQGFWRWISAQTNRARNGELYRYIA  
 225431790 IGMLSDRSKPIIFSMARLDVKNITGLVECFGKSSKLRELVLNVLVIVAGYIDVTKSRDREIEIEIEKMHDLIKTYNLFQGFWRWISAQTNRARNGELYRYIA  
 255551835 IGVLDQSKPIIFSMARLDVKNITGLVECYGKNSKLRELANLVVIVAGYIDVKKSDREEIEIEIEKMHDLIKTYNLFQGFWRWISAQTNRARNGELYRYIA  
 168009716 IG-VIDKSKPIIFSMARLDVKNITGLVECYGKNSKLRELANLVVIVAGYIDVTKSRDREIEIEIEKMHDLIKTYNLFQGFWRWISAQTNRARNGELYRYIA  
 168035060 VG-IIDKSKPIIFSMARLDVKNITGLVECYGKNSKLRELANLVVIVAGYIDVTKSRDREIEIEIEKMHDLIKTYNLFQGFWRWISAQTNRARNGELYRYIA  
 168058907 IG-LIDKSKPIIFSMARLDVKNITGLVECYGKNSKLRELANLVVIVAGYIDVTKSRDREIEIEIEKMHDLIKTYNLFQGFWRWISAQTNRARNGELYRYIA  
 168029793 IGSLKDRKPIIFSMARLDVKNISGLVECFGKSSKLRELVLNVLVIVAGYIDVTKSRDREIEIEIEKMHDLIKTYNLFQGFWRWISAQTNRARNGELYRYIA  
 94266940 LGRLEAPDKPLLFITARLDRIKNTGLVEAYGRDSELQRVNLVIVAGYIDVTKSRDREIEIEIEKMHDLIKTYNLFQGFWRWISAQTNRARNGELYRYIA  
 94264333 LGRLEAPDKPLLFITARLDRIKNTGLVEAYGRDSELQRVNLVIVAGYIDVTKSRDREIEIEIEKMHDLIKTYNLFQGFWRWISAQTNRARNGELYRYIA  
 297569306 LGRLEAPDKPLLFITARLDRIKNTGLVEAYGRDSELQRVNLVIVAGYIDVTKSRDREIEIEIEKMHDLIKTYNLFQGFWRWISAQTNRARNGELYRYIA  
 254416162 YGKLDNDPTKRPLFSIARLDRIKNTGLVECFGKSSKLRELVLNVLVIVAGYIDVTKSRDREIEIEIEKMHDLIKTYNLFQGFWRWISAQTNRARNGELYRYIA  
 332712456 FGKLDYPNKRPIIFSMARLDRIKNTGLAECFGKSKLQERCNLIILVAGKLRVIEDSSDSEEEKAEIIEKLYQIIEEYNLYGKIRWLGVRSLKSDSGEYRVIA  
 17232477 FGKLDYPNKRPIIFSMARLDRIKNTGLAECFGKSKLQERCNLIILVAGKLRVIEDSSDSEEEKAEIIEKLYQIIEEYNLYGKIRWLGVRSLKSDSGEYRVIA  
 75908500 FGKLDYPNKRPIIFSMARLDRIKNTGLAECFGKSKLQERCNLIILVAGKLRVIEDSSDSEEEKAEIIEKLYQIIEEYNLYGKIRWLGVRSLKSDSGEYRVIA  
 186682280 FGKLDYPNKRPIIFSMARLDRIKNTGLAECFGKSKLQERCNLIILVAGKLRVIEDSSDSEEEKAEIIEKLYQIIEEYNLYGKIRWLGVRSLKSDSGEYRVIA  
 119512682 FGKLDYPNKRPIIFSMARLDRIKNTGLAECFGKSKLQERCNLIILVAGKLRVIEDSSDSEEEKAEIIEKLYQIIEEYNLYGKIRWLGVRSLKSDSGEYRVIA  
 334117431 FGKLDYPNKRPIIFSMARLDRIKNTGLAECFGKSKLQERCNLIILVAGKLRVIEDSSDSEEEKAEIIEKLYQIIEEYNLYGKIRWLGVRSLKSDSGEYRVIA  
 218440696 FGKLDYPNKRPIIFSMARLDRIKNTGLAECFGKSKLQERCNLIILVAGKLRVIEDSSDSEEEKAEIIEKLYQIIEEYNLYGKIRWLGVRSLKSDSGEYRVIA  
 159031025 FGKLDYPNKRPIIFSMARLDRIKNTGLAECFGKSKLQERCNLIILVAGKLRVIEDSSDSEEEKAEIIEKLYQIIEEYNLYGKIRWLGVRSLKSDSGEYRVIA  
 220907171 WGLDHPDKRPLFSMARLDRIKNTGLAECFGKSKLQERCNLIILVAGKLRVIEDSSDSEEEKAEIIEKLYQIIEEYNLYGKIRWLGVRSLKSDSGEYRVIA  
 22298591 YGYLEAPEKRPLFSMARLDRIKNTGLAECFGKSKLQERCNLIILVAGKLRVIEDSSDSEEEKAEIIEKLYQIIEEYNLYGKIRWLGVRSLKSDSGEYRVIA  
 158339122 FGKLDYPNKRPLFSMARLDRIKNTGLAECFGKSKLQERCNLIILVAGKLRVIEDSSDSEEEKAEIIEKLYQIIEEYNLYGKIRWLGVRSLKSDSGEYRVIA  
 284053161 FGKLDYPNKRPLFSMARLDRIKNTGLAECFGKSKLQERCNLIILVAGKLRVIEDSSDSEEEKAEIIEKLYQIIEEYNLYGKIRWLGVRSLKSDSGEYRVIA  
 209523126 FGKLDYPNKRPLFSMARLDRIKNTGLAECFGKSKLQERCNLIILVAGKLRVIEDSSDSEEEKAEIIEKLYQIIEEYNLYGKIRWLGVRSLKSDSGEYRVIA  
 17228554 FGKLDYPNKRPLFSMARLDRIKNTGLAECFGKSKLQERCNLIILVAGKLRVIEDSSDSEEEKAEIIEKLYQIIEEYNLYGKIRWLGVRSLKSDSGEYRVIA  
 75909957 FGKLDYPNKRPLFSMARLDRIKNTGLAECFGKSKLQERCNLIILVAGKLRVIEDSSDSEEEKAEIIEKLYQIIEEYNLYGKIRWLGVRSLKSDSGEYRVIA  
 186685043 LGHLDYPNKRPIIFSVSSISIKNLGLAECFGKSKLQERCNLIILVAGKLRVIEDSSDSEEEKAEIIEKLYQIIEEYNLYGKIRWLGVRSLKSDSGEYRVIA  
 119510624 IGLDNDPNKRPIIFSVAPITSVKNITGLAECFAKNGRLQEHNCNLIIFITTKLYVQATNPKEAEEIQRLHDIIINQYELHGNIRCIIGMRPLSPDLGEAYRVIA  
 298489784 LGNLDYPNKRPIIFSVAPITSVKNITGLAECFAKNGRLQEHNCNLIIFITTKLYVQATNPKEAEEIQRLHDIIINQYELHGNIRCIIGMRPLSPDLGEAYRVIA  
 220909283 LGHLDYPNKRPIIFSVAPITSVKNITGLAECFAKNGRLQEHNCNLIIFITTKLYVQATNPKEAEEIQRLHDIIINQYELHGNIRCIIGMRPLSPDLGEAYRVIA

332708740 VGYLNSPNQRPILSIAPLTSIKNLSGLVECFASSKELQQKCNLILITSHVVRVEDATDPEEKGEIEKLNQLIKQYNLHGKIRWIGLRLTTPDIGESYRVIA  
 Clustal Consensus . : : : : . \* : : \* : : . . \* . \* : . \* \* :

710 720 730 740 750 760 770 780 790 800

....|....|....|....|....|....|....|....|....|....|....|....|....|....|....|....|....|....|....|....|....|

114331077 DKKRGI FVQPALFEAFGLTII EAMASG-----LPTFATRYGGPLEI IQHNRSGFHDIPNQGTATADLIADFL EKSHEKPLEWERLSQ GALARVASRYT  
 30249199 DKKRGI FVQPALFEAFGLTII EAMASG-----LPTFATRYGGPLEI IQHNRSGFHDIPNQGAATADLIADFF EKNLENPQEWERISQ GALTDRVASRYT  
 82703384 DRRGI FVQPARFEAFGLTII EAMASG-----LPVFATCYGGPREI IQHGVSGYHFDPN DGLAGASAMADFF ERVAADPGFWDRI SQALQRVEARYT  
 198283392 DSRGCFVQPALFEAFGLTVI EAMSSG-----LPVFATRFGGPLEI IEDGVS GFHDIPNNQQETA EKLADFL EAAAAADIRVWETISD GALARVGAHYT  
 344199811 DTHGCFVQPALFEAFGLTVI EAMSSG-----LPVFATRFGGPLEI IEDGVS GFHDIPNNQQETA EKLADFL EAAAAADIRVWETISD GALARVSTHYT  
 255021595 DGRGVFVQPALFEAFGLTVI EAMSSG-----LPVFATRFGGPLEI IEDGVS GFHDIPNNQQETA EKLADFL EAAERPKYWL EISDAALARVAERYT  
 77166514 DSRGAFVQPALFEAFGLTVI EAMSSG-----LPTFATCYGGPLEI IQEGVSGFHDIPNHG EKAADRIADFF EHCQTEAGYWDKFSQ GALLRRIKNHYT  
 300115586 DSRGAFVQPALFEAFGLTVI EAMSSG-----LPTFATCYGGPLEI IQEGVSGFHDIPNHG EKVANRIADFF EHCQTEAGYWDKFSQ GALLRRIKNHYT  
 292493898 DSRGAFVQPALFEAFGLTVI EAMSSG-----LPTFATCYGGPLEI IQDEISGFHDIPNHG EEAAGSIADFF ERCQVEPEYEWENLSQ GALLRRI RRYT  
 350552412 DRRGVFVQPALFEAFGLTVI EAMVSG-----LPTFATHYGGPLEI IEHQS GFHDIPMRGDQASQ LLAFLRECEQDPDYWVRISHGGM ERVERHYT  
 220933364 DRRGVFVQPALFEAFGLTVI EAMASG-----LPTFATRYGGPLEI IEDGVS GFHDIPNHG EQAARIIMEFLERCASDP DHWQQISRSAIRRVEQRYT  
 350574485 DHQGA FVQPALFEAFGLTVI EAMSCG-----LPTFATCYGGPSEI IEHGLS GFHDIPNHG DQAAALILEFFDAC SQNPAHWQTFSTAAMARVQERYT  
 95929190 DQKGVFVQPALFEAFGLTVI EAMATG-----LPIFATQYGGPLEI IVDGKSGFHDIPNDNE EMAEKICTFF ERAANHPQYWKVISDACITRVEENYT  
 298528445 DSRGAFVQPALFEAFGLTVI EAMNSG-----LPTFATIFGGPLEI IEDGKSGFHDIPTHGDEAAGL MANFFSRCRADASYWDTISNNSIKRVEEKN  
 297602308 DTKGAFVQPALYEA FGLTVI EAMNCG-----LPTFATNQGGPAEII IVDGVS GFHVPNPNGREAGIKIADFFQKCKEDPSYWNK VSTAGLQRIYECYT  
 115457664 DTKGAFVQPALYEA FGLTVI EAMNCG-----LPTFATNQGGPAEII IVDGVS GFHVPNPNGREAGIKIADFFQKCKEDPSYWNK VSTAGLQRIYECYT  
 326504012 DSKGAFVQPALYEA FGLTVI EAMNCG-----LPTFATNQGGPAEII IVDGVS GFHVPNPNGREAGIKIADFFQKCKEDPSYWNK VSTAGLQRIYECYT  
 115450038 DTKGAFVQPALYEA FGLTVI EAMNCG-----LPTFATNQGGPAEII IVDGVS GFHVPNPNGREAGIKIADFFQKCKEDPSYWNK VSTAGLQRIYECYT  
 326531526 DTRGAFVQPALYEA FGLTVI EAMNCG-----LPTFATNQGGPAEII IVDGVS GFHVPNPNGREAGIKIADFFQKCKEDPSYWNK VSTAGLQRIYECYT  
 242063616 DTRGAFVQPALYEA FGLTVI EAMNCG-----LPTFATNQGGPAEII IVDGVS GFHVPNPNGREAGIKIADFFQKCKEDPSYWNK VSTAGLQRIYECYT  
 42568160 DTRGAFVQPAHYEA FGLTVI EAMSCG-----LVTFATNQGGPAEII IVDGVS GFHDIPSNNGEESSDKIADFF EKSGMDPDYWNMFST EQLQRIYECYT  
 297805240 DTRGAFVQPAHYEA FGLTVI EAMSCG-----LVTFATNQGGPAEII IVDGVS GFHDIPSNNGEESSDKIADFF EKSGMDPDYWNMFST EQLQRIYECYT  
 313770765 DTKGAFVQPALYEA FGLTVI EAMNCG-----LPTFATNQGGPAEII IVDGVS GFHDIPKNNGDESSNIIADFF EKCKVDPGHWNKYSL EQLKRIYECYT  
 313770767 DTKGAFVQPALYEA FGLTVI EAMNCG-----LPTFATNQGGPAEII IVDGVS GFHDIPKNNGDESSNIIADFF EKCKVDPGHWNKYSL EQLKRIYECYT  
 255584097 DTKGAFVQPALYEA FGLTVI EAMNCG-----LPTFATNQGGPAEII IVDGVS GFHDIPKNNGDESSNIIADFF EKCKIDAEYWNKFSE DGLKRIYECYT  
 225466221 DTKGAFVQPAIYEA FGLTVI EAMNCG-----LPTFATNQGGPAEII IVDGVS GFHDIPNIGDESSNIIADFF EKCRDSDHWNKISKAGLQRIYECYT  
 313770769 DTKGAFVQPALYEA FGLTVI EAMNCG-----LPTFATNQGGPAEII IVDGVS GFHDIPNNGDESSNIIADFF EKCKTDAEYWNKMSAAGLQRIYECYT  
 313770771 DTKGAFI QPALYEA FGLTVI EAMNCG-----LPTFATNQGGPAEII IVDGVS GFHDIPNNGDESSNIIADFF EKCKTDAEYWNKMSAAGLQRIYECYT  
 255570671 DTKGAFVQPALYEA FGLTVI EAMNCG-----LPTFATNQGGPAEII IVDGVS GFHDIPNNGDESSNIIADFF EKCKADPECWNKMSAAGLQRIYECYT  
 15219457 DTKGVFVQPALYEA FGLTVI EAMNCG-----LPTFATNQGGPAEII IVDGVS GFHDIPNNGDESSVTKIGDFFSKCRSDGLYWDNISQ GGLKRIYECYT  
 297842089 DTKGVFVQPALYEA FGLTVI EAMNCG-----LPTFATNQGGPAEII IVDGVS GFHDIPNNGDESSVTKIGDFFSKCRSDGLYWDNISQ GGLKRIYECYT  
 115466896 DTKGVFVQPAFYEA FGLTVI EAMTCG-----LPTIATCHGGPAEII IVDGVS GLHIDPYHSDKAADILVNFF EKCKQDSTYWDNISQ GGLQRIYEEKYT  
 17980243 DTKGVFVQPAFYEA FGLTVI ESMT CG-----LPTIATCHGGPAEII IVDGVS GLHIDPYHSDKAADILVNFF EKCKEDPTYWDNISQ GGLQRIYEEKYT  
 162460741 DTKGAFVQPAFYEA FGLTVI ESMT CG-----LPTIATCHGGPAEII IVDGVS GLHIDPYHSDKAADILVNFF EKCKADPSYWDNISQ GGLQRIYEEKYT  
 329984690 DTKGAFVQPAFYEA FGLTVI EAMTCG-----LPTIATCHGGPAEII IVDGVS GLHIDPYHSDKAADILVNFF EKSTADPSYWDNISQ GGLQRIYEEKYT  
 162460681 DTKGAFVQPAFYEA FGLTVI EAMTCG-----LPTFATAYGGPAEII IVDGVS GFHDIPYQGDKASALLV DFFDKCQAEPSHWSKISQ GGLQRIEEEKYT  
 242035533 DTKGAFVQPAFYEA FGLTVI EAMTCG-----LPTFATAYGGPAEII IVDGVS GFHDIPYQGDKASALLV DFFDKCQAEPSHWSKISQ GGLQRIEEEKYT  
 62865493 DTKGAFVQPAFYEA FGLTVI ESMT CG-----LPTFATAYGGPAEII IVDGVS GFHDIPYQGDKASALLV EFFEKCQDPHSHWTKISQ GGLQRIEEEKYT  
 17980241 DTRGAFVQPAFYEA FGLTVI ESMS CG-----LPTFATAYGGPAEII IVDGVS GFHDIPYQGDKASALLV EFFEKCQDPAHWTKISQ GGLQRIEEEKYT  
 115453437 DTKGAFVQPAFYEA FGLTVI ESMT CG-----LPTFATAYGGPAEII IVDGVS GFHDIPYQGDKASALLV EFFEKCQEDPSHWTKISQ GGLQRIEEEKYT  
 115473359 DMRGAFVQPALYEA FGLTVI EAMTCG-----LPTFATAYGGPAEII IVDGVS GFHDIPYQNDKASALLV EFFEKCQEDPNHWIKISQ GGLQRIEEEKYT  
 3980298 DMKGAFVQAAFYEA FGLTVI EAMTCG-----LPTFATAYGGPAEII IVDGVS GFHDIPYQNDKASALLV DFFKCKQEDPSHWNKISQ GGLQRIEEEKYT

15242073 DTKGAFVQPALYEAFGLTVVEAMTCG-----LPTFATCKGGPAEIIIVHGKSGFHIDPYHGDQAADTLADFFTKCKEDPSHWDEISKGGQLRIEEKYT  
297812265 DTKGAFVQPALYEAFGLTVVEAMTCG-----LPTFATCKGGPAEIIIVHGKSGFHIDPYHGDQAANTLADFFTKCKEDPSHWDEISKGGQLRIEEKYT  
22331535 DTKGAFVQPALYEAFGLTVVEAMTCG-----LPTFATCNGGPAEIIIVHGKSGFHIDPYHGDKAABSLADFFTKCKHDP SHWDQISLGGLERIQEKYT  
297818772 DTKGAFVQPALYEAFGLTVVEAMTSG-----LPTFATCNGGPAEIIIVHGKSGFHIDPYHGDQAABTLADFFTKCKHDP SHWDQISLGGLERIQEKYT  
313770759 DTKGAFVQPALYEAFGLTVVEAMTCG-----LPTFATCNGGPAEIIIVHGKSGFHIDPYHGEKAAELLVDFFEKCKVDPAHWDKISHGGQLRIQEKYT  
313770761 DTKGAFVQPALYEAFGLTVVEAMTCG-----LPTFATCNGGPAEIIIVHGKSGFHIDPYHGVQAABELLVDFFEKCKADPSYWDKISQGGQLRIQEKYT  
255550319 DTKGVFVQPALYEAFGLTVVESMTCG-----LPTFATCNGGPAEIIIVHGKSGFNIDPYHGDQAABELLVEFFEKCKADPCVWDEISKGGQLRIQEKYT  
324984223 DTKGAFVQPALYEAFGLTVVEAMTCG-----LPTFATCNGGPAEIIIVHGKSGFNIDPYHGDQAADILVDFFEKCKDPSHWKISQGGQLRIEEKYT  
258489633 DTKGAFVQPALYEAFGLTVVEAMTCG-----LPTFATCNGGPAEIIIVHGKSGFNIDPYHGDQAADILVDFFEKCKDPSHWKISQGGQLRIEEKYT  
324984221 DTKGAFVQPALYEAFGLTVVEAMTCG-----LPTFATCNGGPAEIIIVHGKSGFNIDPYHGDQAADILVDFFEKCKDPSHWKISQGGQLRIEEKYT  
324984229 DTKGAFVQPALYEAFGLTVVEAMTCG-----LPTFATCNGGPAEIIIVHGKSGFNIDPYHGDQAADILVDFFEKCKDPSHWKISQGGQLRIEEKYT  
6683114 DTKGAFVQPALYEAFGLTVVEAMTCG-----LPTFATCKGGPAEIIIVHGKSGFHIDPYHGEQAABELLVDFFEKCKADPSYWDKISLGGQLRIEEKYT  
4584690 DTKGAFVQPAVYEAFGLTVVEAMATG-----LPTFATLNGGPAEIIIVHGKSGFHIDPYHGDRAADLLVEFFEKVKVDP SHWDKISQGGQLRIEEKYT  
3915046 DTKGAFVQPAVYEAFGLTVVEAMATG-----LPTFATLNGGPAEIIIVHGKSGFHIDPYHGDRAADLLVEFFEKVKADPSHWKISQGGQLRIEEKYT  
3766299 DTKGAFVQPAVYEAFGLTVVEAMATG-----LPTFATLNGGPAEIIIVHGKSGFHIDPYHGDRAADLLVEFFEKVKDPSHWKISQGGQLRIEEKYT  
3377764 DTKGAFVQPAVYEAFGLTVVEAMATG-----LPTFATLNGGPAEIIIVHGKSGFHIDPYHGDRAADLLVEFFEKVKDPSHWKISQGGQLRIEEKYT  
225444613 DTKGVFVQPAFYEAFGLTVVEAMTCG-----LPTFATCNGGPAEIIIVHGKSGFHIDPYHGDKAABELLANFFEKCKADPTHWEKISKAGLKRRIEEKYT  
3660531 DTKGAFVQPAFYEAFGLTVVEAMTCG-----LPTFATNNGGPAEIIIVHGKSGFHIDPYHGEQAADLLADFFEKCKKEPSHWETISTGGLKRRIQEKYT  
31455440 DTKGAFVQPAFYEAFGLTVVEAMTCG-----LPTFATNNGGPAEIIIVHGKSGFHIDPYHGEQAADLLADFFEKCKKEPSHWETISTGGLKRRIQEKYT  
304651488 DTKGAFVQPAFYEAFGLTVVEAMTCG-----LPTFATNNGGPAEIIIVHGKSGFHIDPYHGEQAADLLAEFFEKCKVDP SHWEAISKGGQLRIQEKYT  
28629438 DTRGAFVQPAFYEAFGLTVVEAMTCG-----LPTFATNNGGPAEIIIVHGKSGFHIDPYHGEQAADLLADFFEKCKVDP SHWEAISKGGQLRIQEKYT  
115310618 DTRGAFVQPAFYEAFGLTVVEAMTCG-----LPTFATNNGGPAEIIIVHGKSGFHIDPYHGEQVSELLANFFERCKKEPSYWDTISAGGLKRRIQEKYT  
345286417 DTKGAFVQPAFYEAFGLTVVEAMTRG-----LPTFATLNGGPAEIIIVHGKSGFHIDPYNGEQVAETLVSFEEKCNKDP SHWEAISTGGLKRRIQEKYT  
38425095 DTRGAFVQPAFYEAFGLTVVEAMTCG-----LPTFATCHGGPAEIIIVHGKSGFHIDPYHGDKAADLLVDFFEKSTADPSYWNENISKGGQLRIEEKYT  
15235300 DTRGAFVQPAFYEAFGLTVVEAMTCG-----LPTFATCHGGPAEIIIVHGKSGFHIDPYHPEQAAGNIMADFFERCKEDPNHWKKSVDAGLQRIERYT  
297814081 DTRGAFVQPAFYEAFGLTVVEAMTCG-----LPTFATCHGGPAEIIIVHGKSGFHIDPYHPEQAAGNIMADFFERGRDPNHWKKSVDAGLQRIERYT  
6682841 DTKGAFVQPAFYEAFGLTVVEAMTCG-----LPTFATCHGGPAEIIIVHGKSGFHIDPYHPEQAABELMADFFGCKKENPSHWKKISDGGQLRIERYT  
255564236 DTKGAFVQPAFYEAFGLTVVEAMTSG-----LPTFATCHGGPAEIIIVHGKSGFHIDPYHPEQAANLMADFFDRCKQDP DHVWNISAGLQRIERYT  
313770763 DTKGAFVQPAFYEAFGLTVVEAMTCG-----LPTFATCHGGPAEIIIVHGKSGFHIDPYHPEQAANLMADFFERCKQDPNHWVKISAGLQRIERYT  
3915037 DTKGAFVQPAFYEAFGLTVVEAMTCG-----LPTFATNNGGPAEIIIVHGKSGFHIDPYHPEQAABELLVDFFQCKEDPNHWKKSVDAGLQRIERYT  
225437428 DTRGIFVQPAFYEAFGLTVVEAMTCG-----LPTFATCHGGPAEIIIVHGKSGFHIDPYHPEQAANLMADFFERCKQDPNHWVKISAGLQRIERYT  
162458268 DTHGAFVQPAFYEAFGLTVVEAMTCG-----LPTFATLNGGPAEIIIVHGKSGFHIDPYHPEQAANLMADFFERCKQDPNHWVKISAGLQRIERYT  
242035817 DTHGAFVQPAFYEAFGLTVVEAMTCG-----LPTFATLNGGPAEIIIVHGKSGFHIDPYHPEQAANLMADFFERCKQDPNHWVKISAGLQRIERYT  
115452927 DTHGAFVQPAFYEAFGLTVVEAMTCG-----LPTFATLNGGPAEIIIVHGKSGFHIDPYHPEQAANLMADFFERCKQDPNHWVKISAGLQRIERYT  
241896730 DTHGAFVQPALYEAFGLTVVEAMTCG-----LPTFATLNGGPAEIIIVHGKSGFHIDPYHPEQAANLMADFFERCKQDPNHWVKISAGLQRIERYT  
304651490 DKRGIFVQPAFYEAFGLTVVEAMTCG-----LPTFATCHGGPAEIIIVHGKSGFHIDPYHPEQAANLMADFFERCKQDPNHWVKISAGLQRIERYT  
29289943 DKRGIFVQPAFYEAFGLTVVEAMTCG-----LPTFATCHGGPMETIIQDGVSGYHIDPYHPNKAABELMVEFFQRCQNP THWENISASGLQRIERYT  
115310620 DKRGIFVQPAFYEAFGLTVVEAMTCG-----LPTFATCHGGPMETIIQDGVSGYHIDPYHPNKAABELMVEFFQRCQNP THWENISASGLQRIERYT  
4468153 DTRGIFVQPAFYEAFGLTVVEAMTCG-----LPTFATSHGGPMETIIQDGVSGYHIDPYHPNKAABELMVEFFQRCQNP THWENISASGLQRIERYT  
345286419 DKRGIFVQPAFYEAFGLTVVEAMTCG-----LPTFATSHGGPMETIIQDGVSGYHIDPYHPNKAABELMVEFFQRCQNP THWENISASGLQRIERYT  
4468151 DKRGIFVQPAFYEAFGLTVVEAMTCG-----LPTFATSHGGPMETIIQDGVSGYHIDPYHPNKAABELMVEFFQRCQNP THWENISASGLQRIERYT  
151176306 DKGGIFAQPAFYEAFGLTVVEAMTCG-----LPTFATCHGGPAEIIIVHGKSGFHIDPYHADQAABKMTFFVCKREDPNYWTKISAGGLLRIKERYT  
14530225 DKGGIFAQPAFYEAFGLTVVEAMTCG-----LPTFATCHGGPAEIIIVHGKSGFHIDPYHADQAABKMTFFVCKREDPNYWTKISAGGLLRIKERYT  
15239816 DTKGVFVQPAFYEAFGLTVVESMTCA-----LPTFATCHGGPAEIIIVHGKSGFHIDPYHADQAABKMTFFVCKREDPNYWTKISAGGLLRIKERYT  
297795665 DTKGVFVQPAFYEAFGLTVVESMTCA-----LPTFATCHGGPAEIIIVHGKSGFHIDPYHADQAABKMTFFVCKREDPNYWTKISAGGLLRIKERYT  
225431790 DTKGAFVQPAFYEAFGLTVVEAMTCG-----LPTFATCHGGPAEIIIVHGKSGFHIDPYHADQAABKMTFFVCKREDPNYWTKISAGGLLRIKERYT  
255551835 DAKGVFVQPAFYEAFGLTVIEAMTCG-----LPTFATCHGGPAEIIIVHGKSGFHIDPYHADQAABKMTFFVCKREDPNYWTKISAGGLLRIKERYT

```

168009716 EAGGVFVQPALYEGFGLTVVEAMTCG-----LPTFATLHGGPAEIIHGISGFHIDPYHPDEVADELVTFFEKVKSDSSFWTKISEAALQRIYSSFT
168035060 DAGGVFVQPALYEGFGLTVVEAMTCG-----LPTFATMHGGPAEIIVNGISGFHIDPYHPGVAEVLVSFFEKVKTDPGVWTRISEAALQRIYSNFT
168058907 DSQGAFFVQPALYEGFGLTVVEAMTSG-----LPTFATSHGGPAEIIHGISGYHIDPYYPDEAAEQIVAFFEKCKNEPGLWNKVSEAGLQRIYSSYT
168029793 DSHGAFVQPALYEGFGLTVIEAMTCG-----LPTFATCHGGPKIEIVSDVSGFHDPPFHPESASKIIVDFFERCCKEYTKLSDGGLERIRTKYT
94266940 DRGGVFVQPALFEAFGLTILEAMHSG-----LPVFATQFGGPLEIIEHEHSGFLINPTDPQAMTARLNEFFAACQADPRHWQGFSGRGLERARSFT
94264333 DRGGVFVQPALFEAFGLTILEAMHSG-----LPVFATQFGGPLEIIEHEHSGFLINPTDPQAMTARLNEFFAACQADSRHWQGFSGRGLERARSFT
297569306 DRRGVFVQPALFEAFGLTILEAMHSG-----LPVFATQFGGPLEIIEHEKSGFLINPTDPQAMTARLREFFHHCEENPRYWQGFSGRGLERARSFT
254416162 DHRGIFVQPALFEAFGLTILEAMISG-----LPTFGTQFGGPLEIIQDKVNGFLINPTNLEETAQKILEFLSKCEQNPDYWLEISNRGMERVYSTYT
332712456 DRHGIFVQPALFEAFGLTILESMISG-----LPTFGTQFGGPLEIIQDKVNGILINPTNQEEMAQKILDFTVKCEENPQYWEESNQGIERVYSTYT
17232477 DRQGFVQPALFEAFGLTILESMISG-----LPTFATQFGGPLEIIQDKINGFYINPTNLEETATKILDFTVKCEQNPYWNIISEKAIDRVYSTYT
75908500 DRQGFVQPALFEAFGLTILESMISG-----LPTFATQFGGPLEIIQDQINGFYINPTNLEETATKILDFTVKCEHNPYWKIIEKAIDRVYSTYT
186682280 DRQGFVQPALFEAFGLTILESMVSG-----LPTFATQFGGPLEIIQDKVNGFLINPTNLEETATKIVDFITKCEQNPYWNIEISQIGIDRVYSTYT
119512682 DRKGIFVQPALFEAFGLTILESMVSG-----IPTFATQFGGPLEIIQDKVNGFYINPTNLEETAQKILEFVTKCEQSSHYWDVASEAIAKRVLTYYT
334117431 DTQGFVQPALFEAFGLTILEAMITG-----IPTFGTQFGGPLEIIQDGVNGFYINPTNHEETAQKILDFTLSCENPNYWEISTRGIDRVYSTYT
218440696 DRRGVFVQPALFEAFGLTILEAMISG-----LPTFATQFGGPLEIIQDKVNGFYINPTNLEETAQKILEFVTKCDHNPQHWIQLSNKAMERVYSTYT
159031025 DRQGFVQPALFEAFGLTILEAMITG-----LPIFATQFGGPREIIEHNGGFLINPTNLEETATMILDFLAKCRQDPDYWREISEQAIQRVYSTYT
220907171 DHQGFVQPALFEAFGLTILEAMITG-----LPTFATQFGGPLEIIEQGVNGFLINPTQPEATAAKILQYVRQCEDNPQTWQSISERAIERVYSTYT
22298591 DRQGFVQPALFEAFGLTILEAMISG-----LPTFGTQFGGPLEIIQDGVNGFYINPTNLEEMAETIVRFLACDRDPQEWQRISKAGIERVYSTYT
158339122 DHKGIFVQPALFEAFGLTVLEAMISG-----LPTFATQFGGPLEIIRDGIDGFYINPTNLEETATKILDEFKACEATNPQYQQISEQAIERVYSTYT
284053161 DHKGIFVQPALFEAFGLTILEAMISG-----LPTFATQFGGPLEIIRDKINGFYINPTNLEETAQKILDEFVLRQYNGFWEISQIGMDRVYSTYT
209523126 DHGVFVQPALFEAFGLTILEAMISG-----LPTFATQFGGPLEIIRDKINGFYINPTNLEETAQKILDEFLLRCQYNGFWEISQIGMDRVYSTYT
17228554 DYRGYIYHFAFARFEAFGRSILEAMISG-----LPTFATKFGGSLEIMEDQNGFRINPTDLEGTAEKILAFFQECETHPEHWQEVSWMSQRIRHOKYN
75909957 DYRGYIYHFAFARFEAFGRSILEAMISG-----LPTFATKFGGSLEILEEDQNGFRINPTDLEGTAEKILAFFQECETHPEHWQEVSWMSQRIRHOKYN
186685043 DCQGISVHFAFARFEAFGRSILEAMISG-----LPTFATQFGGPLEIIEQEEFNVNPTDLVETAKKILDFEKKCNTHPEHWQEVSEWMSQRVHNRYN
119510624 DAQGIYVHFAFARFEAFGRSILEAMVSG-----LPTFVTKFGGAVEIIEQDETFHINPTDFKATAHQILNFDQCEQPERWTEVSWMSQRVINKYN
298489784 DYQGIYIHFALYEAFFGRSILEAMISG-----LPTFATKFGGSSEILEEDLQTFHINPTNLEERTAKTILNFDLKDCAANPEYQWETSQWMIQRIRHOKYN
220909283 DQRGFFVHFAFARFEAFGQTILEAMISG-----LPAFATQFGGPLEIIEQDENGFHNPTDPEGTVKKILAFIHACAADPTYWQGISERAIERVQQQYN
332708740 DLGGFLVHFAFARFEAFGLTVLEAMISG-----LPTFATQFGGPLEIIEQNGDNGFLINPTDLQDTAEKIQQFISKCEHTPDYWQKISQAGIKRVDRKYN
Clustal Consensus : * : .: :...: : ** **: .:* : : * : *

```

810 820 830 840 850 860 870 880 890 900

```

114331077 WKLYAERMMTLSRIYSFWKFVS-GLEREETDLYLNMFYHLQFRPLANRLAGDA-----
30249199 WKLYAERMMTLSRIYGFWKFVS-GLEREETDLYLNMFYHLQFRPLANRLAHEI-----
82703384 WRLYAERMMTLSRIYGFWKFVS-KLEHEETARYLNMFYHLQFRPLAQALPQ-----
198283392 WGNYYAAQMTLARIFGFWRFML-KADRHAAARYLQMFQHLQWRPLAHAVPLGES-----
344199811 WGNYYATQMTLARIFGFWRFML-KTDHHAARYLQMFQHLQWRPLAHAVPLGES-----
255021595 WERYAERLMTIARIFGFWRFVL-DRESQVMERYLQMFRLQWRPLAHAVPME-----
77166514 WELYAERMMTLSRIYGFWKYVT-NLERAEERRYLEMFYNLQFRPLAQQIEH-----
300115586 WELYAERMMTLSRIYGFWKYVT-NLERAEERRYLEMFYNLQFRPLAQQMEH-----
292493898 WDLYAERMMTLSRIYGFWKYVT-NLERAEERRYLEMFYNLQFRPLAQQMEH-----
350552412 WSLYAQRMTLSRIYGFWKYVT-NLERAEARRYLEMFYALQYRPLARSLTGE-----
220933364 WKLYAERMMTLSRIYGFWKYVT-NLERAEERRYLEMFHALQYRPLALLK-----
350574485 WRRYAERMMTLSRIYGFWKYVT-DLERAEERRYLEMFYTLKLRPLAKAQG-----
95929190 WSLYARRLLTSLRYGFWKYVS-NLERAEERRYLEMFHGLMFRNLASETQ-----
298528445 WRLYAQRLLSFSRIYGFWKYVS-NLERDETRRYLDMFYSLKMRSLSH-----
297602308 LWQEQGINRLGKPKQAWRLKAA-DSDAKDLNQVSRAEASSF-----

```

115457664 WKIYATRVLNMGSTYSFWKTLN-KEERQAKQRYLQIFYNVQYRNLAAMARAGDQQAQTG---VAPSEIVVRPKERKPQTRMQRILTRLAQGQKPPVS  
326504012 WKIYATKVLNMGSMYGFWRTLN-KEERQAKQRYMOMFYNLQYRNLVKTVPVGEQPPRPAASTGAVAERNQIVARPRERKPQGRVQRMMSLLGPKPPTY  
115450038 WQIYATKVLNMAISYGFWRTLN-KEERQAKQHYLHMFYNLQFRKLAKNVPTLGEQPAQ---PTESAEPNRIIPRPKERQVCPFLRNLLKKETGNN---  
326531526 WQIYATKVLNMGSMYGFWRTLN-KEERQAKQLYLQMFYNLLFRQLVKTVPKLGEPQAQ---PTTAP--ARIAPRPRERRPQTRIQRATSLGQVPLPTS  
242063616 WQIYATKVLNMGSMYGFWRTLN-KEERQAKQQLYQMFYNLHFRKLANAVPKVGEQPEQ---ATAVPLPDRSAPRPKERQVCPLLRNLLKIKWGSN---  
42568160 WKIYANKVINMGSTYSYWRHLN-KDQKLAKQRYIHSFYNLQYRNLVKTIPILSDIPPEPPLPPKPLVKPSASKGSKRTQPRLSFRLFGA-----  
297805240 WKIYANKVINMGSTYSYWRHLN-KDQKLAKQRYIHSFYNLQYRNLVKNQILSDIPQPPPPPPKPLVKPSASKGSRRTQSRLSFRLFGA-----  
313770765 WKIYANKLLNMGNVYSFWRQLN-KEQKLAKQRYIQLFNLFKRELVSVPPIPTEEAQTPASEPTARTQSSAR-----  
313770767 WKIYAKLLNMGNMYSFWRQLN-KEQKLAKQRYIQMLYNLQFRRLVWVSLSCNQEAWIRTAIILCHLTLLNMFHNVFYLLLSFNFVSVYDH-----  
255584097 WKIYANKVLNMGCIYTYWRQMN-KEQKQAKRRYIQLFYNLQRLKLVKNVPIPTEEAQQQPAPKPVNKASSRQVP-----  
225466221 WKIYANKVLNMGCVFSFWRQLN-TEHKQAKQKYIHMFTYLQFRNLVKNIPIPASEVQPPVSRATKHHHQALTVSTGKVKPKSGLTDYPASAFSQVKNDL  
313770769 WKIYANKVLNMGSVYGFWRQTN-KEQKLAKQRYIEAFYNLQFRNLVGVYCGQLVL-----  
313770771 WKIYANKVLNMGSVYGFWRQMN-KEQKLLKQRYIEAFYNLQFRNLVGVYFRQLVT-----  
255570671 WKIYANKVLNMGSVYGFWRQLN-KEQKHLAKQRYIETFYNLHFRNLVKNVPIASVGPQKQPSSSAGTSKTQEPSPPPATTKSSQSQPTPKPKRKEESQKEKP  
15219457 WKIYAEKLLKMGSLYGFWRQVN-EDQKAKKRYIEMLYNLQFKQLTKKVITIPEDKPLPLRLASLRNLLPKKTTNLGAGSKQKEVTEETKTKQKSKDGOEQ  
297842089 WKIYAEKLLKMGSIYGFWRQVN-EDQKAKQRYIELLYNLQFKQLTKKVITIPEDKPLPLRLASLRNLLPKKTTPLGAGSKQKEVTEAEKTKQKSKDGOEQ  
115466896 WKLYSERLMTLTGVYGFWKYVS-NLERRETRRYIEMFYALKYRSLASAVPLAVDGEESTSK-----  
17980243 WKLYSERLMTLTGVYGFWKYVS-NLERRETRRYIEMFYALKYRSLASAVPLAVDGDSSAAN-----  
162460741 WKLYSERLMTLTGVYGFWKYVS-NLERRETRRYIEMFYALKYRSLASQVPLSFD-----  
239984690 WKLYSERLMTLTGVYGFWKYVS-NLERRETRRYIEMFYALKYRSLAAVPLAVDGESEGN-----  
162460681 WKLYSERLMTLTGVYGFWKYVS-NLERRETRRYIEMLYALKYRTMASTVPLAVEGEPSK-----  
242035533 WKLYSERLMTLTGVYGFWKYVS-NLERRETRRYIEMLYALKYRTMASTVPLAVEGEPSK-----  
62865493 WKLYSERLMTLTGVYGFWKYVS-NLERRETRRYIEMLYALKYRTMASTVPLAVDGEPSK-----  
17980241 WKLYSERLMTLTGVYGFWKYVS-NLERRETRRYIEMLYALKYRKMMASTVPLAVEGEPSNK-----  
115453437 WKLYSERLMTLTGVYGFWKYVS-NLERRETRRYIEMLYALKYRTMASTVPLAVEGEPSNK-----  
115473359 WKLYSERLMTLGSVYGFWKYVT-NLDRRETRRYIEMLYALKYRKMATTVPLAIEGEASTK-----  
3980298 WKLYSERLMTLGSVYGFWKYVS-NLDRRETRRLTKCSMPSSSTAKWLQLSHWLLRARPRANDLSLPEK-----  
15242073 WQIYSQRLTLTGVIYGFWKHVS-NLDRLEARRYIEMFYALKYRPLAQAVPLAQDD-----  
297812265 WQIYSQRLTLTGVIYGFWKHVS-NLDRLEARRYIEMFYALKYRPLAQAVPLAQDD-----  
22331535 WQIYSQRLTLTGVIYGFWKHVS-NLDRLESRRYIEMFYALKYRPLAQAVPLAHEE-----  
297818772 WQIYSERLLTLTGVIYGFWKHVS-NLDRLESRRYIEMFYALKYRPLAQAVPLAQEE-----  
313770759 WQIYSQRLTLTGVIYGFWKHVS-NLDRLESRRYIEMFYALKYRKLAEVPLTKE-----  
313770761 WQIYSQRLTLTGVIYGFWKHVS-NLDRLESRRYIEMFYALKYRKLADSVPLTIE-----  
255550319 WQIYSQRLTLTGVIYGFWKHVS-KLDRRESRRYIEMFYALKYRKLADSVPLTVE-----  
324984223 WKIYSERLLTLTGVIYGFWKHVS-NLERRESRRYIEMFYALKYRKLAEVPLAEE-----  
258489633 WKIYSERLLTLTGVIYGFWKHVS-NLERRESRRYIEMFYALKYRKLAEVPLAEE-----  
324984221 WKIYSERLLTLTGVIYGFWKHVS-NLERRESRRYIEMFYALKYRKLAEVPLAEE-----  
324984229 WKIYSERLLTLTGVIYGFWKHVS-NLERRESRRYIEMFYALKYRKLAEVPLAEE-----  
6683114 WKIYSQRLTLTGVIYGFWKHVS-NLDRLESRRYIEMFYALKYRKLAEVPLAVE-----  
4584690 WTIYSQRLTLTGVIYGFWKHVS-NLDRLESRRYIEMFYALKYRKLAEVPLAVE-----  
3915046 WTIYSQRLTLTGVIYGFWKHVS-NLDRLESRRYIEMFYALKYRKLAEVPLAVE-----  
3766299 WQIYSQRLTLTGVIYGFWKHVS-NLDRLESRRYIEMFYALKYRKLAEVPLAVEE-----  
3377764 WQIYSQRLTLTGVIYGFWKHVS-NLDRLESRRYIEMFYALKYRKLAEVPLAVEE-----  
225444613 WKIYSERLLTLAGVIYGFWKHVS-NLDRRETRRYIEMFYALKYRKLQSVPLAVEE-----  
3660531 WQIYSERLLTLAAVYGFWKHVS-KLDRLEIRRYIEMFYALKYRKLMAEAVPLAAE-----  
31455440 WQIYSERLLTLAAVYGFWKHVS-KLDRLEIRRYIEMFYALKYRKLMAEAVPLAAE-----  
304651488 WQIYSERLLTLAAVYGFWKHVS-KLDRLEIRRYIEMFYALKFRKLAEVPLAVE-----



28629438 WQIYSDRLTLAAVYGFWKHVS-KLDRLEIRRYLEMFYALKFRKLAQLVPLAVE-----  
115310618 WQIYSDRLTLAGVYGFWKCVS-KLDRQEIRRYLEMFYALKYRKLAQVPLAVDQ-----  
345286417 WQIYSDRLTLAGVYGFWKYVS-KLDRLEIRRYLEMFYALKYRKLAQVPLAVE-----  
38425095 WKIYSDRLTLAGVYGFWKYVS-NLDRREARRYLEMFYALKYKLAESVPLAIEDAN-----  
15235300 WKIYSERLMTLAGVYGFWKYVS-KLERRETRRYLEMFYILKFRDLVKTVPSTADD-----  
297814081 WNIYSERLMTLAGVYGFWKYAS-KLERRETRRYLEMFYILKFRDLVKTVPSTADD-----  
6682841 WKIYSERLMTLAGVYGFWKYVS-KLERRETRRYLEMFYILKFRDLVKSVPPLASENQH-----  
255564236 WKIYSERLTLAGVYGFWKYVS-KLERRETRRYLEMFYILKFRDLVQTVPLAIDDQH-----  
313770763 WKIYSERLMTLAGVYGFWKYVS-KLERRETRRYLEMFYILKFRDLVKTVPSTIEDWH-----  
3915037 WKIYSERLMTLAGVYGFWKYVS-KLERRETRRYLEMFYILKFRDLANSVPIAKG-----  
225437428 WKIYSERLMTLAGVYGFWKYVS-KLSRRETRRYLEMFYILKFRDLAKSVPLAIDDQH-----  
162458268 WKIYSERLMTLAGVYGFWKYVS-KLERLETRRYLEMFYILKFRDLAKTVPLAIDQPQ-----  
242035817 WKIYSERLMTLAGVYGFWKYVS-KLERRETRRYLEMFYILKFRDLAKTVPLAIDQPQ-----  
115452927 WKIYSERLMTLAGVYGFWKYVS-KLERRETRRYLEMFYILKFRDLAKTVPLAVDEAH-----  
241896730 WKIYSERLMTLAGVYGFWKYVS-KLERRETRRYLEMFYILKRLVKSVPPLALDETH-----  
304651490 WKIYSERLMTLAGVYGFWKLVS-KLERRETRRYLEMFYILKFRDLVKSVPPLAVDEKQ-----  
29289943 WKIYSERLMTLAGVYGFWKLVS-KLERRETRRYLEMFYILKFRDLVKSVPPLAIDDKH-----  
115310620 WKIYSERLMTLAGVYGFWKYVS-KLERRETRRYLEMFYILKRLVKSVPPLAVDDQH-----  
4468153 WKKYSERLMTLAGVYGFWKHVS-KLERRETRRYLEMFYILKFRDLVNSVPPYAVDGS-----  
345286419 WKIYSERLMTLAGVYGFWKYVS-KLERRETRRYLEMFYILKFRDLVTSVPLAVDGS-----  
4468151 WNIYSERLMTLAGVYGFWKYVS-KLERRETRRYLEMFYILKFRDLAKSVPYATE-----  
151176306 WQKYSERLMTLAGVYGFWKYVS-KLERRETRRYLEMFYILKFRDLANSVPLATDEEPSTTDAVATFRGP-----  
14530225 WQKYSERLMTLAGVYGFWKYVS-KLERRETRRYLEMFYILKFRDLANSVPLATDEEPSTTDAVATFRGP-----  
15239816 WKKYSERLTLAGVYAFWKHVS-KLERRETRRYLEMFYILKFRDLANSIPLATDEN-----  
297795665 WKKYSERLTLAGVYAFWKHVS-KLERRETRRYLEMFYILKFRDLANSIPLATDEN-----  
225431790 WKIYTERLTLAGVYGFWKHVS-KLERRETRRYLEMFYILKRLDLATSIPPLAVDEH-----  
255551835 WKIYSKRLTLAGVYGFWKHVS-KLERREIRRYLEMFYILKFNNLVKSIPLAVDDQQ-----  
168009716 WKLYAERLMTLTRVYGFWKYVS-NLHRREARRYLEMFYTLKFRDLVRSLTLPHPILHLQLHNRQLLYSICIVNSTFQLSTICGNLCDQVKTVPLSKDD-----  
168035060 WKLYAERLMTLTHVYGFWKYVS-NLQRRESKRYLEMFYTLKRYRELVRKSPCPTYSFFIVSNFLMKNLMASYKFQ-----  
168058907 WKIYAERLMTLSAVYGFWKYVS-KLHRQEARRYLEMFYILKFRDLARTVPLSKDDEDVLEKVEKKAQLGPGVGAIVGEAATAVEARKAVTGH-----  
168029793 WEIYAERLMTLSRVYGFWKFVS-KLGRRETRRYLEMFYILKFRDLVKTVPVASDDKSYLEKEKKV-----  
94266940 WQLHCRSLTRLTKVYGFWRYSSISQAKTRLNQYSEVLYHLYFKERAANLL-----  
94264333 WQLHCRSLTRLTKVYGFWRYSSISQAKTRLNQYSEVLYHLYFKERAANLL-----  
297569306 WQRHCRSLTRLTKVYGFWRYSSISQAKMRLNQYSEVLYHLYFKARAEQIR-----  
254416162 WKIHTSRLSLARIYGFWNYTS-KEKREDLLRYTESLFYLIYKPRQQQLLEHHLKR-----  
332712456 WKIHTTRLRLSLARIYGFWNYTS-KANQEDMLRYLEALFHLIYKPRAKLLEHHLTPARA-----  
17232477 WKIHTTKLLTLARIYGFWNFTS-KEKREDLLRYTESLFYLIYKPRQQQLLEQHKKYR-----  
75908500 WKIHTTKLLTLARIYGFWNFAS-KEKREDLLRYTESLFYLIYKPRQQQLLEQHKKYR-----  
186682280 WKIHTSKLLSLARIYGFWNFTS-KENREDLLRYLEALFYLIYKPRQQQLLEQHKKYR-----  
119512682 WKIHTTKLLSLARIYGFWNFTS-KENREDLLRYLEALFYLIYKPKAQELLEQHQR-----  
334117431 WKIHTTKLLTLARTYGFWNYSS-KENREDMLRYTESLFYLIYKPKAKALLAEHANR-----  
218440696 WKIHTSKLLSLARIYGFWNFIS-KENREDILRVESLFYLLFKPRAKELLEQHMR-----  
159031025 WKIHTTRLRLSLARIYGFWNHTS-QENREELLRYIETLFYLLFKPRAQHLEIHGQR-----  
220907171 WKIHTTRLRLSLARTYGFWNYSL-QENREDLLRYTESLFYLLFKPRAQQLAEHLQR-----  
22298591 WKIHTCRLRLSLAKIYGFWNFSS-QENREDMMRYEALFHLIYKPRQAALLAEHLQR-----  
158339122 WKIHTSRLSLAKIYGFWNYTS-REKREDMLRYIETIFYLLYKPMAKLLAKHMD-----  
284053161 WKIHTSRLTLTRVYGFWKYVS-KEKRAMMRYLEALFYLIYKPRCQELLEQHHLQR-----

```

209523126 WKIHTSRLLTLTRVYGFWKYIS-KEKRADMMRYLEALFYLIYKPRSQELLQQLQR-----
17228554 WQLHTSQLLALTKIYSFWNFIR-PESSEARVRYMESLFHLYYKPRAEQILAKHMSCH-----
75909957 WQLHTSQLLALTKIYSFWNFIR-PESSEARVRYMESLFHLYYKPRAEQILAKHMSCH-----
186685043 WLYSNQLLLLAKMFTFWNFVA-PENNEARDRYMETLFHLYYKPRAEKILEKHMGAN-----
119510624 WHLHTSQILLAKIFSFWNFAL-PENNAAKHRYLETFLYLIYKPRAEKILEKHQQYSVIMNH-----
298489784 WESYTEQLLLIKIFSFWNFIV-PEANDARDRYMEILFHLIYKPRAEQIIGQHQQRYAHYIK-----
220909283 WPSHIRQLLLLTKIYGFWNCMA-QQQREALLNYMDALYHLYYKPRAAETLAQHLYR-----
332708740 WQLHTKQLLSLAKIYGFWSETS-KESREALLRYLEALFYLIYKPRATNLLAKHRSR-----
Clustal Consensus :
          910      920      930      940      950      960      970      980
...|...|...|...|...|...|...|...|...|...|...|...|...|...|...|...|...
114331077 -----
30249199 -----
82703384 -----
198283392 -----
344199811 -----
255021595 -----
77166514 -----
300115586 -----
292493898 -----
350552412 -----
220933364 -----
350574485 -----
95929190 -----
298528445 -----
297602308 -----
115457664 E-----
326504012 EQNGYR-----
115450038 -----
326531526 NFSQDAA-----
242063616 -----
42568160 -----
297805240 -----
313770765 -----
313770767 -----
255584097 -----
225466221 -----
313770769 -----
313770771 -----
255570671 KPETITTRHVI-----
15219457 HDVKVGEREVREGLLAADASERVKKVLESSEKQKLEKMKIAYGQQHSQGASPVRNLFWSVVVCLYICYILKQRRFFGANSQAQEV
297842089 NDGKVGGERDVSETFLAAEASERTKKVLETSEKQKLEKMKIAYGQQNQGASPVRNLFWSVVVCLYICYILKQRRFFGANSQAQEV
115466896 -----
17980243 -----
162460741 -----
239984690 -----

```

162460681  
242035533  
62865493  
17980241  
115453437  
115473359  
3980298  
15242073  
297812265  
22331535  
297818772  
313770759  
313770761  
255550319  
324984223  
258489633  
324984221  
324984229  
6683114  
4584690  
3915046  
3766299  
3377764  
225444613  
3660531  
31455440  
304651488  
28629438  
115310618  
345286417  
38425095  
15235300  
297814081  
6682841  
255564236  
313770763  
3915037  
225437428  
162458268  
242035817  
115452927  
241896730  
304651490  
29289943  
115310620  
4468153  
345286419



4468151	-----
151176306	-----
14530225	-----
15239816	-----
297795665	-----
225431790	-----
255551835	-----
168009716	EGPEEKTE <del>TKAR</del> LGPQAIVGTPASA-----
168035060	-----
168058907	-----
168029793	-----
94266940	-----
94264333	-----
297569306	-----
254416162	-----
332712456	-----
17232477	-----
75908500	-----
186682280	-----
119512682	-----
334117431	-----
218440696	-----
159031025	-----
220907171	-----
22298591	-----
158339122	-----
284053161	-----
209523126	-----
17228554	-----
75909957	-----
186685043	-----
119510624	-----
298489784	-----
220909283	-----
332708740	-----
Clustal Consensus	

SucSase sequences from *P. patens* subsp. *patens* (group IV) are clearly separated from those of vascular plants (Figure 35). Interestingly, groups V and VII are further divided in two major branches, containing the sequences from dicots (green) and monocots (blue), respectively. This separation is less clear in group VI (Figure 35). SucSase from *N. europaea* is in a small branch with other  $\beta$ -proteobacteria in group III (proteobacteria). Clearly, *Neu*SucSase is well separated from plant and cyanobacterial enzymes, though they share a significant similarity among all of them. For instance the identity between *Neu*SucSase and *Ath*SucSase is 52.2% and between *Neu*SucSase and SucSase from *T. elongatus* is 48.5%.

### **Protein Expression and Characterization**

The gene of the putative SucSase in *N. europaea* (NCBI Protein ID NP\_841269) codes for 794 amino acids. To shed light on Suc metabolism of group III (Figure 35), we amplified this sequence and expressed the recombinant protein in *E. coli* cells. The enzyme was purified to homogeneity by HisTrap column and gel filtration chromatography as mentioned in “Materials and Methods”. The recombinant protein migrated in SDS-PAGE as a single band of ~95 kDa (data not shown), which is in good agreement with the predicted molecular mass of 93 kDa (including the His-tag provided by the pET28c vector). *Neu*SucSase eluted from the Superdex 200 (size exclusion) column as a protein of ~360 kDa (data not shown), suggesting a tetrameric quaternary structure, as it was reported for cyanobacterial and plant SucSases<sup>77, 80, 84</sup>.

### Substrate Specificity of *Neu*SucSase

SucSases from plants have shown a certain degree of promiscuity to transfer glucoses from ADP-Glc and UDP-Glc, though UDP-Glc is generally preferred. We tested the substrate specificity of SucSase from *N. europaea* in the Suc synthesis direction (Table 4), and observed that ADP-Glc is a more efficient substrate than UDP-Glc. The main difference is not given by  $V_{\max}$ , but by a higher apparent affinity towards ADP-Glc. The  $S_{0.5}$  for ADP-Glc is 0.044 mM in presence of optimal concentrations of Fru (20 mM); whereas the  $S_{0.5}$  for UDP-Glc is 0.98 mM in presence of optimal concentrations of Fru (500 mM). On the other hand, the apparent affinity for Fru is higher in presence of ADP-Glc rather than UDP-Glc. The  $S_{0.5}$  for Fru at saturated concentrations of ADP-Glc is 5.6 mM whereas the  $S_{0.5}$  for Fru in presence of UDP-Glc is significantly higher. Because of the high concentrations of Fru needed to reach saturation, it is not possible to measure the  $S_{0.5}$  for Fru with high precision; but it is at least ~20-fold higher (120 mM). The catalytic efficiencies calculated for ADP-Glc and Fru<sub>(ADP-Glc)</sub> were 17- and 37-fold higher than those obtained for UDP-Glc and Fru<sub>(UDP-Glc)</sub>, respectively (Table 4). These results indicate that *Neu*SucSase prefers ADP-Glc over UDP-Glc as substrate. Similar conclusions were obtained for the enzyme from the cyanobacterium *T. elongatus*, which showed a 26-fold higher catalytic efficiency for ADP-Glc than UDP-Glc <sup>77</sup>.

Table 4. Kinetic parameters for substrates of *NeuSocSase* in the direction of sucrose synthesis. Assays were performed using the conditions described in the “Materials and Methods” section. Analogous values to catalytic efficiency ( $V_{\max}/S_{0.5}$ ) were calculated using the predicted molecular mass of 93 kDa.

Substrate	$S_{0.5}$ (mM)	$V_{\max}$ (U mg <sup>-1</sup> )	$n_H$	$V_{\max}/S_{0.5}$ (mM <sup>-1</sup> s <sup>-1</sup> )
UDP-Glc	0.89 ± 0.05	4.3 ± 0.1	1.1	7.5
ADP-Glc	0.044 ± 0.006	3.7 ± 0.1	1.3	130.3
Fru <sub>(UDP-Glc)</sub>	120 ± 10	2.8 ± 0.2	1.3	0.036
Fru <sub>(ADP-Glc)</sub>	5.6 ± 0.4	4.8 ± 0.2	1.6	1.33

### X-ray Diffraction, Data Processing, Model Building, and Refinement

The best data set collected at synchrotron beamline was processed to 3.05 Å and indexed as space group P65. It was integrated and scaled producing good statistics (Table 5). After the molecular replacement search, four copies of the starting model described in “Materials and Methods” were found in one asymmetric unit. Iterative cycles of model building and refinement were conducted yielding a well-defined structure for *NeuSocSase* with  $R_{\text{work}}$  and  $R_{\text{free}}$  values of 17.37 % and 21.75 %, respectively (Table 5). The truncated GT-B(D) domain was built according to the electron density map. The final structural model contains all the residues except the first three at the N-terminus and the last two at the C-terminus of the *NeuSocSase* amino acid sequence (Figure 36).

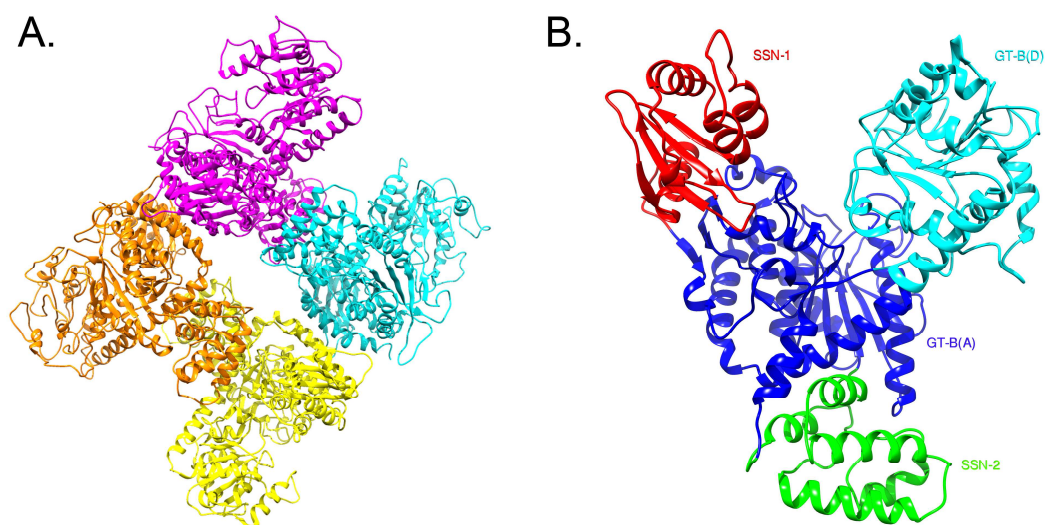


Figure 37. The crystal structure of *NeuSucSase*. A. Tetrameric structure of *NeuSucSase*. B. Monomeric structure and its four different domains: SSN-1, SSN-2, GT-B(A), and GT-B(D).

### Structural Analysis of *NeuSucSase*

*Overall structure.* Although the resolution of the data set was 3.05 Å, the backbone of the protein and some of the key residues side chains were well defined by the electron density (Figure 38 and Figure 39). This allowed us to conduct detailed structural analysis on SucSase's conformational changes involving backbone movement, which are relevant to the catalytic cycle. The crystal structure of *NeuSucSase* displayed a similar fold to the previously reported structural model of *AthSucSase* (PDB ID 3S29)<sup>84</sup>. *NeuSucSase* is a tetramer composed of four identical subunits (Figure 36A), where each monomer contains four domains (Figure 36B). The first domain designated as “Sucrose Synthase N-terminal-1” (SSN-1) domain included residues 1-119 (Figure 36B, red) and contained five  $\alpha$ -helices and four  $\beta$ -strands. The second domain, which included residues 159-264, is the “Sucrose Synthase N-terminal- (SSN-2) domain (Figure 36B, green) with five  $\alpha$ -

helices. The third is the GT-B(D) domain (Figure 36B, cyan), which included residues 514-742 with eight  $\alpha$ -helices and three  $\beta$ -strands. This domain functions in the GT-B family as the sugar donor (D) in catalysis<sup>84, 86, 91</sup>. The fourth domain is the GT-B(A) domain (Figure 36B, blue), which consists of residues from three separate regions: 120-158, 265-513, and 743-794. These separate regions are encompassed by the SSN-1, SSN-2 and GT-B(D) domains in the center of the monomer. The GT-B(A) domain included nine  $\alpha$ -helices and eight  $\beta$ -strands and functions in the GT-B family as the sugar acceptor (A) in catalysis<sup>84, 86, 91</sup>. Both the GT-B(D) and GT-B(A) domains directly facilitate the glycosyltransferase reaction<sup>84</sup>.

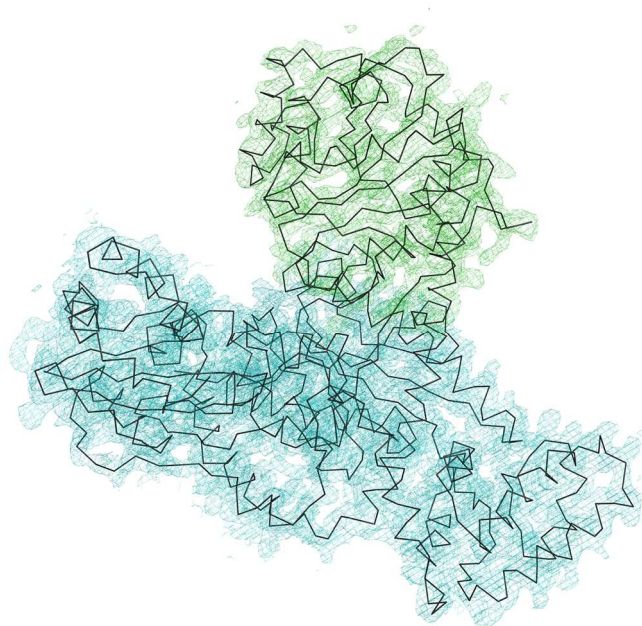


Figure 38. The *NeuSase* monomer structure is shown in backbone trace. The electron density (2Fo-Fc map at 1 sigma) is shown as meshes. The green portion of the electron density covers the GT-B (D) domain in the “open” position, while the cyan portion of the electron density covers the SSN-1, SSN-2, and GT-B (A) domains.

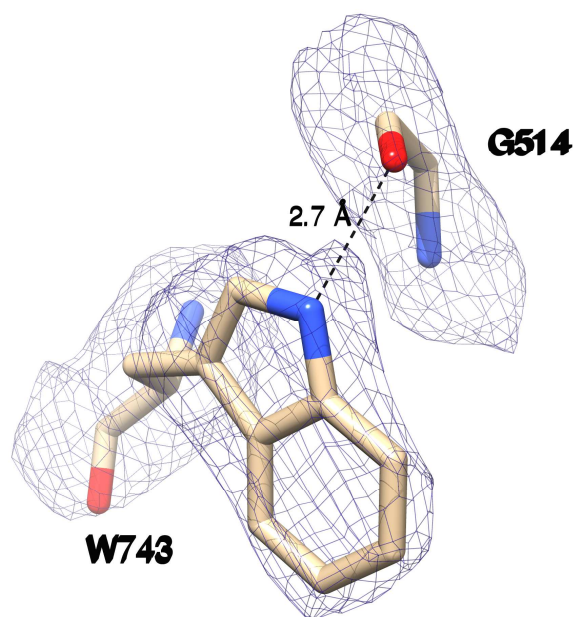


Figure 39. The “hinge”. The picture displays the hydrogen bond between W73 and G514. The electron density (2Fo-Fc map) is shown as blue mesh at 1.5 sigma level.

The obtained *NeuSocSase* structure with no substrates bound has a clearly different overall conformation when compared to *AthSocSase* with UDP and Fru<sup>84</sup>. This implies that substrate binding induces significant conformational changes (Figure 40). After superimposition of only the GT-B(A) domains of *AthSocSase* and *NeuSocSase* (using the least squares function in COOT), the SSN-1, SSN-2, and GT-B(A) domains from both structures overlapped well while the GT-B(D) domains were in a different relative position. The angle between the GT-B(A) and GT-B(D) domains in *NeuSocSase* was about 23.5 degrees wider than in the *AthSocSase* structure. Based on such comparison, we suggest that the *NeuSocSase* structure in this work was in an “open” conformation whereas the *AthSocSase* was “closed”<sup>84</sup>. We have identified some distinct

structural determinants (hinges and latches) related to the movements of the sugar (GT-B(A)) and nucleotide (GT-B(D)) binding domains.

*Sugar-binding GT-B(A) domain.* Analysis of a difference distant matrix map of the Fru-binding GT-B(A) domain as described in “Materials and Methods” (Figure 41) highlights three main regions that move closer upon sugar binding. These are 325-375 to 280-290 ( $\sim 5$  Å), 425-435 to 280-290 ( $\sim 4$  Å), and 425-435 to 325-375 ( $\sim 3$  Å) (Figure 41). Other pair of regions that move towards each other are 280-290 to 490-505 ( $\sim 3$  Å) and 280-290 to 450-460 ( $\sim 2$  Å) (Figure 41). From this analysis, the area 280-290 is the most involved in an induced fit interaction with Fru. Further inspection of these areas reveals that Fru induces local conformational changes via superimposition of the GT-B(A) domains of the *Ath*SucSase (closed) and the *Neu*SucSase (open) (Figure 42). These include the side chain of K431 and the backbone of residues 288-290. The re-shaping of the Fru binding site facilitates the closing via a set of inter-domain hydrogen bonds (Figure 42 in green). These local conformational changes along with the presence of Fru further promote the interactions between the GT-B(A) and GT-(D) domains. Thus, we



propose that Fru binding contributes to the induced fit closing of the structure.

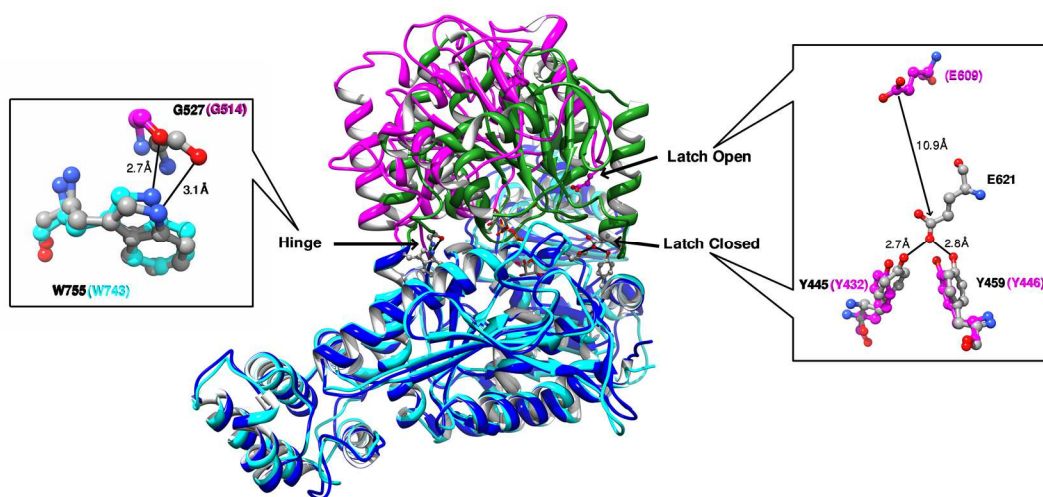


Figure 40. Comparison of the open and closed monomeric forms. The open form structure is represented by the *NeuSocSase* structure reported in this paper; the closed form is represented by the *AthSocSase* structure (PDB ID 3S29). The SNN-1, SNN-2 and GT-B(A) domains are shown in blue for the open form structure and in cyan for the closed form structure. The GT-B(D) domain is shown in magenta for the open form and in green for the closed form. The “hinge-latch” features of the domain movement are shown in blown-up views.

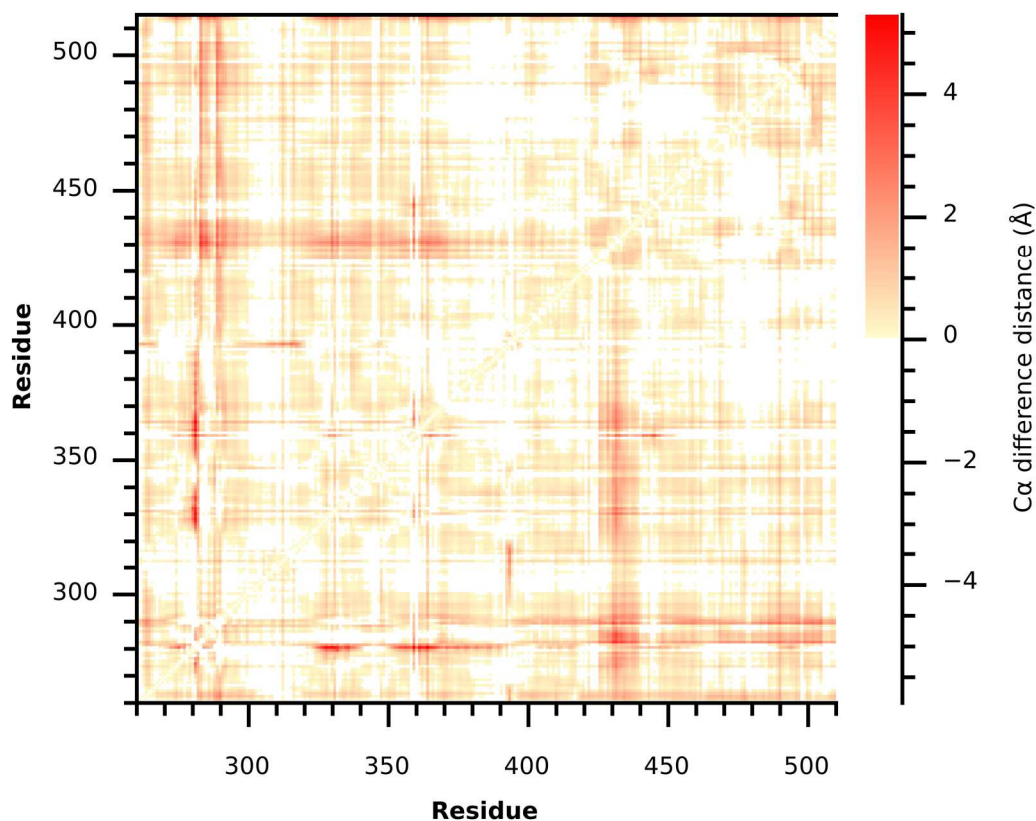


Figure 41. Difference distance matrix map of the GT-B(A) domain. Distances were calculated between all pair of C $\alpha$  carbon of the open structure (*NeuSocSase*). A second pairwise distance matrix was calculated for the close structure (homology model of *NeuSocSase* using *AthSocSase* as template as described in “Materials and Methods”). Afterwards, these two matrices were subtracted, and the  $\Delta$ distance was color coded. The negative and zero values are represented in white. Red colors (higher  $\Delta$ distance values) are pairs of C $\alpha$  carbon that are getting closer upon closing of the enzyme. Only residues from 260 to 510 are shown, which correspond to the GT-B(A) domain.

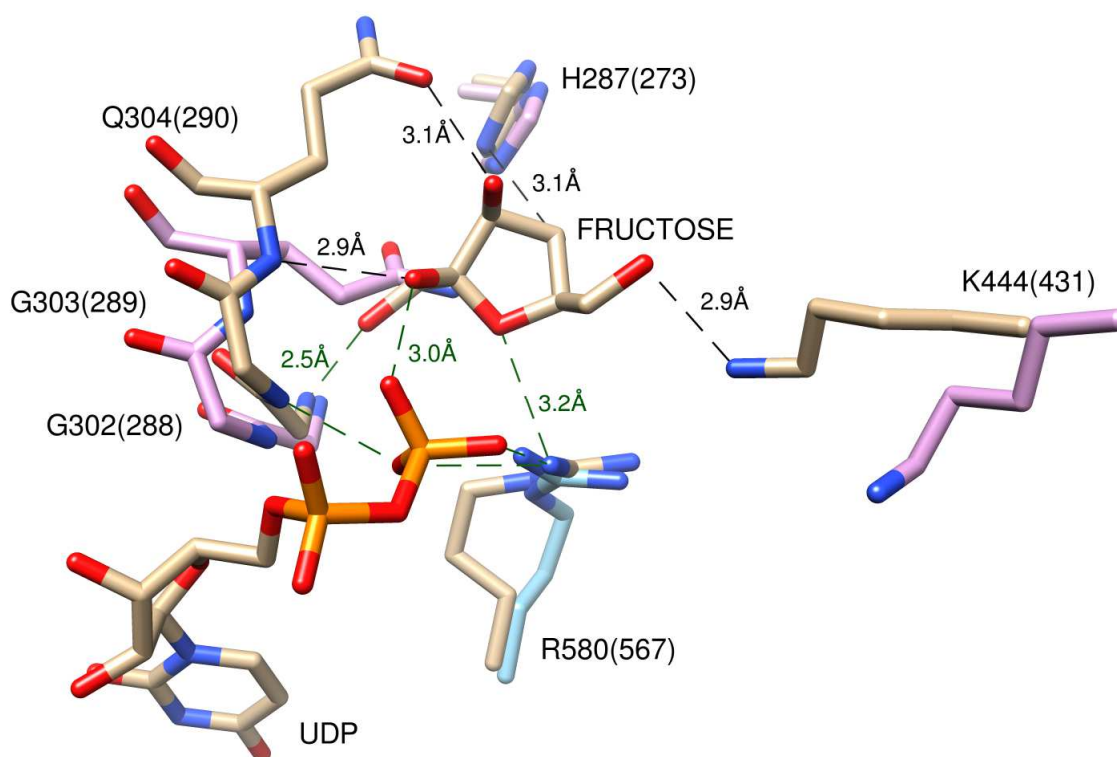


Figure 42. Overlap comparison of the fructose binding sites of the open (*NeuSucSase*) and closed (*AthSucSase*, PDB ID 3S29) structures. The carbon atoms in the closed form structure are in pale yellow. The carbon atoms in the open form structure are in cyan (GT-B(A) domain) and pink (GT-B(D) domain). Conserved residues between two structures are labeled with respective residue numbers; the residue numbers of the open form structure (*NeuSucSase*) are in parenthesis. The hydrogen bonds in the GT-B(D) domain are shown in black. The hydrogen bonds in between GT-B(A) and GT-B(D) domains and the ones in GT-B(A) domains are shown in green.

*Nucleotide-binding GT-B(D) domain.* The GT-B(D) domain binds to sugar nucleotide (synthesis direction) or nucleotide (cleavage direction) substrates. When overlapping GT-B(D) domains from both *AthSucSase* and *NeuSucSase*, residues interacting with the phosphate and ribose moieties of the nucleotides are not only conserved, but also at the same positions (Figure 43). On the other hand, two residues interacting with the nucleotide base are not conserved. Residues Q648 and N654 from *AthSucSase* are replaced by R636 and A642 in *NeuSucSase*, respectively. This difference

creates a more spacious binding site in *NeuS*Sase, which may accommodate bulkier adenosine nucleotide substrates. Similar sequence differences were observed in the *SucS*ase from *T. elongatus*<sup>77</sup>. Based on sequence analysis and homology modeling it was suggested that these two residues could be responsible for the preference towards ADP/ADP-Glc over other nucleotides such as UDP/UDP-Glc in the cyanobacterial enzyme. It is important to notice that the side chains in R636 and A642 in *NeuS*Sase are not conserved in the *E. coli* Glycogen synthase, which is another glycosyltransferase that binds ADP-Glc<sup>92</sup>. *E. coli* Glycogen synthase has a different motif in that position with a Tyr and Ser instead of Arg and Ala<sup>86, 92, 93</sup>, implying a different structural arrangement for accommodating ADP-Glc. Overall, the nucleotide binding to the GT-B(D) domain does not seem to trigger significant local conformational changes (Figure 43). The direct interactions with the nucleotide do not make major contributions to the induced fit mechanism.

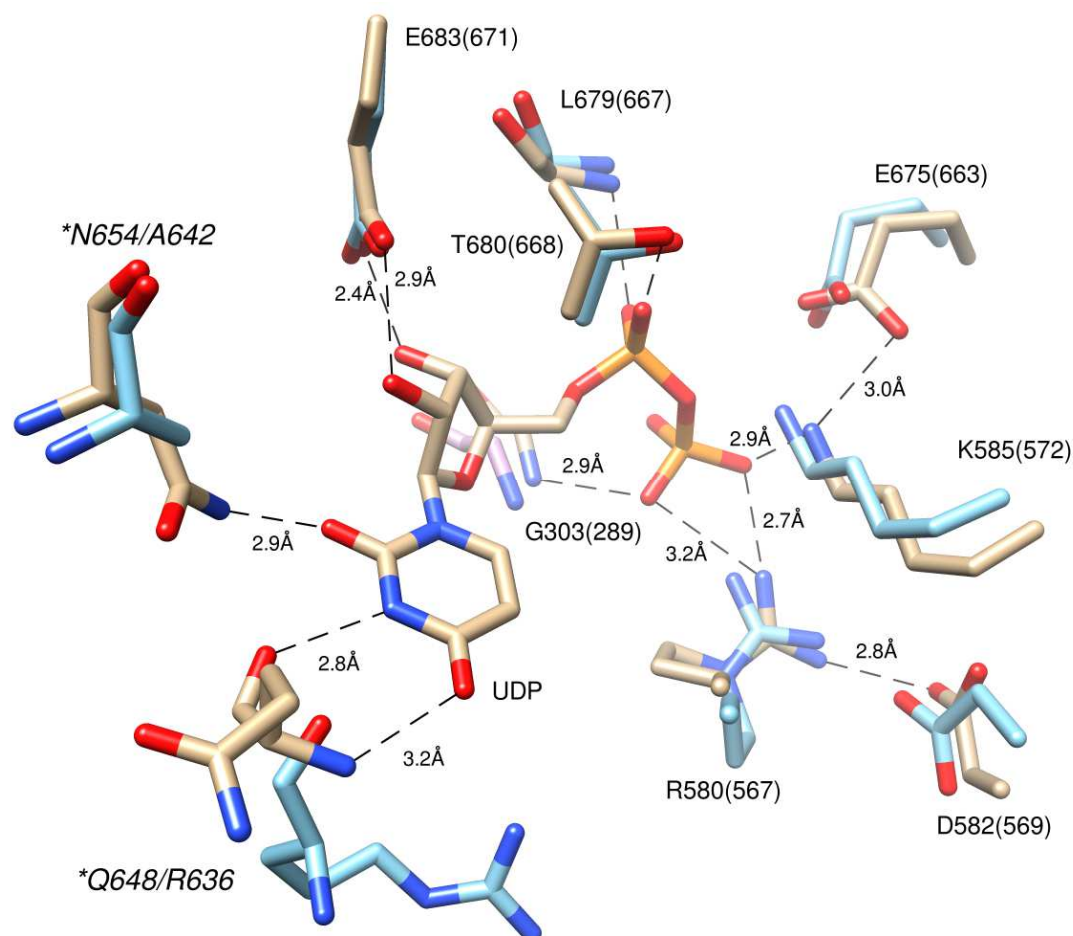


Figure 43. Overlap comparison of the nucleotide binding sites of the open (*NeuSucSase*) and closed (*AthSucSase*, PDB ID 3S29) structures. The carbon atoms in the closed form structure are in pale yellow. The carbon atoms in the open form structure are in cyan (GT-B(A) domain) and pink (GT-B(D) domain). Conserved residues between two structures are labeled with respective residue numbers; the residue numbers of the open form structure (*NeuSucSase*) are in parenthesis. The asterisks indicate the non-conserved binding residues with the closed form residues labeled in front of the ones in the open form structure.

*Hinge Analysis.* We scanned the structures of the acceptor and donor domains for hinges and subtle conformational changes that could be functionally important in catalysis. We used the in-house program *hingescan* described in “Materials and Methods”. Using several window sizes we detected several local conformational changes (Figure 44). For a window size of 51, we detected two clear hinge elements near residues

~515 and ~744 (Figure 45). These two elements actually form a single “hinge” that comprises a hydrogen bond between two conserved residues (G514 and W743) in a flexible area (Figure 40, Figure 39, and Figure 44). These two residues remain at the same position in both the open and the closed conformations of the enzyme. For smaller windows, we found other significant local secondary structure rearrangements (Figure 44, Figure 46, and Figure 45). Upon closing, two  $\alpha$ -helices in the GT-B(D) domain are extended, and a  $\beta$ -strand replaces a previously coiled stretch. The outcome is a more ordered peripheric structure of the GT-B(D) domain. We propose that this secondary structure rearrangement, despite the local entropy decrease, would release extra energy to close the conformation facilitating the binding of substrates.

*Latches.* A feature that contributes to the stabilization of the closed form is a “latch”, E609, which comprises the highly conserved E609 residue located at the periphery of the GT-B(D) domain (Figure 37). Going from an open to a closed conformation, this glutamate residue moves  $\sim 11$  Å towards the GT-B(A) domain and ends up hydrogen-bonded to two tyrosine residues (Y432 and Y446) stabilizing the closing (Figure 40 and Figure 47). Interestingly, there were small secondary structure

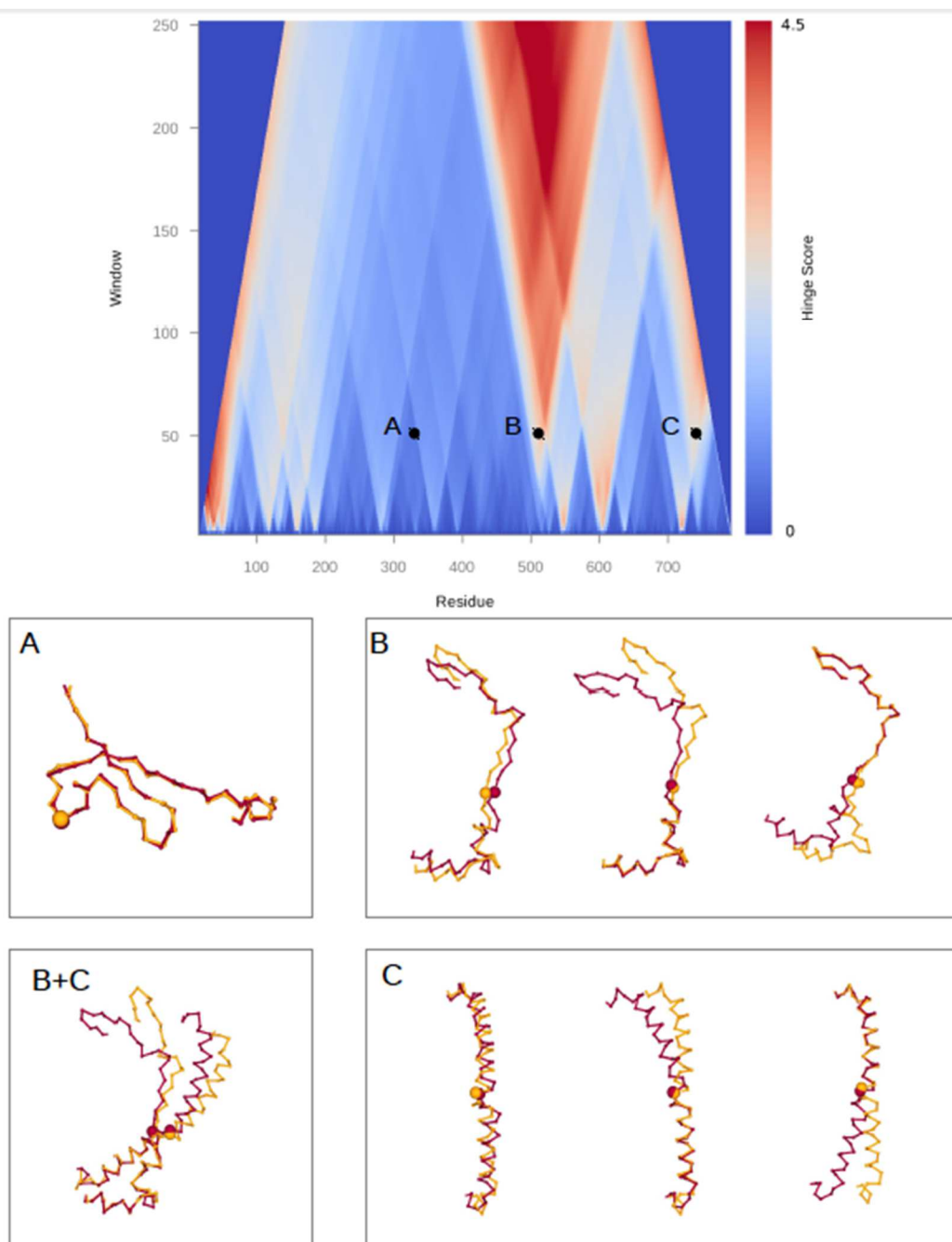


Figure 44. Hinge analysis of *NeuSucSase*. Comparison between the open form and the modeled closed form of the enzyme was performed with the program hingescan as described in Materials and Methods. In the top panel, a color coded hinge score (0 to 4.5) is plot for different window sizes at each residue. Three points are highlighted, A (control) and two hinge regions that are near in space (B and C). In all four panels (A, B, C, and B+C), maroon structures belong to the closed form, and yellow ones to the open form. Panel A shows optimal rigid body superposition of regions 307-357 of the open and closed form. Panel B displays regions 489-539 of both the close and open form.

The left, center and right overlaps are optimal rigid body superposition of the C $\alpha$  of residues 489-539, 514-539, and 489-514, respectively. The center and right overlaps were performed to highlight the differences on the other half of the region. Spheres represent center residue 514. Panel C displays regions 718-768 of both the close and open form. The left, center and right overlaps are optimal rigid body superposition of the C $\alpha$  of residues 718-768, 718-743, and 743-768, respectively. The center and right overlaps were performed to highlight the differences on the other half of the region. Spheres represent center residue 743. Panel B+C shows both regions (489-539 and 718-768), in which the optimal superposition was performed based on C $\alpha$  of residues 514-539 and 718-743.

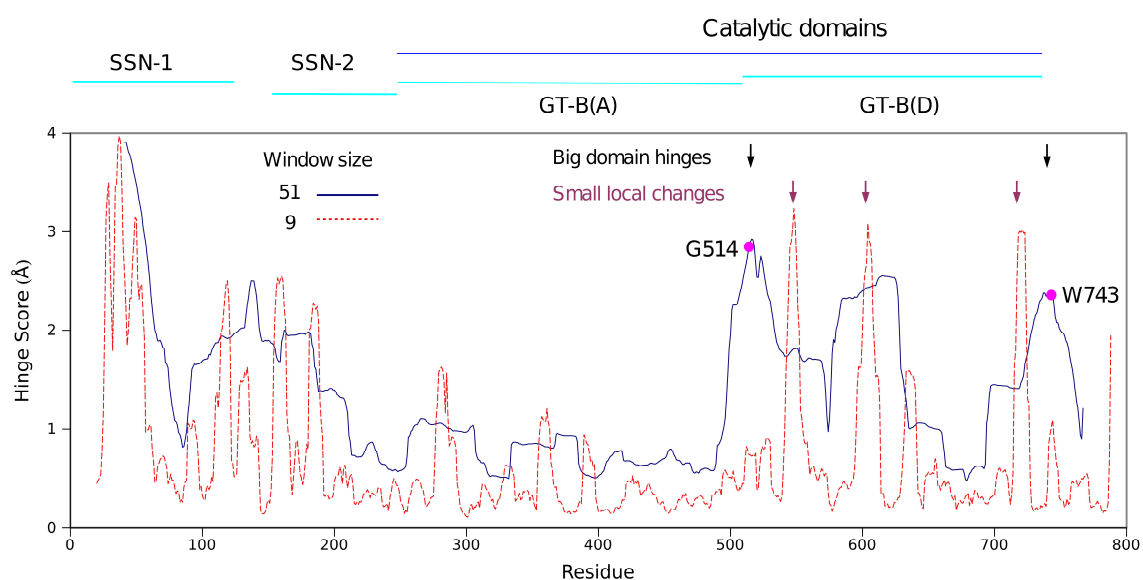


Figure 45. Hinge analysis by comparison of the open v. closed conformations. The blue and red show the “hinge score” using 51 and 9 windows, respectively. The magmata dots (also point with black arrows) shows the two distinct hinges: G514 and W743. The purple arrows points at the region displaying the secondary structure rearrangements.



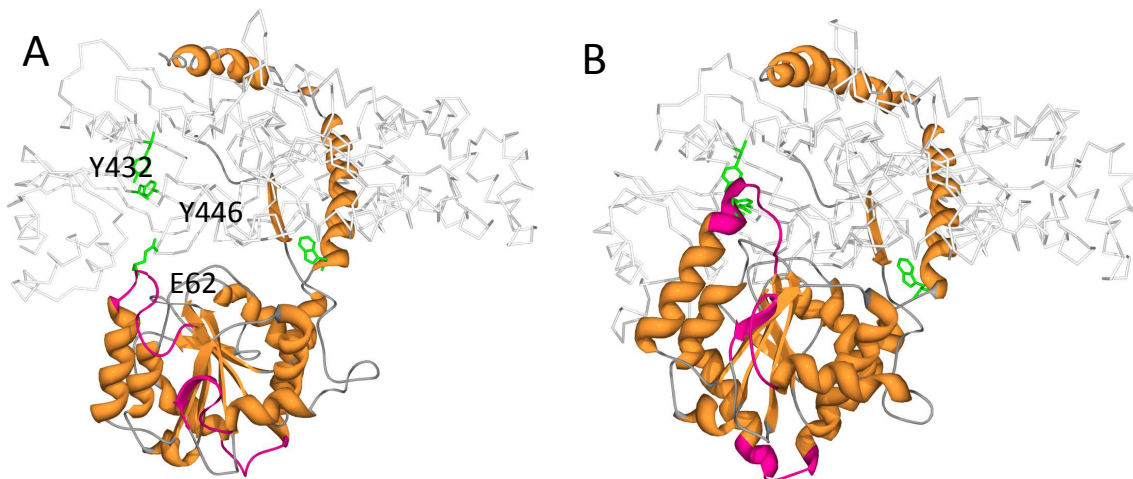


Figure 46. Secondary structure rearrangement during conformational changes between open and closed structures of bacterial SucSases. A. Open conformation of the *Neu*SucSase structure. B. Closed conformation of the *Ath*SucSase structure (PDB ID 3S29). The GT-B(D) domain and a long bending helix is show in orange. The SNN-1, SNN-2, and GT-B(A) domains are in grey. The side chains of the residues in the “latch” and the “hinge” are shown as green sticks. The secondary structural rearrangement is shown in magenta. T

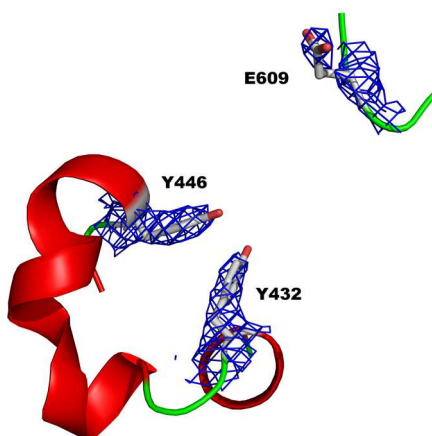


Figure 47. The open “latch”. E609, Y446 and Y432 are shown in sticks. The electron density (2Fo-Fc map) is shown as blue mesh at 1.0 sigma level around there key residues. Local secondary structure fetures are shown in cartoon style.

rearrangements in the vicinity of this latch, which could facilitate the interaction between E609 and the two tyrosines (Figure 46). On the other side of the active site, opposite to

the latch described, there is a hydrophobic patch that contributes to seal the closing (Figure 48). Two hydrophobic residues (M635, L637) in the GT-B(D) domain get in contact with a hydrophobic cluster (V281, L282 and L284) in the GT-B(A) domain, upon closing. The side chain of N280 also provides a methylene to build a non-polar pocket that latches on to M635 and L637 (Figure 48). On the other hand, the amide polar group is exposed to the solvent.

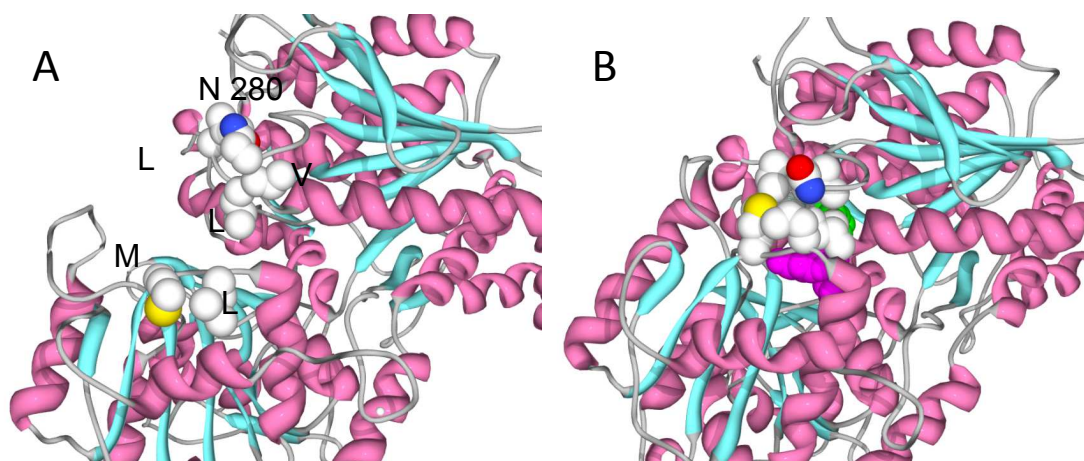


Figure 48. Hydrophobic residues contribute to the latch action. Panel A depicts the open (*NeuSucSase* crystal structure) and B a homology model of a closed structure, which was built as described in the “Materials and Methods” section. Upon closing, the hydrophobic residues: M635, L637 in the GT-B (D) domain and N280, V281, L282 and L284 in GT-B(A) domain generate a hydrophobic environment that stabilize the close action.

The closed structure seems to induce stronger interactions with the nucleotide and vice versa. In *NeuSucSase*, the conserved E671 is in the same position as E369 in the *E. coli* trehalose-6-phosphate synthase (OtsA)<sup>92, 94</sup>. In OtsA, as well as in the close conformation of *AthSucSase* (E683), the carboxylate of this side chain forms two hydrogen bonds with the hydroxyl groups of the ribose of the nucleotide. In these enzymes, the carboxylate is surrounded by hydrophobic residues (Y520, Y646, L667,

T668 in *NeuSocSase*, Y533, Y658, L679 and T680 in *AthSocSase*), which makes the hydrogen bonds stronger in the non-polar environment. In the open form of the *NeuSocSase* structure, V291 (V306 in *AthSocSase*) moves away from the side chain of the glutamate residue (Figure 49). This implies that the closing recruits a non-polar side chain to completely surround the carboxylate. Consequently, nucleotide binding stabilizes the carboxylate charge and facilitates the interaction with V291 upon closing. Interestingly, in another glycosyltransferase such as bacterial glycogen synthase, E671 has been replaced by a Tyr, and V291 was replaced by Asp, thus, switching their roles<sup>92</sup>. Therefore, this ligand-dependent interaction may be a common feature in this family of enzymes.

### **Site Directed Mutagenesis of Critical Residues**

Previously, important residues for catalysis were identified in other retaining GT-B glycosyltransferases. A triad of critical residues has been found in the active site of maltodextrin phosphorylase<sup>95, 96</sup> and glycogen synthase from *E. coli*<sup>97</sup>. Based on X-ray structures, these residues were also predicted to be important for catalysis in OtsA<sup>94</sup> and *AthSocSase*<sup>84</sup>. The homologue residues in *NeuSocSase* are R567, K572, and E663 (Figure 50). When any of those residues were replaced by alanine the activity in the direction of Suc synthesis severely decreased, either in presence of ADP-Glc or UDP-Glc (Table 6). The most active of all these mutants was E663A in presence of ADP-Glc, but it was still 200-fold less active than the wild type. These results indicate that this triad is critical in *NeuSocSase*. Consequently, it also suggests that *NeuSocSase* together with all

other retaining glycosyltransferases with a GT-B fold share the same reaction mechanism (Figure 50).

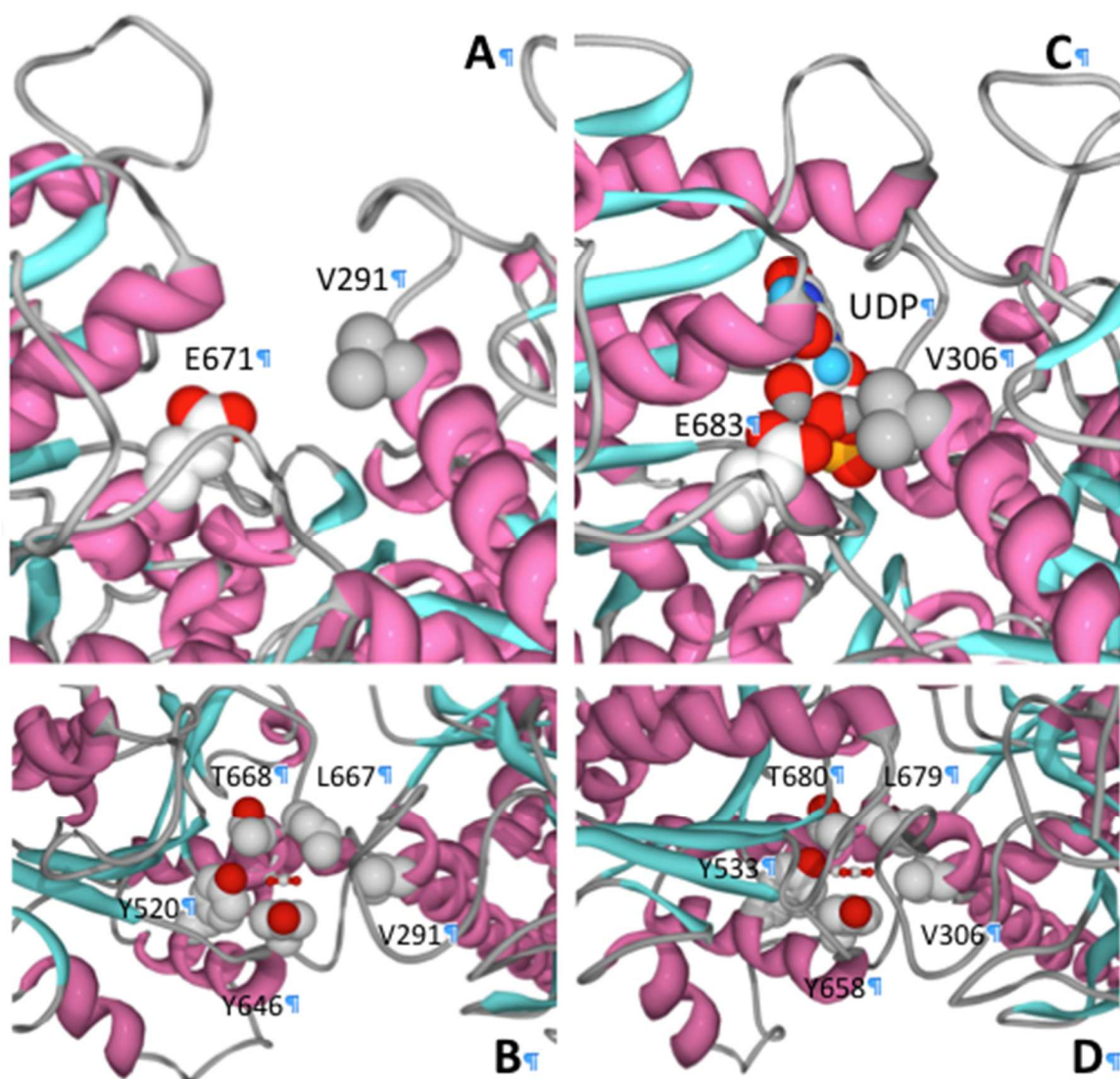


Figure 49. Conserved hydrophobic residues are involved in substrate binding in both open conformation of *NeuSocSase* (A and B), and closed conformation of *AthSocSase* (PDB ID: 3S29) (C and D). In the open conformation, V291, E691 two conserved hydrophobic residues are shown in sticks in figure A, and V291, Y520, Y646, L667, T668 (rotate 90 degree from A) are shown in sticks in figure B. In the closed conformation, V 306 and E 683 are conserved hydrophobic residues in figure C, and V306, Y533, Y658, L679 and T680 (rotate 90 degree from C) are shown in sticks in figure D.

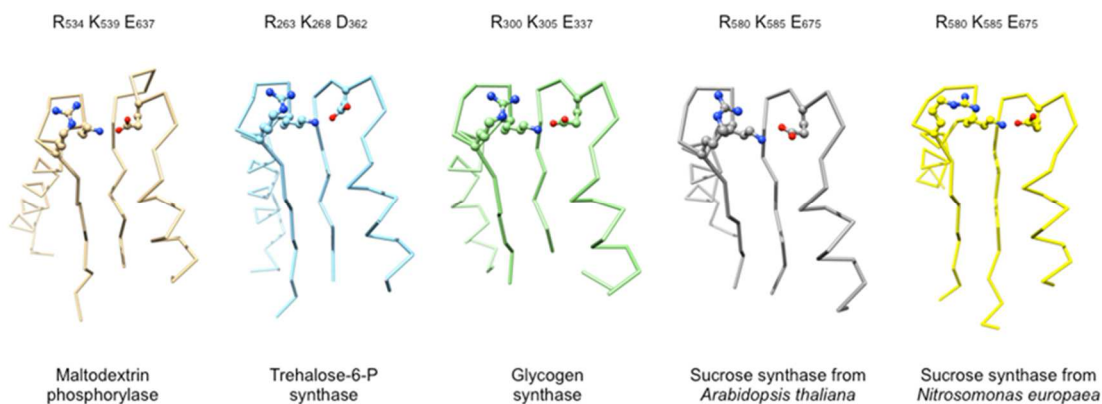


Figure 50. Three highly conserved catalytic residues in different members of the retaining GT-B glycosyltransferase family. The structures analysed in this figure are maltodextrin phosphorylase (PDB ID 1E4O), trehalose-6-phosphate synthase (PDB ID 1GZ5), and glycogen synthase (PDB ID 2ZQS) from *E. coli*, *AthSocSase* (PDB ID 3S29), and *NeuSocSase* (this work).

Table 5. Data collection and refinement statistics for *NeuSucSase*

Data Processing	
Space group	P65
Cell dimensions	
a; b; c (Å)	236.90; 236.90; 231.44
$\alpha$ ; $\beta$ ; $\gamma$ (°)	90.00; 90.00; 120.00
Resolution (Å)	3.05
Mosaicity (°)	0.47
<sup>a</sup> R <sub>merge</sub>	0.169 (0.963)
I/sigma	9.6 (2.1)
Completeness	97.9 (98.6)
Multiplicity	6.3 (6.3)
Refinement	
Resolution (Å)	3.05
No. reflections	794715
No. unique reflections	126170
<sup>b</sup> R <sub>work</sub> / <sup>c</sup> R <sub>free</sub>	17.37/21.75
<sup>d</sup> RMSD Bond length (Å)	0.009
RMSD Bond angle (°)	1.439

The values for the highest resolution bin are in parentheses.

<sup>a</sup>Linear  $R_{\text{merge}} = \sum |I_{\text{obs}} - I_{\text{avg}}| / \sum I_{\text{avg}}$

<sup>b</sup> $R = \sum |F_{\text{obs}} - F_{\text{calc}}| / \sum F_{\text{obs}}$ .

<sup>c</sup>Five percent of the reflection data were selected at random as a test set and only these data were used to calculate  $R_{\text{free}}$ .

<sup>d</sup>RMSD, root mean square deviation.

Table 6. Activity of wild type and mutants of *NeuSocSase*. Assays were performed using the conditions described in the “Materials and Methods” section.

Substrate	$V_{\max}$ (U mg <sup>-1</sup> )			
	WT	R567A	K572A	E663A
UDP-Glc	4.3 ± 0.1	< 0.0017	< 0.0019	< 0.01
ADP-Glc	3.7 ± 0.1	< 0.0014	< 0.0016	0.020 ± 0.02

## Materials and Methods

**Materials:** Chemicals and coupled enzymes used for activity assays were from Sigma-Aldrich (St. Louis, MO). *Escherichia coli* BL21 (DE3) cells were purchased from New England BioLabs (Ipswich, MA). Bacterial growth media and antibiotics were from Fisher Scientific (Pittsburgh, PA) and Sigma-Aldrich. Crystallization screen solutions and other supplies were purchased from Hampton Research (Aliso Viejo, CA) and Emerald Bio (Bedford, MA). All the other chemicals were of the highest quality available.

**Cloning:** The sequence coding for *NeuSocSase* was amplified by PCR using genomic DNA from *N. europaea* ATCC 19718 as template, the specific oligonucleotides CATATGACCACGATTGACACACTCGCCACCTGTACCC (forward, *NdeI* site underlined) and GTCGACTCATATCTCATGGGCCAGCCTGTTTGCCAGCGGCC (reverse, *SalI* site underlined) as primers, and Phusion HF DNA polymerase (Thermo Fisher Scientific, Rockford, IL) following the manufacturer’s instructions. The program used included an initial denaturation of 30 s at 98 °C; 30 cycles of 98 °C for 5 s, 50 °C for 20 s, and 72 °C for 2 min; and a final extension of 72 °C for 5 min. The PCR product was purified after agarose gel electrophoresis and inserted into the pSC-B vector using

the StrataClone Blunt PCR cloning kit (Agilent Technologies, Santa Clara, CA).

Sequence identity was checked by automated DNA sequencing at CRC (Comprehensive Cancer Center at University of Chicago, IL). Afterwards, the sequence was subcloned into the pET28c vector (Merck KGaA, Darmstadt, Germany) between *NdeI* and *SalI* sites to obtain pNESS1, which is the plasmid that encodes the recombinant *NeuSocSase* with an N-terminal His<sub>6</sub>-tag.

*Site-directed mutagenesis:* Site-directed mutagenesis was performed by PCR overlap extension as previously described using Phusion DNA polymerase<sup>98, 99</sup>. Plasmid encoding the *NeuSocSase* (pNESS1) was used as a template for mutagenesis.

To introduce mutations in the sequence coding for *NeuSocSase* we used the following

primers: TTTACCATGGCGgcgCTGGATCGGATC (forward) and

GATCCGATCCAGcgcCGCCATGGTAAA (reverse) for mutant R567A;

CTGGATCGGATCgcgAACATTACCGGC (forward) and

GCCGGTAATGTTcgcGATCCGATCCAG (reverse) for mutant K572A; and

CCAGCCCTGTTCgcgGCATTCGGCCTG (forward) and

CAGGCCGAATGCcgcGAACAGGGCTGG (reverse) for mutant E663A. PCR

conditions were the same as those described above. Flanking primers for the PCR overlap extension were the same used for cloning (described above). All mutations were confirmed by DNA sequencing.

*Protein expression and purification:* Transformed *E. coli* BL21 (DE3) cells with pNESS1 were grown in 4 x 1 L of LB supplemented with 100 µg/ml carbenicillin. This was performed in a 2.8 L Fernbach flask at 37 °C and 250 rpm until OD<sub>600 nm</sub> reached



~0.6. Protein expression was induced by the addition of 0.5 mM isopropyl- $\beta$ -D-1-thiogalactopyranoside. Cells were incubated at 25 °C and harvested after 16 h by centrifuging at 5000 x g and 4 °C for 15 min. The cell paste was resuspended in Buffer C [20 mM Tris-HCl pH 8.0, 200 mM NaCl, 5% (v/v) glycerol, 10 mM imidazole] and disrupted by sonication. The resulting suspension was centrifuged twice at 30000 x g and 4 °C for 15 min and the soluble fraction (crude extract) was loaded onto a 5 ml HisTrap column (GE Life Sciences, Piscataway, NJ) containing  $\text{Ni}^{2+}$  and previously equilibrated with Buffer C. Elution of the retained proteins was achieved with a linear imidazole gradient (20 column volumes, 10-300 mM). Fractions containing SucSase activity were pooled, concentrated to 2 ml, and loaded onto a 16/60 Superdex 200 column (GE Life Sciences) previously equilibrated with 50 mM HEPES-NaOH pH 8.0 and 300 mM NaCl. Fractions containing enzyme activity were pooled, concentrated, supplemented with 5% (v/v) glycerol, and stored at -80 °C until use. Under these conditions the enzyme remained stable and fully active for at least 3 months.

*Protein assay and detection:* Protein concentration was determined by measuring the protein absorbance at 280 nm using a NanoDrop 1000 (Thermo Fisher Scientific) and an extinction coefficient of  $1.153 \text{ ml mg}^{-1} \text{ cm}^{-1}$ , determined from the amino acid sequence using the ProtParam server (<http://web.expasy.org/protparam/>). Denaturing protein electrophoresis was performed as described by Laemmli<sup>100</sup>.

*Enzyme assays:* Activity assays were performed as previously described<sup>77</sup>, with minor modifications. In the direction of Suc synthesis, the reaction medium contained 50 mM HEPPS pH 8.0, 10 mM  $\text{MgCl}_2$ , 5 mM UDP-Glc, 500 mM Fru, 0.3 mM

phosphoenolpyruvate, 0.3 mM NADH, 1 U pyruvate kinase, 1 U lactate dehydrogenase, 0.2 mg ml<sup>-1</sup> BSA, and enzyme in an appropriate dilution in a final volume of 50 µl. Alternatively, activity was measured with 1 mM ADP-Glc and 20 mM Fru. NADH oxidation was followed by measuring the absorbance at 340 nm in a Multiskan Ascent microplate reader (Thermo Fisher Scientific) at 37 °C. One unit of enzyme activity (U) is defined as the amount of protein necessary to produce 1 µmol of product in 1 min under the specified conditions.

*Kinetic characterization:* Data of initial velocity ( $v$ ) versus substrate concentration ( $S$ ) were plotted and fitted to a modified Hill equation:  $v = V_{\max} S^{n_H} / (S_{0.5}^{n_H} + S^{n_H})$ , where  $S_{0.5}$  is the concentration of substrate necessary to obtain 50% of the maximal velocity ( $V_{\max}$ ) and  $n_H$  is the Hill coefficient. Fitting was performed by a non-linear least-squares algorithm provided by the software Origin 7.0 (OriginLab Corporation). Kinetic parameters were obtained using the averages of two independent datasets that were reproducible within errors of  $\pm 10\%$ .

*Phylogenetic analysis:* We searched for protein sequences using the term “sucrose synthase” and the RefSeq filter in the National Center for Biotechnology Information (NCBI) database. Sequences were analyzed with the program BioEdit 7.0.5.3<sup>101</sup>, manually curated, and aligned using the ClustalW server (<http://www.genome.jp/tools/clustalw/>). Tree reconstruction was performed using the Neighbor-Joining algorithm with a bootstrap of 1000 in the program SeaView 4.4.0<sup>102</sup>. The tree figure was prepared using the FigTree 1.4.0 software (<http://tree.bio.ed.ac.uk/software/figtree/>).

*Crystallization and data collection:* After the initial crystallization screen and optimization, the recombinant protein was crystallized via the hanging drop method. The hanging drops were prepared with 1  $\mu$ l of 15 mg ml<sup>-1</sup> *NeuSocSase* protein solution and 1  $\mu$ l of the reservoir solution, containing 5% Tacsimate pH 5.0, 5% (w/v) PEG 3350, and 0.1 M sodium citrate pH 5.6. The hanging drops were kept at 20 °C for crystallization. Crystals appeared in 3 days and were allowed to continue growing at 20 °C for 4 more days until they reached their maximum sizes. Crystals with good morphology and large sizes were transferred to a cryo-condition, which contained 25% glycerol in addition to the components of the reservoir solution, before being frozen in liquid nitrogen.

X-ray diffraction data sets were collected at the SBC19-ID beamline at the Advanced Photon Source (Argonne National Laboratory, Chicago, IL). The wavelength used in the monochromatic data collection was 1.008 Å. All the collected data sets were indexed and integrated using iMosflm and scaled with Scala in the CCP4 program suite (Collaborative Computational Project Number 4) <sup>103</sup>. The resolution cut-off was decided by applying all following criteria on the highest resolution bin: i)  $I/\sigma > 2$ , ii) completeness  $> 90\%$ , and iii)  $R_{\text{merge}} < 1.0$ .

*Phasing, model building, and refinement:* Molecular replacement was carried out using the program Phaser <sup>61</sup> from the CCP4 program suite. The starting search model in molecular replacement was modified from the known *A. thaliana* SucSase structural model (PDB ID: 3S29) <sup>84</sup>. We truncated the GT-B(D) domain (cyan domain in Figure 36B) and used the rest of the molecule as the search model for molecular replacement in Phaser. Once a solution was obtained, model building was conducted in COOT <sup>45</sup>. The

GT-B(D) domain was built according to the electron density maps. Rigid body refinement and restrained refinement were conducted in *refmac5*<sup>104</sup>. In order to remove model bias and achieve the best refinement results possible, simulated annealing refinement and ordered solvent identification were conducted using *PHENIX.refine*<sup>44</sup>. Final model and the structure factor have been deposited in the RCSB Protein Data Bank with the accession code 4RBN.

*Homology modeling:* A model of the monomeric closed form of *NeuS* (residues 16 to 788) was constructed with the program *Modeller* 9.11 (<http://salilab.org/modeller/>)<sup>105</sup>. As template we used the atomic coordinates of the *A. thaliana* sucrose synthase (3S27) with the ligands UDP and fructose<sup>84</sup>. Before the modeling process, sequence alignment was performed manually to match functionally conserved residues and secondary structures. An identity of 52.2% ensured a high confidence alignment since we only had to introduce four one-residue indels. The accuracy of the models was assessed with the *Verify3D* Structure Evaluation Server ([http://nihserver.mbi.ucla.edu/Verify\\_3D/](http://nihserver.mbi.ucla.edu/Verify_3D/))<sup>106</sup>.

*Difference distance matrix map:* We used an *ad hoc* program written in C applying previously developed concepts to detect domain motion and identify regions that move closer upon conformational changes<sup>107</sup>. Distances were calculated between all pair of  $C_{\alpha}$  of one reference structure (open), and a second pairwise distance matrix was calculated for the target (closed) structure. Afterwards, the target matrix was subtracted from the reference matrix to calculate the  $\Delta$ distance plot (<https://github.com/ballicoragroup/didimama>).

*Hinge analysis:* In order to detect possible local conformations or hinges, we performed an analysis with the ad hoc program “hingescan” (<https://github.com/ballicoragroup/hingescan>). We compared the open crystal structure of *NeuSocSase* with a *NeuSocSase* homology model based on the template provided by the close structure of the *AthSocSase*. To detect if there is a significant local conformational change around a given residue (“hinge”), we extracted the coordinates of a given number (n) of C $\alpha$  before the putative hinge and the same given number (n) of residues after (window size = 2n+1). This was done for both the open and closed forms and obtained two fragments to compare. After optimal rigid body superposition of only these two set of coordinates, an average distance was calculated (RMSD). This RMSD calculated in these conditions was called the “hinge score”. When this score is at a peak, the “flanking” n number of C $\alpha$  at both sides display a maximum change between the two structures. For that reason, a hinge is detected. The bigger the window, the bigger the domain movement is detected surrounding the hinge. To identify hinges that link small and bigger domains, different window sizes can be scanned.

## CHAPTER SIX

### CONCLUSIONS

We analyzed the sequences of SucSases from divergent organisms, including proteobacteria, cyanobacteria, and plants. The obtained phylogenetic tree shows that sequences from proteobacteria (including the one from *N. europaea*) are clearly separated from those present in cyanobacteria and plants. To the best of our knowledge, SucSases from proteobacteria have never been characterized. In this work, we expressed, purified the recombinant *Neu*SucSase, and solved its crystal structure. In addition, our analysis provided evidence for a proposed “open” conformation for SucSases. Based on the comparison with a previously published “closed” *Ath*SucSase structure<sup>84</sup>, a “hinge-latch” combination was identified as critical features responsible for the open-close enzyme actions.

We also mutated three highly conserved amino acids proposed to be critical for catalysis. These mutations severely reduced the activity of *Neu*SucSase; therefore, we conclude that the triad composed of residues R567, K572, and E663 (numbers according to *Neu*SucSase) plays a key role for catalysis not only in SucSases, but probably also in all the retaining GT-B glycosyltransferases<sup>84, 94-97</sup>.

With both structural and kinetic results we propose that *Neu*SucSase has a substrate preference in favor of ADP/ADP-Glc over UDP/UDP-Glc. This behavior is

similar to the one observed for *T. elongatus* SucSase<sup>77</sup>. It was proposed that the difference in specificity towards the nucleotide substrate in the cyanobacterial enzyme could be due to changes in two specific residues, R647 and S653 (Q648 and N654 in *Ath*SucSase). Interestingly, we found that *Neu*SucSase presents similar evolutionary variances to those observed in *T. elongatus* SucSase: R636 (R647) and A642 (S653). Residues Q648 and N654 from *Ath*SucSase are strictly conserved in plants and the moss *P. patens*, whereas they are more variable in cyanobacteria and proteobacteria. Based on this finding and taking into account kinetic and structural data obtained for SucSases from *T. elongatus*<sup>77</sup>, *Ath*SucSase<sup>84</sup> and *Neu*SucSase (this work), we hypothesize that these residues may contribute to determining the specificity towards the nucleotide substrate.

The evolutionary origin of enzymes from Suc metabolism in proteobacteria has been previously discussed<sup>65, 66, 69</sup>. The evolution of SucSases in cyanobacteria, proteobacteria, and plants is not yet fully understood, but most likely it involved horizontal gene transfers. On one hand, *Neu*SucSase is closer to plant enzymes in the phylogenetic tree (Figure 35), but on the other hand, the specificity for nucleotides is similar to several cyanobacterial enzymes examined<sup>69, 77</sup>. It is possible that *Neu*SucSase evolved from a protein already present in the common ancestor of proteobacteria and cyanobacteria<sup>71</sup>.

## REFERENCE LIST

- [1] Davidson, D. J., and Porteous, D. J. (1998) Genetics and pulmonary medicine. 1. The genetics of cystic fibrosis lung disease, *Thorax* 53, 389-397.
- [2] Rojo, F. (1999) Repression of transcription initiation in bacteria, *Journal of bacteriology* 181, 2987-2991.
- [3] Lewis, P. J., Doherty, G. P., and Clarke, J. (2008) Transcription factor dynamics, *Microbiology* 154, 1837-1844.
- [4] Grose, J. H., Bergthorsson, U., and Roth, J. R. (2005) Regulation of NAD synthesis by the trifunctional NadR protein of Salmonella enterica, *Journal of bacteriology* 187, 2774-2782.
- [5] Browning, D. F., and Busby, S. J. (2004) The regulation of bacterial transcription initiation, *Nature reviews. Microbiology* 2, 57-65.
- [6] Haydon, D. J., and Guest, J. R. (1991) A new family of bacterial regulatory proteins, *FEMS microbiology letters* 63, 291-295.
- [7] Yoshida, K. I., Fujita, Y., and Ehrlich, S. D. (2000) An operon for a putative ATP-binding cassette transport system involved in acetoin utilization of Bacillus subtilis, *Journal of bacteriology* 182, 5454-5461.
- [8] Klemm, J. D., Schreiber, S. L., and Crabtree, G. R. (1998) Dimerization as a regulatory mechanism in signal transduction, *Annual review of immunology* 16, 569-592.
- [9] Littlefield, O., and Nelson, H. C. (1999) A new use for the 'wing' of the 'winged' helix-turn-helix motif in the HSF-DNA cocystal, *Nature structural biology* 6, 464-470.
- [10] Vindal, V., Suma, K., and Ranjan, A. (2007) GntR family of regulators in Mycobacterium smegmatis: a sequence and structure based characterization, *BMC genomics* 8, 289.
- [11] Park, Y. W., Yeo, H. K., and Lee, J. Y. (2012) Crystallization and preliminary X-ray diffraction analysis of a fatty-acid metabolism regulatory protein, FadR, from Bacillus halodurans, *Acta crystallographica. Section F, Structural biology and crystallization communications* 68, 975-977



- [12] Allison, S. L., and Phillips, A. T. (1990) Nucleotide sequence of the gene encoding the repressor for the histidine utilization genes of *Pseudomonas putida*, *Journal of bacteriology* 172, 5470-5476.
- [13] Quail, M. A., Dempsey, C. E., and Guest, J. R. (1994) Identification of a fatty acyl responsive regulator (FarR) in *Escherichia coli*, *FEBS letters* 356, 183-187.
- [14] Chen, C. M., Ye, Q. Z., Zhu, Z. M., Wanner, B. L., and Walsh, C. T. (1990) Molecular biology of carbon-phosphorus bond cleavage. Cloning and sequencing of the *phn* (*psiD*) genes involved in alkylphosphonate uptake and C-P lyase activity in *Escherichia coli* B, *The Journal of biological chemistry* 265, 4461-4471.
- [15] Resch, M., Schiltz, E., Titgemeyer, F., and Muller, Y. A. (2010) Insight into the induction mechanism of the GntR/HutC bacterial transcription regulator YvoA, *Nucleic acids research* 38, 2485-2497.
- [16] Rigali, S., Derouaux, A., Giannotta, F., and Dusart, J. (2002) Subdivision of the helix-turn-helix GntR family of bacterial regulators in the FadR, HutC, MocR, and YtrA subfamilies, *The Journal of biological chemistry* 277, 12507-12515.
- [17] Gao, Y. G., Yao, M., Itou, H., Zhou, Y., and Tanaka, I. (2007) The structures of transcription factor CGL2947 from *Corynebacterium glutamicum* in two crystal forms: a novel homodimer assembling and the implication for effector-binding mode, *Protein science : a publication of the Protein Society* 16, 1878-1886.
- [18] Hoskisson, P. A., Rigali, S., Fowler, K., Findlay, K. C., and Buttner, M. J. (2006) DevA, a GntR-like transcriptional regulator required for development in *Streptomyces coelicolor*, *Journal of bacteriology* 188, 5014-5023.
- [19] Franco, I. S., Mota, L. J., Soares, C. M., and de Sa-Nogueira, I. (2006) Functional domains of the *Bacillus subtilis* transcription factor AraR and identification of amino acids important for nucleoprotein complex assembly and effector binding, *Journal of bacteriology* 188, 3024-3036.
- [20] Jain, D., and Nair, D. T. (2013) Spacing between core recognition motifs determines relative orientation of AraR monomers on bipartite operators, *Nucleic acids research* 41, 639-647.
- [21] Kim, J. S., Kim, B. H., Jang, J. I., Eom, J. S., Kim, H. G., Bang, I. S., and Park, Y. K. (2014) Functional insight from the tetratricopeptide repeat-like motifs of the type III secretion chaperone SicA in *Salmonella enterica* serovar Typhimurium, *FEMS microbiology letters* 350, 146-153.

- [22] Lee, M. H., Scherer, M., Rigali, S., and Golden, J. W. (2003) PlmA, a new member of the GntR family, has plasmid maintenance functions in *Anabaena* sp. strain PCC 7120, *Journal of bacteriology* 185, 4315-4325.
- [23] Wiethaus, J., Schubert, B., Pfander, Y., Narberhaus, F., and Masepohl, B. (2008) The GntR-like regulator TauR activates expression of taurine utilization genes in *Rhodobacter capsulatus*, *Journal of bacteriology* 190, 487-493.
- [24] Belitsky, B. R. (2004) *Bacillus subtilis* GabR, a protein with DNA-binding and aminotransferase domains, is a PLP-dependent transcriptional regulator, *Journal of molecular biology* 340, 655-664.
- [25] Belitsky, B. R., and Sonenshein, A. L. (2002) GabR, a member of a novel protein family, regulates the utilization of gamma-aminobutyrate in *Bacillus subtilis*, *Molecular microbiology* 45, 569-583.
- [26] Bramucci, E., Milano, T., and Pascarella, S. (2011) Genomic distribution and heterogeneity of MocR-like transcriptional factors containing a domain belonging to the superfamily of the pyridoxal-5'-phosphate dependent enzymes of fold type I, *Biochemical and biophysical research communications* 415, 88-93.
- [27] Kirsch, J. F., Eichele, G., Ford, G. C., Vincent, M. G., Jansonius, J. N., Gehring, H., and Christen, P. (1984) Mechanism of action of aspartate aminotransferase proposed on the basis of its spatial structure, *Journal of molecular biology* 174, 497-525.
- [28] Schneider, G., Kack, H., and Lindqvist, Y. (2000) The manifold of vitamin B6 dependent enzymes, *Structure* 8, R1-6.
- [29] Ouchi, T., Tomita, T., Miyagawa, T., Kuzuyama, T., and Nishiyama, M. (2009) Dual roles of a conserved pair, Arg23 and Ser20, in recognition of multiple substrates in alpha-aminoadipate aminotransferase from *Thermus thermophilus*, *Biochemical and biophysical research communications* 388, 21-27.
- [30] Gajiwala, K. S., and Burley, S. K. (2000) Winged helix proteins, *Current opinion in structural biology* 10, 110-116.
- [31] Eliot, A. C., and Kirsch, J. F. (2004) Pyridoxal phosphate enzymes: mechanistic, structural, and evolutionary considerations, *Annual review of biochemistry* 73, 383-415.
- [32] Smith, D. L., Almo, S. C., Toney, M. D., and Ringe, D. (1989) 2.8-A-resolution crystal structure of an active-site mutant of aspartate aminotransferase from *Escherichia coli*, *Biochemistry* 28, 8161-8167.

- [33] Storici, P., Qiu, J., Schirmer, T., and Silverman, R. B. (2004) Mechanistic crystallography. Mechanism of inactivation of gamma-aminobutyric acid aminotransferase by (1R,3S,4S)-3-amino-4-fluorocyclopentane-1-carboxylic acid as elucidated by crystallography, *Biochemistry* 43, 14057-14063.
- [34] Marchler-Bauer, A., Lu, S., Anderson, J. B., Chitsaz, F., Derbyshire, M. K., DeWeese-Scott, C., Fong, J. H., Geer, L. Y., Geer, R. C., Gonzales, N. R., Gwadz, M., Hurwitz, D. I., Jackson, J. D., Ke, Z., Lanczycki, C. J., Lu, F., Marchler, G. H., Mullokandov, M., Omelchenko, M. V., Robertson, C. L., Song, J. S., Thanki, N., Yamashita, R. A., Zhang, D., Zhang, N., Zheng, C., and Bryant, S. H. (2011) CDD: a Conserved Domain Database for the functional annotation of proteins, *Nucleic acids research* 39, D225-229.
- [35] van Aalten, D. M., DiRusso, C. C., and Knudsen, J. (2001) The structural basis of acyl coenzyme A-dependent regulation of the transcription factor FadR, *The EMBO journal* 20, 2041-2050.
- [36] Raman, N., Black, P. N., and DiRusso, C. C. (1997) Characterization of the fatty acid-responsive transcription factor FadR. Biochemical and genetic analyses of the native conformation and functional domains, *The Journal of biological chemistry* 272, 30645-30650.
- [37] Storici, P., De Biase, D., Bossa, F., Bruno, S., Mozzarelli, A., Peneff, C., Silverman, R. B., and Schirmer, T. (2004) Structures of gamma-aminobutyric acid (GABA) aminotransferase, a pyridoxal 5'-phosphate, and [2Fe-2S] cluster-containing enzyme, complexed with gamma-ethynyl-GABA and with the antiepilepsy drug vigabatrin, *The Journal of biological chemistry* 279, 363-373.
- [38] Tomchick, D. R., Turner, R. J., Switzer, R. L., and Smith, J. L. (1998) Adaptation of an enzyme to regulatory function: structure of *Bacillus subtilis* PyrR, a pyr RNA-binding attenuation protein and uracil phosphoribosyltransferase, *Structure* 6, 337-350.
- [39] Sinha, S. C., Krahn, J., Shin, B. S., Tomchick, D. R., Zalkin, H., and Smith, J. L. (2003) The purine repressor of *Bacillus subtilis*: a novel combination of domains adapted for transcription regulation, *Journal of bacteriology* 185, 4087-4098.
- [40] Jain, D., Kim, Y., Maxwell, K. L., Beasley, S., Zhang, R., Gussin, G. N., Edwards, A. M., and Darst, S. A. (2005) Crystal structure of bacteriophage lambda cII and its DNA complex, *Molecular cell* 19, 259-269.
- [41] Otwinowski, Z., and Minor, W. (1997) Processing of X-ray diffraction data collected in oscillation mode, *Method Enzymol* 276, 307-326.

- [42] Collaborative Computational Project, N. (1994) The CCP4 suite: programs for protein crystallography, *Acta crystallographica. Section D, Biological crystallography* 50, 760-763.
- [43] Holm, L., and Rosenstrom, P. (2010) Dali server: conservation mapping in 3D, *Nucleic acids research* 38, W545-549.
- [44] Adams, P. D., Afonine, P. V., Bunkoczi, G., Chen, V. B., Davis, I. W., Echols, N., Headd, J. J., Hung, L. W., Kapral, G. J., Grosse-Kunstleve, R. W., McCoy, A. J., Moriarty, N. W., Oeffner, R., Read, R. J., Richardson, D. C., Richardson, J. S., Terwilliger, T. C., and Zwart, P. H. (2010) PHENIX: a comprehensive Python-based system for macromolecular structure solution, *Acta Crystallogr. D Biol. Crystallogr.* 66, 213-221.
- [45] Emsley, P., and Cowtan, K. (2004) Coot: model-building tools for molecular graphics, *Acta Crystallogr. D Biol. Crystallogr.* 60, 2126-2132.
- [46] Edayathumangalam, R., Wu, R., Garcia, R., Wang, Y., Wang, W., Kreinbring, C. A., Bach, A., Liao, J., Stone, T. A., Terwilliger, T. C., Hoang, Q. Q., Belitsky, B. R., Petsko, G. A., Ringe, D., and Liu, D. (2013) Crystal structure of *Bacillus subtilis* GabR, an autorepressor and transcriptional activator of *gabT*, *Proceedings of the National Academy of Sciences of the United States of America* 110, 17820-17825.
- [47] Jochmann, N., Gotker, S., and Tauch, A. (2011) Positive transcriptional control of the pyridoxal phosphate biosynthesis genes *pdxST* by the MocR-type regulator PdxR of *Corynebacterium glutamicum* ATCC 13032, *Microbiology* 157, 77-88.
- [48] Belitsky, B. R. (2014) Role of PdxR in the activation of vitamin B6 biosynthesis in *Listeria monocytogenes*, *Molecular microbiology* 92, 1113-1128.
- [49] El Qaidi, S., Yang, J., Zhang, J. R., Metzger, D. W., and Bai, G. (2013) The vitamin B(6) biosynthesis pathway in *Streptococcus pneumoniae* is controlled by pyridoxal 5'-phosphate and the transcription factor PdxR and has an impact on ear infection, *Journal of bacteriology* 195, 2187-2196.
- [50] Liu, W., Peterson, P. E., Langston, J. A., Jin, X., Zhou, X., Fisher, A. J., and Toney, M. D. (2005) Kinetic and crystallographic analysis of active site mutants of *Escherichia coli* gamma-aminobutyrate aminotransferase, *Biochemistry* 44, 2982-2992.
- [51] Adams, P. D., Grosse-Kunstleve, R. W., Hung, L. W., Ioerger, T. R., McCoy, A. J., Moriarty, N. W., Read, R. J., Sacchettini, J. C., Sauter, N. K., and Terwilliger, T. C. (2002) PHENIX: building new software for automated crystallographic structure

determination, *Acta crystallographica. Section D, Biological crystallography* 58, 1948-1954.

[52] Liu, W., Peterson, P. E., Carter, R. J., Zhou, X., Langston, J. A., Fisher, A. J., and Toney, M. D. (2004) Crystal structures of unbound and aminooxyacetate-bound *Escherichia coli* gamma-aminobutyrate aminotransferase, *Biochemistry* 43, 10896-10905.

[53] Silverman, R. B., and Levy, M. A. (1981) Mechanism of inactivation of gamma-aminobutyric acid-alpha-ketoglutaric acid aminotransferase by 4-amino-5-halopentanoic acids, *Biochemistry* 20, 1197-1203.

[54] Liu, D., Pozharski, E., Fu, M., Silverman, R. B., and Ringe, D. (2010) Mechanism of inactivation of *Escherichia coli* aspartate aminotransferase by (S)-4-amino-4,5-dihydro-2-furancarboxylic acid, *Biochemistry* 49, 10507-10515.

[55] Liu, D., Pozharski, E., Lepore, B. W., Fu, M., Silverman, R. B., Petsko, G. A., and Ringe, D. (2007) Inactivation of *Escherichia coli* L-aspartate aminotransferase by (S)-4-amino-4,5-dihydro-2-thiophenecarboxylic acid reveals "a tale of two mechanisms", *Biochemistry* 46, 10517-10527.

[56] Lepore, B. W., Liu, D., Peng, Y., Fu, M., Yasuda, C., Manning, J. M., Silverman, R. B., and Ringe, D. (2010) Chiral discrimination among aminotransferases: inactivation by 4-amino-4,5-dihydrothiophenecarboxylic acid, *Biochemistry* 49, 3138-3147.

[57] Schnackerz, K. D., Tai, C. H., Simmons, J. W., 3rd, Jacobson, T. M., Rao, G. S., and Cook, P. F. (1995) Identification and spectral characterization of the external aldimine of the O-acetylserine sulfhydrylase reaction, *Biochemistry* 34, 12152-12160.

[58] Griswold, W. R., Castro, J. N., Fisher, A. J., and Toney, M. D. (2012) Ground-state electronic destabilization via hyperconjugation in aspartate aminotransferase, *Journal of the American Chemical Society* 134, 8436-8438.

[59] Griswold, W. R., Fisher, A. J., and Toney, M. D. (2011) Crystal structures of aspartate aminotransferase reconstituted with 1-deazapyridoxal 5'-phosphate: internal aldimine and stable L-aspartate external aldimine, *Biochemistry* 50, 5918-5924.

[60] Onuffer, J. J., and Kirsch, J. F. (1995) Redesign of the substrate specificity of *Escherichia coli* aspartate aminotransferase to that of *Escherichia coli* tyrosine aminotransferase by homology modeling and site-directed mutagenesis, *Protein science : a publication of the Protein Society* 4, 1750-1757.

- [61] McCoy, A. J., Grosse-Kunstleve, R. W., Adams, P. D., Winn, M. D., Storoni, L. C., and Read, R. J. (2007) Phaser crystallographic software, *Journal of applied crystallography* 40, 658-674.
- [62] Koch, K. (2004) Sucrose metabolism: regulatory mechanisms and pivotal roles in sugar sensing and plant development, *Current opinion in plant biology* 7, 235-246.
- [63] Lunn, J. E. (2008) Sucrose Metabolism, In *Encyclopedia of Life Sciences*, John Wiley & Sons.
- [64] Winter, H., and Huber, S. C. (2000) Regulation of sucrose metabolism in higher plants: localization and regulation of activity of key enzymes, *Critical reviews in biochemistry and molecular biology* 35, 253-289.
- [65] MacRae, E., and Lunn, J. (2012) Photosynthetic Sucrose Biosynthesis: An Evolutionary Perspective, In *Photosynthesis* (Eaton-Rye, J. J., Tripathy, B. C., and Sharkey, T. D., Eds.), pp 675-702, Springer Netherlands.
- [66] Salerno, G. L., and Curatti, L. (2003) Origin of sucrose metabolism in higher plants: when, how and why?, *Trends in plant science* 8, 63-69.
- [67] Cumino, A. C., Marcozzi, C., Barreiro, R., and Salerno, G. L. (2007) Carbon cycling in *Anabaena* sp. PCC 7120. Sucrose synthesis in the heterocysts and possible role in nitrogen fixation, *Plant physiology* 143, 1385-1397.
- [68] Curatti, L., Giarrocco, L., and Salerno, G. L. (2006) Sucrose synthase and RuBisCo expression is similarly regulated by the nitrogen source in the nitrogen-fixing cyanobacterium *Anabaena* sp., *Planta* 223, 891-900.
- [69] Kolman, M. A., Torres, L. L., Martin, M. L., and Salerno, G. L. (2012) Sucrose synthase in unicellular cyanobacteria and its relationship with salt and hypoxic stress, *Planta* 235, 955-964.
- [70] Yamanaka, T. (2008) *Chemolithoautotrophic Bacteria: Biochemistry and Environmental Biology*, Springer, Japan.
- [71] Teske, A., Alm, E., Regan, J. M., Toze, S., Rittmann, B. E., and Stahl, D. A. (1994) Evolutionary relationships among ammonia- and nitrite-oxidizing bacteria, *J. Bacteriol.* 176, 6623-6630.

- [72] Vannelli, T., Logan, M., Arciero, D. M., and Hooper, A. B. (1990) Degradation of halogenated aliphatic compounds by the ammonia- oxidizing bacterium *Nitrosomonas europaea*, *Applied and environmental microbiology* 56, 1169-1171.
- [73] Chain, P., Kurtz, S., Ohlebusch, E., and Slezak, T. (2003) An applications-focused review of comparative genomics tools: capabilities, limitations and future challenges, *Briefings in bioinformatics* 4, 105-123.
- [74] Hooper, A. B. (1969) Biochemical basis of obligate autotrophy in *Nitrosomonas europaea*, *J. Bacteriol.* 97, 776-779.
- [75] Baroja-Fernandez, E., Munoz, F. J., Saikusa, T., Rodriguez-Lopez, M., Akazawa, T., and Pozueta-Romero, J. (2003) Sucrose synthase catalyzes the de novo production of ADPglucose linked to starch biosynthesis in heterotrophic tissues of plants, *Plant & cell physiology* 44, 500-509.
- [76] Delmer, D. P. (1972) The purification and properties of sucrose synthetase from etiolated *Phaseolus aureus* seedlings, *J. Biol. Chem.* 247, 3822-3828.
- [77] Figueroa, C. M., Asencion Diez, M. D., Kuhn, M. L., McEwen, S., Salerno, G. L., Iglesias, A. A., and Ballicora, M. A. (2013) The unique nucleotide specificity of the sucrose synthase from *Thermosynechococcus elongatus*, *FEBS letters* 587, 165-169.
- [78] Grimes, W. J., Jones, B. L., and Albersheim, P. (1970) Sucrose synthetase from *Phaseolus aureus* seedlings, *J. Biol. Chem.* 245, 188-197.
- [79] Morell, M., and Copeland, L. (1985) Sucrose synthase of soybean nodules, *Plant physiology* 78, 149-154.
- [80] Porchia, A. C., Curatti, L., and Salerno, G. L. (1999) Sucrose metabolism in cyanobacteria: sucrose synthase from *Anabaena* sp. strain PCC 7119 is remarkably different from the plant enzymes with respect to substrate affinity and amino-terminal sequence, *Planta* 210, 34-40.
- [81] Ross, H. A., and Davies, H. V. (1992) Purification and Characterization of Sucrose Synthase from the Cotyledons of *Vicia faba* L., *Plant physiology* 100, 1008-1013.
- [82] Tanase, K., and Yamaki, S. (2000) Purification and characterization of two sucrose synthase isoforms from Japanese pear fruit, *Plant & cell physiology* 41, 408-414.

- [83] Curatti, L., Giarrocco, L. E., Cumino, A. C., and Salerno, G. L. (2008) Sucrose synthase is involved in the conversion of sucrose to polysaccharides in filamentous nitrogen-fixing cyanobacteria, *Planta* 228, 617-625.
- [84] Zheng, Y., Anderson, S., Zhang, Y., and Garavito, R. M. (2011) The structure of sucrose synthase-1 from *Arabidopsis thaliana* and its functional implications, *J. Biol. Chem.* 286, 36108-36118.
- [85] Lairson, L. L., Henrissat, B., Davies, G. J., and Withers, S. G. (2008) Glycosyltransferases: structures, functions, and mechanisms, *Annu. Rev. Biochem.* 77, 521-555.
- [86] Sheng, F., Jia, X., Yep, A., Preiss, J., and Geiger, J. H. (2009) The crystal structures of the open and catalytically competent closed conformation of *Escherichia coli* glycogen synthase, *J. Biol. Chem.* 284, 17796-17807.
- [87] Hardin, S. C., Winter, H., and Huber, S. C. (2004) Phosphorylation of the amino terminus of maize sucrose synthase in relation to membrane association and enzyme activity, *Plant physiology* 134, 1427-1438.
- [88] Klotz, K. L., Finger, F. L., and Shelver, W. L. (2003) Characterization of two sucrose synthase isoforms in sugarbeet root, *Plant Physiol. Biochem.* 41, 107-115.
- [89] Schäfer, W. E., Rohwer, J. M., and Botha, F. C. (2004) A kinetic study of sugarcane sucrose synthase, *Eur. J. Biochem.* 271, 3971-3977.
- [90] Wolosiuk, R. A., and Pontis, H. G. (1974) Studies on sucrose synthetase. Kinetic mechanism, *Archives of biochemistry and biophysics* 165, 140-145.
- [91] Gibson, R. P., Tarling, C. A., Roberts, S., Withers, S. G., and Davies, G. J. (2004) The donor subsite of trehalose-6-phosphate synthase: binary complexes with UDP-glucose and UDP-2-deoxy-2-fluoro-glucose at 2 Å resolution, *The Journal of biological chemistry* 279, 1950-1955.
- [92] Yep, A., Ballicora, M. A., and Preiss, J. (2006) The ADP-glucose binding site of the *Escherichia coli* glycogen synthase, *Archives of biochemistry and biophysics* 453, 188-196.
- [93] Buschiazzo, A., Ugalde, J. E., Guerin, M. E., Shepard, W., Ugalde, R. A., and Alzari, P. M. (2004) Crystal structure of glycogen synthase: homologous enzymes catalyze glycogen synthesis and degradation, *The EMBO journal* 23, 3196-3205.



- [94] Gibson, R. P., Turkenburg, J. P., Charnock, S. J., Lloyd, R., and Davies, G. J. (2002) Insights into trehalose synthesis provided by the structure of the retaining glucosyltransferase OtsA, *Chemistry & biology* 9, 1337-1346.
- [95] Schinzel, R., and Drueckes, P. (1991) The phosphate recognition site of *Escherichia coli* maltodextrin phosphorylase, *FEBS letters* 286, 125-128.
- [96] Schinzel, R., and Palm, D. (1990) *Escherichia coli* maltodextrin phosphorylase: contribution of active site residues glutamate-637 and tyrosine-538 to the phosphorolytic cleavage of alpha-glucans, *Biochemistry* 29, 9956-9962.
- [97] Yep, A., Ballicora, M. A., and Preiss, J. (2004) The active site of the *Escherichia coli* glycogen synthase is similar to the active site of retaining GT-B glycosyltransferases, *Biochem. Biophys. Res. Commun.* 316, 960-966.
- [98] Kuhn, M. L., Falaschetti, C. A., and Ballicora, M. A. (2009) *Ostreococcus tauri* ADP-glucose pyrophosphorylase reveals alternative paths for the evolution of subunit roles, *The Journal of biological chemistry* 284, 34092-34102.
- [99] Sambrook, J., and Russell, D. W. (2001) *Molecular Cloning: A laboratory Manual*, Vol. 2, 3rd ed., Cold Spring Harbor Laboratory Press, Cold Spring Harbor, NY.
- [100] Laemmli, U. K. (1970) Cleavage of structural proteins during the assembly of the head of bacteriophage T4, *Nature* 227, 680-685.
- [101] Hall, T. A. (1999) BioEdit: a user-friendly biological sequence alignment editor and analysis program for Windows 95/98/NT, *Nucl. Acids Symp. Ser.* 41, 95-98.
- [102] Gouy, M., Guindon, S., and Gascuel, O. (2010) SeaView version 4: A multiplatform graphical user interface for sequence alignment and phylogenetic tree building, *Molecular biology and evolution* 27, 221-224.
- [103] Winn, M. D., Ballard, C. C., Cowtan, K. D., Dodson, E. J., Emsley, P., Evans, P. R., Keegan, R. M., Krissinel, E. B., Leslie, A. G., McCoy, A., McNicholas, S. J., Murshudov, G. N., Pannu, N. S., Potterton, E. A., Powell, H. R., Read, R. J., Vagin, A., and Wilson, K. S. (2011) Overview of the CCP4 suite and current developments, *Acta Crystallogr. D Biol. Crystallogr.* 67, 235-242.
- [104] Murshudov, G. N., Vagin, A. A., and Dodson, E. J. (1997) Refinement of macromolecular structures by the maximum-likelihood method, *Acta Crystallogr. D Biol. Crystallogr.* 53, 240-255.

- [105] Sali, A., and Blundell, T. L. (1993) Comparative protein modelling by satisfaction of spatial restraints, *Journal of molecular biology* 234, 779-815.
- [106] Luthy, R., Bowie, J. U., and Eisenberg, D. (1992) Assessment of protein models with three-dimensional profiles, *Nature* 356, 83-85.
- [107] Richards, F. M., and Kundrot, C. E. (1988) Identification of structural motifs from protein coordinate data: secondary structure and first-level supersecondary structure, *Proteins* 3, 71-84.

## VITA

Rui Wu was born in Linfen, Shanxi, China. She was 23 when moved to Chicago, Illinois, where she attended graduate school. Between 2006 and 2010 she attended Sichuan University, Chengdu, China, where she earned a Bachelor of Science in